THESIS

A SIMPLE LUMPED PARAMETER MODEL OF THE CARDIOVASCULAR SYSTEM

Submitted by

Canek Phillips

Department of Mechanical Engineering

In partial fulfillment of the requirements

For the Degree of Master of Science

Colorado State University

Fort Collins, Colorado

Summer 2011

Masters Committee:

Advisor: L Prasad Dasi

Sue James
Chrisopher Kawcak

ABSTRACT

A SIMPLE LUMPED PARAMETER MODEL OF THE CARDIOVASCULAR SYSTEM

Congestive heart failure is caused when untreated heart diseases affect malfunction in the heart to a point where the heart can no longer pump enough blood to the body. The additional energy cost taxed onto the heart by heart diseases is the root cause of congestive heart failure. Currently, a disease severity guideline is used in the medical field to differentiate disease cases and their relative risk of causing congestive heart failure. The current disease severity guideline does not take into consideration workload when assessing the severity of a disease case.

A zero-dimensional computational model of the left ventricle was developed to simulate physiological and pathophysiological characteristics to quantify workload of hypothetical normal and diseased patient cases. The development of the computational model has revealed that workload calculation possesses utility in differentiating the severity of risk that left ventricular diseases have on affecting congestive heart failure. Results of heart disease simulations for aortic stenosis, aortic regurgitation, mitral regurgitation, and hypertension show the energy cost the diseases impose on the left ventricle compared to a normal patient model. Additional results of simulations with combined mild cases of heart diseases show an amplified impact on energy cost

- more than the energy cost of individual mild cases added together separately. The calculation of workload in computational simulations is an important step towards using workload as a universal indicator of risk of development of congestive heart failure and updating treatment guidelines so that prevention of congestive heart failure is more successful.

ACKNOWLEDGEMENTS

First and foremost I would like to thank my mother who has always supported me to pursue a higher education.

Next I would like to recognize the outstanding support throughout my research that my adviser Dr L Prasad Dasi provided. His kindness and understanding as I toiled during the development stages of the project made it very easy to want to accomplish the aims of the project. I would also like to thank my committee members for adding their expertise to this project. Dr Chris Kawcak was my first lab adviser when I started at CSU in 2009 and I thank him for sticking with me as I progressed through my graduate work at CSU. Dr Sue James was the chair of the School of Biomedical Engineering when I first met her and I appreciate that she would lend her time to this project as I finish my work at CSU.

I would like to thank the School of Biomedical Engineering for the support given to me my first year at CSU. I had the honor of being able to do lab rotations the BME Dept my first year as a grad student which introduced me to Dr Kawcak and Dr Dasi, something that I am very thankful for. Dr Dasi provided me with an assistantship my final semester at CSU, a factor that allowed me to easily finish my studies at CSU.

I would like to thank my lab, the Cardiovascular and Biofluids Mechanics Laboratory, for all the support they have given. My officemate, Brennan, was a lot of fun and great company.

I would also like to thank the Diversity Offices and Apartment Life at CSU for giving me something to do outside of engineering that I really enjoyed. I would also really like to thank Kate Wormus, a coordinator for the Vice President of Student Affairs at CSU. She was an exceptional friend and I don't really think I could ever thank her for the work she did.

TABLE OF CONTENTS

LIST OF FIGURES

LIST OF TABLES

1 INTRODUCTION

1.1 Introduction

In 2006, it was estimated that 81.1 M people were living with some form of heart disease in the US. Heart disease caused more than one out of four deaths in 2006 – the leading cause of death for both men and women that year. (National Center for Chronic Disease Prevention and Health Promotion)

Untreated heart and circulatory system diseases lead to congestive heart failure. Untreated diseases like valvular disease, coronary heart disease, or hypertension will influence heart malfunction through different means that will eventually result in the same end; the heart will not be able to pump enough blood to the rest of the body. Congestive heart failure is known to those it affects through the symptoms that include fatigue, shortness of breath, and swelling. The symptoms of congestive heart failure are what the public often mistakenly refers to as the actual disease, which is part of the problem in understanding what heart disease actually is. (Cicala 1997)

Understanding how heart disease leads to congestive heart failure is paramount in preventing congestive heart failure. One problem in understanding how congestive heart failure develops is the resiliency of the heart in its attempt to pump enough blood to the body while being overloaded by heart disease. The heart essentially becomes its own worst enemy as it fights a losing battle to pump enough blood. In the meantime, mild cases of heart diseases remain disguised as the heart pumps harder to compensate for their effects. As a result, when congestive heart failure finally does overtake the heart, treatment options may not exist for the patient.

Research is required into being able to actually quantify when a heart disease is beginning to cause congestive heart failure. The relationship between heart disease and added workload on the heart is not fully understood in the medical field. If the relationship can be understood, it may increase the level of treatment management for a life-threatening condition.

1.2 Background and motivation

Congestive heart failure is caused by diseases that impose an extra workload on the heart. The heart grows so that it might overcome the extra load that it must work against; but its growth is a double edged sword. While the heart is able to compensate by the extra work it must perform, eventually too much heart growth leads to congestive heart failure. The walls of the heart that thicken to provide extra pumping force take up volume that would have otherwise been used to hold blood. The lack of space to hold blood volume leads to the inability to pump enough blood to the rest of the body.

At the root of the condition of congestive heart failure is work. The heart must perform work to pump blood to the body. Thermodynamically speaking, the heart performs work when its chambers change in volume as it contracts and expands. The classical definition of pressure-volume work is: $W = \int_{V_i}^{V_f} p\, dV$. A system performs positive work when contracting from an initial volume to a smaller final volume. The left ventricle performs positive work when it contracts blood during systole out to systemic circulation.

Congestive heart failure is most easily caused by heart diseases that make the left ventricle have to work harder and undergo hypertrophy to withstand the extra load placed upon it. The left ventricle's role as the chamber that pumps blood out to the body makes its proper functioning as the most crucial of the four chambers of the heart. It is easy to then understand that when the left ventricle is unable to pump enough blood out to the body, a life threatening situation is imminent.

Four causes of increased workload to the left ventricle are mitral regurgitation, aortic stenosis, aortic regurgitation, and hypertension. The four causes can be grouped accordingly to how they create extra workload on the left ventricle. Aortic stenosis and hypertension both create a scenario where the left ventricle must contract harder due to a greater pressure overload that it must work against. Aortic stenosis is the narrowing of the aortic valve through which blood exits the left ventricle. The narrowing of the valve increases the resistance against blood traveling through the aortic valve into the aortic sinus. The increase in resistance through the aortic valve creates a greater pressure gradient from which the left ventricle must pump harder to overcome. Hypertension is a disease that is caused when systemic capillaries harden and decrease in diameter. The loss in compliance and increase in resistance of systemic vessels increases the afterload that the heart pumps against, again requiring an increase in the pumping force of the left ventricle.

Conversely, aortic and mitral regurgitation create volume overloads in different ways, but with the same result of making the left ventricle increase its contraction strength to pump an increased volume of blood. Aortic regurgitation occurs when blood initially pumped out by the left ventricle into the aortic sinus leaks back into the heart due to valve malfunction. The constant backflow of blood caused by a leaky valve increases the amount of volume that the left ventricle must eject, increasing workload. Mitral regurgitation involves blood leaking back from the left ventricle through a faulty mitral valve into the left atrium. The left ventricle has to increase stroke volume to compensate for the amount of blood that it loses through the mitral valve, again making the heart work harder.

The left ventricle tries, albeit with futility, to overcome the extra workloads imposed on it by the pressure and volume overload disease cases. In its attempt to overcome pressure overload, the left ventricle thickens its walls so that it can pump more forcefully. While this method of remodeling called hypertrophy does allow the heart to pump harder, it also decreases the amount of blood volume available within the ventricle to pump out to the body. The loss of stroke volume

causes the left ventricle to try to pump even harder and thicken its walls even more. The vicious cycle caused by hypertrophy makes the risk of congestive heart failure even greater. (Cicala 1997)

With volume overload cases, the left ventricle dilates so that it can hold more blood to make up for the blood volume that is leaking through faulty valves. The dilation is referred to medically as left ventricular cardiomyopathy – a term that describes the weakening of the left ventricle muscle's strength caused by the dilation of the chamber. While the dilation of the ventricle allows it to hold more volume, it also weakens the muscle in the walls lining the ventricle, eventually so that the left ventricle no longer has the strength to pump enough blood out to the body. (Cicala 1997)

The relationship between heart disease and extra workload leading to the onset of congestive heart failure needs to be understood if congestive heart failure is to be treated. Currently, the medical field is in the nascent stages of connecting heart disease with the extra workload it causes. Research is required if understanding of the relationship is to be furthered for the benefit of congestive heart treatment.

The current guidelines that are used to treat cases of diseases that cause congestive heart failure stemming in the left ventricle do not focus on the extra energy costs that those diseases tax on the left ventricle:

Table 1 Guidelines for differentiating disease severity for hypertension, aortic stenosis, and aortic and mitral regurgitation. (Bonow 2007)

Hypertension		
	SBP mmHg	DBP mmHg
mild	120 - 139	or 80 - 89
moderate	140 - 159	or 90 - 99
severe	≥160	and ≥100
Source: US Dept of Health and Human Services		

Aortic stenosis	
	Mean dP
mild	<25 mmHg
moderate	25 mmHg < dP < 40 mmHg
severe	≥40 mmHg
Source: ACC/AHA 2006 Pocket Guideline	

Mitral regurgitation	
	Regurgitant Fraction
mild	<30%
moderate	30% < RF < 49%
severe	≥50%
Source: ACC/AHA 2006 Pocket Guideline	

Aortic regurgitation	
	Regurgitant Fraction
mild	<30%
moderate	30% < RF < 49%
severe	≥50%
Source: ACC/AHA 2006 Pocket Guideline	

The severity of hypertension and aortic stenosis cases are differentiated by pressure. The severity of mitral and aortic regurgitation cases both use regurgitant fraction, the amount of blood leaking through the faulty valve in question versus the amount of blood that passes through. The quantification of actually how hard the heart is working while operating under diseased conditions is never fully answered.

The risk of developing congestive heart failure is not truly captured by the guidelines above because the primary factor in developing congestive heart failure is work. While in a sense there is some aspect of work that is factored into the consideration of regurgitant fraction (increased volume), and increased pressure (pressure is after all the integral of pressure with change in volume), the guideline lose some scope of applicability in certain situations where inherent patient conditions invalidate the usefulness of the guidelines.

The guidelines used to differentiate severity often fall prey to assumptions about patient conditions that might soften the appearance of disease severity. Pressure drop across the aortic valve might not be as great in a patient who has already had congestive heart failure. Furthermore, a heart with several mild conditions might not be considered severely overworked either. A patient with mild hypertension and mild mitral regurgitation will not have a blood pressure deemed too high or a regurgitant fraction severe enough to be deemed at risk for congenital heart failure yet it might be entirely possible that the heart is being overworked. With the weakness of the current guideline system employed to gage disease severity exposed, it is hypothesized that *using a workload calculation to characterize disease severity would better serve to capture the severity of heart diseases and the risk they pose in causing congestive heart*

failure. Such a workload calculation would be better able to assess the true workload impact that an individual case or combined cases would be having on the heart. A second hypothesis to be explored is that *the combination of mild diseases adds non-linearly to the energy cost that they place upon the heart*.

The second hypothesis relates that two combined mild cases may add together a greater energy cost than the sum of the energy cost each results in separately.

To test the hypotheses stated, specific aims have been constructed. The specific aims are:

Specific aim I: The development of a computational model of the left ventricle that is able to simulate physiological and pathophysiological characteristics and quantify workload from those characteristics.

Specific aim II: Utilization of the computational model to test how multiple disease scenarios affect energy cost on the left ventricle.

Results from the computational model developed for this research have been promising. A zero-dimensional model, also known as a lumped parameter model, was developed that could accurately simulate blood flow and pressure throughout the left pumping chambers and systemic circulation of the human cardiovascular system. Direct calculation of workload within normal and diseased left ventricular simulations provided evidence of the utility of workload as a universally applicable measure in differentiating the risk of developing congestive heart failure. Additional results of simulations with combined mild cases of heart diseases show a greater combined impact on energy cost than the energy cost of individual mild cases added together separately, supplying evidence that workload as a severity measure of a disease better captures what current guidelines may overlook as a potentially serious life-threatening condition.

A background of the mechanics of the cardiovascular system, heart diseases affecting the left ventricle, as well as a literature review of lumped parameter modeling is presented in chapter 2. Chapter 3 presents the methods used to accomplish the specific aims defined in this chapter. Chapter 4 contains the results of the computational simulations of normal and diseased patient

cases. Research is summarized and an explanation of future work is submitted in Chapter 5. The C code of the lumped parameter model is attached in the appendix.

2 THE CARDIOVASCULAR SYSTEM AND ITS COMPONENTS

2.1 Blood

Blood is partly made up of cells as well as liquid. The liquid part of blood is known as plasma and is made up of organic and inorganic substances in aqueous solution. The plasma solution is itself mostly protein by weight. Plasma proteins are classified as albumins, globulins, or fibrinogens. The non-liquid portion of blood is composed of cells. Over ninety-nine per cent of blood cells are erythrocytes, also known as red blood cells. Other cells in the blood are leukocytes that protect against pathogens and cancer, and finally platelets which are more like cell fragments than actual cells. Hematocrit is a term used to denote the blood volume percentage that is taken by red blood cells. A normal hematocrit is 45% for men and 42% for women.(Vander, Sherman et al. 2001)

2.2 The cardiovascular circuit

The idea of blood being pumped in a circuit within the body has been documented as early as 1628 by William Harvey. Harvey was the first to conclude that the same blood that exited the heart also returned back to the heart. (Vander, Sherman et al. 2001)

The transport of blood is accomplished through two circuits within the cardiovascular system: the systemic and pulmonary circuit. Each circuit begins and ends at the heart, and the heart itself is divided longitudinally. The left and right sides of the heart are each divided into two chambers, the atrium and ventricle. The atrium is the upper chamber of the heart and it empties blood into the ventricle, the lower chamber.(Vander, Sherman et al. 2001)

When blood is pumped through the pulmonary circuit, it is pumped from the right ventricle to the lungs and eventually to the left atrium. The pulmonary circuit allows red blood

cells to expel carbon dioxide and replenish oxygen which is carried into the systemic circuit. In systemic circulation, blood travels from the heart's left ventricle to the organs of the body and back to the right atrium.

The vessels carrying blood away from the heart are known as arteries, and vessels that allow for the return of blood are veins. Arterial networks demonstrate non-linear visco-elastic behavior. Inside arteries, flow is pulsatile, and the blood itself exhibits complex non-Newtonian behavior. Blood vessels do not obey Hooke's law and gain stiffness as stress increases. (Bronzino 1995)

Blood vessels have three layers. The inner layer, called the intima, is mainly composed of endothelial cells that have the ability to change the vessel's diameter. The middle layer, called the media, is made of elastin, collagen, and smooth muscle whose composition determines the elastic properties of the vessel. The adventitia is the outer layer of the vessel that is mostly connective tissue. (Bronzino 1995)

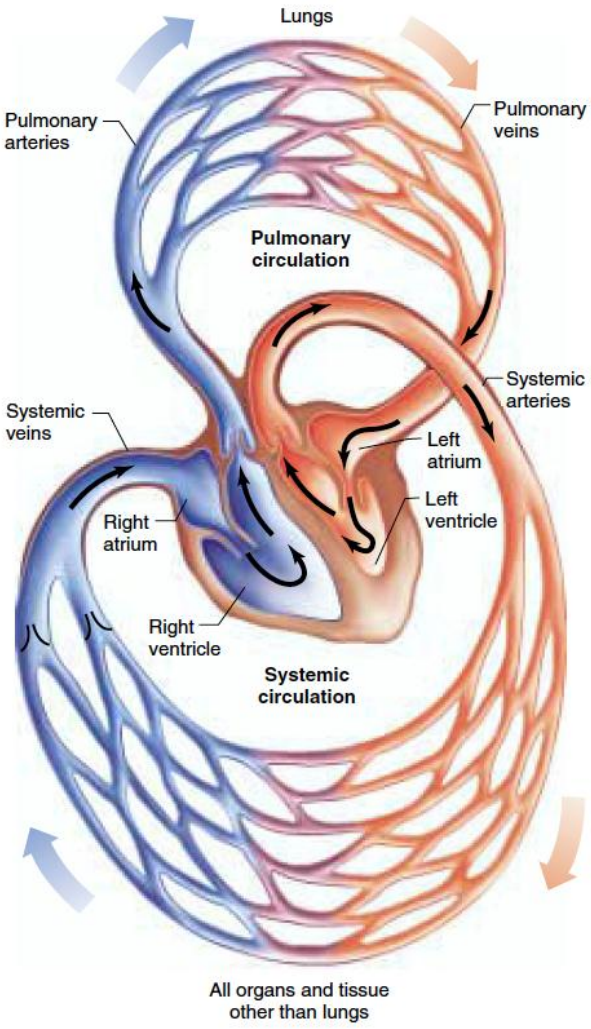

Figure 1 The cardiovascular circuit. (Vander, Sherman et al.)

Blood transport through the systemic circuit begins when the blood leaves the left ventricle via the aorta. Vessels branch from the aorta into arteries, arteries divide into arterioles, and arterioles branch into capillaries

which are estimated to number in the range of ten billion. Capillaries regroup into larger sized venules that unite to form veins. Veins unite to form the inferior and superior vena cava that return blood from the upper and lower regions of the body and return the blood to the right atrium. (Vander, Sherman et al. 2001)

In pulmonary circulation blood leaves the right ventricle through the pulmonary trunk which divides into two arteries, each artery traveling to a separate lung. Similarly, arteries ultimately divide into capillaries, and capillaries ultimately regroup into veins. Four pulmonary veins empty blood coming from the lungs back into the left atrium completing the pulmonary circuit.

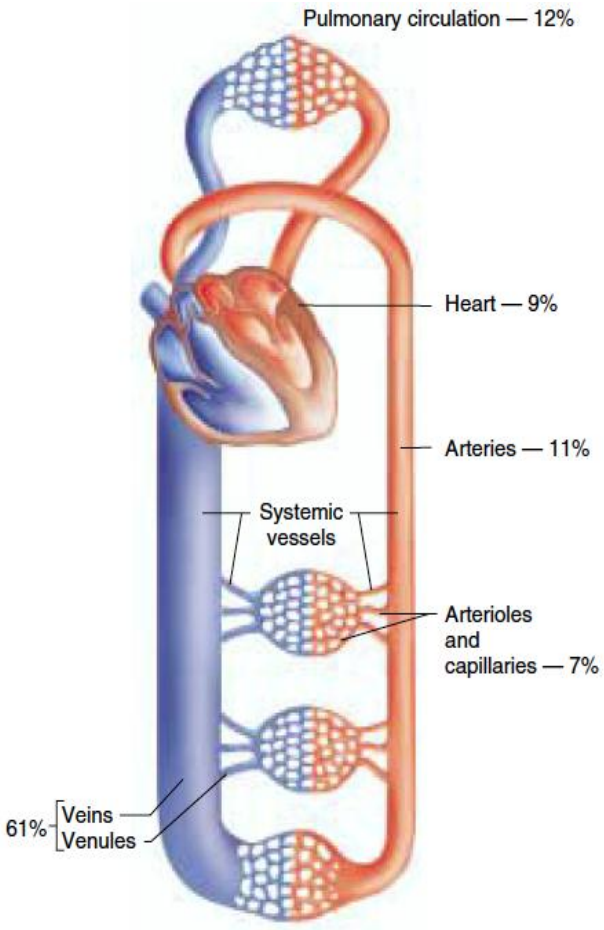

Figure 2 Illustration of blood volume by cardiovascular segment in human circulation. (Vander, Sherman et al.)

The bulk movement of blood is accomplished through the pressure created from the pumping heart. 95% of circulating blood is contained within the larger blood vessels, but it is within the capillaries that the end functions of gaseous and nutrient exchange that allows for normal functioning of the body occurs. The cardiovascular system can be ultimately summed up as a system whose aim is to supply adequate blood flow to the capillaries of the body. (Vander, Sherman et al. 2001)

As a useful comparison to the human cardiovascular system, the geometric parameters of the canine systemic and pulmonic branches have been quantified. Total blood circulation in the

systemic system contains 83% of blood volume, with 12% of blood in the pulmonic branch, and 5% within the heart. Most of systemic blood is contained in the veins where it is used to maintain a mean circulatory blood pressure through use of compliance of veins. (Bronzino 1995)

2.3 Pressure, resistance and blood flow

The rate of blood flow is determined by pressure and resistance. Blood flow (Q) is calculated by dividing the difference in pressure between two points (dP) by the resistance (R) to flow between the same two points, i.e. $Q = \frac{dP}{R}$. Resistance is a value for the friction that slows down flow across a vessel.

Blood flow always follows a path from a region of higher pressure to a lower one. In the cardiovascular system, the pressure exerted by the heart is the driving force that moves blood. In the medical field, blood flow is usually measured in liters per minute (L/min), and blood pressure is measured in millimeters of mercury (mmHg). Resistance (mmHg-min/L) is encountered as blood travels through the blood vessels of the body.

Resistance in a tubular vessel can be calculated using the following equation:

$$R = \frac{8\mu L}{\pi r^4}$$

Where μ represents kinematic fluid viscosity (mmHg-min-in^3/L), L is length of the tube (inches), and r equals the inner radius of the tube (inches). (Verdonck and Perktold 1998) Examining the resistance formula for a tube and its relationship with blood flow; a change in radius size of a tube will have a great impact on blood flow indeed, much more so than changing fluid viscosity or tube length.(Vander, Sherman et al. 2001)

The diameter of blood vessels is actively regulated by the body. Vasoconstrictors like norepinephrine and vasodilators such as nitroprusside are two examples of compounds with the ability to change blood vessel diameter. As the names suggest, vasoconstrictors shorten the length of the diameter of a vessel and vasodilators enable the opposite task. Norepinephrine and

nitroprusside can be used to create change in blood flow through the change in resistance to flow that vessels create when vessel diameter is changed. (Bronzino 1995)

Major simplification of blood flow fluid properties is often implemented to create useful hemodynamic models as a result of the complex nature of cardiovascular flow. The complex nature of blood flow is a result of the matrix of suspended cells and particles that form blood and give it its complex non-Newtonian properties. Large blood vessels are more accurately described using Newtonian assumptions of fluid, but small vessels around 100 μm in diameter do not behave accordingly. Wall shear stress values from blood-like fluids inside small vessels have been shown to deviate from the values calculated within larger vessels. (Bronzino 1995)

Arterial hemodynamics is affected by the viscoelasticity of the blood vessel. The Moens-Korteweg relationship calculates the wave propagation speed through the wall of vessel undergoing pulsatile flow such as an artery: $c = \sqrt{\frac{Eh}{2\rho r}}$, where E is the elastic modulus, h is the wall thickness, ρ is the blood density, and r is vessel radius. The Moens-Kortweg relationship therefore allows a means for studying the affect of wave propagation on rate of blood flow. Wave speed is faster in humans in the aorta than the pulmonary artery due to the higher pressure that the aorta withstands which creates a higher modulus of elasticity. As vessels branch to smaller sizes, it is generally a rule that wave speeds become greater due to the smaller radius of the branched vessel. (Bronzino 1995)

The reflection of waves propagated through vessels can occur at the branching of vessels. Wave refection is a consequence of imperfect impedance matching that occurs when a somewhat rigid vessel branches into a more elastic vessel. For a rigid vessel, the impedance is essentially just its resistance. The impedance for an elastic vessel is related to the frequency of fluctuations in pressure and flow. The mismatch of impedance is a result of the incongruity of material property between two unlike vessels. (Bronzino 1995)

The most efficient network of vessels would be a system with perfect impedance matching, preventing any energy being culled by wave reflections. The reflection coefficient is a ratio that compares the relative characteristic impedance at the junction of two vessels: $R = \frac{Z_0^{-1} - Z_1^{-1} - Z_2^{-1}}{Z_0^{-1} + Z_1^{-1} + Z_2^{-1}}$, where Z_1 and Z_2, represent the impedance values of the parent vessel and Z_0 the value for the daughter vessel. For perfect impedance matching to occur, R would equal zero, meaning that $Z_0^{-1} = Z_1^{-1} + Z_2^{-1}$. The relative impedance ratios at local branching junctions in the arterial system are typically 0.2 indicating a good rate of efficiency. The low reflection coefficient at a local junction is overshadowed by the high global coefficient which sums the imperfect impedance matching at sites distal to a given site and is largely responsible for the inefficiency of the arterial system. (Bronzino 1995)

The elastic modulus of a vessel is also important because it determines how much blood a vessel can hold during diastole when the heart is not pushing flow throughout the body. (Bronzino 1995)

2.3.1 Circulation pressures

The pressure of blood exiting the left and right ventricles is significantly different due to architectural difference between each ventricle. The left ventricle wall is thicker than the right ventricle, presumably because of the greater force required by the left ventricle to circulate blood to the entire body. Systolic and diastolic systemic arterial pressures are 120 and 70 mmHg on average while they are only 24 and 8 mmHg for pulmonic arterial circulation. (Vander, Sherman et al. 2001)

2.4 The semilunar valves

The left and right sides of the heart each contain two one way valves. The left side of the heart contains the mitral and aortic valve. The right side contains the tricuspid and pulmonary valves. While the functions of the valves are all the same, to regulate the flow of blood, location

of each valve within the heart and exposure to different amount of blood flow has created differences between each valve.(Vander, Sherman et al. 2001)

The left ventricle pumps much more blood than the right ventricle (the left side of the must generate enough pressure to circulate blood around the body), and as a result the valves of the left side of the heart must withstand a greater pressure than the right side. The tricuspid and pulmonic valves must counter a 30 mmHg pressure when closed compared to the 100 mmHg that the aortic and mitral valves must withstand on the left side of the heart.(Bronzino 1995)

2.4.1 The aortic valve

The aortic valve is made up of three leaflets situated inside a connective tissue sleeve. The leaflets are also referred to as semilunar cusps because they resemble a half moon shape when viewed from above.

Each cusp is composed of a dense collagenous core facing the high pressure side of the aorta with a lining of endothelial cells. The side of the leaflet facing the aorta is the major fibrous layer of the leaflet and as a result is called the fibrosa of the leaflet. On the other side of the leaflet, the ventricular side, the composition is mainly collagen and elastin. The side of the leaflet facing the ventricle is commonly called the ventricularis for obvious reasons. The ventricularis presents a very smooth surface to blood flow and is not as thick as the fibrosa layer of the leaflet. When facing the pressure of blood flow, the fibers of collagen within the fibrosa reorient in direction to a circumferential orientation and returns to an unorganized state when no blood flow presents stress. (Bronzino 1995)

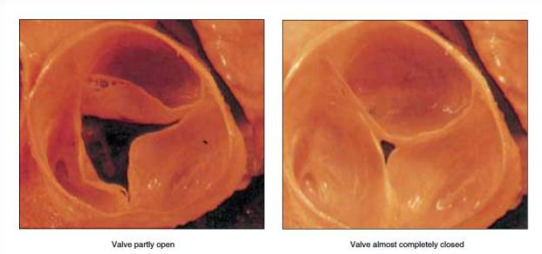

Figure 3 Aortic valve (opened and closed). (Vander, Sherman et al.)

The aorta is separated from the left ventricle by the annular ring of the aortic valve. The sinus of Valsalva lies superior to the aortic valve and is composed of three bulges found at the

root of the aorta. Each bulge is aligned with a corresponding valve leaflet so that each leaflet and bulge is named according to anatomical location within the aorta. Coronary arteries branch off from two of the sinuses. (Bronzino 1995)

2.4.2 The pulmonic valve

Anatomically the pulmonic valve is similar to the aortic valve. The main difference between the two valves lies in the smaller sinuses and the larger pulmonic valve annulus versus the aortic valve. (Bronzino 1995)

2.5 The atrioventricular (AV) valves

The AV valves, also known as the mitral valve in the left chamber of the heart and the tricuspid valve in the right chamber of the heart, serve to regulate flow between the atria and ventricles of the heart. Flow between the atrium and ventricle proceeds when there is a higher pressure in the atrium than in the adjacent ventricle and the AV valve opens. The AV valve shuts when pressure in the ventricle reaches a greater value than the pressure of the atrium. (Vander, Sherman et al. 2001)

The AV valves are similar in structure with four primary elements: a valve annulus, valve leaflets, papillary muscles, and chordate tendinae.

2.5.1 The mitral valve

The mitral annulus has a three-dimensional form like that of a suction cup. Its dense collagenous tissue surrounded by muscle translates and changes size during the cardiac cycle. Circumference of the mitral annulus is between 8 to 12 mm when the atrium is filling. (Bronzino 1995)

The mitral valve is formed by two leaflets that are actually one continuous piece of tissue separated into anterior and posterior leaflets by regularly placed indentations in the valve tissue called commissures. Endothelium reinforced with collagen is the main tissue type found in each leaflet which also includes blood vessels, non-myelinated nerve fibers, and striated muscle cells. Healthy leaflets combined form a much larger area than necessary to seal the mitral orifice

allowing for proper functioning if the valves ever do become diseased. The anterior mitral leaflet is a bit larger than the posterior leaflet. Also, the anterior leaflet has a semilunar shape while the posterior leaflet is more rectangular. The posterior leaflet covers about 2/3 of the mitral annulus and extends from the mural endocardium from the free walls of the left atrium. The anterior leaflet serves essentially connects the wall of the ascending aorta, the aortic valve, and the atrial septum. The posterior leaflet can be divided into three regions by scallops that are indentations on the leaflet. The three divisions are the media, central, and lateral scallop.(Bronzino 1995)

The rough zone of the mitral leaflet is the thicker region from valve's line of closure to the end of the extra tissue beyond the line of closure. The chordae tendinae that insert in this aforementioned region create a rough texture which lends to calling the region 'rough'. Extending from the line of closure to the annulus is a clear zone of the leaflet that is thinner and translucent. (Bronzino 1995)

Papillary muscles are connected to the mitral valve by the chordae tendinae. Two sets of chordae tendinae extend from the papillary muscles, the marginal and basal chordae. Each chordae tendinae is comprised of loosely meshed elastin and collagen fibers that surround an inner core of collagen fibers. Encircling the meshed elastin and collagen is an outer layer of endothelial cells. The marginal chordae insert at the free edge of the leaflet and serves to keep the leaflet stationary. The basal chordae acts as a support for the leaflet and inserts at a higher level near the annulus. (Bronzino 1995)

Attached at the ventricular free wall and connected to the mitral valve by the chordae tendinae are two papillary muscles. The papillary muscle/chordae tendinae structure prevents mitral valve prolapse into the left atrium during systole. (Bronzino 1995)

Histological studies of mitral tissue show that the tissue is composed of three layers defined by differentiated cellularity and collagen density. The anterior leaflet can withstand greater tensile loads than its posterior counterpart indicating a difference in material structure that may affect surgical interventions in patients undergoing mitral repair. (Bronzino 1995)

Finite element models of the complete mitral complex has estimated peak principal stresses to be 5.7 x 10^6 dyne/cm^2 at the annulus, and stresses ranging from 2 x 10^6 dyne/cm^2 to 4 x 10^6 dyne/cm^2 sustained by the anterior leaflets. Other models that use force balance on a closed valve present that at least half the force of fluid flow is sustained by the chordae tendinae. (Bronzino 1995)

The mitral valve, like the heart as a whole, changes in shape during the cardiac cycle. Reduction in area of the annulus can range from 10 to 25% from diastole to systole. The reduction in area aids in the ease at which leaflets are able to seal the annulus. Translation of the annulus is also significant. The annulus moves towards the atrium, theoretically aiding in filling of the ventricle. (Bronzino 1995)

The papillary muscles have been shown not to move significantly despite the movement of other heart structures. The papillary muscles are responsible for maintaining proper mitral valve positioning and any significant movement might cause prolapsed of the valve and regurgitation of blood. (Bronzino 1995)

2.5.2 Flow profile through the mitral valve

Blood flows through the mitral valve when pressure in the left atrium is greater than the pressure in the left ventricle. The flow profile at the annulus during this period is slightly skewed and not flat.

Active relaxation of the left ventricle maintains the positive pressure difference across the mitral valve and accelerates filling. The flow velocity curve during this period of active relaxation of the ventricle is termed the E-wave. The primary filling phase of transmitral flow reaches peak values between 50 to 80 cm/s before decelerating when the ventricle ends its period of relaxation. A secondary acceleration of fluid occurs through the mitral orifice when the atrium contracts during late diastole called the A-wave. The late diastolic contraction of the atrium produces flow velocities about 2/3 the amplitude of the E-wave. (Bronzino 1995)

2.5.3 The tricuspid valve

The tricuspid valve is larger and more structurally complicated than the mitral valve. The tricuspid valve has a total of three leaflets: an anterior, posterior, and septal leaflet. The separation of valve tissue leaflets is less pronounced than the separation observed in the mitral valve. Leaflet surface appearance is similar to that of the mitral leaflets except that the basal zone is present in all tricuspid leaflets. (Bronzino 1995)

In addition to having three leaflets, the tricuspid valve has three papillary muscles. It is significant to note that it is common that the eseptal papillary muscle is absent; making the valve only have a total of two papillary muscles. (Bronzino 1995)

The flow profile at the tricuspid annulus is similar to that of the mitral annulus except that the peak velocity is lower due to the larger area of the tricuspid annulus. (Bronzino 1995)

2.6 Cardiac cycle mechanics

Each cycle of the heart consists of two phases: systole and diastole. Systole is the period of ventricular contraction and blood ejection, while diastole is the period of ventricular relaxation and blood filling. (Vander, Sherman et al. 2001)

2.6.1 Systole

Systole can be divided into two parts. The first part of systole is known as isovolumetric contraction. Isovolumetric contraction occurs when the ventricles of the heart are contracting, but no blood is ejected because all the valves of the heart, semilunar and AV valves are closed. Eventually, the contraction of the ventricles create a high enough pressure to open the semilunar valves and eject blood. The semilunar valves open when the pressure inside the ventricles is greater than the pressure within the aorta and pulmonary trunk. (Vander, Sherman et al. 2001)
Isovolumetric contraction acts so rapidly within the ventricles that pressure increases to a point that almost instantaneously ventricle pressure exceeds aortic pressure. Once the semilunar valves open, there is very little resistance to flow across the annuli leading to a very insignificant

pressure gradient value. Ejection of blood from the ventricles is very rapid at first and gradually decreases. The decrease in the strength of ejection of blood is directly correlated to the reduction in the strength of ventricular contraction near the end of systole. As the ejection weakens, the rate of blood leaving the ventricles leaving the heart is less than the rate of blood leaving the aorta and pressure in the aorta decreases. (Vander, Sherman et al. 2001)

The amount of blood ejected from the heart is called the stroke volume (SV) and averages about 70 mL. Not all blood is ejected from the heart during systole – 65 mL on average is left inside the ventricle. The leftover blood from systole is called the end systolic volume (ESV). (Vander, Sherman et al. 2001)

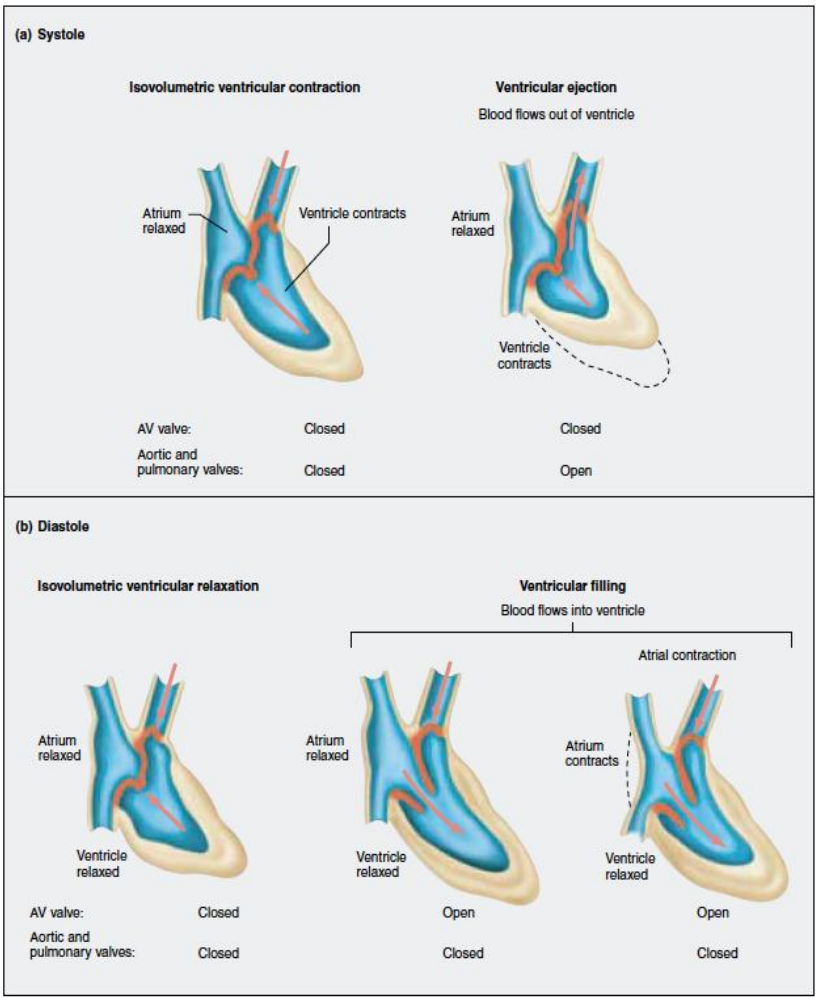

Figure 4 Visual representation of systole and diastole. (Vander, Sherman et al.)

2.6.2 Diastole

Diastole can also be divided into two parts. The first part of diastole begins at the time when the ventricles relax, returning the ventricles to a lower pressure than the aortic and pulmonary trunk that they empty into and closing the semilunar valves. The AV valves are closed at the beginning of the relaxation phase of diastole, meaning that this phase is a period of isovolumetric relaxation since no blood is allowed to enter the heart's chambers. The AV valves re-open once the pressures of the ventricles are lower than the pressure exerted by the blood flowing into the atria commencing the start of the second phase of diastole. Diastole ends when the atria contract to assist in the timely filling of the ventricles. (Vander, Sherman et al. 2001)

The ventricle recoils outwards as the once compressed fibers of the ventricles expand and lowers the overall ventricular pressure. The fibers of the heart act like springs that store potential energy that is released upon the end of contraction. The recoiling of the ventricle enhances ventricular filling. The rapid filling of the ventricles during diastole means that the ventricles are filled even during times when the heart is beating much more rapidly than at rest. When the heart reaches a rate of 200 beats/min, the ventricles are no longer able to be fully filled. (Vander, Sherman et al. 2001)

2.6.3 Heart performance and efficiency calculation

Cardiac output (CO) is the term used to describe the amount of blood pumped by each ventricle per minute. The left ventricle and the right ventricle have the same cardiac output despite the differences in their architecture – it must be that way or an accumulation of blood would exist on one side of the circulatory system causing catastrophic consequences. Cardiac output is calculated by the following formula $CO = SV \cdot HR$, where SV is stroke volume and HR is heart rate. A non-athlete pumps about 20 – 25 L of blood per minute. (Vander, Sherman et al. 2001)

2.6.3.1 Stroke Volume

Stroke volume is the amount of blood ejected from the heart and is related to the strength of contraction of the ventricle. The average ventricle contraction leaves some blood volume left within the ventricle. The stronger a ventricle's contraction, the less blood is left once systole is over. (Vander, Sherman et al. 2001)

The amount of stroke volume can be changed in three ways. The first way is by changing the initial volume within a ventricle at the start of systole (also known as the end-diastolic volume (EDV)).

The Frank-Starling Mechanism is the formal name given to describe the relationship between stroke volume and end-diastolic volume. An increase in the amount of blood occupying a ventricle after diastole results in an increase in contraction. The stronger contraction is a result of the increased amount of blood creating an increased tensile preload on the muscle fibers of the ventricle, creating a greater force of contraction. The Frank-Starling Mechanism kicks in when there is an imbalance of rate of blood flow between separate sides of the heart. If one side of the heart begins to pump blood at a faster rate than the other, the side of the heart with the slower rate of blood flow will demonstrate an increase in venous return, creating a higher EDV in the ventricle, instigating a stronger contraction resulting in a greater stroke volume (Vander, Sherman et al. 2001)

The second way is by input from the sympathetic nervous system. The sympathetic nervous system mobilizes the body's resources during times of stress. When greater cardiac output is required, the body can create stronger ventricular contraction that results in greater stroke volume. (Vander, Sherman et al. 2001)

The third way stroke volume can be changed is through a change in arterial pressure in which the ventricles must empty into. An increase in afterload (the pressure exerted by the arteries onto the ventricle) usually decreases stroke volume because the increased load prevents full contraction of the ventricle's muscle fibers. (Vander, Sherman et al. 2001)

2.6.4 Compliance

Compliant blood vessels would not be necessary if the same amount of blood ejected by the heart exited the arteries per cardiac cycle. In reality, only one third of the stroke volume of the heart exits the arteries and the remaining blood pools in the arteries and raises the blood pressure of the arteries by distending them. The distension of vessels demonstrates the compliant nature of the arterial system. The level of compliance of a vessel can be calculated using the following equation, $C = {dV}/{dP}$, where C is compliance, dV is change in volume, and dP is change in pressure. (Vander, Sherman et al. 2001)

2.6.4.1 Arterial Pressure

After systole, the blood exits the arteries passively as the once stretched arteries begin to contract. The decrease in the volume of blood within the arterial system lowers overall pressure, but never reaches zero because there is always enough blood within the arteries to stretch the arteries. (Vander, Sherman et al. 2001)

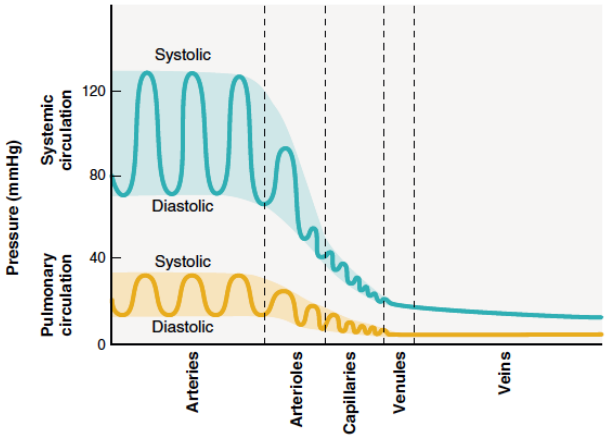

Figure 5 Arterial pressure change during diastole and systole. (Vander, Sherman et al.)

The fluctuation of pressure caused by the change in volume within the arteries creates a pattern of falling and rising pressures. The maximum arterial pressure occurs right after systole and is called systolic blood pressure (SBP). Conversely, minimum arterial pressure occurring right before diastole is diastolic blood pressure (DBP). Average max/min pressures in human arteries is 125/75 mmHg in the US. (Vander, Sherman et al. 2001)

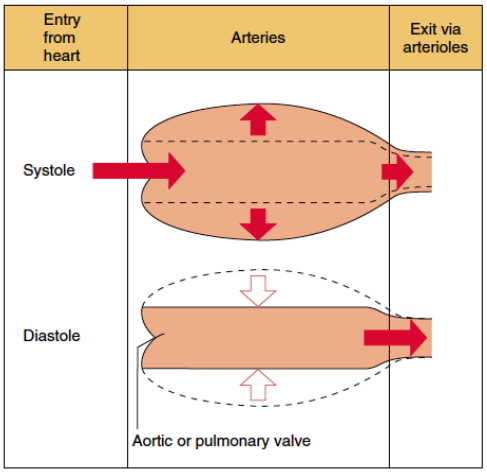

Figure 6 Model of pressure change in arteries. (Vander, Sherman et al.)

The mean arterial pressure (MAP) is the pressure that drives fluid through the body's vessels, and is related to diastolic and systolic pressures by the following equation: $MAP = DP + \frac{1}{3}(SBP - DBP)$. (Vander, Sherman et al. 2001)

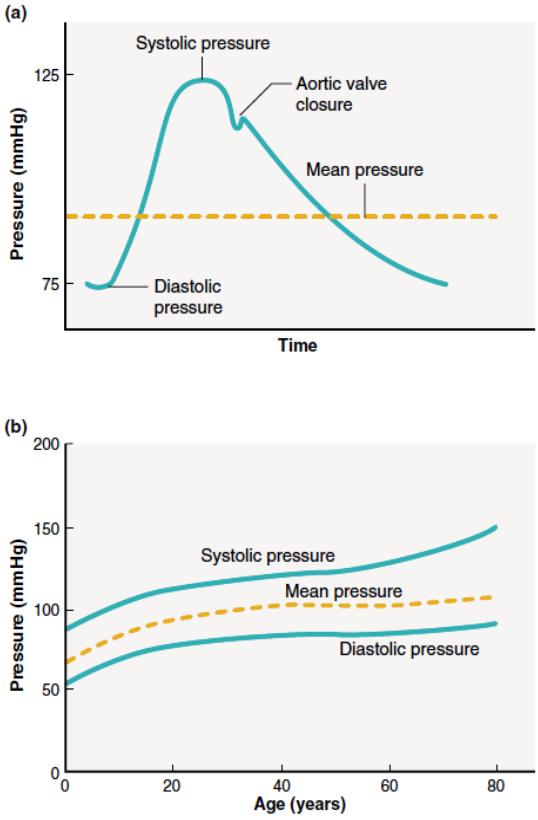

Figure 7 Explanation of Mean Arterial Pressure. (Vander, Sherman et al. 2001)

2.6.4.2 Venous Pressure

Venous pressure deviates much less than arterial pressure despite the fact that much more blood is contained within the veins than in the arteries because of the thinner walls that allow

veins to be much more compliant than arteries. The greater compliance of veins translates into an average overall venous pressure of 10 mmHg in the body despite the fact that 60% of blood is contained in veins. (Vander, Sherman et al. 2001)

2.6.4.3 Pulse

The sudden ejection of blood into the arteries after systole creates a pulse that increases in strength of pressure if stroke volume increases, arteries harden and become less compliant, or the strength of contraction of the ventricle increases. (Vander, Sherman et al. 2001)

2.6.5 Heart disease

The innocuous term heart disease in common vernacular sometimes hides the true underlying nature of what usually is a group of diseases that are disrupting adequate cardiac performance and producing troublesome symptoms for the individual being affected. (Cicala 1997)

Heart disease in reality is often caused by an underlying condition that targets cardiovascular performance in one specific area and then spreads to another over time. The ability for problems to spread across the system is a consequence of how dependent each part of the cardiovascular system is dependent on all the other parts to function properly. (Cicala 1997)

A common underlying condition of heart failure is arteriosclerosis; a condition where the hardening of arteries outside of the heart, acts to make the heart work much harder to pump blood (the overall mechanisms of how arteriosclerosis works to cause heart failure will be described later). The improper functioning of the arteries leading to heart failure illustrate how disease can spread from one area of the cardiovascular system to another causing greater complications for the system as a whole. (Cicala 1997)

2.6.5.1 Congestive heart failure

Congestive heart failure is also known as the “final common pathway” for untreated circulatory system diseases. Untreated diseases like valvular disease, coronary heart disease, or

hypertension will influence heart malfunction through different means that will eventually result in the same end; the heart will not be able to pump enough blood to the rest of the body. Congestive heart failure is known to those it affects through the symptoms that include fatigue, shortness of breath, and swelling. The symptoms of congestive heart failure are what the public often mistakenly refers to as the actual disease, which is part of the problem in understanding what heart disease actually is. (Cicala 1997)

2.6.5.2 Valvular disease

Valvular disease refers to the improper functioning of the valves of the heart for various reasons. For individuals who have mild versions of valvular disease, undergoing thorough examination by a trained physician is usually the only way to diagnose the problem. Valvular disease will often be diagnosed by a doctor when an abnormal sound known as a murmur signals the malfunctioning of a valve initiating further investigation. (Cicala 1997)

A mild problem with a heart valve can take years to grow to become congestive heart failure because the heart is able to adjust its own performance to make up for problems with the valve. Problems with other parts of the cardiovascular system that force the heart to work even harder together with mild valvular malfunction is usually what causes the heart to weaken. (Cicala 1997)

The regularity of valvular disease is not clearly defined in the medical world. While almost one in twenty persons have a mild congenital form of what is known as mitral valve prolapse (the mitral valve does not cover the annulus completely), only one in half a million people suffer from valvular disease that affects adequate pumping to the body by the heart. Diseases of the valves are named by identifying the affected valve and whether the valve is stenotic (narrowed) or regurgitant (leaking). Mitral valve stenosis is an example of the nomenclature for a given valvular disease. (Cicala 1997)

Common causes of valvular disease include congenital defects (a malformation during fetal development), calcium deposits that form as people age, and valvular infections. Less commonly, the deterioration of valvular supportive tissue (the valve no longer seals tightly due) as well as aortic aneurysm (the dilated aorta is too wide for the aortic valve to cover sufficiently) can also cause disease of the valves. Valvular disease affecting the left side of the heart is a much more serious problem than disease of valves on the right side due to the much higher pressure loads that must be withstood on the left side of the heart. (Cicala 1997)

Congenital defects found in valves are usually only one part of a larger set of abnormalities; also known as a syndrome. Congenital abnormalities that accompany valve defects also include holes between heart chambers or unusual formation of large blood vessels. (Cicala 1997)

Developmental malformations in the aortic and pulmonary valves are the most common congenital valvular diseases. The malformation of the semilunar valves allows for stenosis, and requires surgical intervention if severe in babies. Mild cases of stenosis may not be noticed until a person matures, but by this time a person living in the United Stated is usually aware of possible complications in health. (Cicala 1997)

Rheumatic fever and infectious endocarditis are two infectious diseases that can cause disease of the heart valves. Rheumatic fever is caused by the same strain of bacteria that causes strep throat and can infect the heart valves if improper treatment allows for spreading of the bacteria to the heart. The bacteria cause inflammation of the lining of the heart and heart valves, almost always in the mitral valve, and half of the time in the aortic valve. In one out of four cases the patient suffers permanent damage that depletes heart function very slowly. It is usually after decades that a person's symptoms necessitate surgical intervention at the valves. (Cicala 1997)

Infective endocarditis is a much more severe complication that is life threatening to those who contract it. Endocarditis is an actual infection, not just an inflammation, which requires intravenous antibiotics to treat. The bacteria that infect the valves may only cause slight damage,

but the damage may worsen over time. Severe infections that destroy one or more valves require surgery, but only after the infection has been cleared from the bloodstream. (Cicala 1997)

Stenotic valves can be caused in many ways – heart attack, congestive heart failure, aging, or cardiac/aortic aneurysm. In all cases, the support structures of the valve stiffen and the valve loosens resulting in valvular disease and allowing for regurgitation of blood. (Cicala 1997)

Mitral stenosis is caused most often by Rheumatic fever, and less frequently by the aging process that results in the calcification of the valve. Severe cases of mitral stenosis cause a backup of blood in the left atrium, distending the atrial wall. The atrium in turn attempts to compensate for the overfilling over time by thickening so that it can pump blood more forcefully. An enlarged left atrium may inherit rhythm irregularity known as atrial fibrillation where the atrium no longer contracts. Eventually, blood backs up through the pulmonary vein and into the lungs causing pulmonary edema. Pooled blood in the atrium can also clot. If a small piece of the clot in the atrium breaks off into the bloodstream, it could lead to infarction in some other region of the body. (Cicala 1997)

Mild mitral stenosis usually allows for normal heart function with no symptoms. It is not until the disease progresses and causes pulmonary edema where a person suffers shortness of breath when lying down or awakes from sleep because of shortness of breath does a person suffer from symptoms of mitral stenosis. (Cicala 1997)

In the case of backflow of blood through the mitral valve, known as mitral regurgitation, the heart compensates by enlarging. The onset of symptoms only occurs after many years and is similar to those observed with mitral stenosis. Fatigue, weakness, shortness of breath, and eventually pulmonary edema are all symptoms of mitral regurgitation. (Cicala 1997)

The enlarged heart that results because of mitral regurgitation is due to the decrease in the amount of blood flowing out to the body. The decrease in cardiac output causes the heart to compensate by having to work harder. The left atrium actually enlarges because of mitral

regurgitation because it has the extra load of having to push extra blood that has leaked from the ventricle during systole back into the ventricle during each heart cycle. (Cicala 1997)

Aortic stenosis is commonly caused by the aortic valve only having two leaflets. A bicuspid aortic valve becomes stenotic more easily because it more easily calcifies. Aortic stenosis causes the left ventricle to undergo hypertrophy to generate the much higher pressures that the diseased valve imposes on the ventricle to force blood into the body. Eventually the left ventricle hypertrophy leads to congestive heart failure with all its aforementioned symptoms. (Cicala 1997)

Aortic regurgitation can also be caused by a bicuspid aortic valve or a widening of the aorta over time. The left ventricle enlarges to compensate for the extra blood that must be contained because of the backflow of blood re-entering the ventricle from the aortic sinus. The greater force to pump the extra blood also requires the heart to enlarge, leading again to congestive heart failure. (Cicala 1997)

While the right side of the heart more easily tolerates valvular disease than does the left side because of the lower pressure load placed upon the right side, stenosis and regurgitation of the pulmonic and tricuspid valves still exist and arise by similar pathways as valvular disease on the left side of the heart. (Cicala 1997)

High blood pressure, also referred to as hypertension, is a disease where higher resistance in the arteries raises the afterload that the heart must force blood into. In the United states, the upper limit of normal blood pressure is 140/90 mmHg, whereas for people under the age of 45 130/90 mmHg is usually the norm. The norm was decided through thorough clinical studies where blood pressures higher than “normal” levels were 50% more likely to result in death from complications resulting from hypertension. (Cicala 1997)

Hypertension has widespread negative affects across the body, but in terms of the heart and circulatory system, hypertension causes hypertrophy of the heart leading to congestive heart failure. The increased afterload resulting from higher arterial pressure forces the heart to work

harder and enlarge . Eventually the enlargement of the heart leads to congestive heart failure. (Cicala 1997)

2.7 Early lumped parameter modeling overview

Numerous mathematical models of the human cardiovascular system (CVS) have appeared in literature since Womersley in 1957 analyzing blood flow in elastic vessels. (Womersley 1958) CVS models vary considerably in complexity, ranging from simple models that take into account resistance and compliance to complex multisegmental representations of the vascular tree. Simplified descriptions of the CVS with lumped parameters often form part of a model of a larger physiological system. (Elstad, Toska et al. 2002)

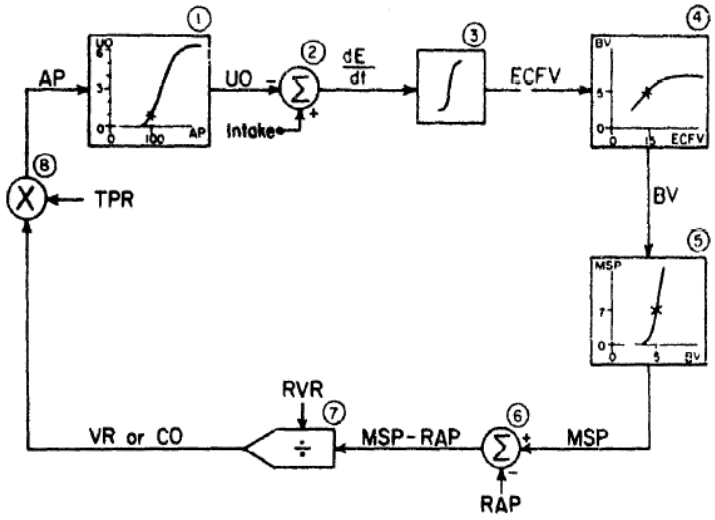

Figure 8 Example of a lumped parameter CVS model. (Guyton, Coleman et al.)

The Guyton model of overall circulation (Figure 9) is an example of a lumped parameter model and is one of the most well-known. (Henderson, Griesdale et al. 2010) The Guyton model includes a three compartment representation for the CVS function that allows for the calculation of mean values of CVS variables. More elaborate mathematical models of the CVS are intended to provide a better understanding of the pressure-flow relationship in the system and how they are affected by external stimuli. (Melchior, Srinivasan et al. 1992)

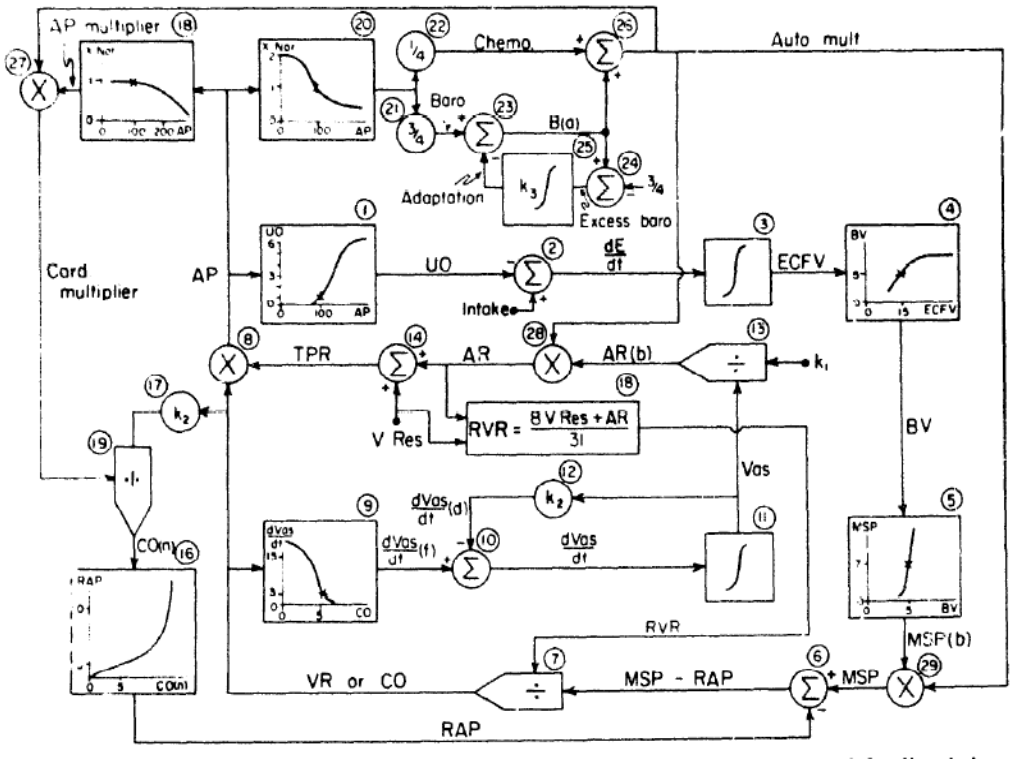

Figure 9 Example of a complex lumped parameter model with variables for local vascular control, nervous control, and pumping function. (Guyton, Coleman et al.)

Advancement in computation allowed for the modeling of transient physiological phenomena. (Terkildsen, Montani et al. 2009) Advancement in computation only tells part of the story of how physiological models have become so abundant in literature. Physiological phenomena are computationally easier to model because of the passive affect that million years of evolution have on the stability of even poorly designed models. Much of the hard programming that is necessary in other types of dynamic modeling is not present when creating physiological models because of the millions of years of evolution that have created stable systems with feedback loops that can be trusted to work. (Montani and Van Vliet 2009) The safety factor created by evolution ensures that even poor models can provide significant insight into physiological functioning. (Guyton, Coleman et al.)

Physiology is itself an attempt to explain how the body functions. (Berne and Levy 2001) Physiology therefore is inclusive of all types of modeling that explains mechanical functioning.

(Montani, Adair et al. 1986) Before computation, most physiological modeling was qualitative. In the 1940's and 50's, the first computational models were based on algebraic and graphical analysis. Equations or intersecting graphical curves were used to analyze steady state function, and rarely differential equations were used to map physiological processes. Analog computing in the 50's and 60's allowed for more sophisticated modeling. (Guyton, Coleman et al.)

Sophisticated CVS models consist of two major parts: the hemodynamic system and autonomic nerve control. (Lu, Clark et al. 2001) The hemodynamics of vessels can be represented by the relationship between blood pressure and blood flow rate in the vascular system. In the lumped model, hemodynamic parameters of the CVS are expressed as a series of equivalent elements in an electric circuit (Figure 10).

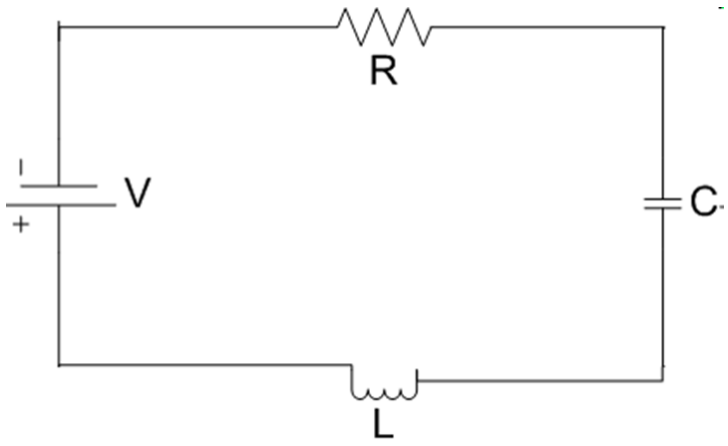

Figure 10 The cardiovascular system represented as an analogous electrical circuit.

The application of Kirchhoff's voltage law to each node in the lumped parameter hemodynamic model leads to the following differential equation for mass conservation in steady-state flow: change in volume over time (L/min) equals $\frac{dV}{dt} = Q_{in} - Q_{out}$ where flow rate (L/min) $Q = \frac{P_{in} - P_{out}}{R}$, P is pressure (mmHg), and R is resistance. (Shim, Sah et al.) In the model above in Figure 10, only one set of equations would be necessary to model for blood flow through the circulatory system since there is only one series of RLC components to pass through.

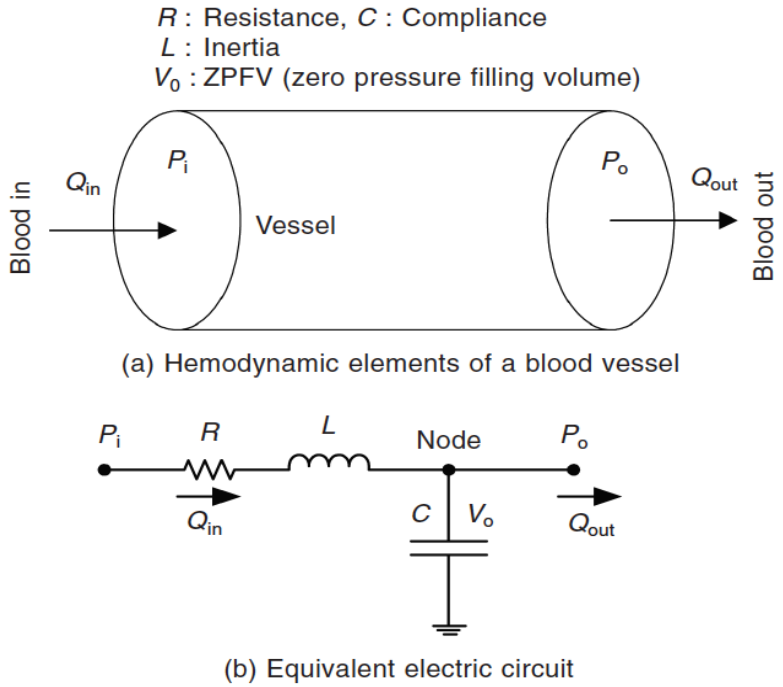

Figure 11 Example of the hemodynamic elements represented as an equivalent electric circuit. (Shim, Sah et al.)

The circuit analog hemodynamic representation makes it so that L which represents inductance in electrical circuit models comes to represent the inertia (fluid density), R describes fluid friction effects, and C is the ability of a vessel to distend and hold fluid. (Fung 1984)The lumped parameter model works by obtaining a new volume from the differential equation already described, and then calculating pressure using the equation (again assuming steady flow) $P = {}^{V}/_{C}$.The application of this formula for pressure to other nodes in the CVS moel enables the solution of lumped information of the cardiac hemodynamics. (Shim, Sah et al.)

2.7.1 The Grodins lumped parameter model

The Grodins model is cited as the first significant lumped parameter model of the CVS. (Wolf and Garner 2007) The model exists as a feedback loop where medullary cardiac and vasometer centers and endocrine glands control the behavior of the heart and arterial network. The outputs of blood flow from the various nodes of the CVS are fed back to the controllers of the CVS and determine the input of the lumped parameter values. (Grodins)

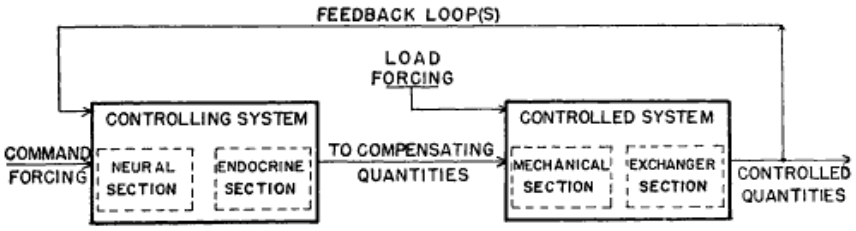

Figure 12 The Grodins full lumped parameter model. (Grodins)

The controlled system in the Grodins model includes the mechanical section, for which the heart and arterial network fall under. Formulation of heart function are defined by equations that determine steady-state heart function for one ventricle at a time. Each ventricle pumps into its own circuit, the pulmonary or the systemic, which are then combined to form the circulatory system. (Wolf and Garner 2007)

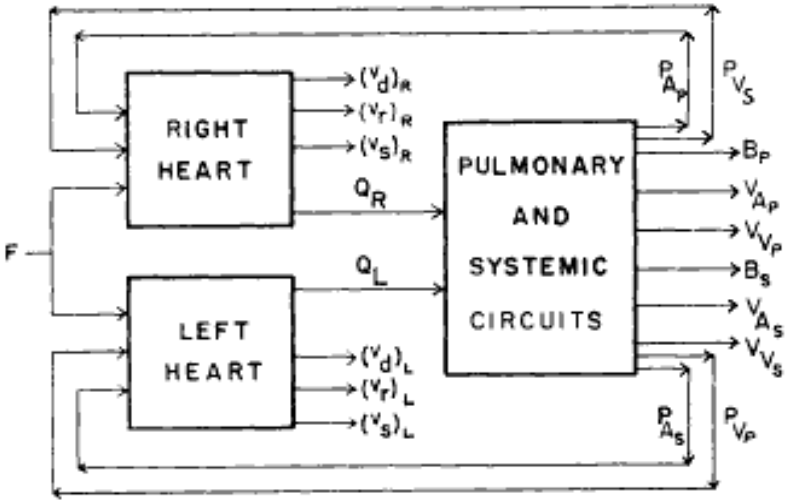

Figure 13 Lumped parameter model of the heart and arterial network made by Grodins. (Grodins)

The Grodins lumped parameter heart model requires pressures inputs from the arteries (the afterload, P_{As}) and veins (P_{Vp}) and outputs diastolic volume (v_d), stroke volume (v_s) and residual volume (the volume of blood left in the ventricle after systole, v_r). The heart model contains no atria. At the beginning of the heart cycle, the heart contains a volume of blood (v_d), then ejects a volume (v_s) against the afterload (P_{As}), with some blood leftover in the ventricle quantified as v_r. The filling of the heart is modeled by assuming the heart with visco-elastic material properties so that compliance of the heart is non-linear. The diastolic volume of the heart

is derived from a first order differential equation resulting in the equation $v_d = CP_V + (v_r - CP_V)e^{-t/RC}$ where R is viscous resistance, C is ventricle compliance, t is time, and P_V is venous pressure. The mean volume flow rate of blood through a given circuit is calculated using the application of Kirchhoff's laws denoted above where $Q = Q_A - Q_V$ where Q_A is the flow of blood through arteries and Q_V the flow through veins. Mean arterial blood pressure was then calculated using $P_A = {}^{V_A}/_{C}$. (Grodins)

2.7.2 Variations on heart modeling

Variations upon the lumped parameter model originally presented have trickled through literature since the 50s. (Shi, Lawford et al. 2011) Much of variation stems from the sub-modeling of the heart that is coupled to circulation. (Avolio 1980) As noted in the description of the Grodins model above, the heart was only functioned with two ventricles with a time-varying compliance. (Bodley 1971)

A lumped parameter model authored by Liang, similar in design to the Grodins' model, uses a 4 chamber time-varying elastic heart along with aspects of the circulatory system that are elastically time-varying as well. (Liang and Liu)

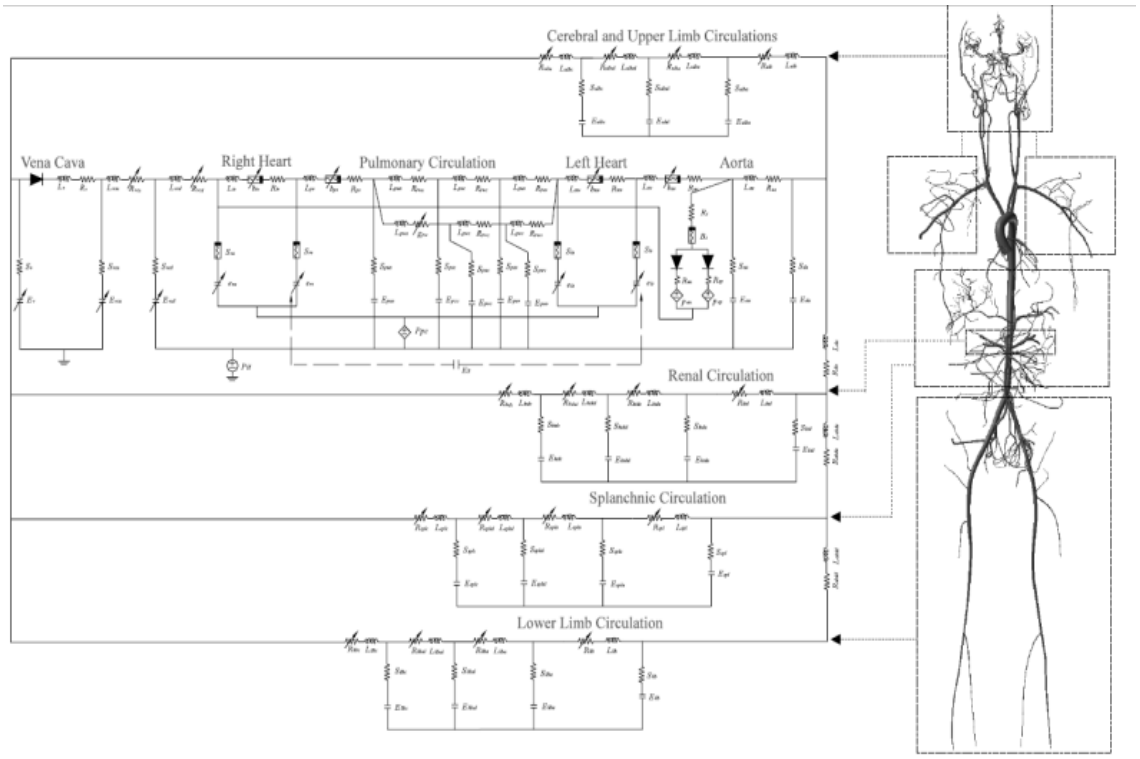

Figure 14 Electrical analog of the Liang lumped parameter CVS model. (Liang and Liu)

The Liang model uses a fourth order Runge-Kutta method to get solutions for blood flow and blood pressure. The governing equations at the nodes are formulated in the following way using the node configuration shown in Figure 15:

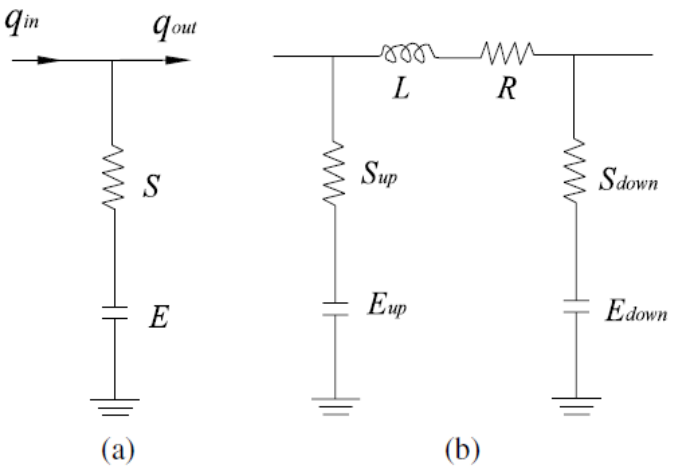

Figure 15 Illustration of node configuration within the analogous electrical wire model of the cardiovascular system. (Liang and Liu)

At node E: $\frac{dv}{dt} = q_{in} - q_{out}$, and at node L: $L\frac{dq}{dt} = C_{up}V_{up} + S_{up}\frac{dv_{up}}{dt} - qR - S_{down}V_{down} + R_{down}\frac{dv_{down}}{dt}$. The Liang model does not assume steady flow with the inclusion of the inertial term ($L\frac{dq}{dt}$) and actually includes a term for vessel viscoelastance ($S\frac{dv}{dt}$) unlike the Grodins model. (Liang and Liu)

Heart mechanics in the Liang model uses a time-varying elastance equation that is later used to calculate chamber pressure. Instantaneous elastance is calculated using the formulas for left atrial and ventricular elastance:

$$e_{lv} = \begin{cases} E_{lva} \cdot F_s \cdot \left(1 - e^{-t/\tau_{lvc}}\right) \cdot \dfrac{1 - e^{-t_{s0}/\tau_{lvc}}}{1 - e^{-t_s/\tau_{lvc}}} \\ \quad + E_{lvb}/F_s \\ \left(e_{lv}\big|_{t_s} - E_{lvb}/F_s\right) \cdot e^{-(t-t_s)/\tau_{lvr}} \\ \quad + E_{lvb}/F_s \end{cases} \begin{array}{l} 0 \le t \le t_s \\ \\ t_s < t < t_r \end{array} \qquad e_{la} = \begin{cases} E_{laa}\left(1 - e^{-(t-tac)/\tau_{lac}}\right) \\ \quad + E_{lab} \\ \left(e_{la}\big|_{t_{ar}} - E_{lab}\right) \cdot e^{-(t-t_{ar})/\tau_{lar}} \\ \quad + E_{lab} \end{cases} \begin{array}{l} t_{ac} \le t \le t_{ar} \\ \\ t_{ar} < t < (t_r + t_{ac}) \end{array} \quad (3$$

The subscript lv and la stand for left ventricle and left atrium, repectively. The subscript ar, ac, vr, and vc all refer to atrial relaxation, atrial contraction, ventricular relaxation, and ventricular contraction, respectively. The variable definitions are as follows: E (elastance), F (a scaling factor for myocontractility relating to Starling law), t_s adnd t_r denote the moment of the peak systolic elastance and a cardiac cycle, respectively. Left ventricular pressure is than calculated using the following formula taking elastance into account: $p_{lv} = E_s \cdot \frac{e_{lv}}{E_s + e_{lv}} \cdot v_{lv} + \frac{e_{lv}}{E_s + e_{lv}} \cdot p_{rv}$, and similarly for left atrial pressure. (Liang and Liu)

Suga found that if a pressure of a number of beats is plotted against volume while pre- or afterload of the heart was varied, points of different cardiac cycles that occur at the same time in the cardiac cycle can be connected to form isochrones. (Lankhaar, Rovekamp et al.)

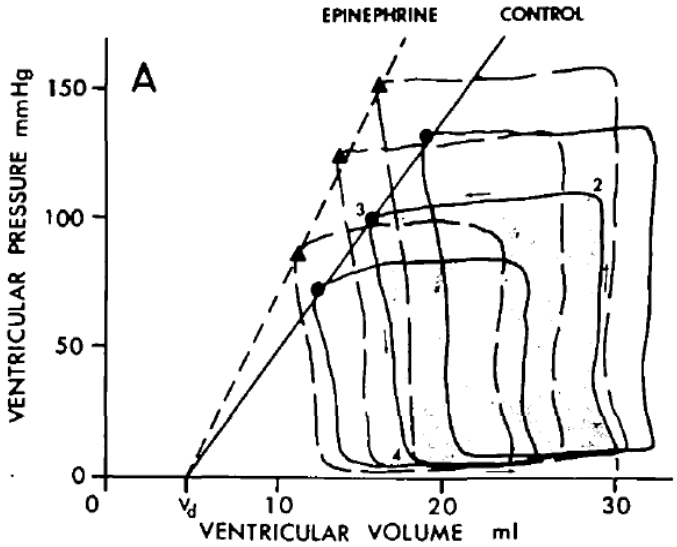

Figure 16 P-V diagrams with an isochrone connecting different cardiac cycles. (Suga, Sagawa et al.)

Suga used isochrone to conclude that time-varying elastance of the left ventricle could be calculated using the following formula: $E(t) = \frac{P(t)}{(V(t) - V_d)}$, where E(t) is instantaneous elastance, P(t) is instantaneous pressure, V(t) is instantaneous volume, and V_d is an experimentally determined volume correction factor. (Suga, Sagawa et al. 1973) Suga's research into the basic P-V relationships within the left ventricle found that P-V curves of the left ventricle were similar in their basic shape and attained their peak near the end of the ejection phase regardless of mechanical load, contractile state, or heart rate. Furthermore, under a constant heart rate and contractile state extensive changes in preload, afterload, or both did not alter the peak value of elastance with respect to the timing of systole, but contractility was very susceptible to the effects of sympathetic nervous input of epinephrine. (Funai and Thames 1988)

Since the conclusion of linearity of isochrones in left ventricular elastance was made by Suga et al., the idea of similarity of shape in the pressure volume curve has been studied extensively and has given birth to more variations in the way time-varying elastance is modeled for the heart. (Lecarpentier, Chuck et al. 1979) The variations in modeling of elastance of the

heart is primarily due to research that has concluded that isochrones are parabolic, logarithmic, or even sigmoidal in relation (Lankhaar, Rovekamp et al.)

The linear model with free intercept (LinFree) is the same as the original Suga model for elastance except now the correction factor V_d is allowed to vary with time so that the new formula for elastance looks like this: $E(t) = \frac{P(t)}{(V(t) - V_d(t))}$. (Lankhaar, Rovekamp et al.)

The Langewouters model results in tangentially curved isochrones because of its formulation: $P(t) = P_0(t) + \frac{P_1(t) tan\pi(V(t) - \frac{1}{2}V_m)}{V_m}$. Originally derived to describe pressure-area relations of arteries, it can also be used to describe the pressure volume relation of the left ventricle. In the formula, V_m represents the maximum volume of the left ventricle. (Langewouters, Wesseling et al. 1984)

The sigmoidal model (S-shaped curve) uses the following PV-relation: $P(t) = A(t) \frac{\left[V(t)/V_{ref}(t)\right]^{\alpha(t)}}{1+\left[V(t)/V_{ref}(t)\right]^{\alpha(t)}} + B(t)$. (Claessens, Georgakopoulos et al. 2006) For the sigmoidal model, A(t) is an amplitude and B(t) a vertical offset. For a given time t, the function is enclosed by two horizontal asymptotes at B and A + B. The bending point of the curve is found at $V = V_{ref}$ and at P = B + A/2. The slope of the curve is proportional to α. (Lankhaar, Rovekamp et al.)

The Shroff model uses evidence from studies that left ventricular PV-relation is a function of systolic resistance. Time varying elastance is modeled as $E(t) = \frac{P(t)}{(V(t) - V_d(t))(1 - \rho \dot{V(t)})}$. In the Shroff model ρ is a fixed resistance proportionality factor and $\dot{V(t)}$ is the instantaneous ventricular outflow. The Shroff model is the same as the Suga model when outflow is equal to zero. (Lankhaar, Rovekamp et al.)

The Burkhoff model for heart-arterial interaction combines an exponential diastolic model for pressure with a linear elastance systolic model which creates isochrones in a smoothly defined transition area between both models. (Burkhoff, Detombe et al. 1993) The systolic model

looks like the following: $P_{es}(V) = E_{max}(V - V_d)$with $P_{es}(V)$ equaling end-systolic pressure, E_{max} being maximum elastance, and V_d the same as it was in the Suga model. The end-diastolic pressure-volume relation is defined as $P_{ed}(V) = A\left(e^{B(V-V_d)} - 1\right)$ where A and B are constant parameters. (Burkhoff, Mirsky et al. 2005)The weighted sum of the end-diastolic and end-systolic pressure-volume models are used to create the isochrones with the equation $P(V,t) = \alpha(t)P_{es}(V) + \left(1 - \alpha(t)\right)P_{ed}(V)$where α(t) is a weight factor with range between 0 and 1. α(t) values are compiled from a fifth order polynomial where $\alpha(t) = a_1t^5 + a_2t^4 + \ldots + a_5t + a_6$ with the limit that α(t) reached 1 at the time of maximum elastance and that α(t)=0 whenever the cardiac cycle was in a period before end-systole and when t = 0. (Lankhaar, Rovekamp et al.)

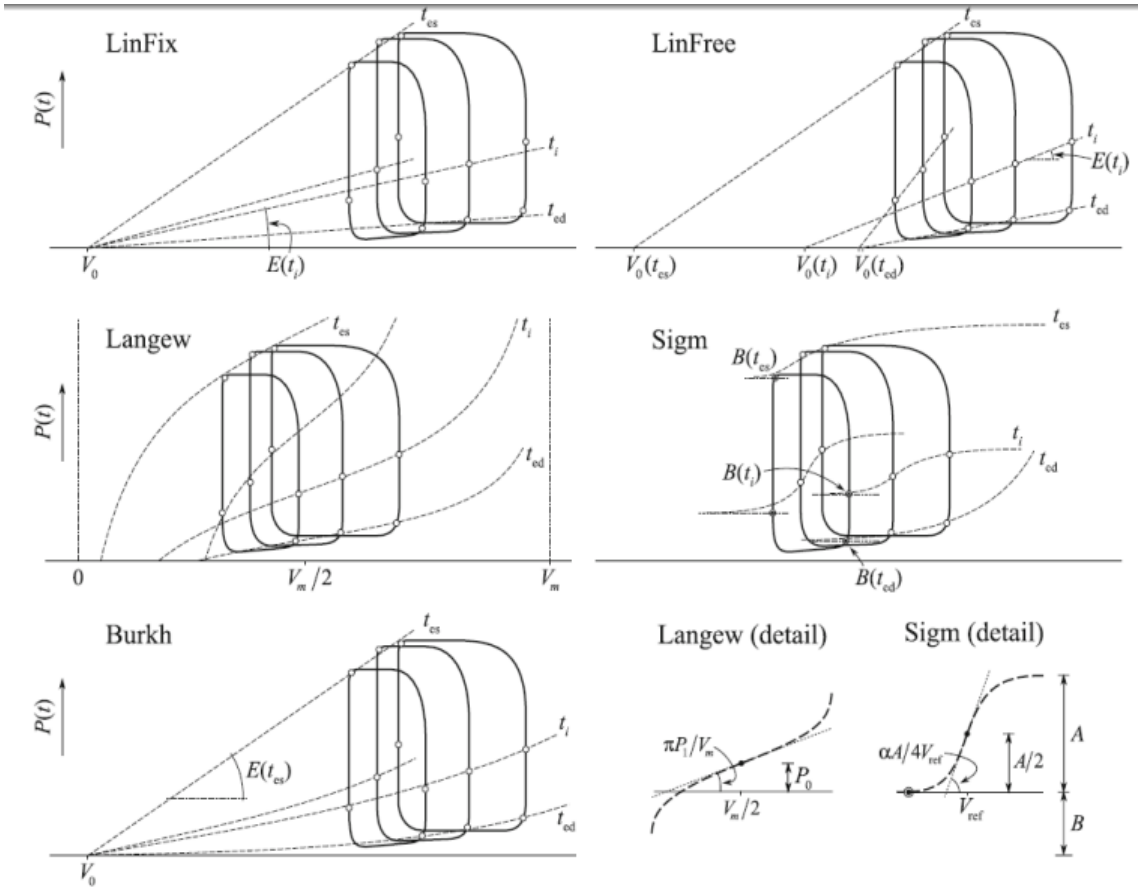

Figure 17 Comparison of five different heart models with the resulting isochrones from each model. (Lankhaar, Rovekamp et al.)

The PV diagrams fit to six different statistical models in Figure 17 are meant to show the level of sophistication that is present in literature as researchers attempt to improve the understanding of how the heart reacts to outside physiological inputs. While level of sophistication has improved to include complicated statistical modeling, it should be noted that the most widely adopted of the isochrones fitting methods is still the LinFree model because of its simplicity.

2.7.3 The evolution of the PV-relationship

Although presented more than a century ago, the pressure-volume relationship of the heart was not accepted widely until the mid-1970s when the PV-diagram was shown to be a good representation of ventricular mechanics. In the early 1980s, ventricular interaction was coupled with afterload relating to arterial elastance and a more effective model of the heart's pumping ability was created. A model of circulatory equilibrium was achieved when ventricular-arterial interaction was coupled with Guyton's circulatory equilibrium in the 2000s. (Sunagawa)

The first known study of the PV-relationship was done by Otto Frank in 1899 (Die Grundform des arteriellen Pulses) which characterizes a frog ventricle's PV-relation. (Noordergraaf, Verdouw et al. 1963) Physiologists and cardiologists did not accept the marked loading history dependence of the end-systolic PV-relation (ESVPR). (Sunagawa)

Later study by Sunagawa in the 1970s found that the ESVPR was linear and insensitive to loading conditions and lead to the theory of isochrones which lead to a greater acceptance of the PV-diagram as an effective tool for explaining ventricular mechanics. The systolic PV-diagram area as a measure of total mechanical area released per contraction was one useful consequence of the acceptance of the PV-diagram. (Sunagawa)

Guyton established that cardiac output is determined as the equilibrium between venous return and cardiac output. In the Guyton framework, the intersection of the systemic venous return curve with the cardiac output curve of the right atrium determined circulatory equilibrium. The concept of determining circulatory equilibrium in the manner performed by Guyton allowed

for a deepened understanding of how the cardiovascular system reacted under varying conditions like hemorrhage and exercise. (Uemura, Sugimachi et al.)

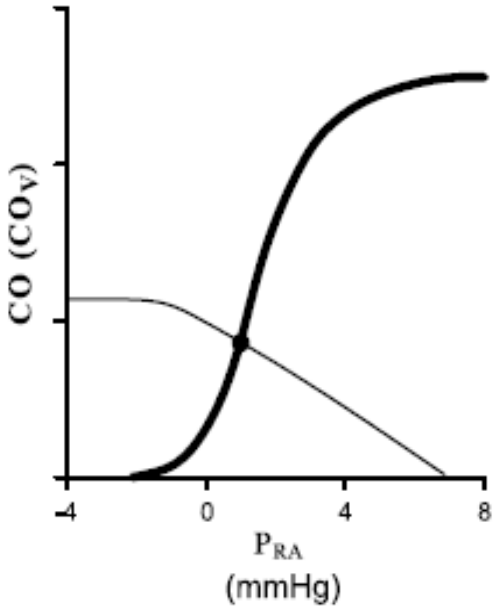

Figure 18 The calculation of circulatory equilibrium using systemic a venous return curve (thin line) and a curve for right atrial cardiac output (thicker line). (Uemura, Sugimachi et al.)

The Guyton methodology for calculating circulatory equilibrium in a clinical setting is complicated because it is an iterative process that uses a somewhat unrealistic two compartment model of the heart (the Guyton heart only has a left and right chamber). (Paredes, Rocha et al. 2011) A newer model developed by Sunagawa et al., the venous return properties of the systemic and pulmonary circulations are integrated so that an equilibrium can be found within the total cardiovascular system. The Sunagawa model uses a linearized model that creates a flat surface venous return surface as a function of venous return (CO_V) for a given stressed volume (V) and right and left atrial pressure. The formulation for the venous return surface is as follows: $CO_V = {}^{V}/_{W} - G_S P_{ra} - G_P P_{la}$, where W is a parameter that defines maximum venous return for the given stressed volume and G_S and G_P are slopes of venous return with respect to the left and right atrial pressures (P_{la} and P_{ra}). (Uemura, Sugimachi et al.)

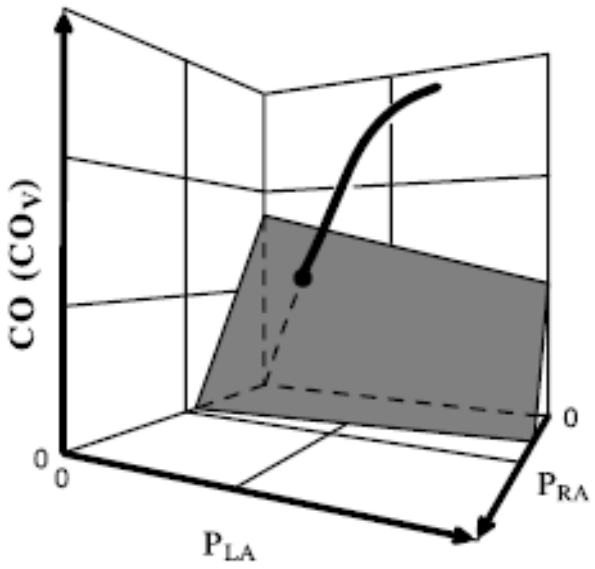

Figure 19 Model of circulatory equilibrium by Sunagawa et al. that implements a flat venous return surface. (Uemura, Sugimachi et al.)

2.8 Final thoughts on lumped parameter modeling literature review

The history of lumped parameter modeling of the cardiovascular system is dominated by attempts to accurately simulate flow and pressure drops occurring in physiological and pathophysiological cases throughout the system. The main goals of the types of modeling reviewed are to understand how the heart adapts to changing inputs from signals given by the body and diseases – goals that are intrinsically different than the goals of the project set forth in this research project.

This research project aims to use a lumped parameter model to directly calculate energy cost in physiological and pathophysiological cases. To calculate energy cost, physiological simulations of flow and pressure change across the cardiovascular system is necessary, but accurate simulation of how the system responds to changing inputs representing diseased cases are not. In fact, a different method is required to calculate energy cost of a working heart.

The different method required is that instead of allowing the heart to remodel its operation when affected by normal or diseased conditions, the heart is instead required to maintain its standard operating parameters – meaning that it will remain outputting the same amount of blood at the same heart rate. Requiring the heart to maintain a standard output even when faced with diseased input parameters creates a situation where workload, and only workload, will vary so that the heart can meet its output demands. The variation in workload that results in this modeling method gives some understanding of why the heart compensates the way it does under diseased conditions, not how it compensates.

The workload analysis performed in the model developed for this project is a novel approach not seen in literature on how to apply lumped parameter modeling to the cardiovascular system. The approach used with the model developed can be used to directly understand the severity of a disease's impact on the heart through the extra workload that the disease causes, not by changes in pressure and flow that have been proven to be unreliable in real patient cases.

In developing the model for this research, a similar model was thoroughly investigated and almost used to directly calculate workload. The Korakianitis and Shi model, referred to as the KM in later chapters was a model that showed great potential in being able to provide direct workload calculation of simulated cardiovascular system operation. The KM was developed for the purpose of studying the response of the heart when affected by the introduction of a ventricular assist device (for more background information on the model, please see Korakianitis, T. and Y. B. Shi (2006). "Numerical simulation of cardiovascular dynamics with healthy and diseased heart valves." Journal of Biomechanics **39**(11): 1964-1982.). Unfortunately, the KM needed to be modified to provide accurate physiological representation of cardiac operation, the modification. Chapter 3.2 tells the story of why and how the KM was modified for the purpose of this research.

3 MATERIALS AND METHODS

3.1 Introduction

Initially, a CVS LPM by Korakianitis and Shi was adopted as a potential CVS simulator that would provide a basis from which cardiac workload could be calculated. Unfortunately, the KM did not provide satisfactory numerical solutions for flow and a new model was adopted. Chapter 3.2 outlines how the KM model works and why it was not ultimately used to model cardiac simulation. Chapter 3.3 describes the new model's construction – the new aspects of the model that were developed to simulate accurate mitral and aortic flow, as well as the use of components from the KM that worked well to govern the calculation of pressure and flow through the systemic circulation loop.

3.2 The Korakianitis model

Zero-dimensional models, also known as lumped parameter models (LPMs), are collections of differential equations that can be applied to model the operation of a system. A CVS LPM allows for the calculation of pressure and flow throughout the system without complex construction of three dimensional meshes. Information concerning the geometry of the CVS in an LPM is contained within the parameters that work to define the system and the behavior of blood flow going through it.

Initially, a LPM created by Korakianitis et al. was adopted to form the initial framework of the current LPM of the CVS for this research. The Korakianitis model (KM) uses a configuration of the heart containing three main parts: the heart, a systemic circulatory system, and a pulmonic circulatory system. In Figure 20, the pulmonic circulation forms the top portion of the circuit diagram, the heart block forms the middle portion, and systemic circulation is shown at the bottom. (Korakianitis and Shi 2006)

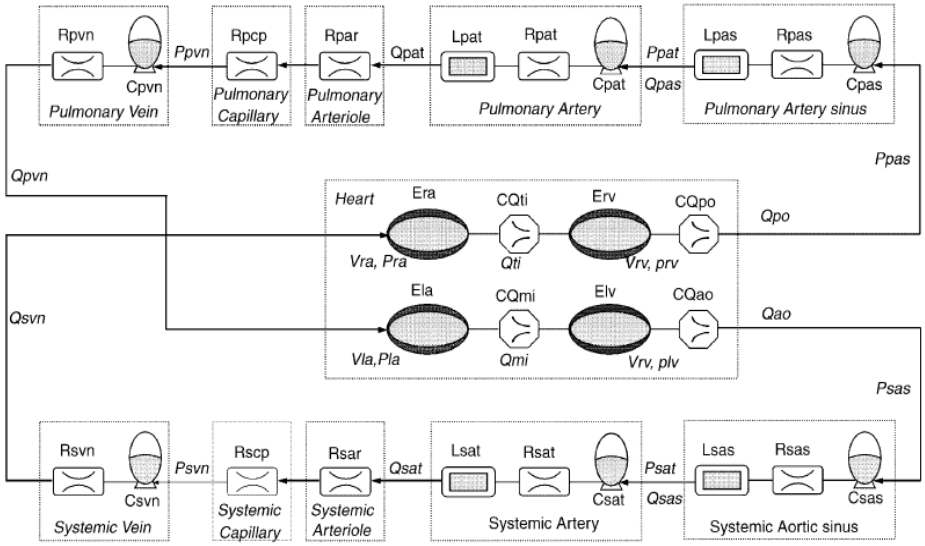

Figure 20 Schematic of the KM CVS. (Korakianitis and Shi 2006)

The heart block in the KM contains four pumping chambers and four valves. The nomenclature used to describe the different mechanisms found in the heart model are shown below in Table 2:

Table 2 Heart parameter and feature names used in the KM. (Korakianitis and Shi 2006)

Heart Nomenclature		
Parameter	*Definition*	*Unit*
E	elastance	mmHg/mL
P	pressure	mmHg
V	volume	mL
Q	flow rate	mL/s
CQ	flow resistance	mL/(s $mmHg^{0.5}$)
AR	orifice area of valve	
e(t)	elastance function	
Feature Label	*Definition*	
la	left atrium	
lv	left ventricle	
ra	right atrium	
rv	right ventricle	
ti	tricuspid valve	
mi	mitral valve	
po	pulmonic valve	
ao	aortic valve	

The pumping chambers of the KM all work the same way, with their only differences existed within the parameters that define their exact performance. Genearlly speaking, pumping chamber operation depends on a pre-defined normalized time-varying elastance function like the one shown in Figure 21. The elastance function shown in Figure 21 is for the left ventricle, with the other three pumping chambers having different elastance functions. The idea is similar for four elastance functions, each is defined by a periodic function like the one for the left ventricle shown directly below:

$$e(t) = \begin{cases} \cos\left(\frac{t}{T_{s1}}\pi\right), & 0 \le t \le T_{s1}, \\ \cos\left(\frac{t + T_{s2} - T_{s1}}{T_{s1}}\pi\right), & T_{s1} \le t \le T_{s2}, \\ 0, & T_{s2} \le t \le T\,. \end{cases}$$

The time-varying elastance functions for the ventricles of the KM operate according to the timing of the peak of systole, characterized by T_{s1}, the end of systole T_{s2}, and the length of the heart beat period T.

The normalized elasticity function is combined with maximum and minimum values of elastance found at systole (denoted by $E_{lv,s}$) and diastole ($E_{lv,d}$) to calculate the elasticity function of the left ventricle. The formula used to describe instantaneous elasticity in the left ventricle is $E_{lv}(t) = E_{lv,d} + \frac{E_{lv,s} - E_{lv,d}}{2} e(t)$.

The corresponding graph of the elasticity function is shown below:

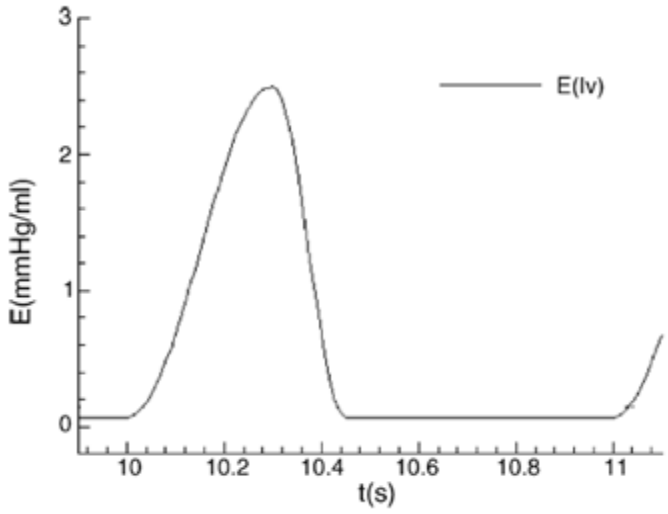

Figure 21 Graph of elasticity versus time in the left ventricle in the KM model. (Korakianitis and Shi 2006)

A volume change is calculated for the left ventricle equal to the flow rate coming into the left ventricle from the mitral valve minus the flow rate exiting the left ventricle through the aortic valve: $\frac{dV_{lv}}{dt} = Q_{mi} - Q_{ao}$. Instantaneous volume ($V_{lv}$) is calculated using a first order Taylor approximation where the solution for volume change is multiplied by the time step and added to an initial value for volume: $V_{lv,new} = V_{lv,old} + (Q_{mi} - Q_{ao})$. Pressure in the left ventricle is calculated using an initial pressure value plus the instantaneous elastance time the volume currently present in the left ventricle: $P_{lv} = P_{lv,0} + e_{lv}(t)\left(V_{lv} - V_{lv,0}\right)$.

The flow rate coming out of the left ventricle is then subject to a conditional statement. Blood flow is only allowed when pressure inside the left ventricle exceeds the pressure of the systemic aortic sinus (P_{sas}). The simple on/off nature of blood flow across the aortic valve is defined by the statement: $AR_{ao} = \begin{cases} 1, & P_{lv} \geq P_{sas} \\ 0, & P_{lv} < P_{sas} \end{cases}$. The AR_{ao} parameter which describes orifice area for the aortic valve simplistically treats the valve as either open or closed depending on whether or not the cardiac cycle is in its systolic (AR_{ao} = 1) or diastolic phase (AR_{ao} = 0). Aortic blood flow coming out of the left ventricle is calculated as $Q_{ao} = \begin{cases} CQ_{ao}AR_{ao}\sqrt{P_{lv} - P_{sas}}, & P_{lv} \geq P_{sas} \\ 0, & P_{lv} < P_{sas}. \end{cases}$ Similarly, the models for the other three pumping

chambers follow the same mode of definition as the left ventricular model. Reference to the article by Korakianitis and Shi is provided in the works cited section if exact specifications are desired.

Parameter values for the KM heart model all are time varying (elastance), or are dependent on where the model is during the cardiac cycle (pressure, volume, and flow rate, orifice area). The one value that is constant is heart valve resistance (CQ). Heart valve resistance parameters are shown in Table 3:

Table 3 Heart valve resistance parameters and values for the KM. (Korakianitis and Shi 2006)

Heart Valve Resistance			
Parameter	*Definition*	*Value*	*Unit*
CQao	aortic valve resistance	350	mL/(s $mmHg^{0.5}$)
CQmi	mitral valve resistance	400	mL/(s $mmHg^{0.5}$)
CQpo	pulmonic valve resistance	350	mL/(s $mmHg^{0.5}$)
CQti	tricuspid valve resistance	400	mL/(s $mmHg^{0.5}$)

The values given for all parmeters in the KM are chosen from the literature review done in conjunction with the model's development. (Korakianitis and Shi 2006)

The heart, like a battery, provides a motive force in the form of pressure that causes blood to flow through the pulmonic and systemic circulation. The behavior of blood flow through the circulation system modeled in the KM depends on governing differential equations analogous to the governing differential equations of an electrical circuit to define blood flow and pressure. The circulatory model of the KM contains three parameters that affect flow. The parameters are inductance ($L = \frac{P_L}{dQ/dt}$), capacitance ($C = \frac{\int Q(t)dt}{P_C}$), and resistance ($R = \frac{P_R}{Q}$). Looking back at Figure 20, you will see symbols for inductance, capacitance, and resistance used often and with different subscripts. Table 4 below describes what each of the circulation parameters mean.

Table 4 Parameter names, values, and definitions for the KM circulatory system. (Korakianitis and Shi 2006)

Circulation parameters				
Branch	*Parameter*	*Definition*	*Value*	*Unit*
Systemic Circulation	Csas	capacitance - aortic sinus	0.08	mL/mmHg
	Rsas	resistance - aortic sinus	0.003	mmHg s/mL
	Lsas	inductance - aortic sinus	0.000062	mmHg s^2/mL
	Csat	capacitance - systemic arteries	1.6	mL/mmHg
	Rsat	resistance - systemic arteries	0.05	mmHg s/mL
	Lsat	inductance - systemic arteries	0.0017	mmHg s^2/mL
	Rsar	resistance - systemic arterioles	0.5	mmHg s/mL
	Rscp	resistance - systemic capillaries	0.52	mmHg s/mL
	Rsvn	resistance - systemic veins	0.075	mmHg s/mL
	Csvn	capacitance - systemic veins	20.5	mL/mmHg
Pulmonic Circulation	Cpas	capacitance - pulmonic sinus	0.18	mL/mmHg
	Rpas	resistance - pulmonic sinus	0.002	mmHg s/mL
	Lpas	inductance - pulmonic sinus	0.000052	mmHg s^2/mL
	Cpat	capacitance - pulmonic arteries	3.8	mL/mmHg
	Rpat	resistance - pulmonic arteries	0.01	mmHg s/mL
	Lpat	inductance - pulmonic arteries	0.0017	mmHg s^2/mL
	Rpar	resistance - pulmonic arterioles	0.05	mmHg s/mL
	Rpcp	resistance - pulmonic capillaries	0.25	mmHg s/mL
	Rpvn	resistance - pulmonic veins	0.006	mmHg s/mL
	Cpvn	capacitance - pulmonic veins	20.5	mL/mmHg

Inductance describes the inertial effect possessed by blood. An increase in inductance in the system would decrease the rate in which blood accelerates with an applied pressure.

Capacitance defines how much blood a blood vessel can hold. An increase in capacitance would increase the volume holding capability of a given blood vessel. Resistance is the average frictional effect that a blood vessel has against blood traveling through it. An increase in resistance decreases the rate of blood flow at a given pressure.

Part of the nature of simplicity of the KM is that it models the circulatory system as a system of three components. The three components are the aortic or pulmonic sinus, systemic or pulmonic arteries, and systemic or pulmonic veins. Unlike more complicated models of the CVS that attempt to solve for pressures and flows of individual vessels, the KM groups individual vessels together based on their classification as one of the three vessel types and than uses a bulk parameter for inductance, resistance, and capacitance applied to calculate pressure and blood flow through each component. The design and parameter values for the systemic circulation loop of the KM model are exactly the same for the current model. Pulmonic circulation is not simulated within the current model.

The governing equations for the systemic loop's compnents all follow the same pattern. A governing equation for pressure calculation defines pressure change at a given node: $\frac{dP_j}{dt} = \frac{Q_i - Q_j}{C_j}$. Blood flow is calculated using the governing differential equation: $\frac{dQ_j}{dt} = \frac{P_j - P_{k-R_j Q_j}}{L_j}$.

As seen previously, a first order taylor approximation is employed to update pressure and flow calculation. Pressure in the aortic sinus is calculated as $P_{sas,new} = P_{sas,old} + \left(\frac{Q_{ao} - Q_{sas}}{C_{sas}}\right) dt$. Blood flow is calculated as $Q_{sas,new} = Q_{sas,old} + \left(\frac{P_{sas} - P_{sat-R_{sas} Q_{sas}}}{L_{sas}}\right) dt$. Flow and pressure are calculated in the aortic sinus in the previous manner described because of the great effect that local tissue elastance and flow variation have on blood in the region. Pressure and flow rate changes are calculated differently in the arterial component of the systemic loop as the arterial component integrates arterioles and capillaries into this part of the model as pure resistance units. (Korakianitis and Shi 2006)

The pressure equation for the arterial section is calculated using the governing equations for pressure change ($\frac{dP_{sat}}{dt} = \frac{Q_{sas} - Q_{sat}}{C_{sat}}$) and flow ($\frac{dQ_{sat}}{dt} = \frac{P_{sas} - P_{svn} - (R_{sat} + R_{sar} + R_{scp})Q_{sat}}{L_{sat}}$). The systemic vein uses the governing equation for pressure change: $\frac{dP_{svn}}{dt} = \frac{Q_{sat} - Q_{svn}}{R_{svn}}$ and dircetly calculates flow rate: $Q_{svn} = \frac{P_{svn} - P_{ra}}{R_{svn}}$. (Korakianitis and Shi 2006) Updating values for pressure and flow uses the same Taylor series approximation method seen for calculating pressure and flow in the aortic sinus. Once flow rate and pressure drop are calculated for the systemic vein, those values become inputs for the governing equations of pressure and flow for the right atrium. No further discussion on the exact governing equations used for the rest of the model is necessary at this point as the rtight side of the heart follows the same model for calculating pressure and flow as the left at each analagous part of the CVS.

For the sake of simplicity, the same nomenclature from the KM was applied to naming of parameters in the current model. Given that only the systemic circulatory component of the KM was adopted within the final model's code, much of the nomenclature that was given in the full KM was not used at all.

The model acts within a time space created by the user that defines when the model begins and ends simulation. The way that the KM model works is that each part of the CVS is divided into a block where initial values of pressure and blood flow are applied to governing differential equations that model each block and decide the output of new pressure and flow values for the next block. For a given time, the model outputs values for pressure and flow, passed to each block one at a time. Time advances forward using a time step value each time the cardiac cycle is completed. The KM model uses a time step of $1x10^{-4}$ s for each cardiac cycle it advances forward.

Timing of the KM is an important concept to understand. While timing was briefly touched upon in discussing the KM's heart model with the timing of systole and diastole on the

governing pressure and flow equations, there is a bit more to explain about the timing parameters used in the KM.

Table 5 Timing parameters for the KM. (Korakianitis and Shi 2006)

Timing Parameters			
Parameter	*Definition*	*Value*	*Unit*
dt	time step	0.0001	s
T	heart period	1	s
Ts	systolic period	0.3	s

Table 5 above introduces the term heart period. The heart period is the inverse value of heart rate, the time it takes for the heart to complete one heart cycle. In the KM, the heart rate is one beat per second, or 60 beats per minute. The systolic duration is 0.3 s, or three-tenths the length of the heart period, leaving the remaining seven-tenths to be the duration of diastole.

The KM heart block is a four chamber variable elastance model with four heart valves. The governing equations of the heart are based on the Suga et al (1975) variable elastance model. (Korakianitis and Shi 2006) Initially, the current model was designed to adopt the same variable elastance model used in the KM. Problems arose with the numerical solutions gathered from the model using KM specifications and a different path was taken to model the heart using a blood flow input rather than a pressure input calculated from the Suga variable elastance model. The reason that the KM was modified for this current model was because of poor resulting flow curves that resulted from the KM. Figure 22 below shows a comparison of KM left atrial, left ventricular, and aortic curves for pressure, volume, and flow rate with physiologically accurate curves.

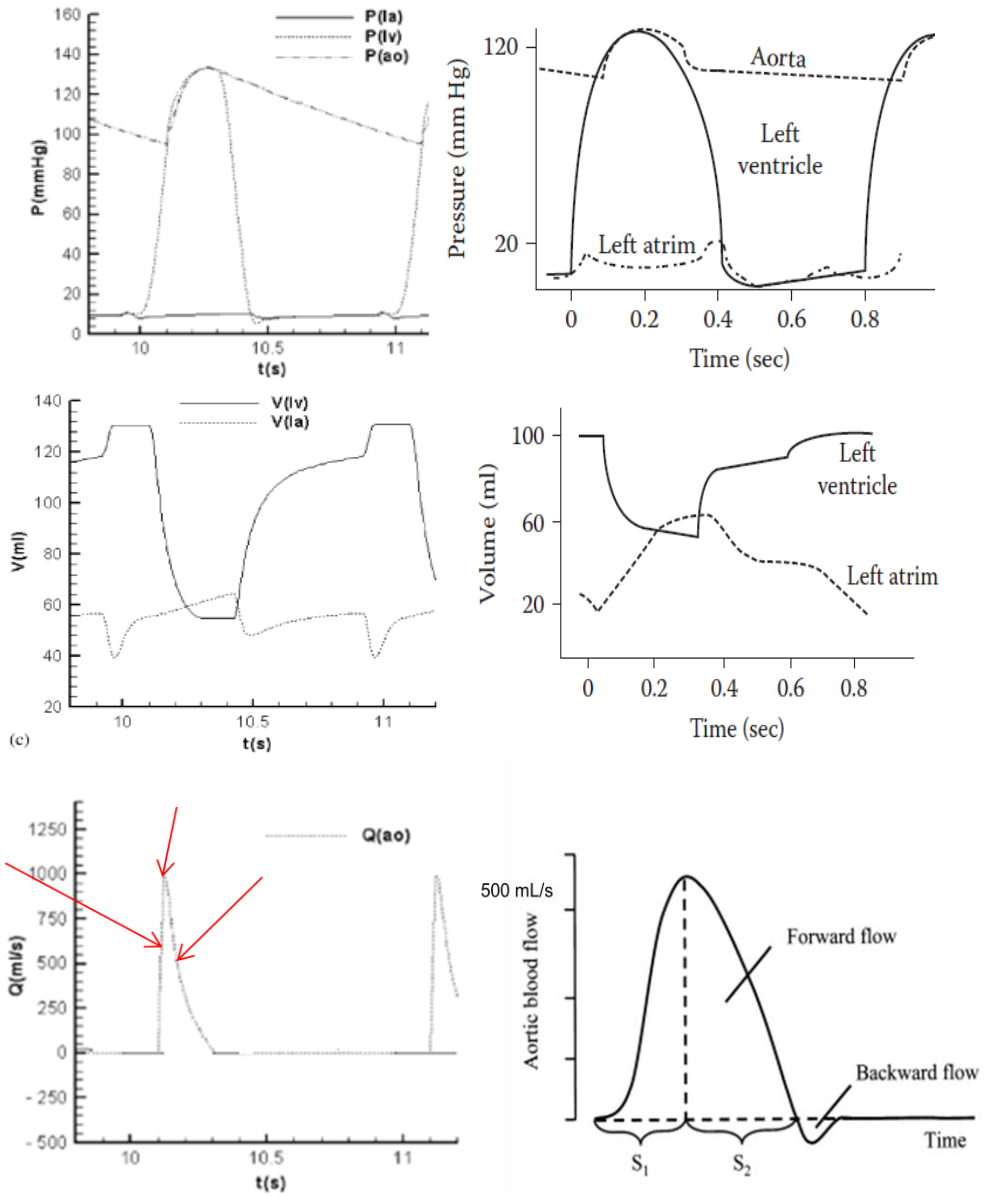

Figure 22 Comparison of KM pressure, flow, and volume curves (left side) to corresponding physiological data (right side). (Korakianitis and Shi 2006) (Kvitting, Ebbers et al. 2004) (Chandran, Rittgers et al. 2007)

With due respect, the pressure and the volume curves representing the left ventricle, left atrium, and aorta appear to correspond well enough with physiologically analogous curves. Without the aortic blood flow curve to show that something is wrong with how the heart is modeled, it would not really be necessary to improve on the KM. The real telltale sign of why the KM is flawed is seen in the aortic flow curve's peak value and overall curve shape (the bottom two graphs shown in Figure 22). The peak resulting flow value from the KM is too high; more

than twice the value of a normal physiologic flow. Additionally, the flow accelerates to its peak value too rapidly as evident in the steep slope starting at the beginning of systole to the peak value. Flow also decelerates too rapidly at the peak of systole to the end of systole. The shape of the curve from the peak of systole to the end of systole is also incorrect, the curve is convex when it should be concave.(Chandran, Rittgers et al. 2007)

What the KM blood flow curves are really doing a good job of showing is that the KM heart is modeled to contract and open too forcefully. A heart squeezing too forcefully will cause heart to eject blood in the fashion described by the KM blood flow curve. There will be little time in between when blood flow is not moving at the beginning of systole and when it has reached its peak flow in the middle of systole. The KM model blood flow curve above illustrates just how forceful the contraction of the heart is, showing almost no lag time between when blood is ejected from the heart and when blood flow hits its peak. (Korakianitis and Shi 2006)

Furthermore, the KM aortic flow curve also fails to account for any aortic regurgitation which will always be present in normal physiological aortic flow. The lack of backflow of blood in the model is an area that needs improvement in the KM because all physiological flows have some sort of closing volume that occurs when blood is pushed back into a pumping chamber when valve leaflets shut. As a result of the shortcomings of the KM, a new model was required so that accomplishment of the specific aims of the project could occur.

One last note on parameter values in general. Without taking units into consideration, and just looking at the parameter values absolutely, one thing that can be seen is that there are some parameters (particularly the parameters that help model circulation) that are several orders of magnitude smaller within the same governing equations as parameters that are much larger. Compare for instance capacitance and inductance. The capacitance of the aortic sinus is 3 orders of magnitude larger than the inductance of the aortic sinus. This might be intuitive to someone with a lot of modeling experience, but if not, the following statement is meant to assist in any future work with the model developed for this project: the smaller valued parameters are much

more sensitive than the bigger ones to numerical adjustment. Changing the values slightly for inductance within the aortic sinus will have a much greater impact on the model than inputting small variations in capacitance for the aortic sinus. When trying to tweak the model, always keep a baseline record of normal case operation to fall back on if there is some problem with how parameter values are causing the model to behave.

3.3 Current model set-up

Given the limitations presented by the KM, a new model was devised that could output physiologically accurate pressure and flow calculations. The final version of the current model shown in Figure 23 contains two pumping chambers, the left atrium and left ventricle, along with a systemic circulation loop that is fed by the left ventricle and empties into the left atrium.

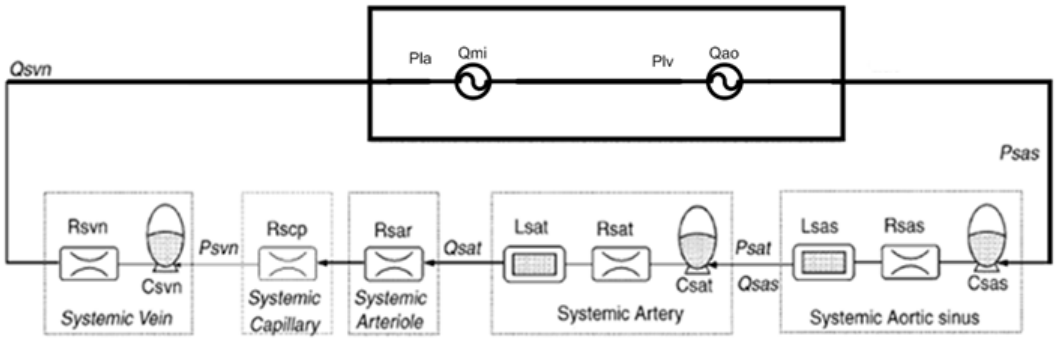

Figure 23 Final schematic of the current model.

The model only considers the left pumping chambers of the heart primarily due to the importance of the left ventricle. Heart diseases impacting the left ventricle are the most life-threatening of all heart diseases because the left ventricle is responsible for pumping blood out to the body. As a result of the extra load that the left ventricle must bare for sustaining systemic circulation, any heart diseases that affect its workload more easily impact the risk of the heart succumbing to congestive heart failure. Therefore, an assumption made by the model is that physiologically accurate response can be achieved by only modeling one half of the heart and hence short circuiting the systemic loop to feed blood back into the left atrium is performed in the model.

The current model has five universal variables that govern how the heart will operate at its most basic level. These variables are heart rate (HR), cardiac output (CO), systolic fraction (the fraction of the heart beat that the heart is contracting), dt (the time step of each iteration of code), and total run time (the amount of time that the heart will beat before the code terminates its operation). A "normal" definition of these universal variables is described below in :

Timing Parameters			
Parameter	*Definition*	*Value*	*Unit*
total_time	simulation duration	0.0001	s
dt	time step	50	s
HR	heart rate	72	beat/min
CO	cardiac output	5	L/min
T	heart period	0.8333333	s
Ts	systolic period	1/3	s

Figure 24 Universal timing parameters used in the current model.

The current model runs for as long as the user tells the model to run. Therefore, the entire model is subject to the total run time definition. The model is told to run as long as the individual iterations of dt have not summed to the value of the total run time value. Therefore, there also is a variable that keeps track of the current code iteration. That variable is ubiquitously called time and it is defined as the sum of all incremental time steps that have collected through each loop of code.

After the definition of the universal variables mentioned above, the current model creates a functioning CVS through the definition of sub-functions that break the CVS down into components.

The current model circumvented the problem of poor modeling of blood flow in the heart by not adopting the Suga et al. model of the heart that used an elastance function to create pressure that would drive blood flow. Instead, the current model implemented a blood flow generating function for aortic and mitral flow.

The idea behind generating a blood flow curve by itself without first defining a pressure function to drive flow goes hand in hand with the idea of having a simple lumped parameter

model. Generating physiologically accurate blood flow curves directly requires less parameterization and complexity than using the Suga model to generate an elastance function that creates pressure to drive blood flow.

Doing away with an elastance function to generate blood flow also does not result in a loss of information that can be gleaned from the model. The shape of a blood flow curve says as much about the way a heart is functioning as any other pressure-volume relationship. A normal blood flow curve still requires that the heart generate the correct pressures while pumping. Therefore, going about the problem of generating blood flow to create pressure still allows for accurate modeling of the heart and allows for the gathering of physiologically correct data from the model.

Understanding how the current model works to simulate the mechanics of a human CVS can be illustrated using the following quasi-code of the model.

```
if (time < total run time)
{
        create aortic blood flow;
        model blood flow through the systemic circuit;
                {
        model blood flow through the aortic sinus;
        model blood flow through systemic arteries;
        model blood flow through the systemic vein;
        }
        model blood flow through the left atrium;
        create mitral blood flow;
        model blood flow through the left ventricle;
time = time + dt;
}
```

The basic mechanics of the quasi-code show that the model first generates an aortic flow curve. The aortic flow curve passes on a numerical solution for aortic sinus pressure that becomes the input for pressure for the aortic sinus component of the systemic circulation. After solving for pressure and blood flow at the exit of the aortic sinus, those solutions are passed on to the systemic arterial component that again creates a solution for pressure and blood flow at the exit of the arterial component. The blood flow and pressure are calculated once more after passing through the systemic vein sub-model and those values are passed on to the left atrium sub-model that calculates the pressure and volume of in the left atrium. Blood flow through the mitral valve is generated and passed on to the left ventricle where the blood flow input is used to calculate pressure and volume in the left ventricle. At that point, the entire cardiac cycle starts over again and time steps forward the amount of the time step value.

Blood flow out of the mitral and aortic valves is modeled using a blood flow function generator that allows the creation of a physiologically accurate blood flow curve through the input of user defined parameters. To create the aortic flow curve, four parameters are required (labeled as A, B, C, D in Figure 26). To create a mitral flow curve, 7 parameters are required (A, A1, A2, A3, B, C, D in Figure 27).

A hypothetical declaration of the shape of an aortic curve is shown below:

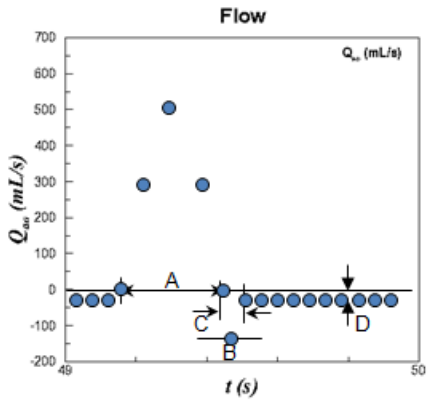

Figure 25 Parameterization of a user-defined aortic flow curve.

Systolic duration defines A, B is the minimum value of regurgitation as part of the closing volume, C defines the length of time it takes for the aortic valve to close, and D represents any backflow occurring after the aortic valve closes. Once the flow curve is parameterized by A, B, C, and D, a spline code works to connect the dots, so to speak, and make the aortic flow curve look physiologic. The end result is the following:

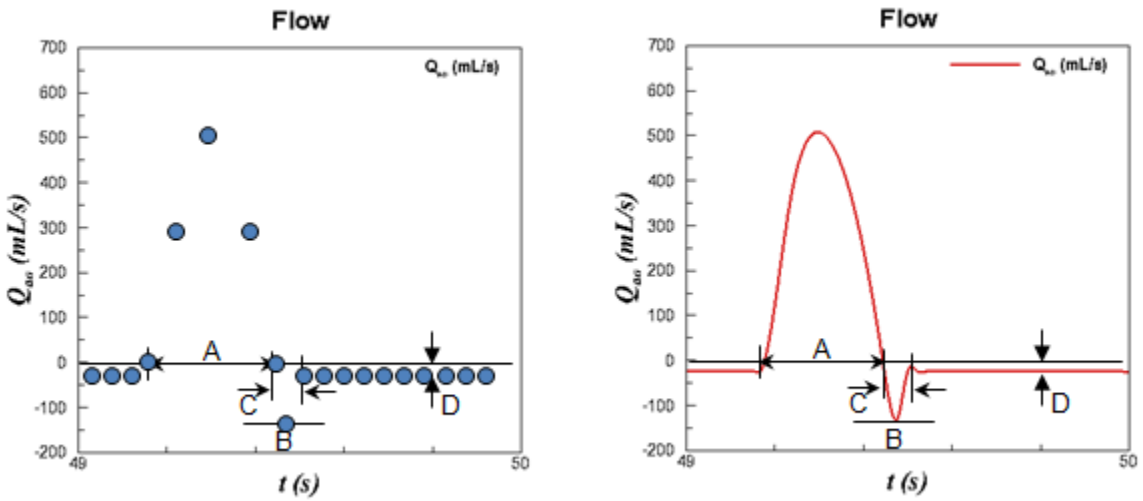

Figure 26 Process illustration of aortic flow curve parameterization to aortic flow curve generation.

The spline code is a sub-routine found in the lump parameter model that creates a twice differentiable continuous function. The continuity of the splined flow curve is important because it would otherwise create unrealistic pressure calculations at discontinuities in the flow curve due to the way pressure is calculated in the previously defined governing equation for pressure within the left ventricle.

The method of splining together a mitral flow curve is exactly the same as in the splining of the aortic flow curve with the only difference being an increase from four to seven parameters required.

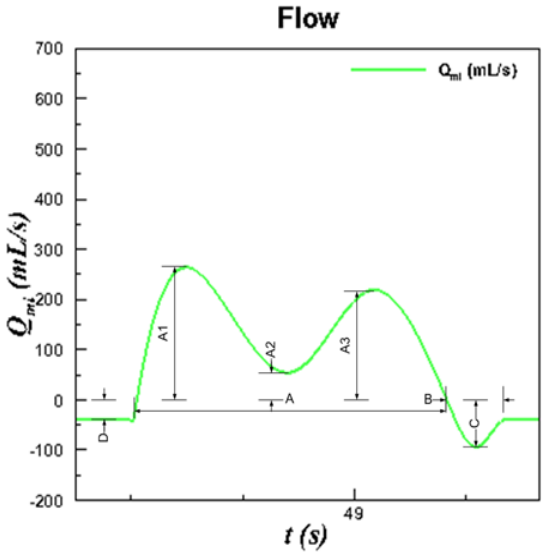

Figure 27 Mitral flow curve with parameter values that define its shape.

The seven parameters that define the mitral flow curve are A (length of systole), A1 (first local maximum), A2 (local minimum), A3 (second local maximum), B (duration of mitral valve closure), C (volume of blood that leaks back during valve closure), and D (regurgitant blood for leaky valves).

In the left atrium as in the left ventricle, pressure is defined from instantaneous blood flow. During systole, pressure is defined in the left ventricle as: $P_{lv} = P_{sas} + L_{ao}dQ_{ao} + \frac{Q_{ao}^2}{CQ_{ao}^2}$ and pressure is defined in left atrium as: $P_{la} = P_{lv} + L_{mi}dQ_{mi} + \frac{Q_{mi}^2}{CQ_{mi}^2}$. During diastole, pressure out of the aortic valve is simply $P_{lv} = -\frac{Q_{ao}^2}{20}$ and pressure out of the left atrium is $P_{la} = -\frac{Q_{mi}^2}{20}$. Consistent with the aims of this research, the lumped parameter model outputs a pressure-volume diagram, a diagram commonly used to study heart workload. Typical pressure-volume diagrams look like the one in Figure 28:

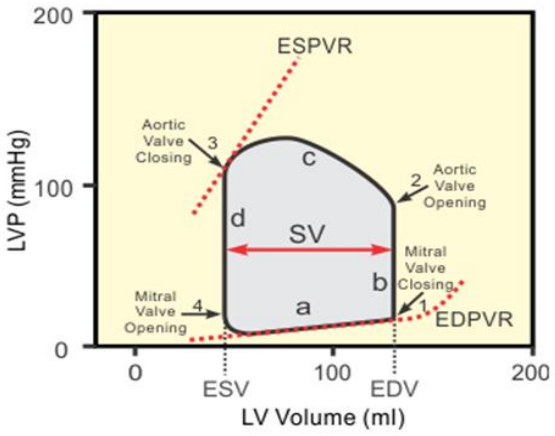

Figure 28 Pressure-volume diagram of the left ventricle. (Klabunde 2005)

The left ventricular pressure-volume diagram above is the result of the mapping of volume and pressure together as shown in

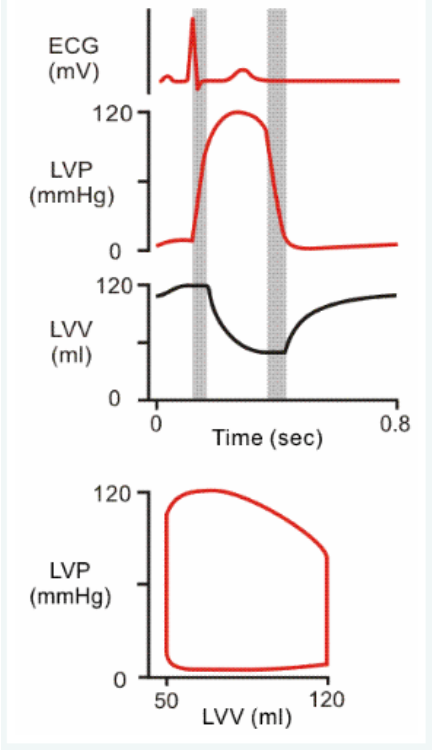

Figure 29 Demonstration of pressure and volume being mapped into a pressure volume diagram. (Klabunde 2005)

Normal values for human stroke volume are within the range of 70 mL, with an end systolic blood volume (ESV) of 65 mL and an end diastolic blood volume of 135 mL. (Vander, Sherman et al. 2001) As work is the integral of work and volume, comparisons of pressure-

volume diagrams allow for an easy understanding of how the heart is working based on changing parameters across several simulations. Changes in stroke volume and the rate at which pressure changes per change in volume across several simulations show how a heart is responding to the parameters defined for a given simulation.

Instantaneous power is also a useful measure of how the simulated heart is working. An instantaneous power graph of the left ventricle from the model looks like the one seen in Figure 30:

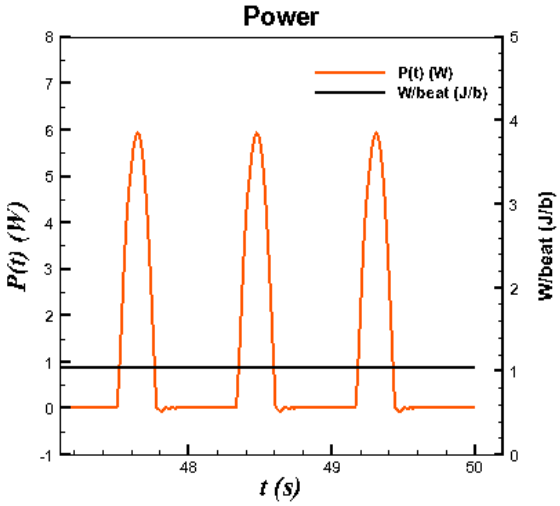

Figure 30 Graph of instantaneous power along with work/beat calculation.

The graph of instantaneous power is important because it is actually from instantaneous power calculation in the code for the lumped parameter model that work per beat is calculated.

For a given heart simulation using the current model, instantaneous power will vary depending on rate of work the heart is performing at. In the simulation, power is calculated as $\dot{W}_{lv}(t) = P_{lv}\frac{dV_{lv}}{dt}$. In general, an overworked heart will have to produce more power to output the same amount of blood as a more efficient heart.

The amount of workload per beat of the heart is also shown in Fig 28. The calculation of workload per beat is the culmination of part of specific aim I outlined earlier to model physiological flow accurately. The work per beat calculation is not exactly the integral of

pressure with respect to change in volume, the classical definition of pressure-volume work ($W = \int_{V_i}^{V_f} p\, dV$). In the model, work per heartbeat is actually calculated using the summation of the average amount of power across the length of time of a heart beat period and applying a first-order Taylor series approximation: $\frac{W}{b} = \left(\sum_{dt}^{T} \frac{\dot{W}}{T/_{dt}}\right) dt$.

C code of the current model is found in the appendix for any further review as desired. One final note should be made to help future researchers in the development of this model for future research: **Do not use MATLAB**. MATLAB is good for many things, but not for lumped parameter modeling using a normal desktop computer. At a time step of 10^{-4} s (two orders of magnitude bigger than the time step of 10^{-6} s used in the current C version of the model) and with a simulated modeling time of 30 seconds (compared to the 50 second simulated duration of cardiac operation in the current C model), it took MATLAB longer than 4 minutes to compile the code for the model. Visual 6 only took around 25 seconds. So please save yourself time and use Visual 6 or better to compile your model.

4 RESULTS AND DISCUSSION

4.1 Introduction

Chapter 4 will be divided into two sections in relating the results of the specific aims. Section 4.2 gives a more detailed view why the KM was not adopted to directly calculate workload. Section 4.3 corresponds with the results of accomplishing specific aim I: The development of a computational model of the left ventricle that is able to simulate physiological and pathophysiological characteristics and quantify workload. Section 4.3 describes the parameters used to create a baseline normal physiological simulation of blood flow and pressure through the CVS as well as the resulting dependent variables that quantify workload for the normal case. The importance of the normal case simulation is that its results serve as baseline values from which workload of the heart is compared to other cases simulated. Section 4.3 holds the results dealing with the fulfillment of specific aim II: Utilization of the computational model to test how multiple disease scenarios affect energy cost on the left ventricle. 4.4 contains the results of simulations of mild, moderate, and severe disease cases of aortic and mitral regurgitation, aortic stenosis, and hypertension.

4.2 Results from modeling the KM with no revisions

The methodology section briefly mentions that the KM had to be revised because of physiologically inaccurate representations of flow. A more detailed account of the resulting flow and pressure from the attempt to directly apply the KM will be given here.

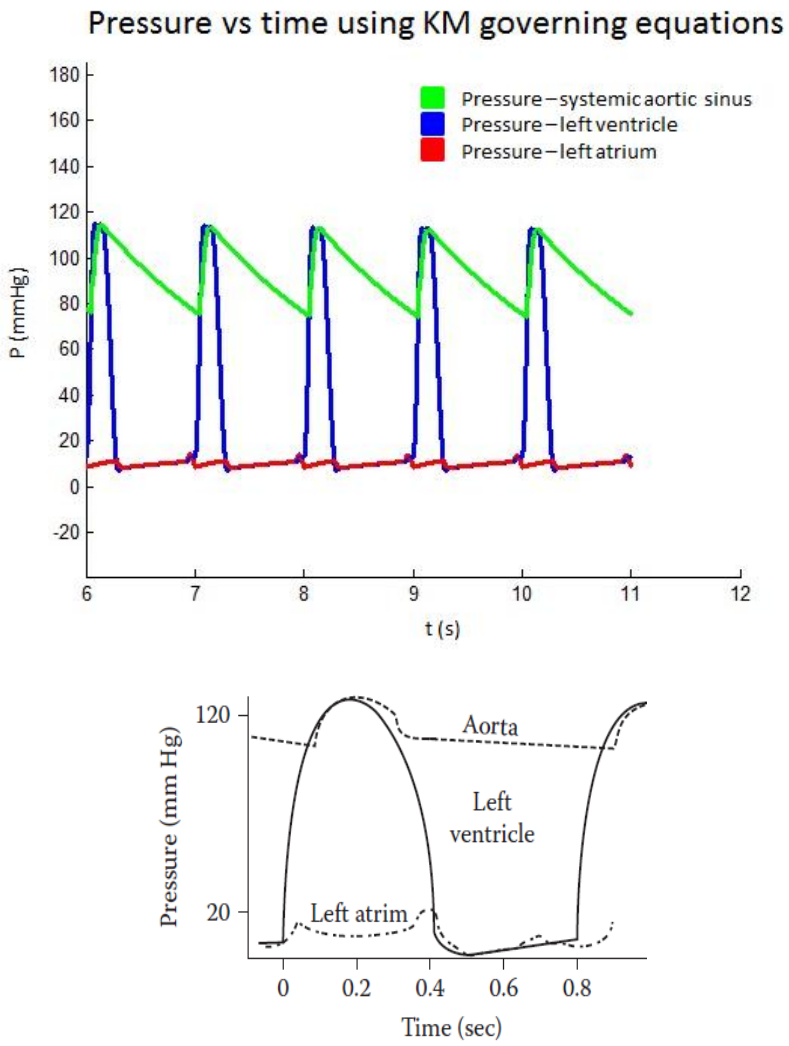

Figure 31 Graph of resulting pressure versus time from KM guided simulations compared to a physiologically accurate representation of pressure vs time. (Kvitting, Ebbers et al. 2004)

The resulting pressure versus time graph (Figure 31) using the KM to guide its calculation does look physiological. The operating pressure range of systole and diastolic blood pressure is a healthy 117/77 mmHg. The left ventricle and the left atrium are behaving physiologically as well.

Looking at the volume versus time graph shown in Figure 32, the left ventricle and left atrial volume versus time graph does not look bad either. The stroke volume is within the range of

70 mL for the left ventricle. There is a somewhat high rate of change of volume at the beginning of systole and at the end of systole, but it is arguably accurate enough to survive any challenges.

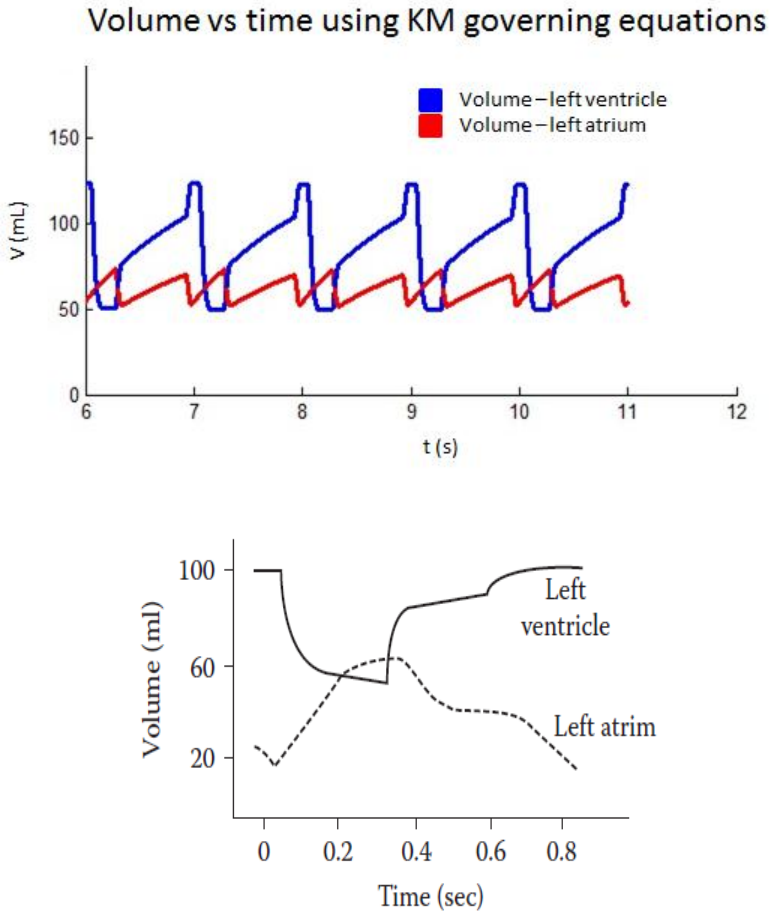

Figure 32 Comparison of left atrial and left ventricular volume from the model using KM cardiac governing equations and physiologically accurate representations of volume vs time from literature. (Kvitting, Ebbers et al. 2004)

The resulting flow curves from the applied KM governing equations were actually worse than the ones published in the Korakianitis paper.

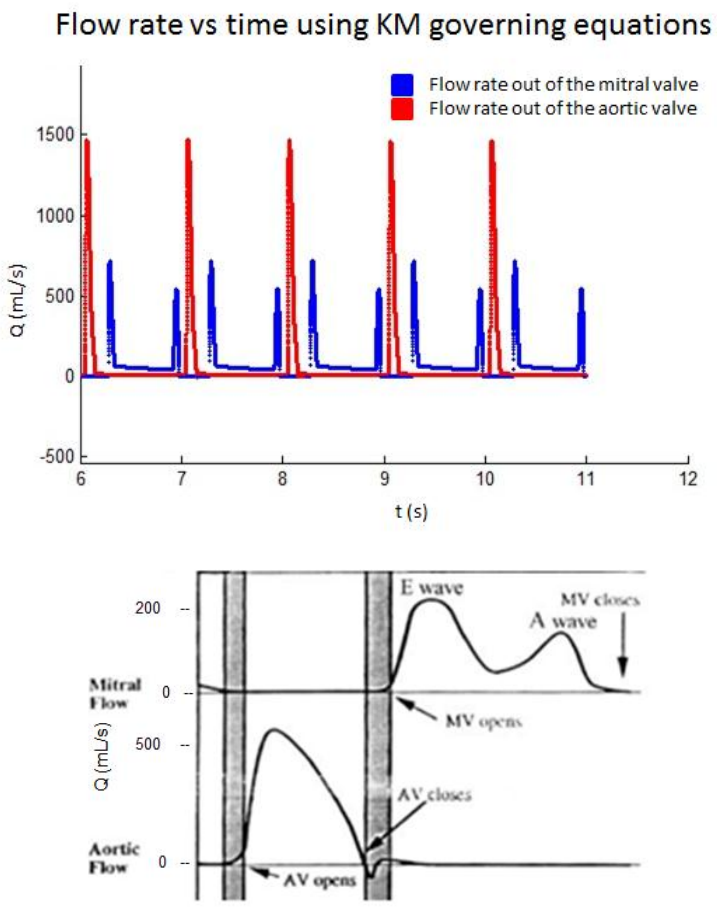

Figure 33 Comparison of mitral and aortic flow rate curves from the attempt at applying the KM in early modeling stages to physiologically accepted representations. (Yoganathan, He et al. 2004)

The flow curves generated with the KM governing equations for cardiac operation were not good physiological models at all (Figure 33). Looking at aortic flow, the peak flow reaches nearly 1.5 L/s, almost three times what a healthy peak flow rate should be. The shape of the aortic flow rate is also mal-formed, with flow accelerating and decelerating much too quickly. The mitral flow curve obtained from using the KM was also not physiologically accurate. Peak flow was again much too high, almost three times as high as should be expected physiologically. The shape of the E and A waves that form the overall mitral flow curves are mal-formed as well.

The application of the KM to direct workload calculation was whole-heartedly attempted, but in the end could not be implemented for the reasons given above due to inaccurate aortic and mitral flow representations.

4.3 Results and discussion for specific aim I

Twenty one parameters are used by the current model to simulate left chamber pumping and systemic loop circulation. The twenty one parameters can be thought of as a hypothetical person's cardiovascular characteristics. The parameters used to describe normal physiological operation of the CVS are used as a baseline and can be considered the characteristics of a healthy patient. The twenty one parameters can be placed into four groupings based on the component of cardiac operation that the parameters affect.

The first grouping of parameters can be thought of as parameters that affect the universal characteristics of cardiac operation (Figure 34). These parameters are heart rate (HR), cardiac output (CO), and fraction of a heart beat that determines the length of systole (systolic fraction).

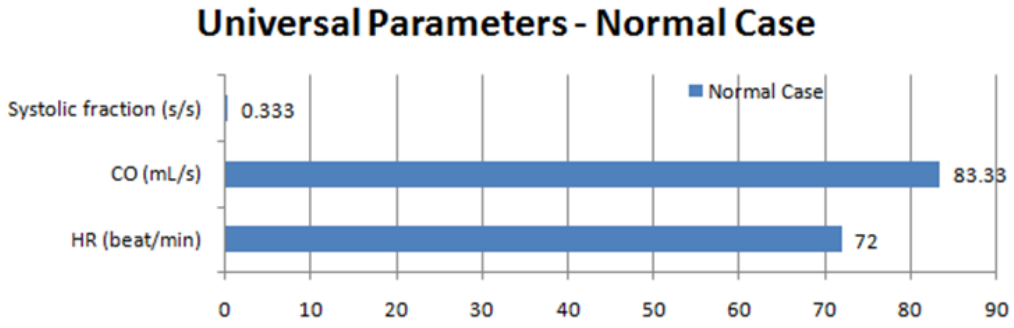

Figure 34 Parameters describing universal performance characteristics of the cardiac cycle.

The systolic fraction equals one-third of the length of a heartbeat, meaning that diastole is two-thirds. The cardiac output selected was 5 L/min, and the heart rate was 72 beats/min. These parameter values are all within normal cardiac performance ranges given from literature. (Vander, Sherman et al. 2001)

Six parameters are used in determining the shape of the aortic and mitral flow curve, three for each curve. B and C_ control the amount of regurgitation that occurs during the time when the aortic and mitral valves initiate and finish closing respectively. C and B_ are values that represent the duration of time that it takes for the aortic and mitral valves to close, respectively. D and D_ take into consideration aortic and mitral regurgitation after the aortic and mitral valves

close, respectively. Figure 35 shows the parameter values used to model normal operation of aortic and mitral flow. In the normal case, there is no backflow of blood after either the mitral or aortic valves have shut. The length of time that lapses for the aortic valve to shut (C) is one-twelfth of a heartbeat, and the shutting period for the mitral valve (B_) is one-eighth of a heartbeat; both within normal physiological ranges. (Chandran, Rittgers et al.)

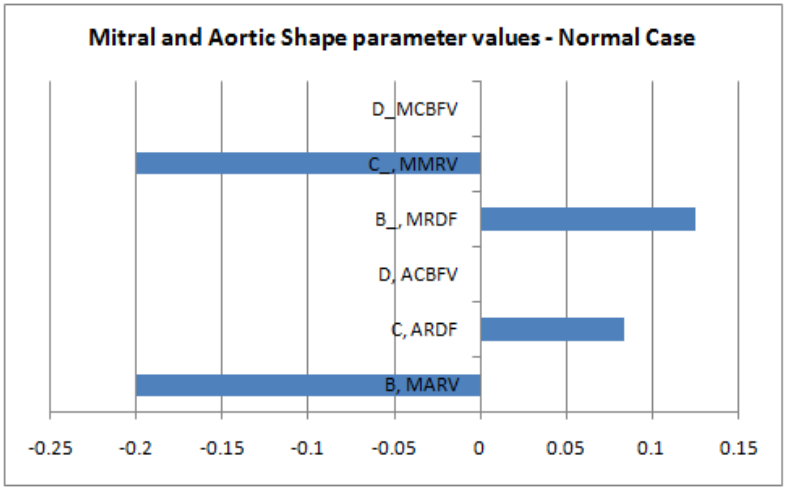

Figure 35 Mitral and Aortic shape parameters for normal case operation.

Figure 36 shows the thirteen parameters that are used to define the operation of systemic circulation. These parameters are the values for inductance, capacitance, and resistance taken from the KM. The same systemic KM parameters were chosen because of the validation done through literature review cited by Korakianitis and Shi in the methods section from the journal article: "Numerical simulation of cardiovascular dynamics with healthy and diseased heart valves." Journal of Biomechanics **39**(11): 1964-1982. The journal article states that parameters were chosen based on values found in various sources. (Korakianitis and Shi 2006)

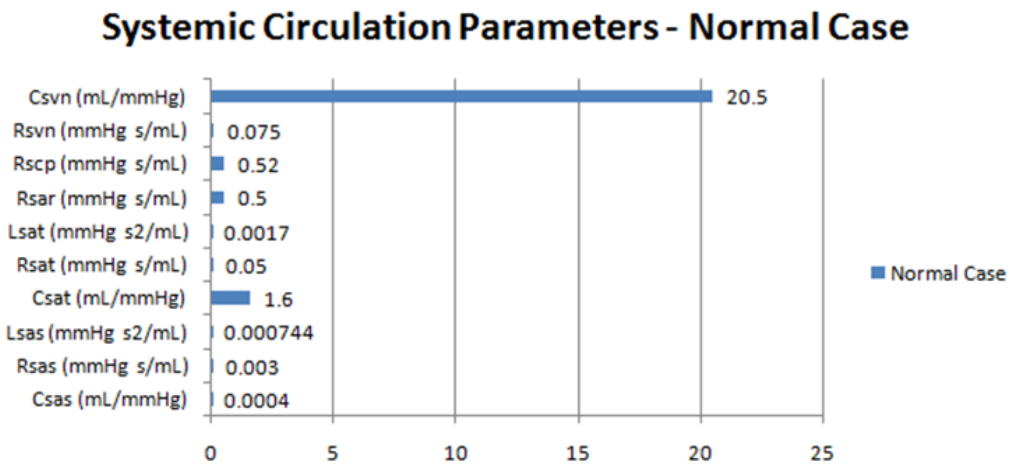

Figure 36 Normal case parameters controlling systemic loop operation.

Only two of the circulation parameters are ever changed to model diseased cases, the compliance of the systemic artery component (C_{sat}) and the resistance of capillaries (R_{scp}) which are changed to simulate hypertension.

The last grouping of parameters is the valve resistance values for the aortic and mitral valves (Figure 37). Aortic valve resistance (CQ_{ao}) is adjusted when modeling aortic stenosis. Mitral stenosis is not modeled so mitral valve resistance (CQ_{mi}) never changes throughout later disease case runs. The valve resistance parameters for normal case operation were taken from the Korakianitis and Shi model which had already validated the values for resistance through literature review. (Korakianitis and Shi 2006) One key difference in the how the valve resistance parameters are presented should be noted to avoid confusion. The inverse of the values of valve resistance given by Korakianitis and Shi are presented in Figure 37 due to how these are used in the governing mitral and aortic flow calculations – valve resistance is a coefficient that divides flow rate as seen in the governing equation that calculates pressure in the left ventricle ($P_{lv} = P_{sas} + L_{ao}dQ_{ao} + \frac{\boldsymbol{Q_{ao}^2}}{\boldsymbol{CQ_{ao}^2}}$). The emboldened term shows that multiplying the inverse of resistance to flow and squaring the value accomplishes the same calculation as dividing the square of valve resistance. The whole reasoning behind inverting the valve resistance values is to simplify the presentation of valve resistance in diseased cases using changing valve resistance as a parameter.

In the case of aortic stenosis simulation where valve resistance will increase, presenting physiologically, using the inverse of valve resistance values illustrates the increase, whereas using the actual values would show a contradictory decrease in aortic valve resistance.

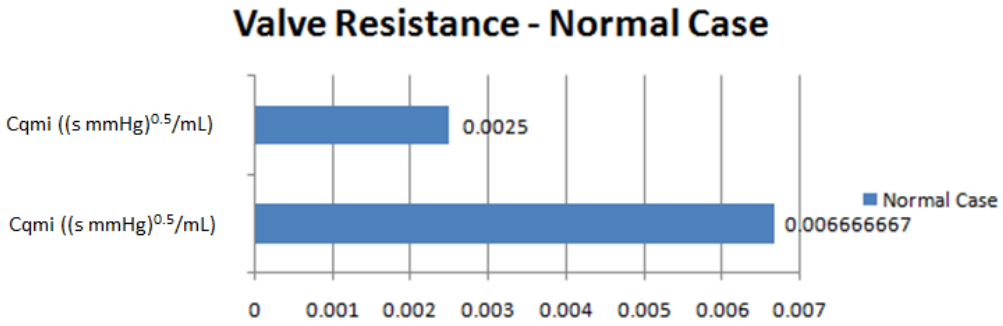

Figure 37 Mitral valve resistance (CQ_{mi}) and aortic valve resistance (CQ_{ao}) parameters.

The resulting graphs from simulation using normal case parameters are shown below.

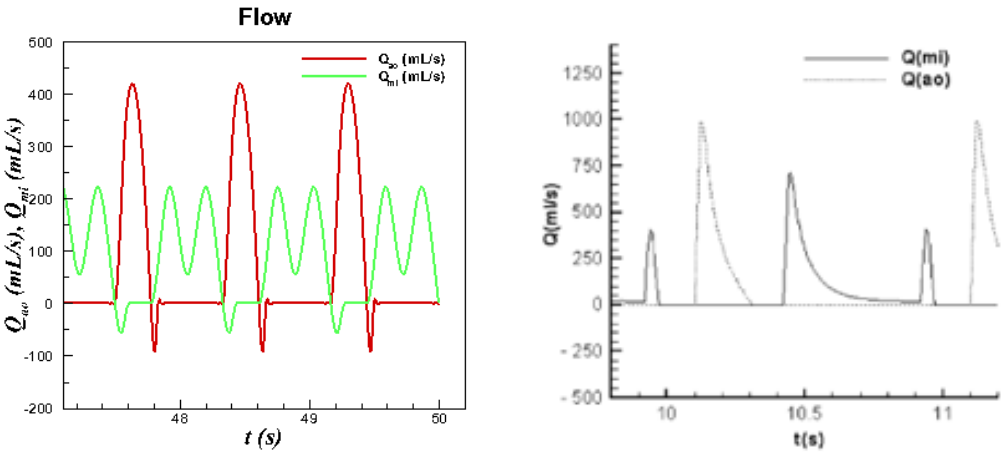

Figure 38 Left: Resulting aortic flow, $Q_{ao}(t)$ (red), and mitral flow, $Q_{mi}(t)$ (green) from current model normal case simulation. Right: Resulting KM curves for aortic and mitral flow. (Korakianitis and Shi 2006)

Figure 38 illustrates the difference between the current model's aortic flow and mitral flow curves with the KM's flow curves. Figure 39 illustrates the similarity between the current model's flow rate representations with what is considered physiologically accurate flow response.

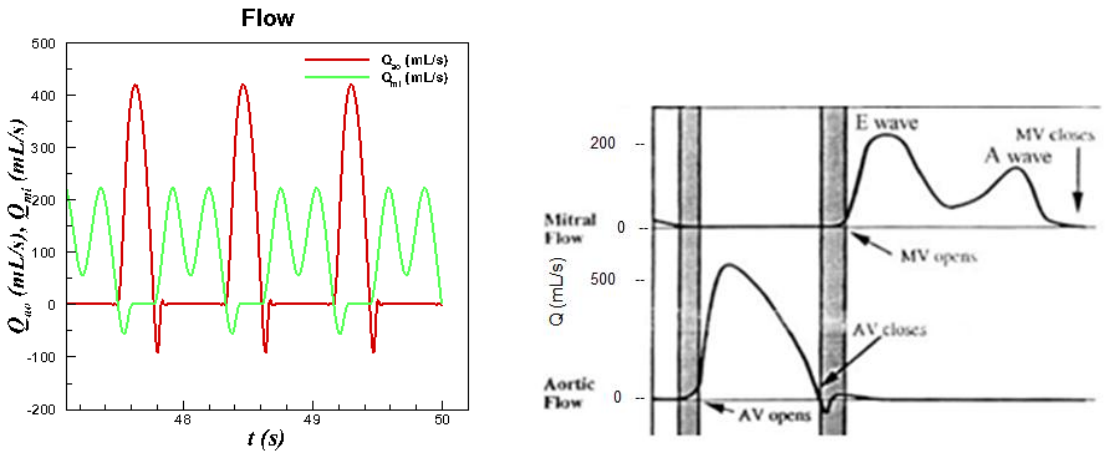

Figure 39 Comparison of the current model's flow rate curves with a physiologically accurate representation of flow rate. (Yoganathan, He et al. 2004)

Side by side comparison of the current model's mitral and aortic flow curves with figures from Yoganathan et al's 'Fluid mechanics of heart valves' show great similarity within peak value and flow rate shapes for mitral and aortic flow. The aortic flow curve has a peak value for flow near 425 mL/s that is within physiological range of normal flow, and mitral flow has a peak value near 200 mL/s which is also considered physiological. The aortic flow curve also includes what is known as a closing volume, or the small regurgitation of blood that occurs after systole in the left ventricle when the small duration of time that occurs while the aortic valve closes allows some blood back into the left ventricle. The closing volume displayed in the current model is considered physiologically representative of accurate aortic flow. The mitral flow curve in the current model also shows backflow due to a closing volume which is also physiologically accurate although it is not shown in Figure 39's mitral flow curve created by Yoganathan et al.

The small difference between the current model and the representation by Yoganathan et al illustrates the variation of flow representation between various sources in literature. Sources tend to give a wide range of what is considered physiologically normal in terms of peak flow rate, flow curve shape, and the existence of closing volume. (Vander, Sherman et al. 2001)(Klabunde 2004)(Yoganathan, He et al 2004). The variation in physiological range of flow rate should not be surprising given the great diversity in human condition provided by age, gender, height, weight

and so many other variables. What matters in determining whether or not a flow curve is physiologically accurate is shape and peak flow rate. In selecting a peak flow rate for aortic and mitral flow during this research project a rule of thumb was to choose one source that had been widely accepted and stick to its interpretation of physiologically accurate flow (Yoganathan, He et al 2004).

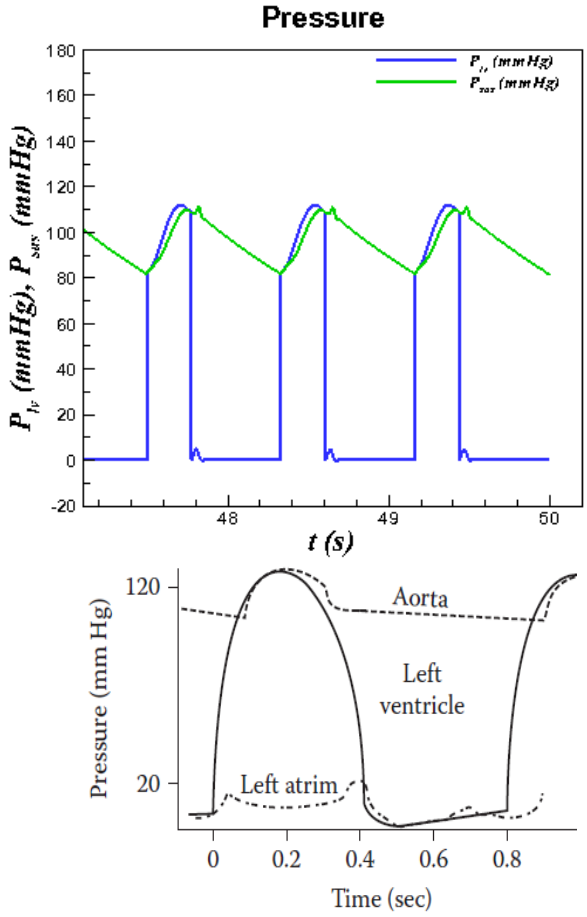

Figure 40 Comparison of the current model's resulting pressure graph from normal case simulation with a physiological representation of pressure for the left left ventricle and aortic sinus. (Kvitting, Ebbers et al. 2004) Left ventricle pressure ($P_{lv}(t)$) is in blue, and aortic sinus pressure ($P_{sas}(t)$) is in green.

Figure 40 above shows the graphs of left ventricle pressure and aortic sinus pressure. The peak systolic aortic sinus pressure commonly referred to as SBP reaches 116 mmHg and it falls to its minimum diastolic value (DBP) at around 81 SBP. The SBP and DBP are within a healthy range for a person to have. (Vander, Sherman et al. 2001)

The left ventricular pressure curve does not follow a completely physiologically accurate path that one would see in a real human patient pressure graph of the left ventricle. The rising and falling of pressure corresponding to contraction and relaxation of the left ventricle is somewhat instantaneous – much faster than what would be seen physiologically. The instantaneous rising and falling of left ventricular pressure is one limitation of the current mode's governing equation for pressure calculation. The current model initiates flow during systole instantaneously from the point when the simulated cardiac cycle finishes diastole. Physiologically, flow would rise gradually due to a gradual rise in ventricular pressure. The gradual rise in pressure is not enough to severely affect the physiological representation of pressure and more importantly, not anywhere near the point at which direct work calculation would be severely affected. The point should be noted that it will be an area of future improvement for the model to have a more gradual rise and fall of pressure in the left ventricle.

During diastole there is no slight rise in pressure that is normally seen as the left ventricle fills with blood and begins to distend. This absence in slight pressure rise during diastole is evident in the zero pressure that is maintained during the duration of diastole seen in Figure 40 in the left ventricle pressure curve. The absence of a diastolic gain in pressure in the left ventricle is another limitation of the current model's ability to represent pressure physiologically, but one that can be easily reasoned as unimportant in the calculation of work. It can be argued that work is only being done by the heart when its walls are contracting and creating volume change in its chambers. During diastole, the left ventricle's walls are not contracting, and the increased pressure change is not doing any useful work. The absence of increased pressure during diastole in the current model does not have an effect on the overall useful work calculation for the left ventricle justified by the reasoning made.

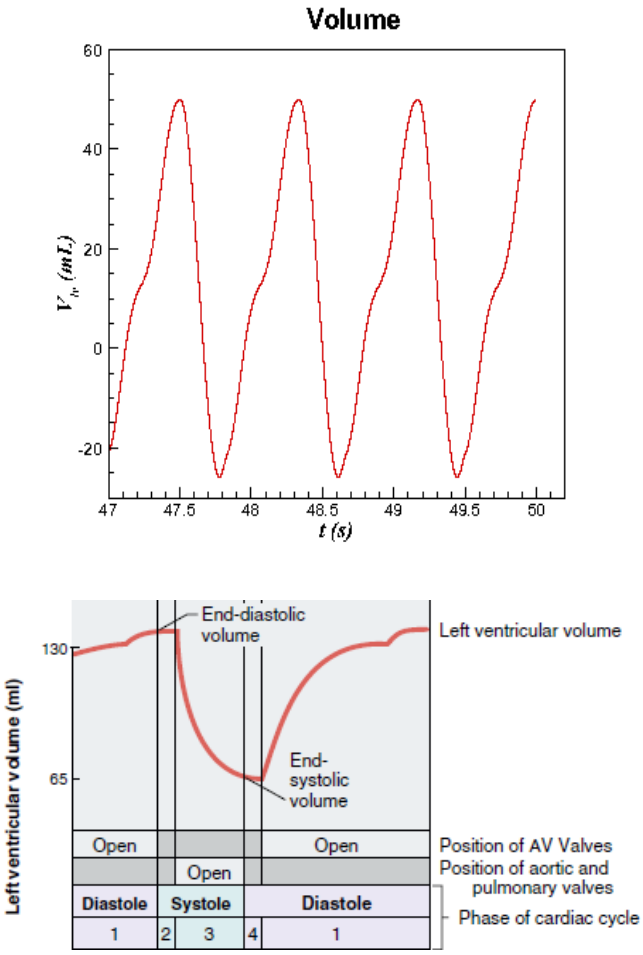

Figure 41 Comparison of resulting volume graph of the left ventricle ($V_{lv}(t)$) created using normal baseline parameters with a physiological representation of left ventricular volume (Vander Sherman et al 2001).

The current model's volume graph shown at the top of Figure 41 shows the left ventricle fills to a maximum near 50 mL of blood before ejecting blood at systole. At the end of systole, the volume graph shows a negative 20 mL value of volume. This negative value represents the closing volume of blood that enters back into the left ventricle after being ejected during the time the aortic valve is closing. The total stroke volume left ventricle, the amount of blood ejected by the heart into systemic circulation, is the total difference in volume of the heart from the end of diastole to the end of systole. In the normal patient case, the stroke volume is 70 mL, a value very much in the range of healthy patient data. (Vander, Sherman et al. 2001) It should be noted to avoid confusion between the volume graph representing the current models volume range with

what is represented as the volume range of the left ventricle by Vander's Human Physiology. The current model does not include an initial volume value for the left ventricle in its governing equation for volume calculation that would add the necessary volume to make the volume range the same as the Vander representation of volume. The different starting and ending values for left ventricular volume do not affect direct workload calculation as the stroke volume is still accurately represented by the volume calculation as seen in Figure 42.

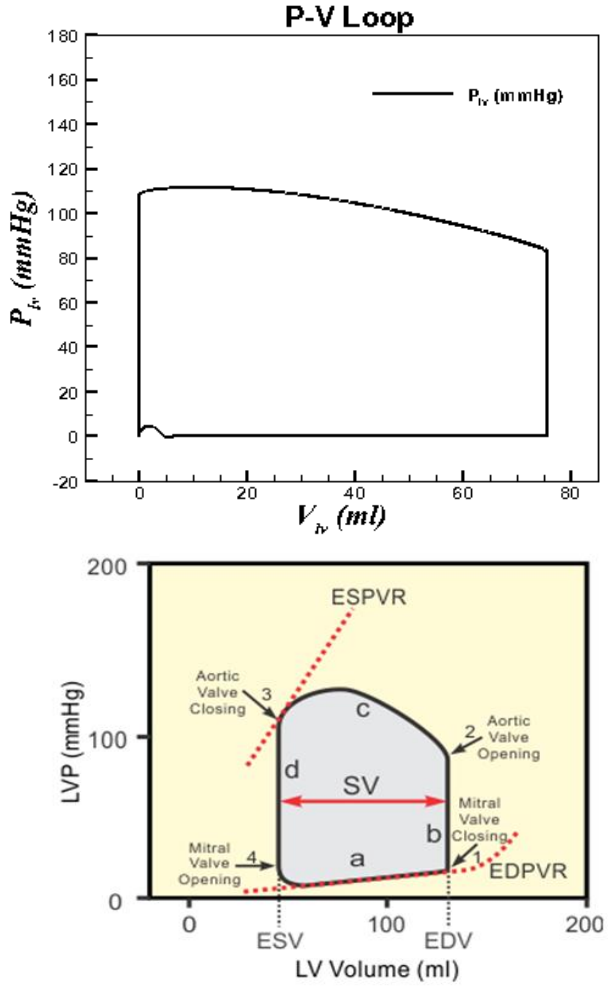

Figure 42 Pressure-volume diagram of the left ventricle using normal case parameters.

The left ventricle pressure-volume diagram shows the physiologically inaccurate nature of the ventricle mechanics during diastole. As said earlier, the pressure should raise about 10 mmHg from the beginning of diastole to the end of diastole. In calculating work, the small rise in

pressure is negligible. In justifying the absence of the small diastolic pressure increase, there is reason to say that pressure volume work really is not being done by the heart during diastole. The reason for the pressure increase during diastole in the left ventricle is due to blood filling pushing up against the walls of the left ventricle. In this case of increased volume causing increased pressure, no useful work is actually being done and should not factor into the workload calculation of the left ventricle. Besides the absence of a pressure gradient in the diastolic portion of the cardiac cycle, the PV-diagram obtained from normal cardiac simulation looks quite similar to the physiological representative diagram presented by Klabunde. The stroke volume and operating pressures are very close. There is a small pressure rise at the beginning of diastole that shows up in the current model's PV-diagram (the small bump begins at 0 mL, 0 mmHg and ends at 10 mL, 0 mmHg) and is actually a result of the pressure rise created by the backflow of blood that occurs during the time it takes the aortic valve to close (i.e. the closing volume).

Instantaneous power of the left ventricle is the final graph generated for the model. Peak instantaneous power occurs right before peak systole, reaching about 6 W. Also, direct calculation of work per beat from instantaneous power was made. Under normal operating parameters, the simulated heart spends 1.03 J per beat.

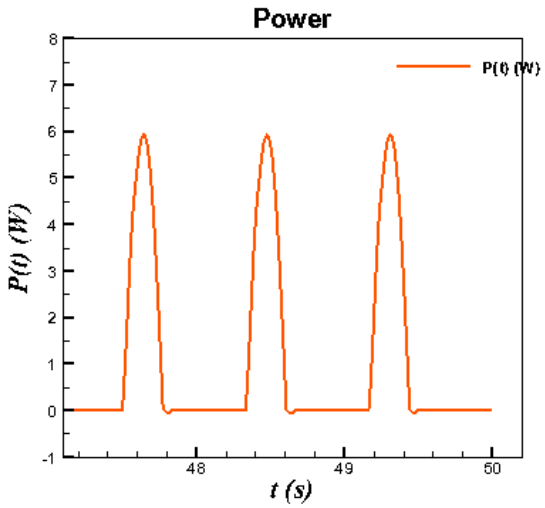

Figure 43 Instantaneous power graph (P(t)) for normal case parameters.

With results delineated using graphs of left ventricular pressure and volume, mitral and aortic flow, a pressure-volume diagram, and instantaneous power, accomplishment of part of specific aim I is made – a satisfactory computational simulation of the left pumping chambers and systemic circulation loop was created. The computational loop allowed for accurate simulation of aortic and mitral flow, as well as direct calculation of work per beat. The work per beat calculation for the normal case was significant as it lays the foundation for accomplishing the rest of specific aim I; calculation of energy cost to operate the heart under diseased conditions.

Analysis of time step sensitivity was also conducted to validate the time step used in the model. The time step advance each simulated cardiac loop of the model forward was $1x10^{-6}$ s. To test sensitivity of time step, results were charted for time step values an order of magnitude greater ($1x10^{-5}$ s) and an order of magnitude smaller ($1x10^{-7}$ s). The resulting pressure-volume graph for the three different time step runs is shown below. The time step runs all overlap one another quite closely so that only one of the three graphs are visible. The equal appearance of the three time step pressure volume graphs suggest that time step sensitivity is not an issue in the range of $1x10^{-6}$s and that the computational runs using one one-millionth of a second as the time step are valid.

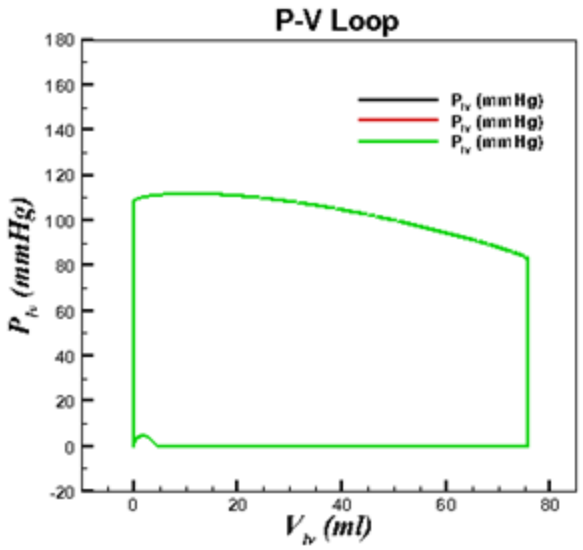

Figure 44 Pressure volume diagram illustrating the equality of pressure and volume calculations at three different time step values.

4.4 Results and discussion for specific aim II

It should be made clear at this point what energy cost means using a systems approach to guide its definition. The operating curves of a hypothetical pump and system are described in the figure below:

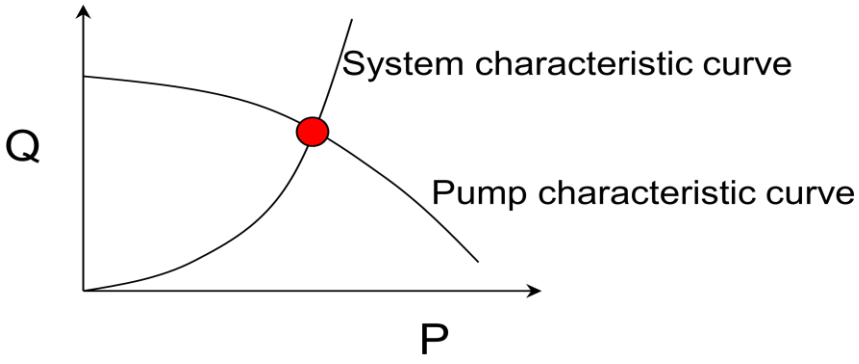

Figure 45 Operating curves of a pump and system connected to the pump.

The curve describing system operation has a higher flow rate as pressure increases. Conversely, a pressure increase affects pump operation by slowing flow down. Where the two operating curves intersect is where the system will operate. Taking the pump to be the left

ventricle of the computational model being used, and the system curve to be systemic circulation, we can apply this systems approach to describe energy cost for any number of diseased systems cases in terms of the work per beat of the left ventricle.

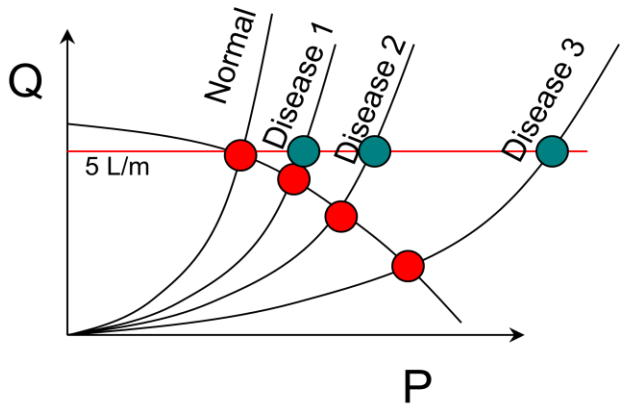

Figure 46 Operating curves for diseased systems in relation to the operating curve of the heart.

Figure 46 shows two concepts that are important in understanding how the model calculates workload. The first point that Figure 46 is showing is how heart diseases would normally affect cardiac output. Under normal conditions, the left ventricle would output 5 L/min. As diseases affect the left ventricle, its output goes down represented by the decreasing heights of the red dots. The red dots represent the physiological response of the left ventricle's cardiac output. Physiologically a bit of a paradox exists in how the heart is operating in that the heart works harder to pump out blood, but it's output is going down due to changes in the outside systems characteristics (i.e. increased resistance outside the heart) or malfunction within the pump (i.e. leaky valves). So it is important to understand that physiologically speaking two variables change when looking at how the system reacts to disease physiologically – workload AND cardiac output.

The second point to understand is that by maintaining output at a constant level for normal and diseased case simulations, the model creates a scenario where workload is no longer coupled with cardiac output in terms of the system's response to disease, allowing for a direct understanding of how workload varies under differing conditions. The green dots in Figure 46

represent the idea of how the left ventricle would operate given a constant cardiac output under differing diseased condition. The increasing distance between the red and green dots across diseases 1, 2, 3 symbolizes the increasing workload that the left ventricle must endure in order to pump out the 5 L/min output level and in turn reflects the concept of disease severity purely in terms of workload – an overarching goal of this research project.

More detailed elaboration of how heart diseases physiologically impact left ventricular operating pressures and volumes is shown in Figure 47.

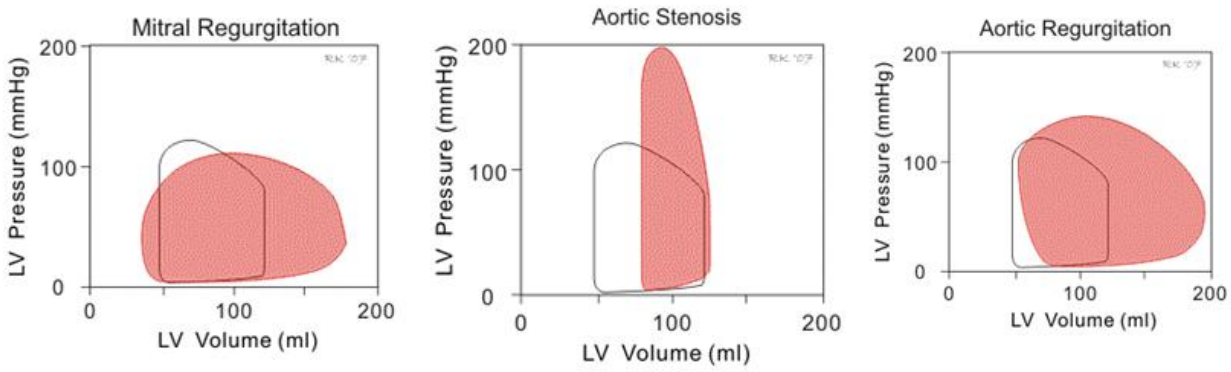

Figure 47 Pressure-volume diagrams showing the effects of mitral and aortic regurgitation, as well as aortic stenosis on left ventricular operating pressures and volumes. (Klabunde)

Mitral regurgitation (the left diagram shown in Figure 47) and aortic regurgitation (the right diagram shown in Figure 47) affect the left ventricle to work harder through volume overload so that the left ventricle's stroke volume increases to compensate for the extra blood it must pump. Aortic stenosis (center, Figure 47) affects the heart by making it pump much harder, while at the same time pumping less blood out to the body. Results of simulations of these three diseased cases will show some of the same characteristics, but will always be different because again, the heart cannot adjust its output of blood when affected by any disease.

Validation of the parameters used to develop the normal case was talked about in section 3.3 for parameters that were used to define inductance, resistance, and capacitance of the systemic circulation as well as valve resistance in the left atrium and left ventricle. Values for systemic circulation and valve resistance parameters were validated indirectly through the

adoption of values used by Korakianitis and Shi for systemic circulation and valve resistance that were validated through their own literature review for their model's development.

In section 4.3 the parameter values used to model aortic and mitral flow were validated differently through comparison of the resulting aortic and mitral flow curves developed by the model with published representations of aortic and mitral flow from literature.

In modeling diseased cases, parameter values were chosen to create diseased conditions based on the severity guidelines presented for hypertension, aortic stenosis, aortic regurgitation, and mitral regurgitation. The diseased guidelines were shown in section 1.2 and are presented again here:

Table 6 Guidelines for differentiating disease severity for hypertension, aortic stenosis, and aortic and mitral regurgitation. (Bonow 2007)

Hypertension		
	SBP mmHg	DBP mmHg
mild	120 - 139 or 80 - 89	
moderate	140 - 159 or 90 - 99	
severe	≥160 and ≥100	
Source: US Dept of Health and Human Services		

Aortic stenosis	
	Mean dP
mild	<25 mmHg
moderate	25 mmHg < dP < 40 mmHg
severe	≥40 mmHg
Source: ACC/AHA 2006 Pocket Guideline	

Mitral regurgitation	
	Regurgitant Fraction
mild	<30%
moderate	30% < RF < 49%
severe	≥50%
Source: ACC/AHA 2006 Pocket Guideline	

Aortic regurgitation	
	Regurgitant Fraction
mild	<30%
moderate	30% < RF < 49%
severe	≥50%
Source: ACC/AHA 2006 Pocket Guideline	

The method of creating a mild hypertension case is quite simply to find parameters that would create an end result where diastolic blood pressure was in the range of 80-89 mmHg or systolic blood pressure is within the range of 120-139 mmHg. In an effort to model the disease physiologically, the parameters for capacitance of arteries and resistance of capillaries were changed to represent what the disease actually does in the body.

Parameter values for mild hypertension, let alone any other disease case modeled in this research project could not be validated further and cannot be validated further than using the guidelines for heart disease severity shown above. In the case of mild hypertension, there are an infinite number of pathophysiological reasons that someone could show pressure values within the range of the guidelines set for identifying mild hypertension. All heart diseases are unique and create responses that are generalized into disease cases, mild hypertension being one of them. Reasoning follows that validation of the parameters used to simulate diseases can rely solely on only changing parameters that correspond to the area of the cardiovascular system that causes the disease that is being simulated with the resulting response of operating pressures and volumes of the left ventricle cross checked with disease severity guidelines to determine the disease severity.

4.4.1 Hypertension model results and discussion

Hypertension modeling is controlled by changing the capacitance of systemic arteries as well as adjusting capillary resistance. The following figure illustrates what mild, moderate, and severe diseased parameter values were used to create each disease case.

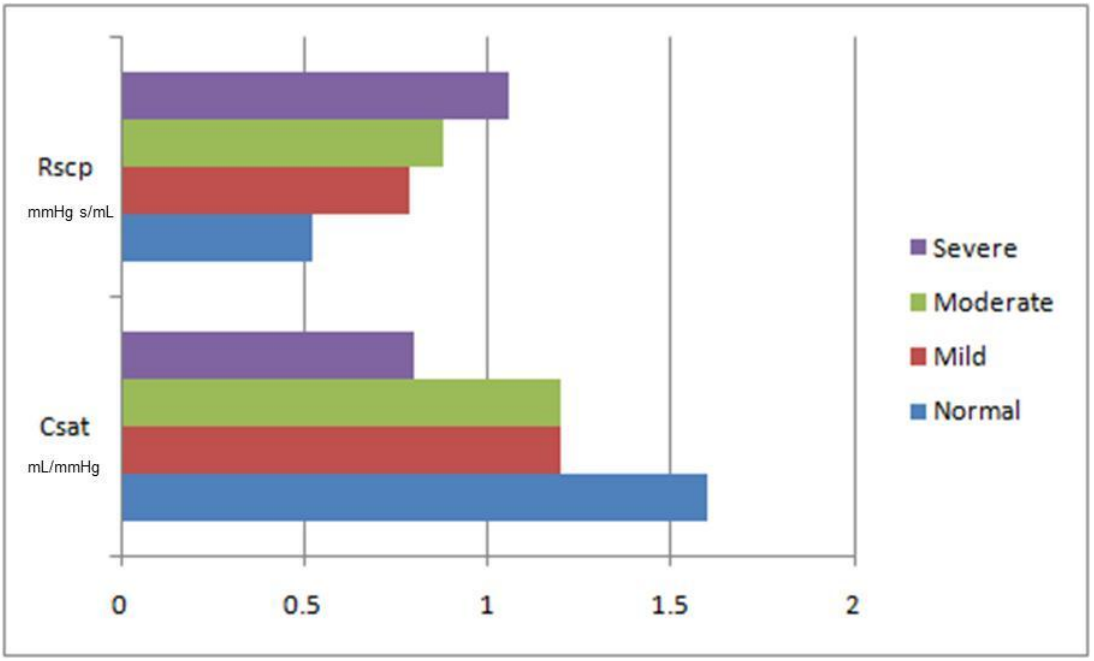

Figure 48 Parameter values reflecting mild, moderate and severe hypertension cases.

Severity of hypertension disease case increased as arterial capacitance decreased and capillary resistance increased.

Results for output dependent variables for mild, moderate, and severe hypertension cases are found on the following three pages.

The hypertension cases are cases of pressure overload on the heart. Stroke volume does not change because flow through the aortic and mitral valves does not change. Hypertension directly affects the afterload pressure that the left ventricle must pump into when it ejects blood. As systemic circulation pressure increases at the aortic sinus, the ventricle must pump harder to eject the same cardiac output. The increased rate at which the left ventricle must increase in pressure is made evident in the severe hypertension case pressure-volume loop. The slope of pressure from the beginning to the end of systole is much steeper than the normal case's pressure slope, showing that the left ventricle is pumping much harder to sustain cardiac output. Table 7 shows the work per beat increase that occurs as hypertension increases in severity.

Table 7 Workload calculation of hypertension cases.

Condition	W/b (J)	% Change
Normal	1.03	0
Hypertension		
mild	1.15	12%
moderate	1.34	30%
severe	1.51	47%

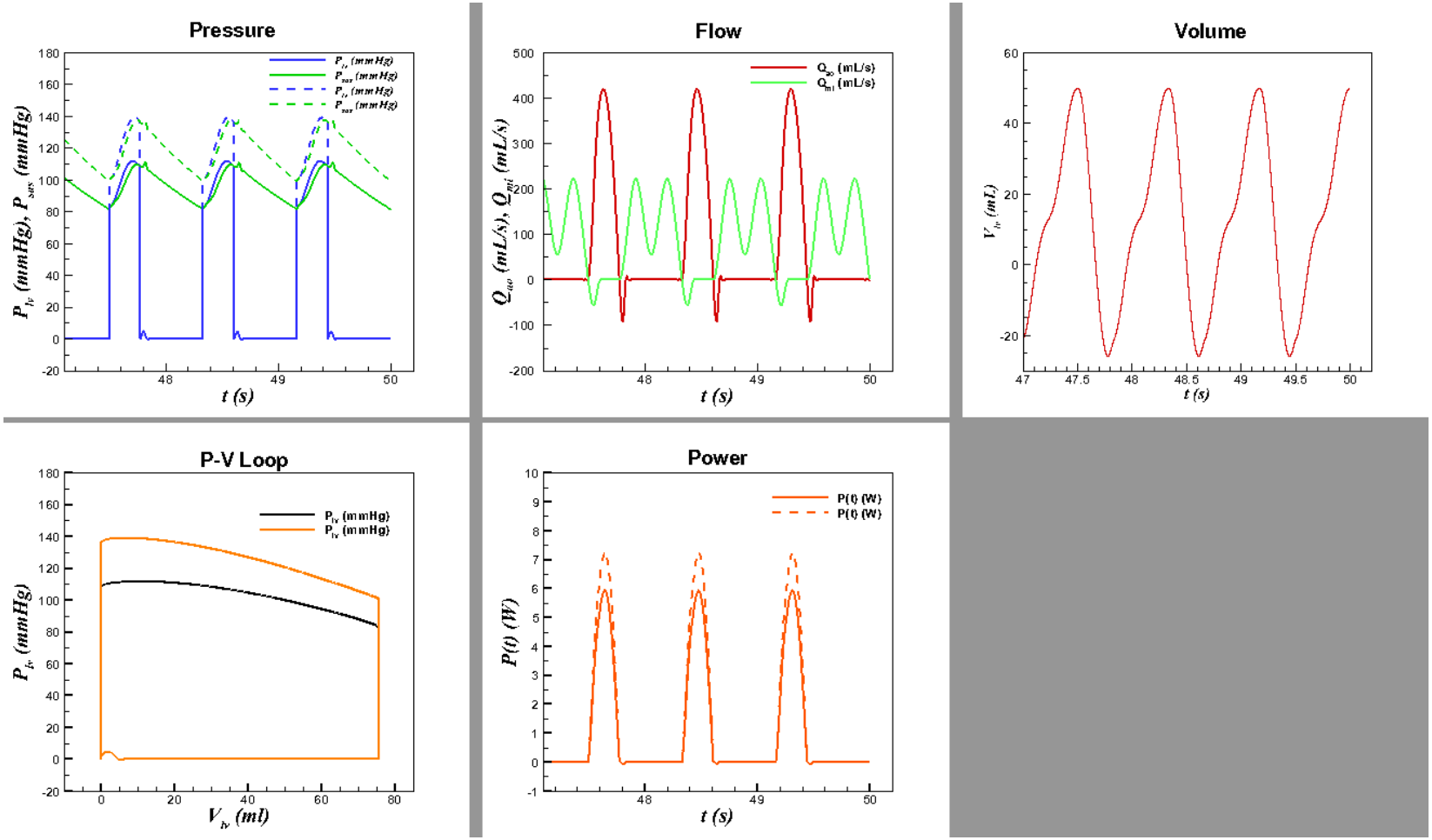

Figure 49 Results for the mild hypertension model. The pressure (upper-left hand corner) and power (bottom-middle) graphs show comparisons between mild hypertension results with the results using normal case parameters (normal case uses solid lines, diseased case uses dashed lines). The flow (top-middle) and volume (upper-right corner) graphs do not change since parameters affecting their calculation do not change to model hypertension. The P-V loop (bottom-left hand corner) shows a comparison between normal and diseased case operating pressure and volumes (normal case is in black, diseased case in orange).

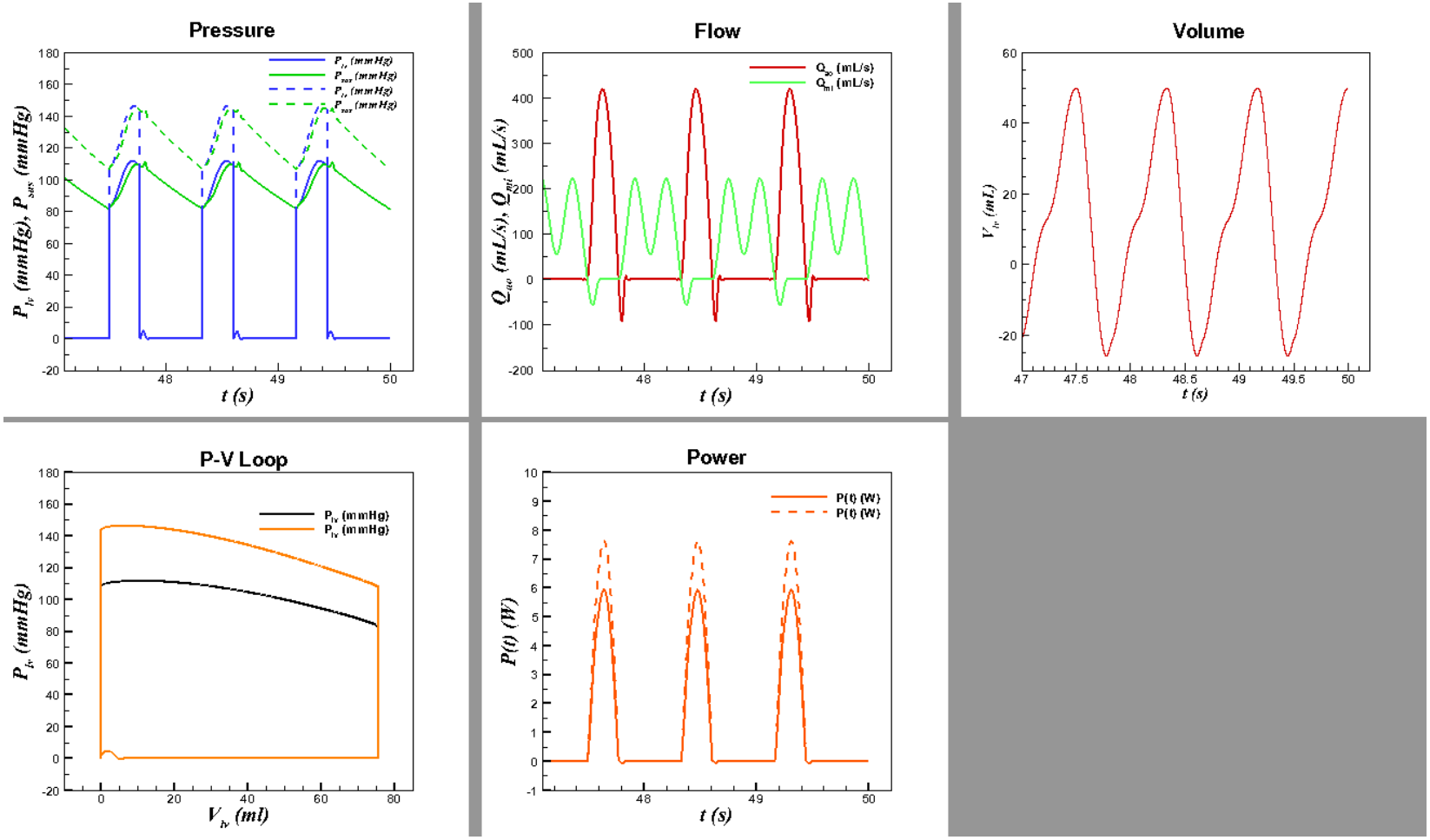

Figure 50 Results for the moderate hypertension model. The pressure (upper-left hand corner) and power (bottom-middle) graphs show comparisons between mild hypertension results with the results using normal case parameters (normal case uses solid lines, diseased case uses dashed lines). The flow (top-middle) and volume (upper-right corner) graphs do not change since parameters affecting their calculation do not change to model hypertension. The P-V loop (bottom-left hand corner) shows a comparison between normal and diseased case operating pressure and volumes (normal case is in black, diseased case in orange).

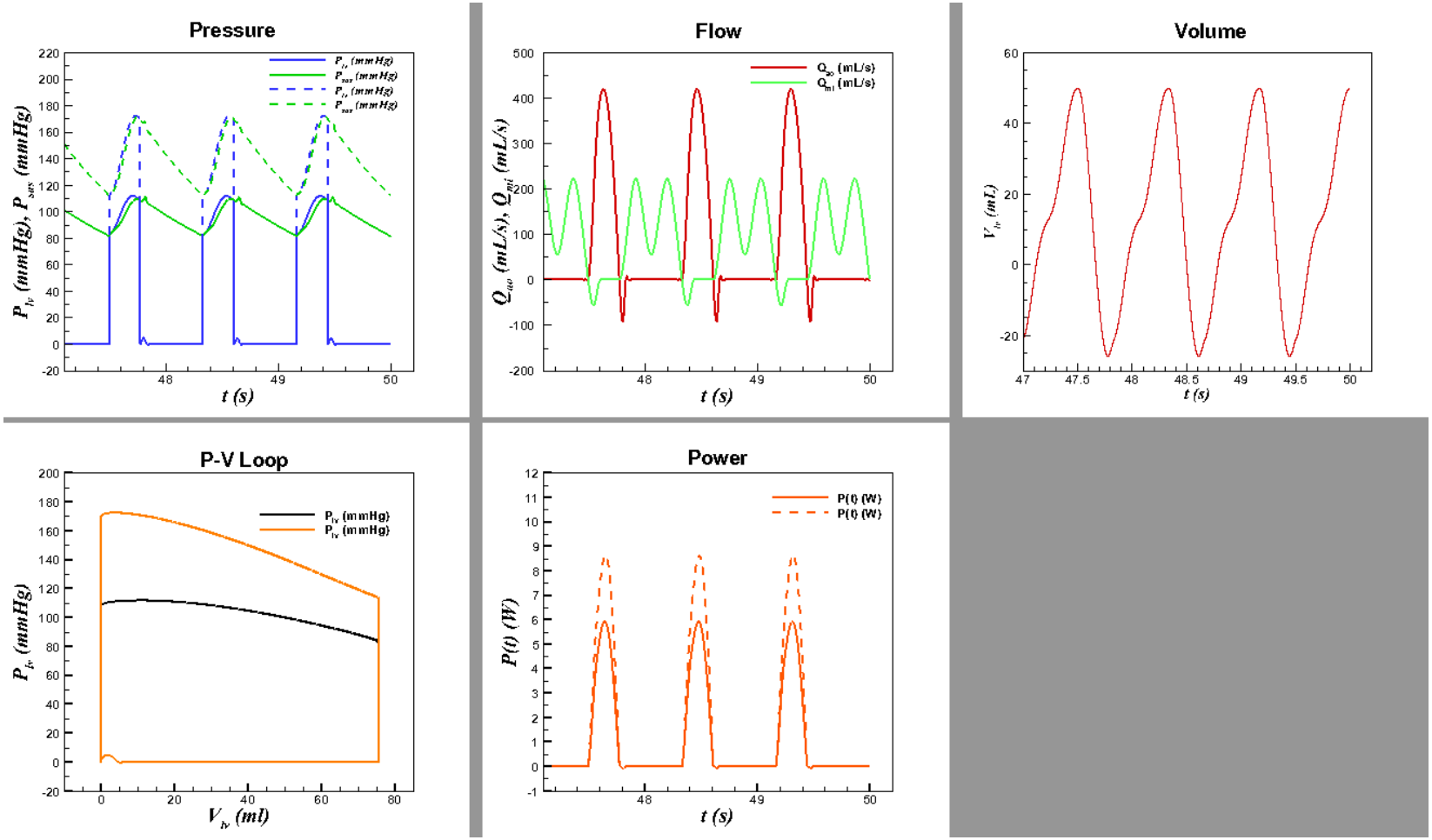

Figure 51 Results for the severe hypertension model. The pressure (upper-left hand corner) and power (bottom-middle) graphs show comparisons between mild hypertension results with the results using normal case parameters (normal case uses solid lines, diseased case uses dashed lines). The flow (top-middle) and volume (upper-right corner) graphs do not change since parameters affecting their calculation do not change to model hypertension. The P-V loop (bottom-left hand corner) shows a comparison between normal and diseased case operating pressure and volumes (normal case is in black, diseased case in orange).

4.4.2 Aortic stenosis model results and discussion

Aortic stenosis modeling is simulated by the adjustment of aortic valve resistance (CQ_{ao}). Below are the CQ_{ao} values used to create mild, moderate, and severe aortic stenosis.

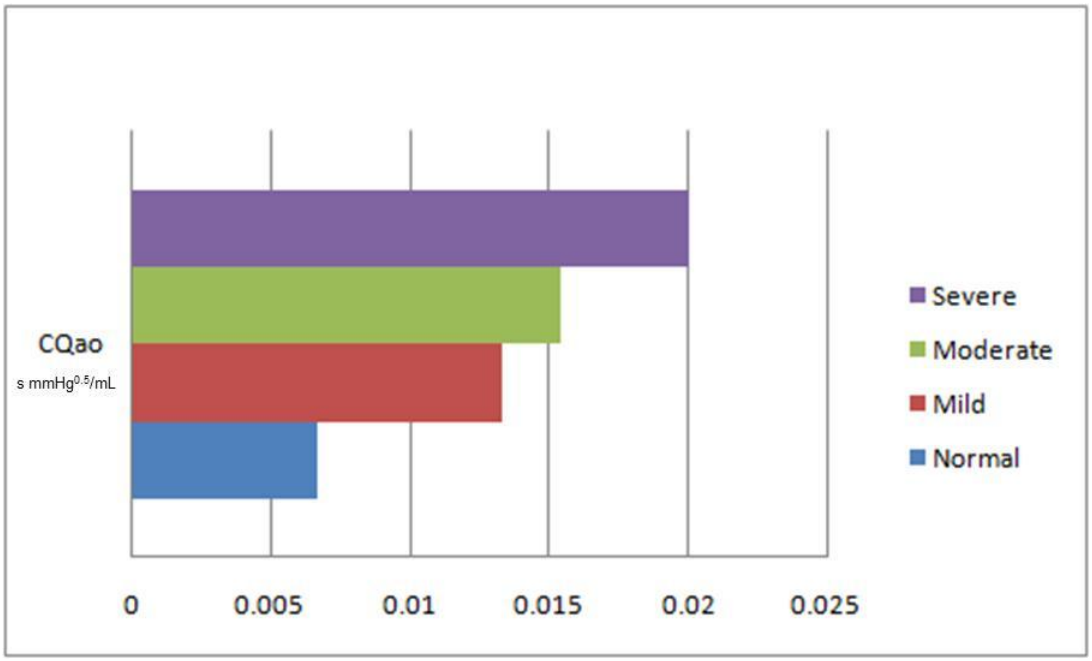

Figure 52 Parameter values reflecting mild, moderate and severe aortic stenosis cases.

As expected severity of aortic stenosis increased as aortic valve resistance increased. Graphs comparing the results for mild, moderate, and severe aortic stenosis with normal case results are found on the following three pages.

Aortic stenosis is a condition that causes the left ventricle to have to pump harder to keep its same cardiac output. As in the hypertension case, the pressure-volume diagrams for aortic stenosis show an increase in the slope of pressure per unit volume as the severity of the disease increases. There is also no increase in stroke volume as the disease increases because mitral and aortic flows are kept the same. The table below shows the work per beat outcomes for aortic stenosis cases.

Table 8 Workload calculation of normal case compared to aortic stenosis cases.

Condition	W/b (J)	% Change
Normal	1.03	0
Aortic Sten		
mild	1.19	16%
moderate	1.27	23%
severe	1.46	42%

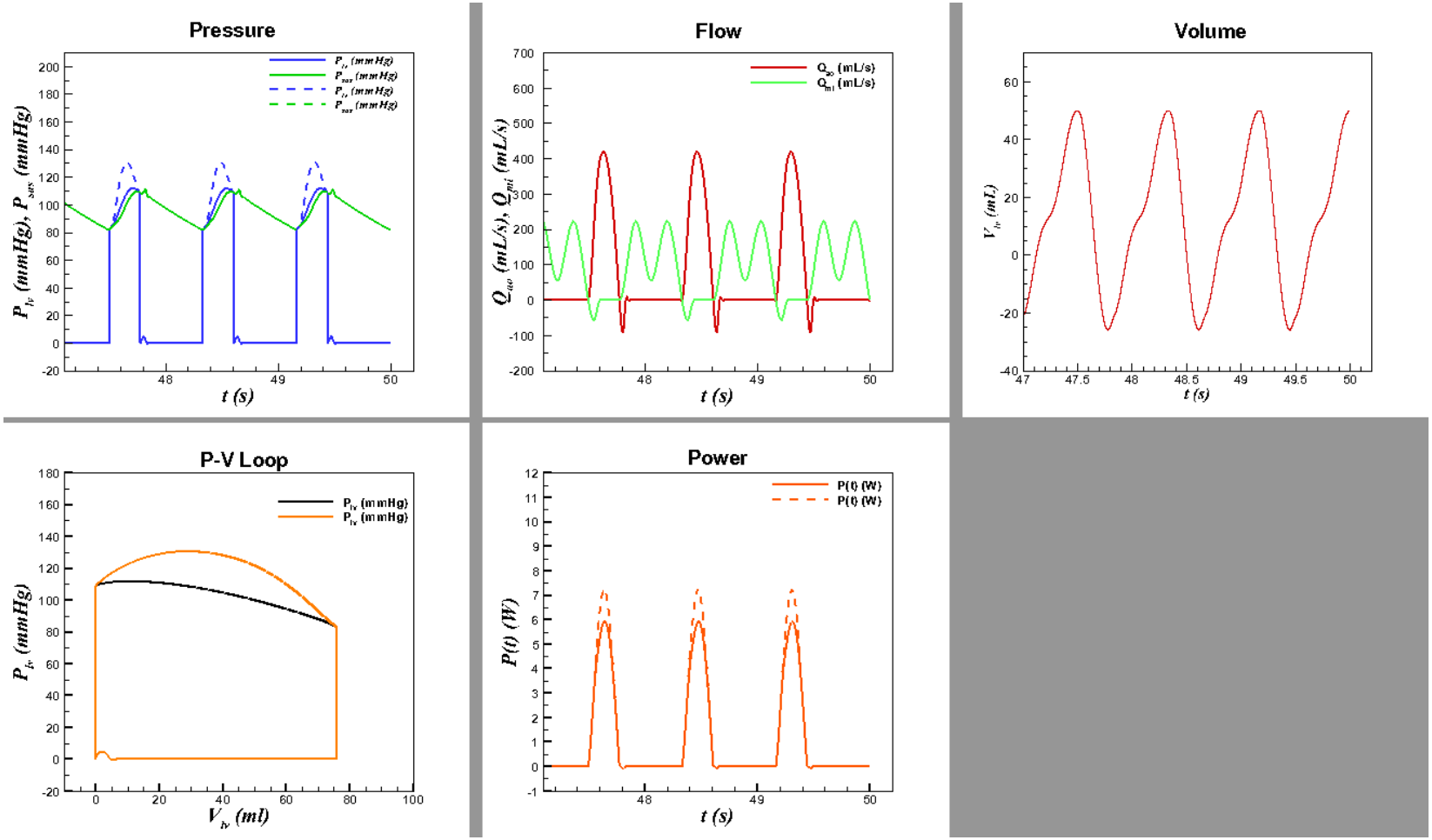

Figure 53 Results for the mild aortic stenosis model. The pressure (upper-left hand corner) and power (bottom-middle) graphs show comparisons between mild aortic stenosis results with the results using normal case parameters (normal case uses solid lines, diseased case uses dashed lines). The flow (top-middle) and volume (upper-right corner) graphs do not change since parameters affecting their calculation do not change to model aortic stenosis. The P-V loop (bottom-left hand corner) shows a comparison between normal and diseased case operating pressure and volumes (normal case is in black, diseased case in orange).

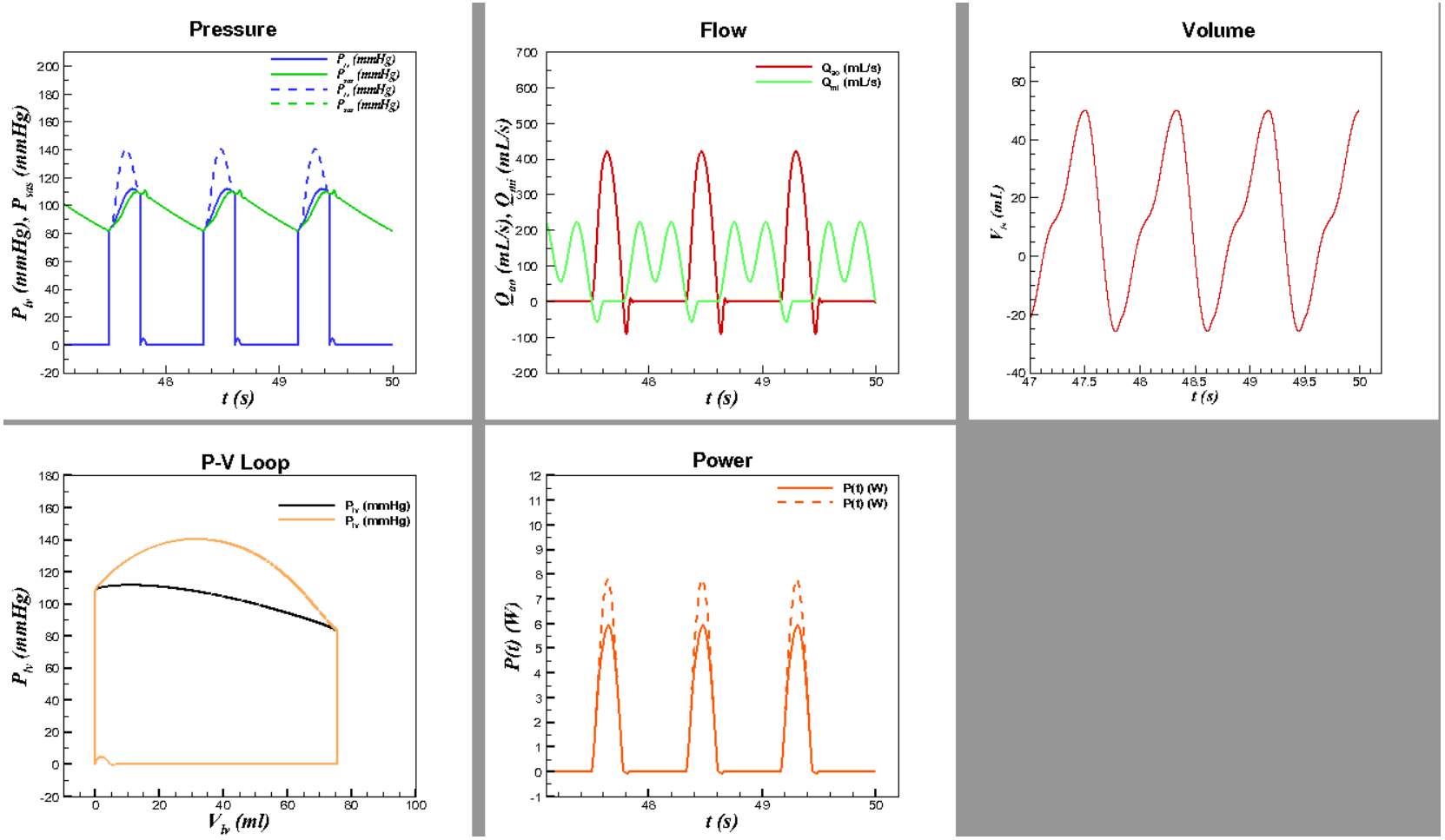

Figure 54 Results for the moderate aortic stenosis model. The pressure (upper-left hand corner) and power (bottom-middle) graphs show comparisons between mild aortic stenosis results with the results using normal case parameters (normal case uses solid lines, diseased case uses dashed lines). The flow (top-middle) and volume (upper-right corner) graphs do not change since parameters affecting their calculation do not change to model aortic stenosis. The P-V loop (bottom-left hand corner) shows a comparison between normal and diseased case operating pressure and volumes (normal case is in black, diseased case in orange).

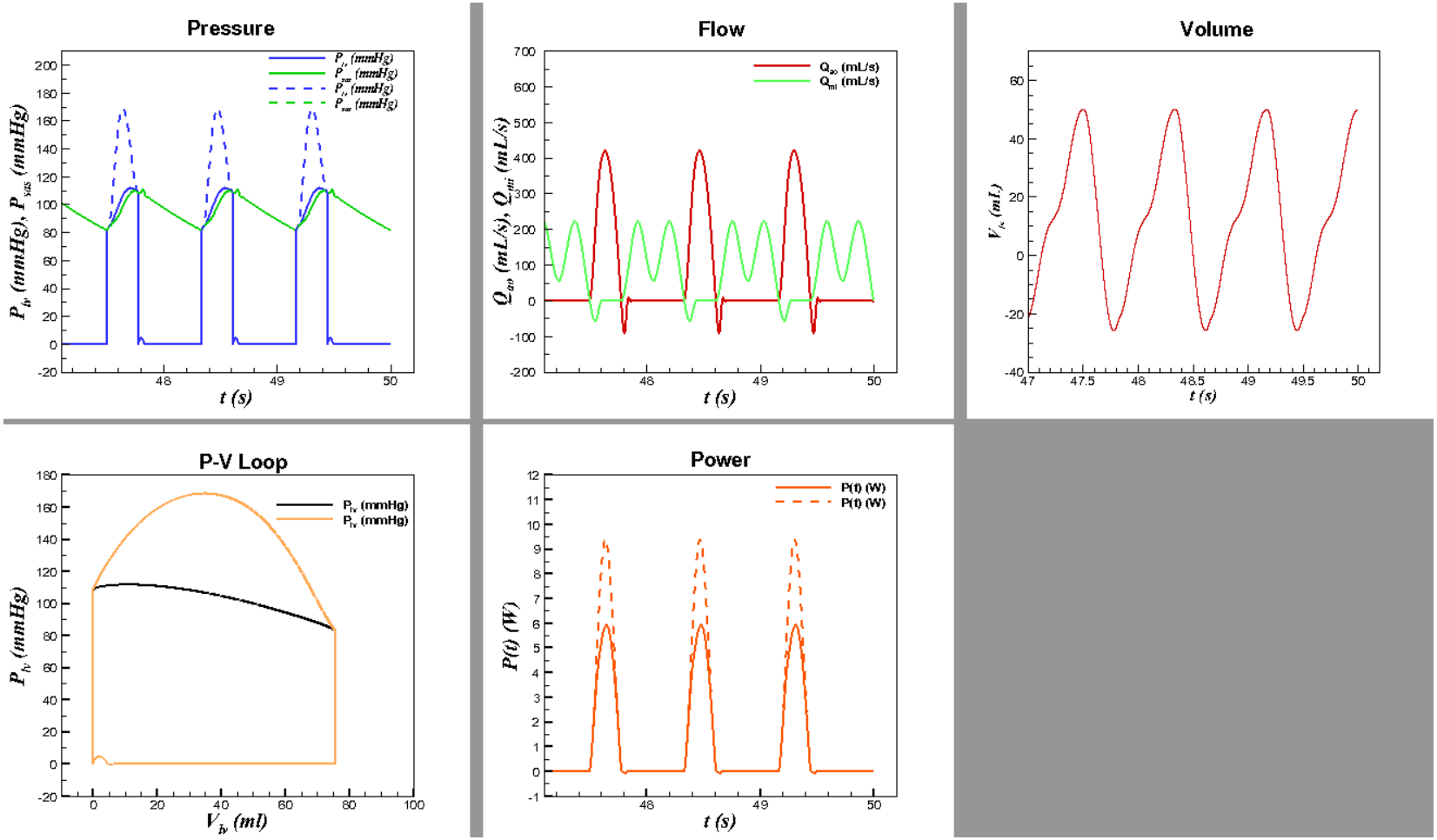

Figure 55 Results for the severe aortic stenosis model. The pressure (upper-left hand corner) and power (bottom-middle) graphs show comparisons between mild aortic stenosis results with the results using normal case parameters (normal case uses solid lines, diseased case uses dashed lines). The flow (top-middle) and volume (upper-right corner) graphs do not change since parameters affecting their calculation do not change to model aortic stenosis. The P-V loop (bottom-left hand corner) shows a comparison between normal and diseased case operating pressure and volumes (normal case is in black, diseased case in orange).

4.4.3 Aortic regurgitation model results and discussion

Modeling of aortic regurgitation is performed by adjusting the values that control regurgitation in the aortic flow function generator, the parameters B and D. Changing the value for B changes the maximum regurgitation value that occurs between the time of the end of systole and the closing of the aortic valve. Changing the value for D adjusts the amount of blood that will backflow through the aortic valve during diastole – creating a leaky valve if the value is not zero. The values of B and D always have the same offset of 0.2 between the values. No matter if the case is normal or diseases, adjusted values are always 0.2 units apart. The reasoning for the constant offset is that it makes the aortic flow look more physiological. Below are the B and D values used to simulate mild, moderate, and severe aortic regurgitation cases.

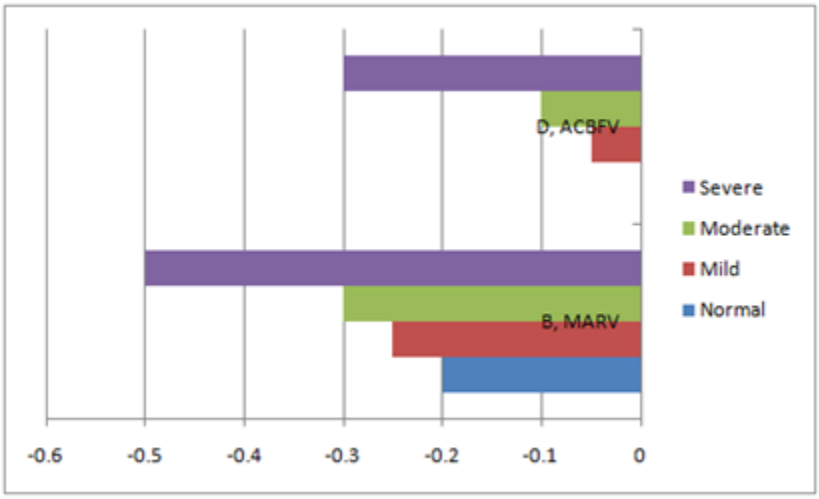

Figure 56 Parameter values reflecting mild, moderate and severe aortic regurgitation cases. The normal case has no regurgitation resulting in a zero value and no blue bar for the normal case for the D parameter value.

Graphs comparing the results for mild, moderate, and severe aortic regurgitation with normal case results are found on the following three pages.

The resulting aortic flow curves from the new parameterizations that include greater backflow as the severity of aortic regurgitation increases show how stroke volume of the left ventricle must compensate for the extra blood it must pump due to aortic valve malfunction. To

accomplish a 5 L/min cardiac output, aortic flow increases during systole to match the loss of blood that occurs during diastole due to backflow. Not only does stroke volume increase due to aortic regurgitation, but the left ventricle must pump much harder to eject the greater volume of blood now located in the left ventricle after each cycle of diastole. The combination of greater stroke volume and added pressure that the left ventricle ejects volume at due to aortic regurgitation makes the condition of aortic regurgitation the most severe of the diseased heart models. Clinically speaking, the increased operating pressure and increased stroke volume are seen in patients as shown in Figure 47 (Klabunde 2004). In terms of a complete picture of what happens physiologically, the left ventricle is forced to dilate to accommodate the extra volume it needs to make up for all the blood that leaks back after it gets pumped out through the aorta. The dilation and associated left ventricular cardiomyopathy create a pressure-volume relationship much different in shape than the one presented in the resulting aortic regurgitation simulations run using the current model. Accurate simulation of ventricular dilation is not the goal of the current model though and is therefore not addressed. Below is a tabulation of the work per beat calculations for the aortic regurgitation case models.

Table 9 Work/beat calculations for aortic regurgitation cases as well as the normal case.

Condition	W/b (J)	% Change
Normal	1.03	0
Aortic Regurg		
mild	1.28	24%
moderate	1.69	64%
severe	2.52	145%

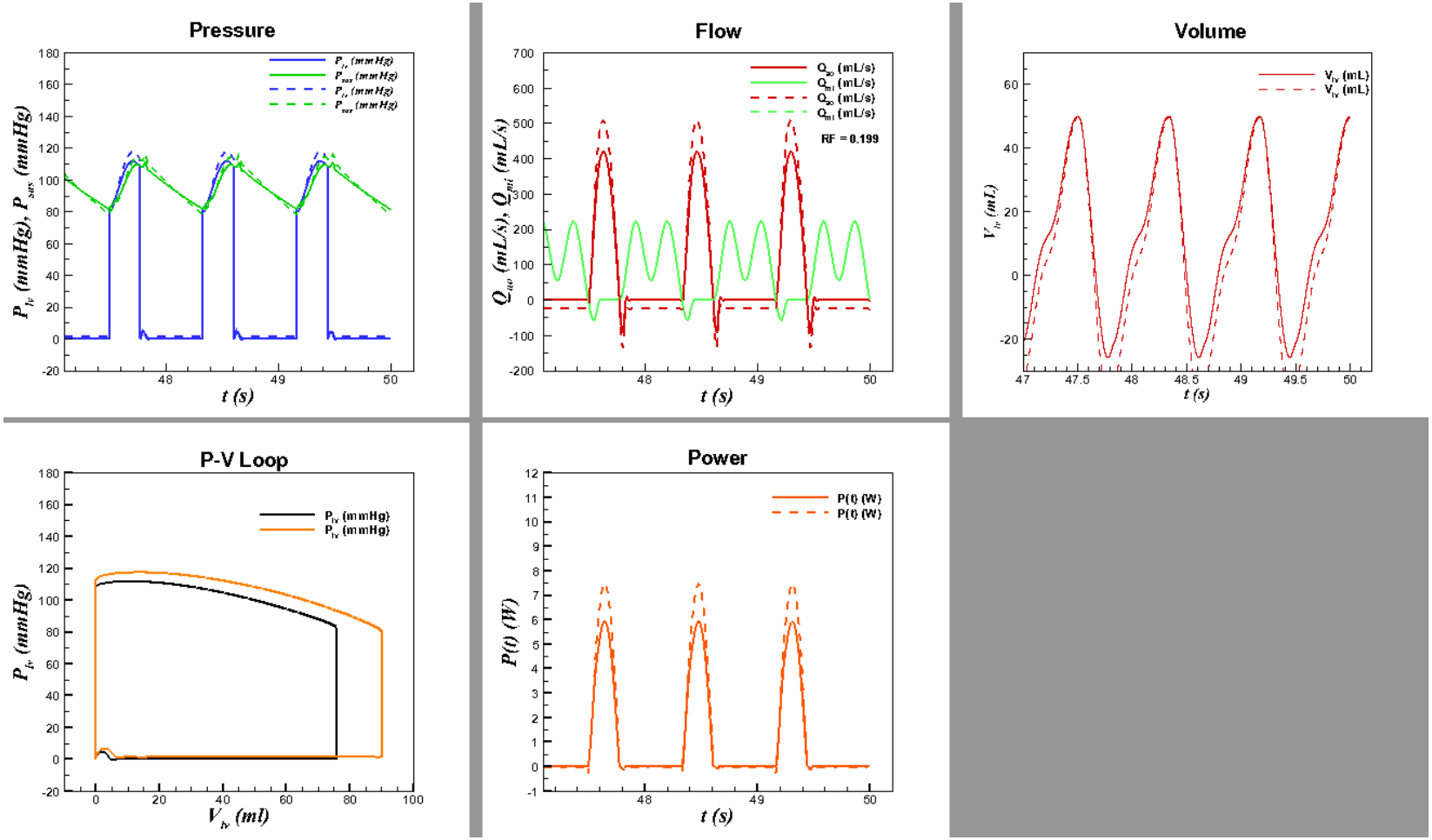

Figure 57 Results for the mild aortic regurgitation model. The pressure (upper-left hand corner), flow (upper-middle), volume (upper-right corner) and power (bottom-middle) graphs show comparisons between mild aortic regurgitation results with the results using normal case parameters (normal case uses solid lines, diseased case uses dashed lines). The P-V loop (bottom-left hand corner) shows a comparison between normal and diseased case operating pressure and volumes (normal case is in black, diseased case in orange).

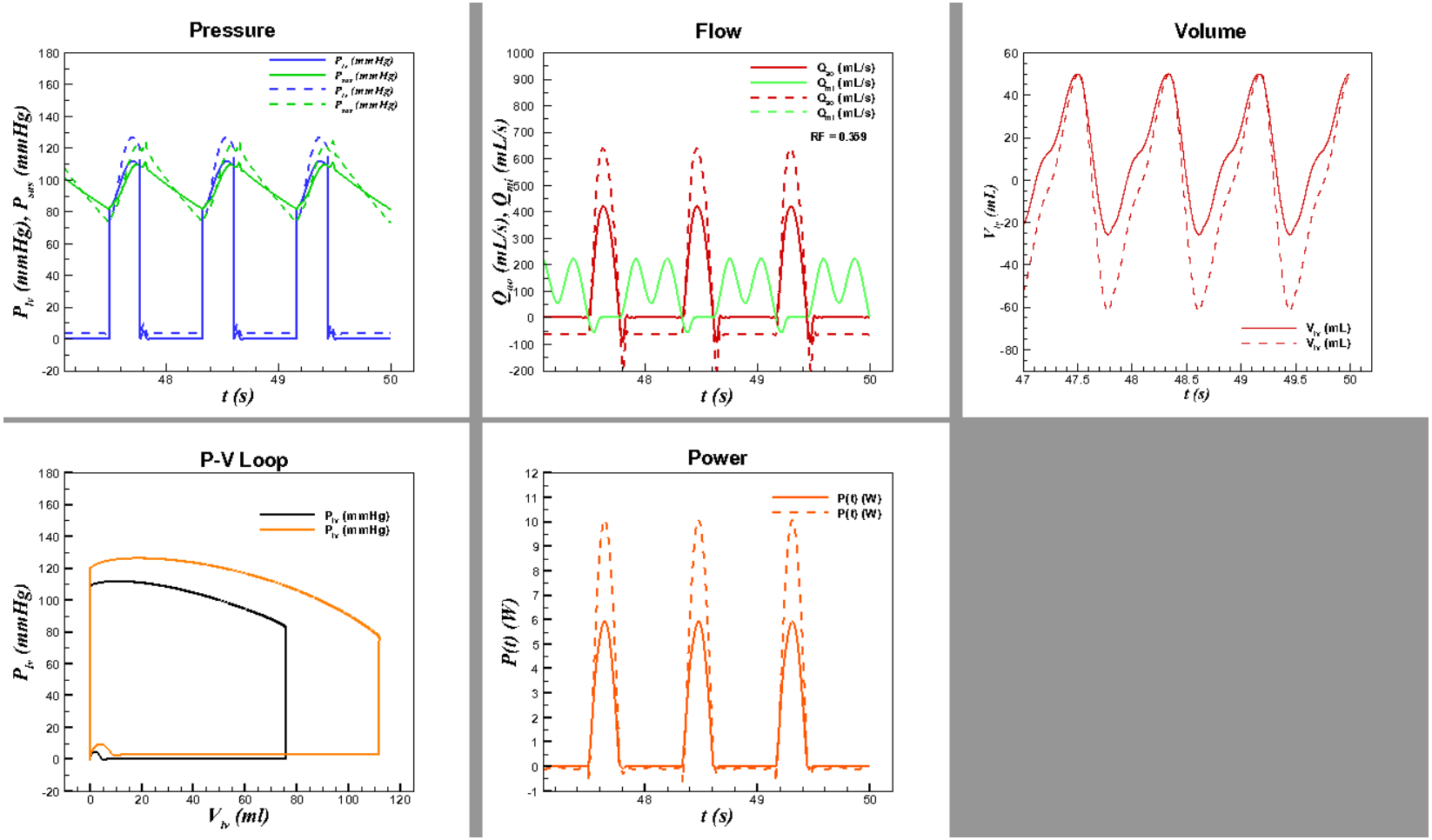

Figure 58 Results for the moderate aortic regurgitation model. The pressure (upper-left hand corner), flow (upper-middle), volume (upper-right corner) and power (bottom-middle) graphs show comparisons between moderate aortic regurgitation results with the results using normal case parameters (normal case uses solid lines, diseased case uses dashed lines). The P-V loop (bottom-left hand corner) shows a comparison between normal and diseased case operating pressure and volumes (normal case is in black, diseased case in orange).

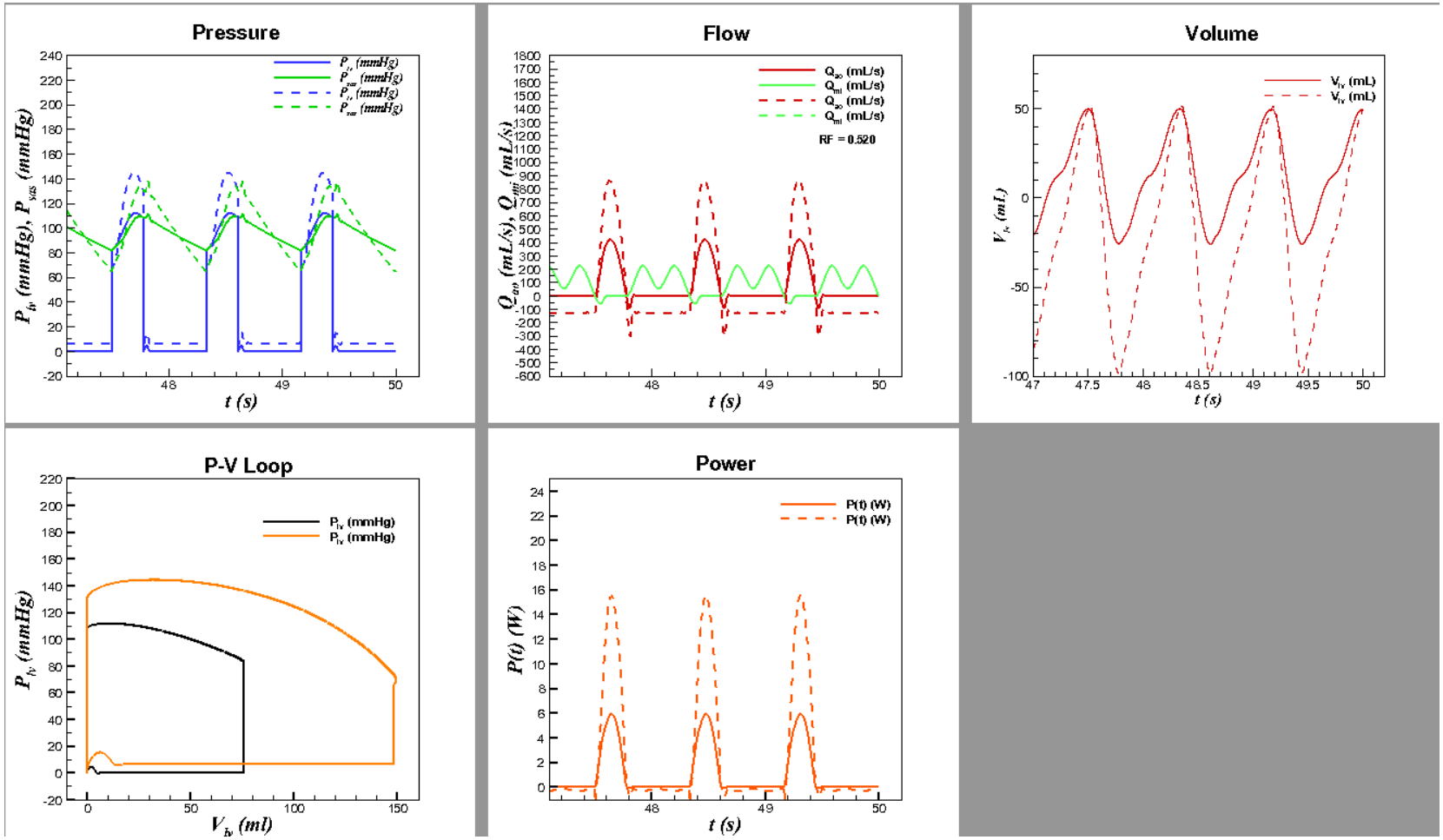

Figure 59 Results for the severe aortic regurgitation model. The pressure (upper-left hand corner), flow (upper-middle), volume (upper-right corner) and power (bottom-middle) graphs show comparisons between severe aortic regurgitation results with the results using normal case parameters (normal case uses solid lines, diseased case uses dashed lines). The P-V loop (bottom-left hand corner) shows a comparison between normal and diseased case operating pressure and volumes (normal case is in black, diseased case in orange).

4.4.4 Mitral regurgitation model results and discussion

Mitral regurgitation can be modeled similarly to how aortic regurgitation was modeled; through adjustment of parameters that affect the mitral flow function generator, the parameters C_ and D_. Changing the value for C_ changes the maximum regurgitation value that occurs between the time of the end of diastole and the closing of the mitral valve. Changing the value for D_ adjusts the amount of blood that will backflow through the mitral valve during systole. Since diastole lasts twice the amount of time as systole in the modeling, the regurgitation parameter values for mitral flow will be greater than the regurgitation values used to acquire the correct regurgitant fraction values that classify disease cases as mild, moderate, or severe. The values of C_ and D_ are always offset by 0.2 as was the case with aortic flow parameters B and D so that flow patterns would look physiologically accurate. Below are the B and D values used to simulate mild, moderate, and severe aortic regurgitation cases.

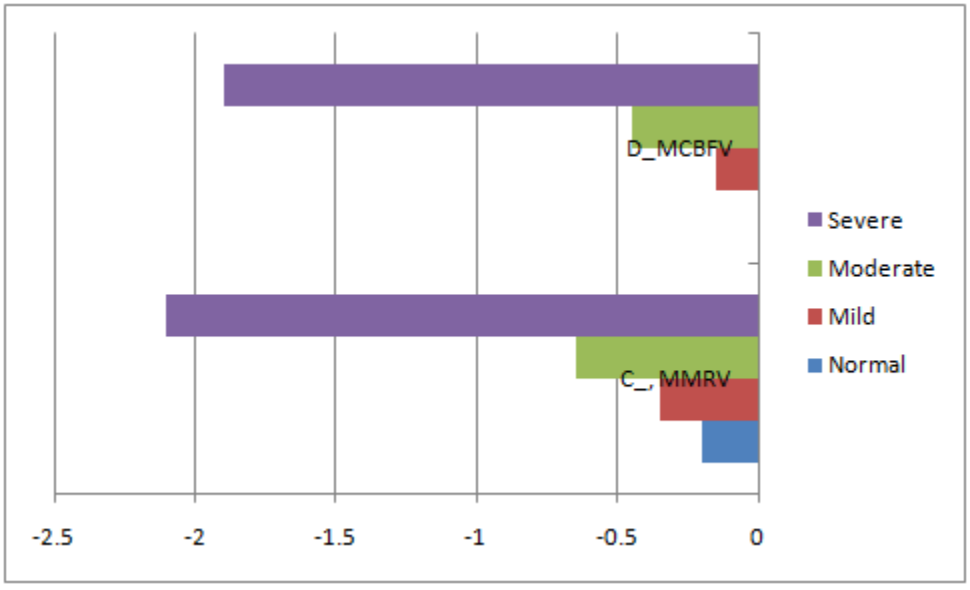

Figure 60 Parameter values reflecting mild, moderate and severe mitral regurgitation cases.

Graphs comparing the results for mild, moderate, and severe aortic regurgitation with normal case results are found on the following three pages.

To accomplish a 5 L/min cardiac output, mitral flow increases during diastole to match the loss of blood that occurs during systole due to backflow. Stroke volume of the left ventricle increases to compensate for the extra volume of blood that it must pump due to mitral regurgitation. The left ventricle also must pump harder as a result of the mitral regurgitation, but not nearly as hard as was the case for aortic regurgitation. While the left ventricle does pump harder due to mitral regurgitation, it is really the left atrium that is affected the most by the increased pressure that it must operate at to push extra blood through to the left ventricle during systole. Below is a tabulation of the work per beat calculations for the mitral regurgitation case models.

Table 10 Work/beat calculations for mitral regurgitation cases as well as the normal case.

Condition	W/b (J)	% Change
Normal	1.03	0
Mitral Regurg		
mild	1.23	19%
moderate	1.65	60%
severe	2.51	144%

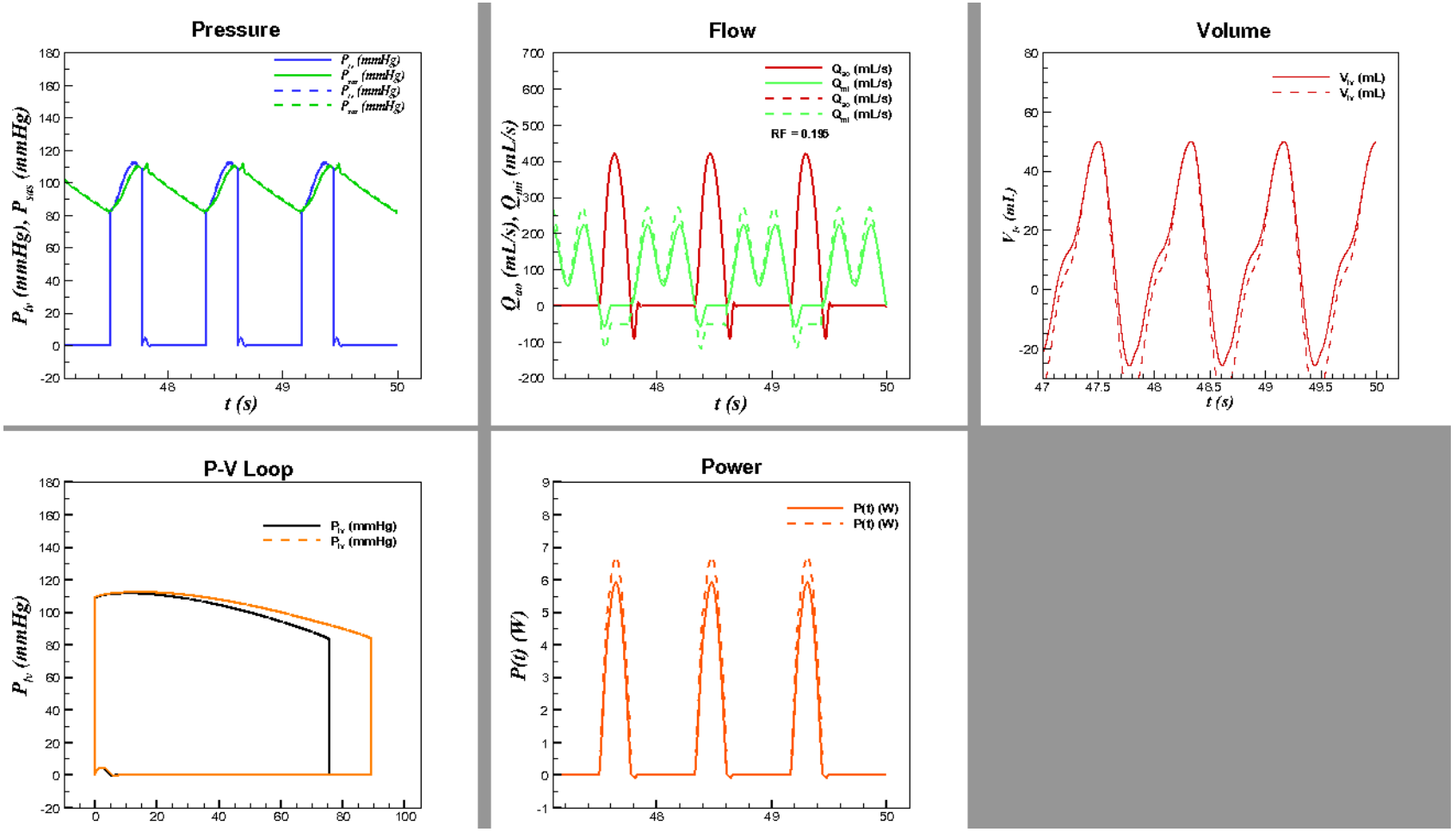

Figure 61 Results for the mild mitral regurgitation model. The pressure (upper-left hand corner), flow (upper-middle), volume (upper-right corner) and power (bottom-middle) graphs show comparisons between mild mitral regurgitation results with the results using normal case parameters (normal case uses solid lines, diseased case uses dashed lines). The P-V loop (bottom-left hand corner) shows a comparison between normal and diseased case operating pressure and volumes (normal case is in black, diseased case in orange).

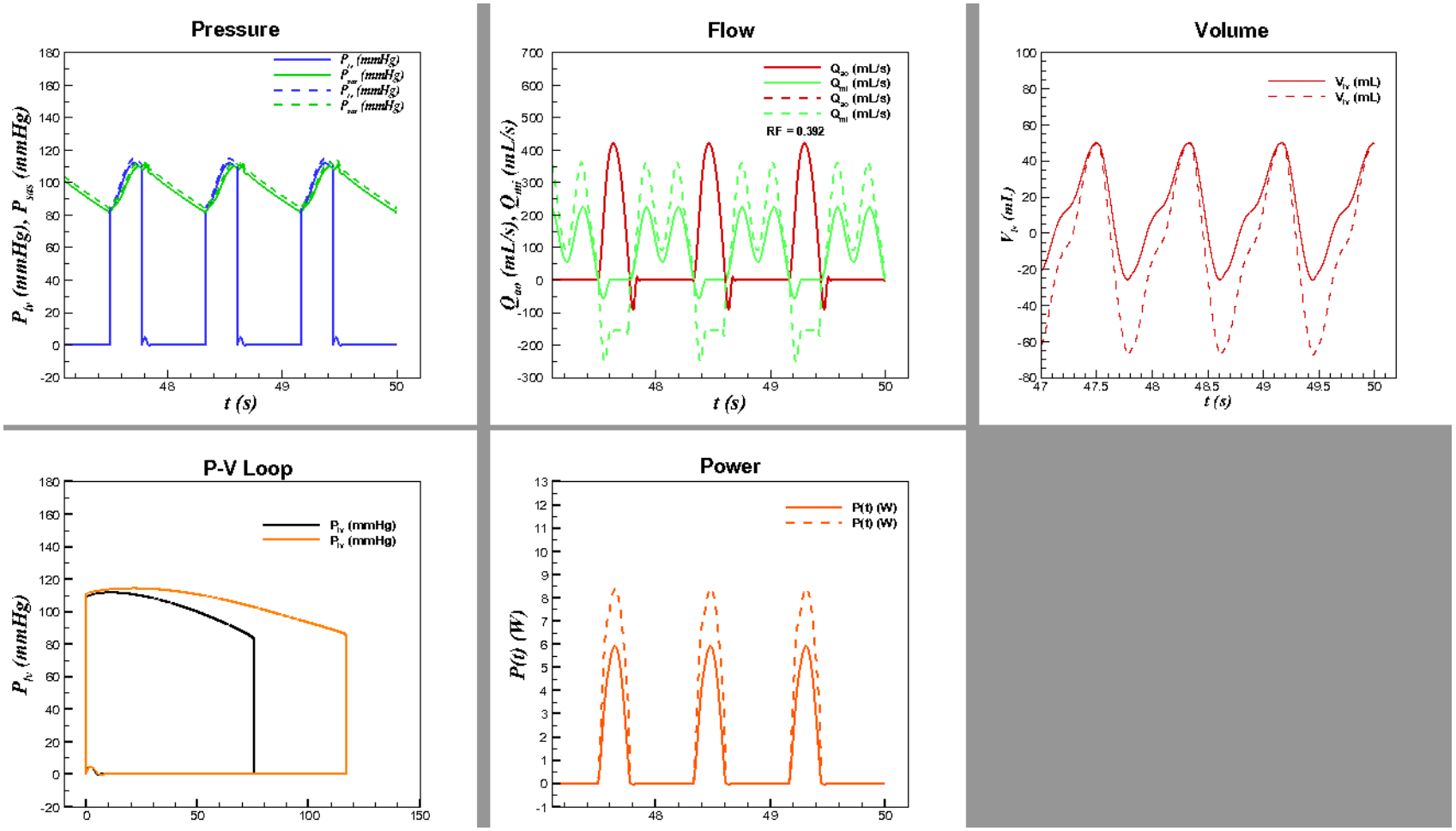

Figure 62 Results for the moderate mitral regurgitation model. The pressure (upper-left hand corner), flow (upper-middle), volume (upper-right corner) and power (bottom-middle) graphs show comparisons between moderate mitral regurgitation results with the results using normal case parameters (normal case uses solid lines, diseased case uses dashed lines). The P-V loop (bottom-left hand corner) shows a comparison between normal and diseased case operating pressure and volumes (normal case is in black, diseased case in orange).

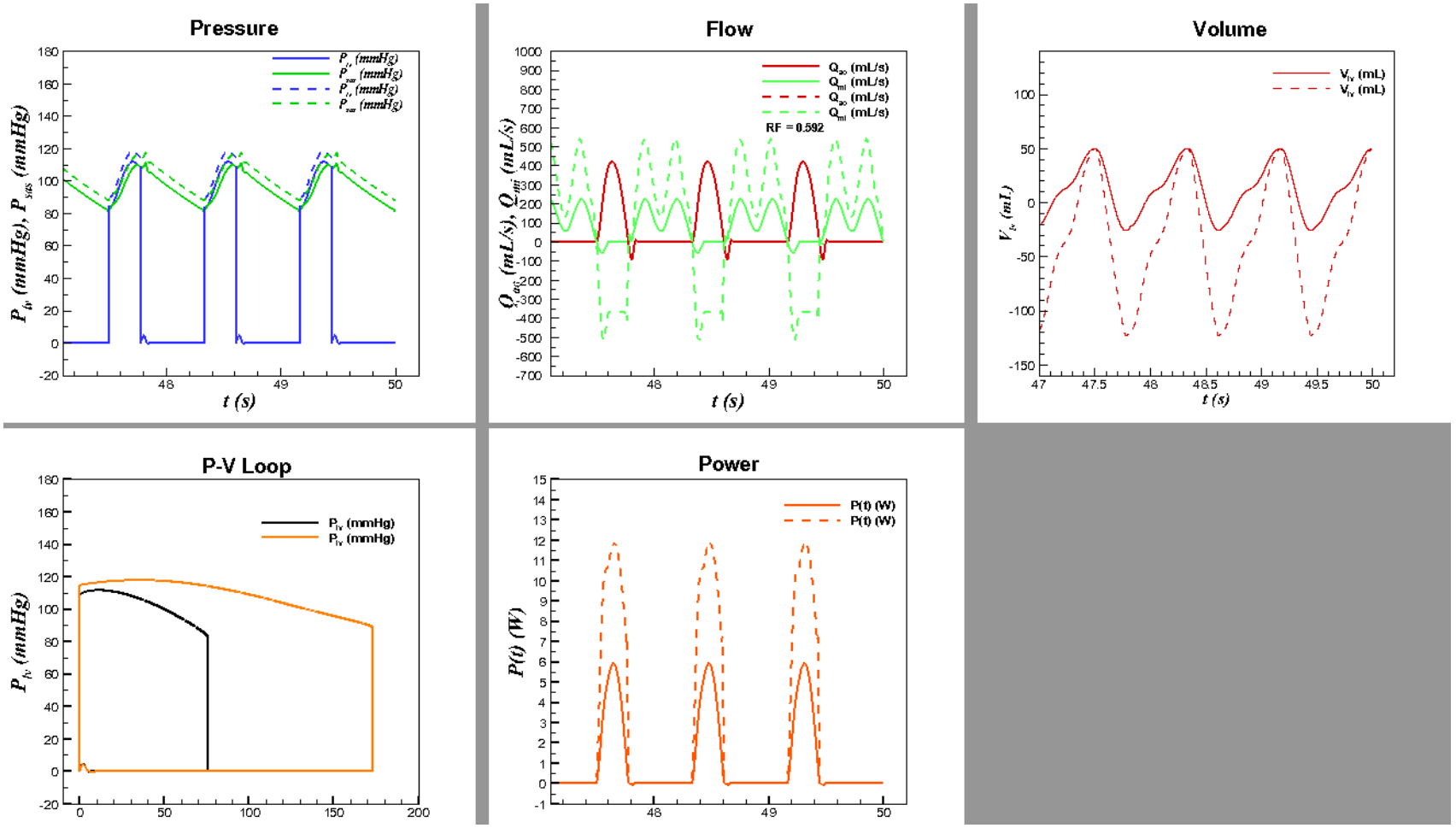

Figure 63 Results for the severe mitral regurgitation model. The pressure (upper-left hand corner), flow (upper-middle), volume (upper-right corner) and power (bottom-middle) graphs show comparisons between severe mitral regurgitation results with the results using normal case parameters (normal case uses solid lines, diseased case uses dashed lines). The P-V loop (bottom-left hand corner) shows a comparison between normal and diseased case operating pressure and volumes (normal case is in black, diseased case in orange).

With the four disease cases modeled according to severity, the following chart illustrates the workload increase that was tabulated as disease severity changed for the diseases modeled.

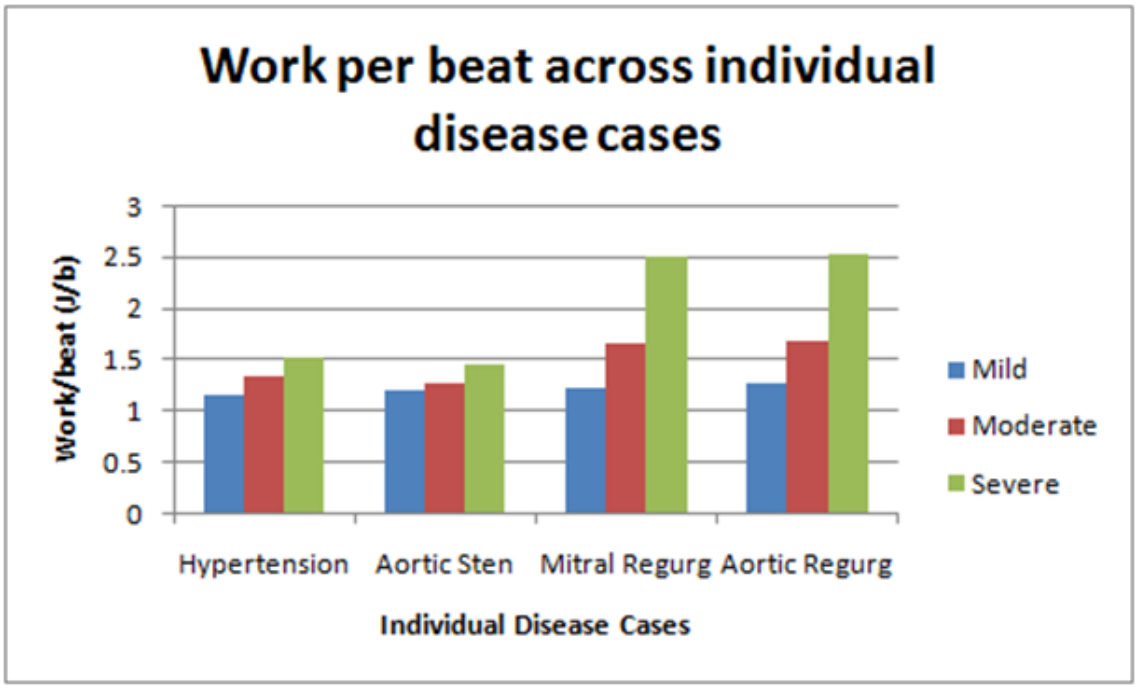

Figure 64 Work per beat comparison for disease severity across all four diseases models.

The diseases modeled that used pressure overload to overwork the heart increased left ventricle workload somewhat linearly as severity of the disease worsened. Diseases that worked through volume overload saw an increase in work that was uniform as well as disease severity worsened, but was much more non-linear in terms of added workload on the left ventricle.

Pressure overload disease cases only affect the left ventricle with increased operating pressures. When disease severity increases it is only because of pressure and workload increase happens linearly due to the linearity of pressure increase that the disease guidelines stipulate. Showing the portion of Table 1that only shows pressure overload disease case guidelines below, the linearity in workload increase is directly related to the fact that the guidelines for hypertension and aortic stenosis severity increase in a linear fashion. For hypertension, severity increases every 20 mmHg systolic blood pressure and for aortic stenosis severity increases at 25 and 40 mmHg pressure drop difference between left ventricle and aortic sinus. Since the guidelines for disease

severity create a scenario where left ventricle workload becomes a function of how severity is defined, the pressure overload cases create a linear and uniform increase in workload as diseases increase in severity due to how pressure guidelines give linear and uniform increases in pressure values.

Hypertension		
	SBP mmHg	DBP mmHg
mild	120 - 139 or 80 - 89	
moderate	140 - 159 or 90 - 99	
severe	≥160 and ≥100	
Source: US Dept of Health and Human Services		

Aortic stenosis	
	Mean dP
mild	<25 mmHg
moderate	25 mmHg < dP < 40 mmHg
severe	≥40 mmHg
Source: ACC/AHA 2006 Pocket Guideline	

Volume overload cases create the same scenario of making workload increase a function of what guidelines stipulate as mild, moderate and severe. Figure 64 shows that workload increase, while very similar as disease severity increases within volume overload diseases, is much more non-linear than pressure overload disease counterparts. Volume overload creates non-linear increases in workload as severity increases because volume overload does not only change the stroke volume of the left ventricle to increase workload, it also creates higher operating pressures for the left ventricle that also adds to the increased workload of the ventricle. The combined effect of added volume and pressure that is not accounted for in the severity guidelines for volume overload cases is the reason for the non-linear workload increase seen within pressure overload cases. The most drastic change in workload is visible in the severe aortic regurgitation case and is mainly a product of the guideline that severe aortic regurgitation occurs at 60% regurgitation of total volume. The 60% volume backflow forces the left ventricle to work incredibly hard, it's stroke volume is more than two times greater in the severe case of aortic regurgitation than it is during normal operation, and it's operating pressure increases to a level that would be considered moderately severe, making the energy cost to maintain a 5 L/min output of blood incredibly high as compared to pressure overload cases of severe left ventricular diseases.

When workload increase is studied across disease cases it can be concluded that increase in disease severity using disease guideline stipulations does not equal the same increase in workload depending on the disease affecting the left ventricle. Stepping up from a moderate to severe pressure overload disease does not involve the same workload commitment by the heart as does stepping up from a moderate to severe volume overload disease. The results from the severe aortic regurgitation model place an especially important spotlight on aortic and mitral regurgitation guidelines to adapt regurgitant fraction guidelines that are more in tune with workload cost and not purely added stroke volume costs.

4.3.5 Combined disease model results and discussion

The combined disease models represent the combination of mild disease parameters for two diseases modeled together. In all there are 6 combined disease cases:

Table 11 Combined disease cases simulated by the current model grouped by how each model overloads the heart.

Combined Disease Cases		
Pressure overload	Volume overload	Pressure and volume overload
Mild aortic stenosis and mild hypertension	Mild mitral regurgitation and mild aortic regurgitation	Mild aortic stenosis and mild aortic regurgitation
		Mild aortic stenosis and mild mitral regurgitation
		Mild hypertension and mild aortic regurgitation
		Mild hypertension and mild mitral regurgitation

The parameters used for combined case of mild aortic stenosis with mild aortic regurgitation are below:

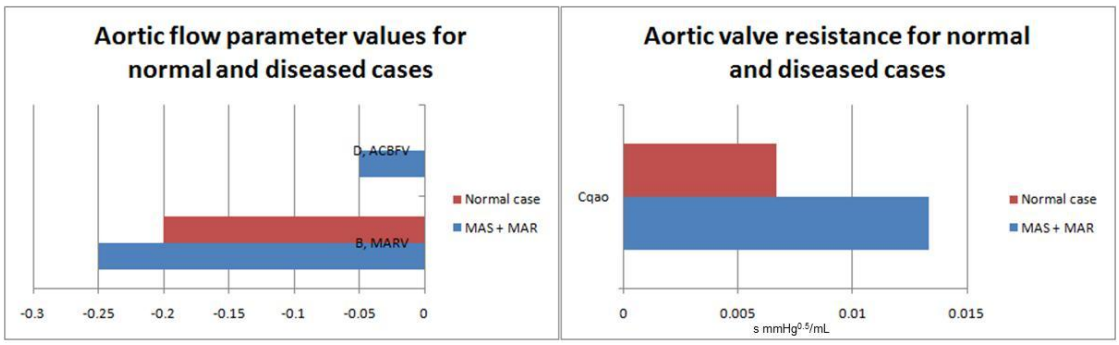

Figure 65 Normal and combined disease parameters for mild aortic stenosis and mild aortic regurgitation.

The combined mild aortic stenosis/mild aortic regurgitation model has pressure overload and volume overload characteristics, reflecting the added stroke volume created by the aortic regurgitation, and the increased resistance through the left ventricle which forces the left ventricle to pump harder. Pressure volume diagrams of illustrating the added stroke volume and increased operating pressure of the mild aortic stenosis/mild aortic regurgitation model are shown below.

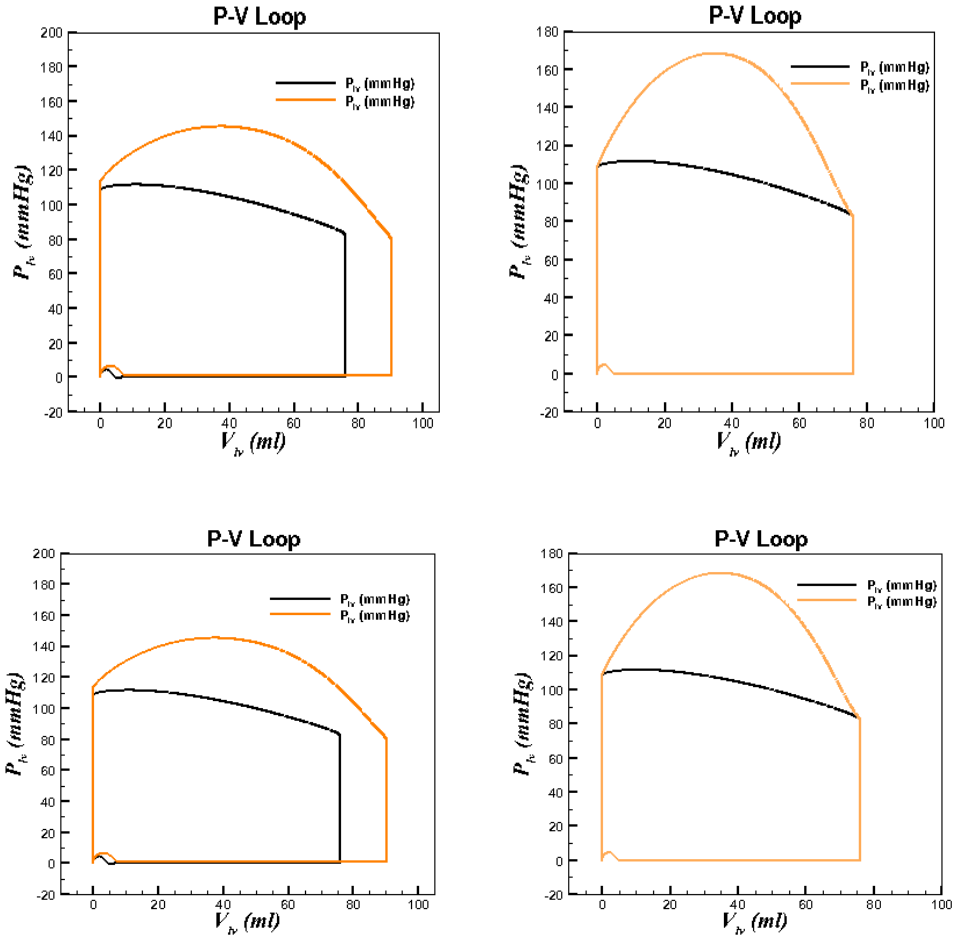

Figure 66 Pressure volume diagrams comparing p-v loops of mild aortic stenosis/mild aortic regurgitation (left column) with severe aortic stenosis (row 1, column 2) and severe aortic regurgitation (row 2, column 2).

The calculated work per beat for the mild aortic stenosis/mild aortic regurgitation case was 1.56 J/beat, an increase of 51% workload compared to the normal case workload. The increase of 51% workload was tied for the greatest increase in workload for all combined disease cases modeled, and was greater than the workload increase of the severest cases of pressure overload diseases modeled.

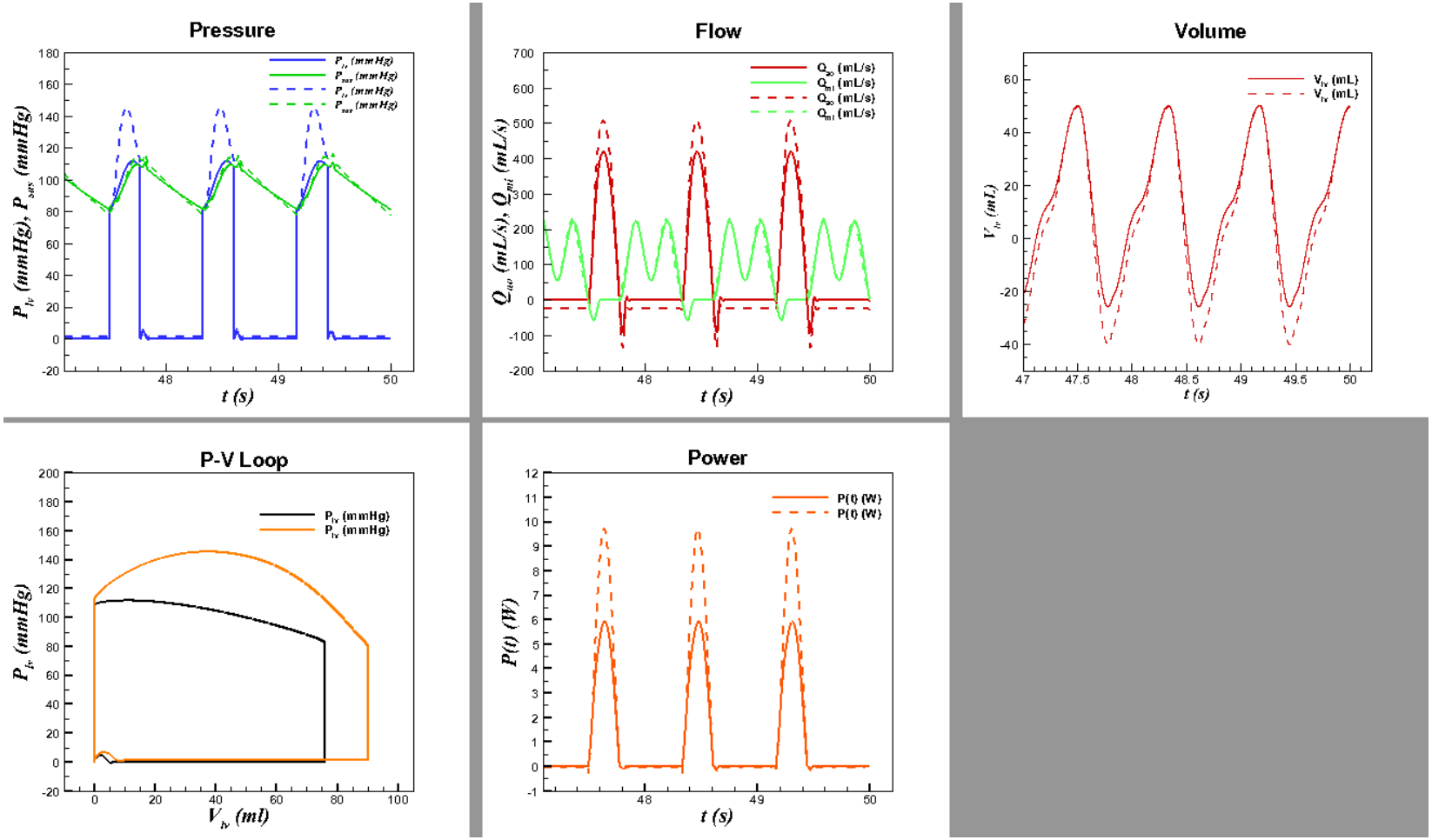

Figure 67 Results for the combined mild aortic stenosis/mild aortic regurgitation model. The pressure (upper-left hand corner), flow (upper-middle), volume (upper-right corner) and power (bottom-middle) graphs show comparisons between the combined disease case results with the results using normal case parameters (normal case uses solid lines, diseased case uses dashed lines). The P-V loop (bottom-left hand corner) shows a comparison between normal and diseased case operating pressure and volumes (normal case is in black, diseased case in orange).

The second case of pressure and volume overload working together in the combined disease models is mild aortic stenosis and mild mitral regurgitation case. The parameters used for the model are shown below:

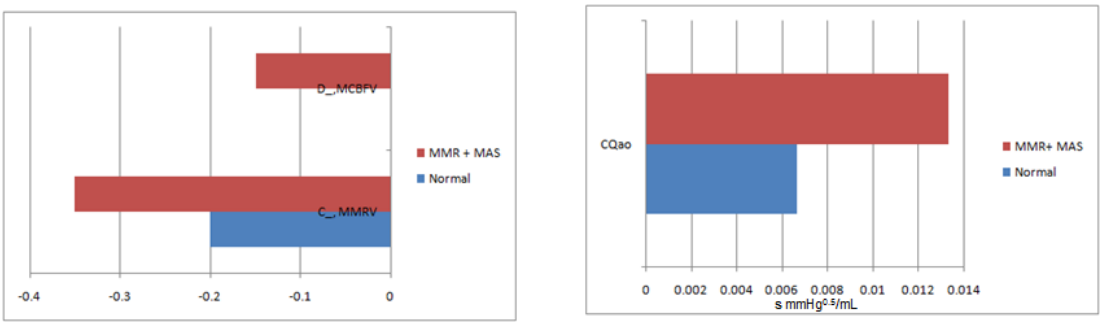

Figure 68 Parameter values used to conduct the mild mitral regurgitation and mild aortic stenosis disease model.

The mild aortic stenosis and mild mitral regurgitation case pressure-volume diagram shows how the added stroke volume caused by mitral regurgitation combined with the greater left ventricle operating pressure caused by aortic stenosis increases heart workload per beat. In all, workload increased 32% in the mild aortic stenosis and mild mitral regurgitation case. The 32% workload increase was the lowest increase in workload for all combined disease cases modeled.

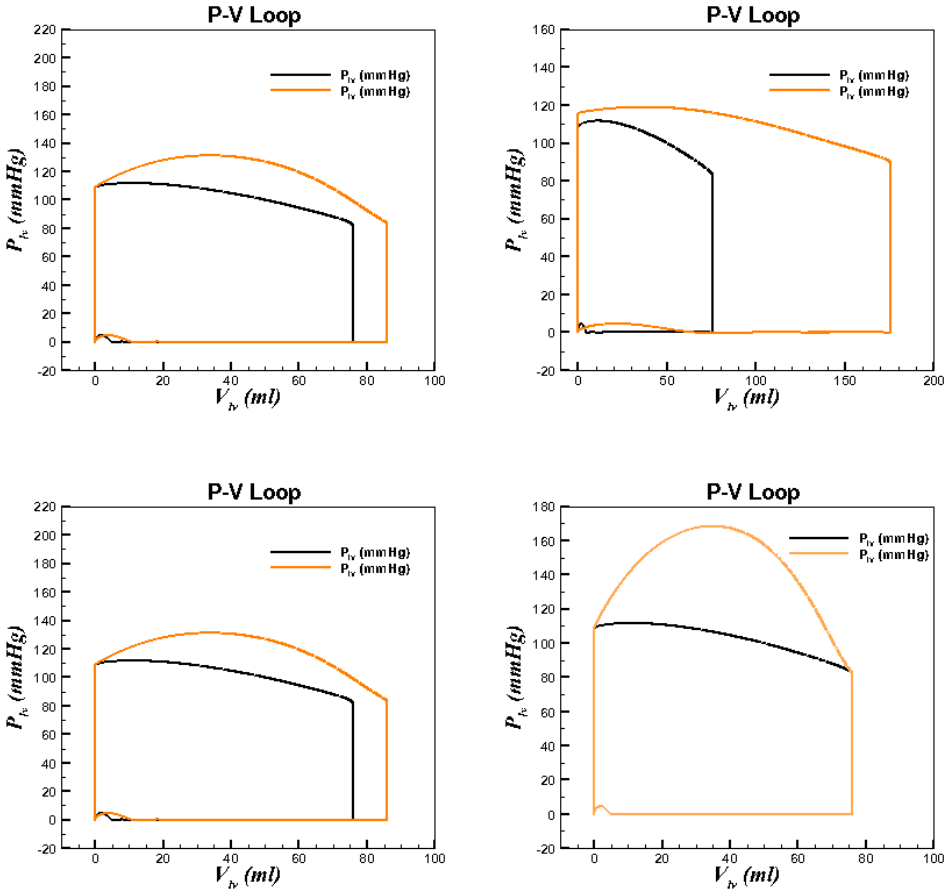

Figure 69 Pressure volume diagrams comparing p-v loops of mild aortic stenosis/mild mitral regurgitation (left column) with severe mitral regurgitation (row 1, column 2) and severe aortic stenosis (row 2, column 2).

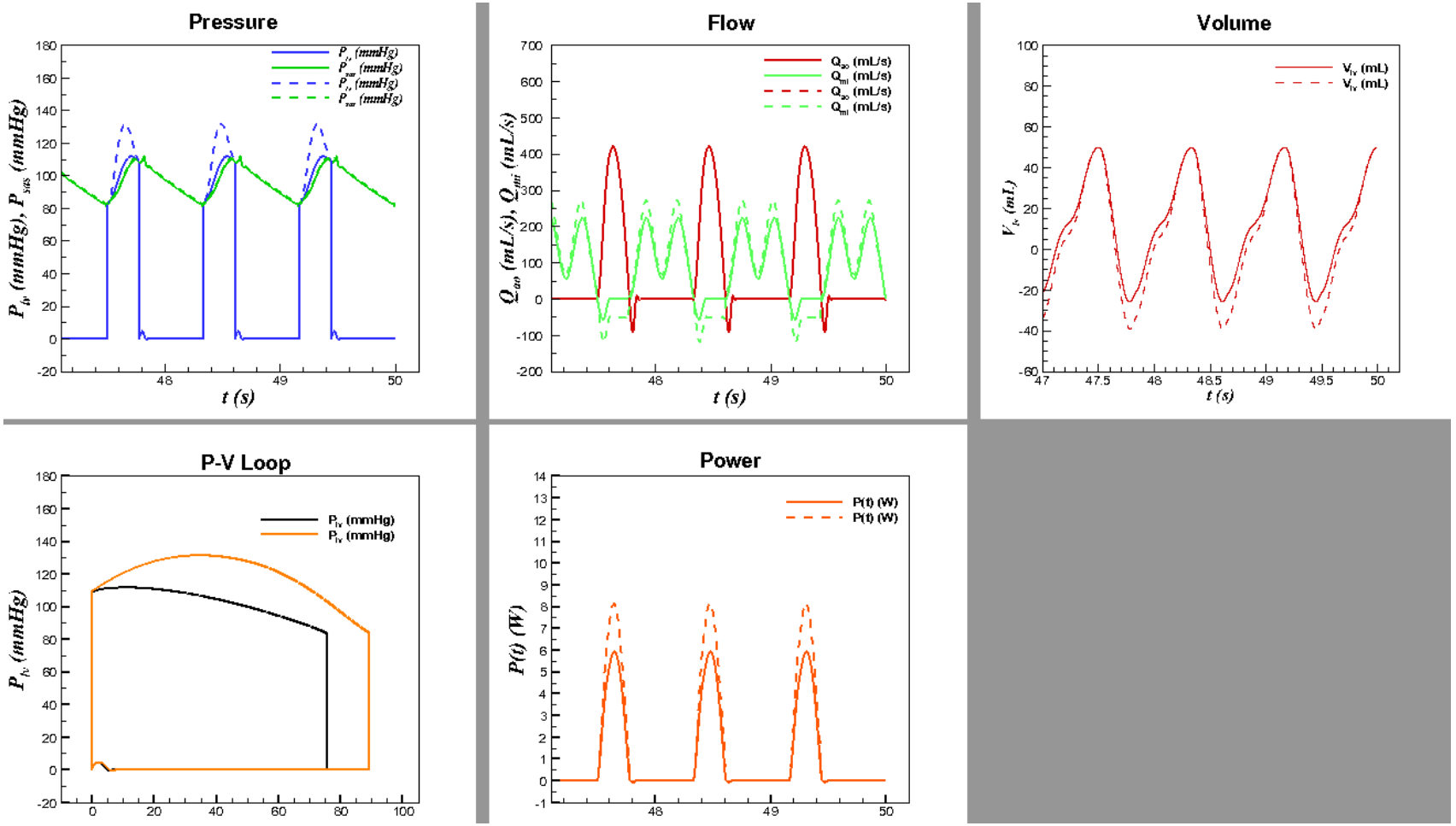

Figure 70 Results for the combined mild aortic stenosis/mild mitral regurgitation model. The pressure (upper-left hand corner), flow (upper-middle), volume (upper-right corner) and power (bottom-middle) graphs show comparisons between the combined disease case results with the results using normal case parameters (normal case uses solid lines, diseased case uses dashed lines). The P-V loop (bottom-left hand corner) shows a comparison between normal and diseased case operating pressure and volumes (normal case is in black, diseased case in orange).

The next case of pressure and volume overload working together in the combined disease case modeling is examined in the mild hypertension and mild aortic regurgitation case. Mild hypertension creates the pressure overload and mild aortic regurgitation the mild volume overload. The parameters used to simulate the combined case are in the figure below:

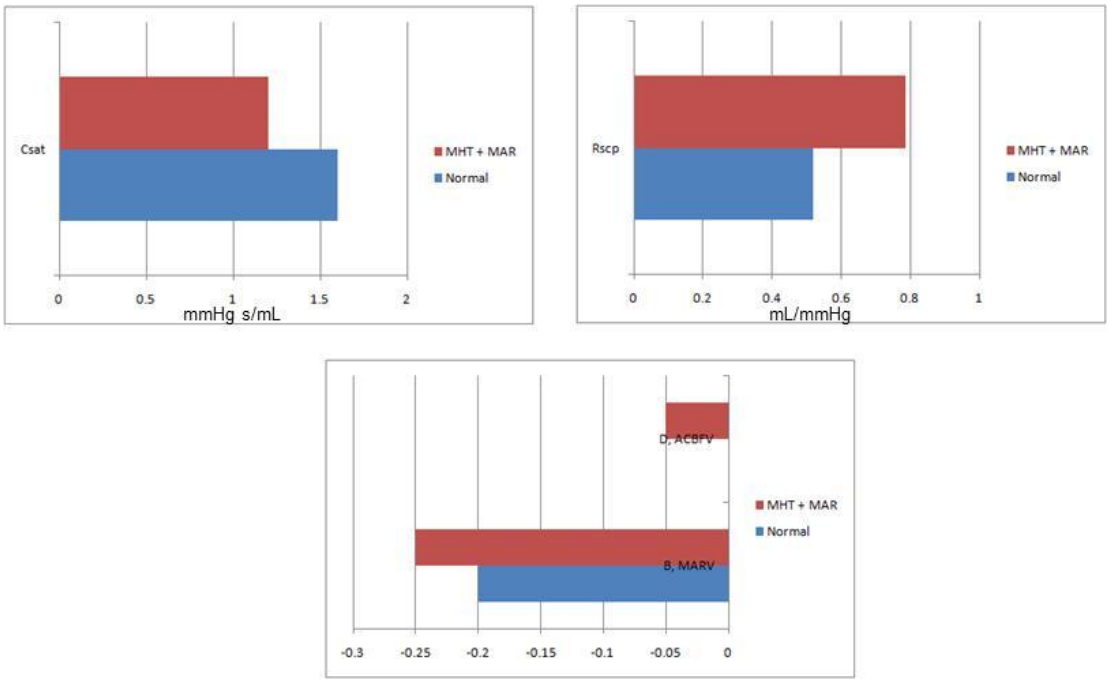

Figure 71 Parameters used to model mild hypertension with mild aortic regurgitation.

The PV-diagram for the mild hypertension mild aortic regurgitation case shows the increased operating pressure the left ventricle is forced to work at due to hypertension as well as the increased stroke volume caused by the aortic regurgitation. Aortic regurgitation, although labeled a volume overload disease, does cause significant work to be done due to added pressure it causes the left ventricle to perform to eject the added regurgitant blood that leaks every cycle. The added pressure work that the left ventricle has to perform, added with the extra pressure work created by hypertension as well as the noted volume work creates an extra workload of +51% compared to the normal case. The workload seen for the combined mild hypertension and mild aortic regurgitation case is the greatest increase in workload caused by any of the combined cases

examined. The increase of 51% in workload was greater than the two severe cases of pressure overload diseases individually modeled, severe aortic stenosis (+42%) and severe hypertension (+47%), meaning that the combined case mild aortic regurgitation and mild hypertension form a formidable force in endangering the onset of congestive heart failure while at the same time not appearing severe under either of the pressure or volume overload guidelines.

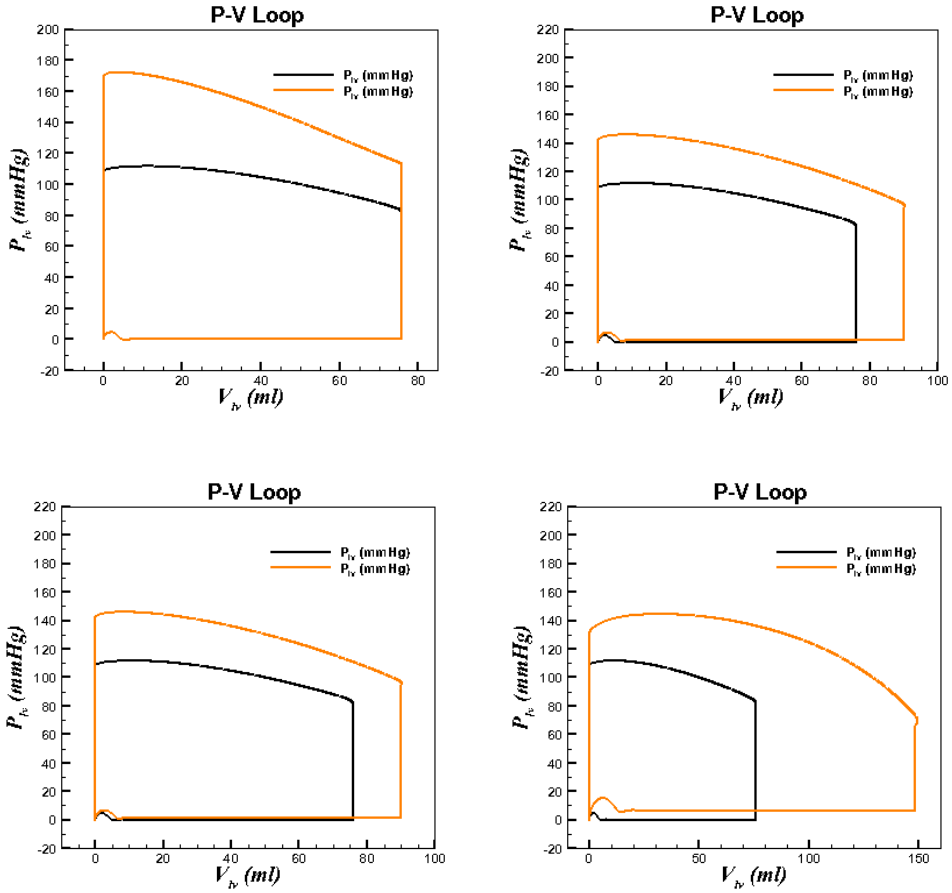

Figure 72 Pressure volume diagrams comparing p-v loops of mild hypertension/mild aortic regurgitation (left column) with severe hypertension (row 1, column 2) and severe aortic regurgitation (row 2, column 2).

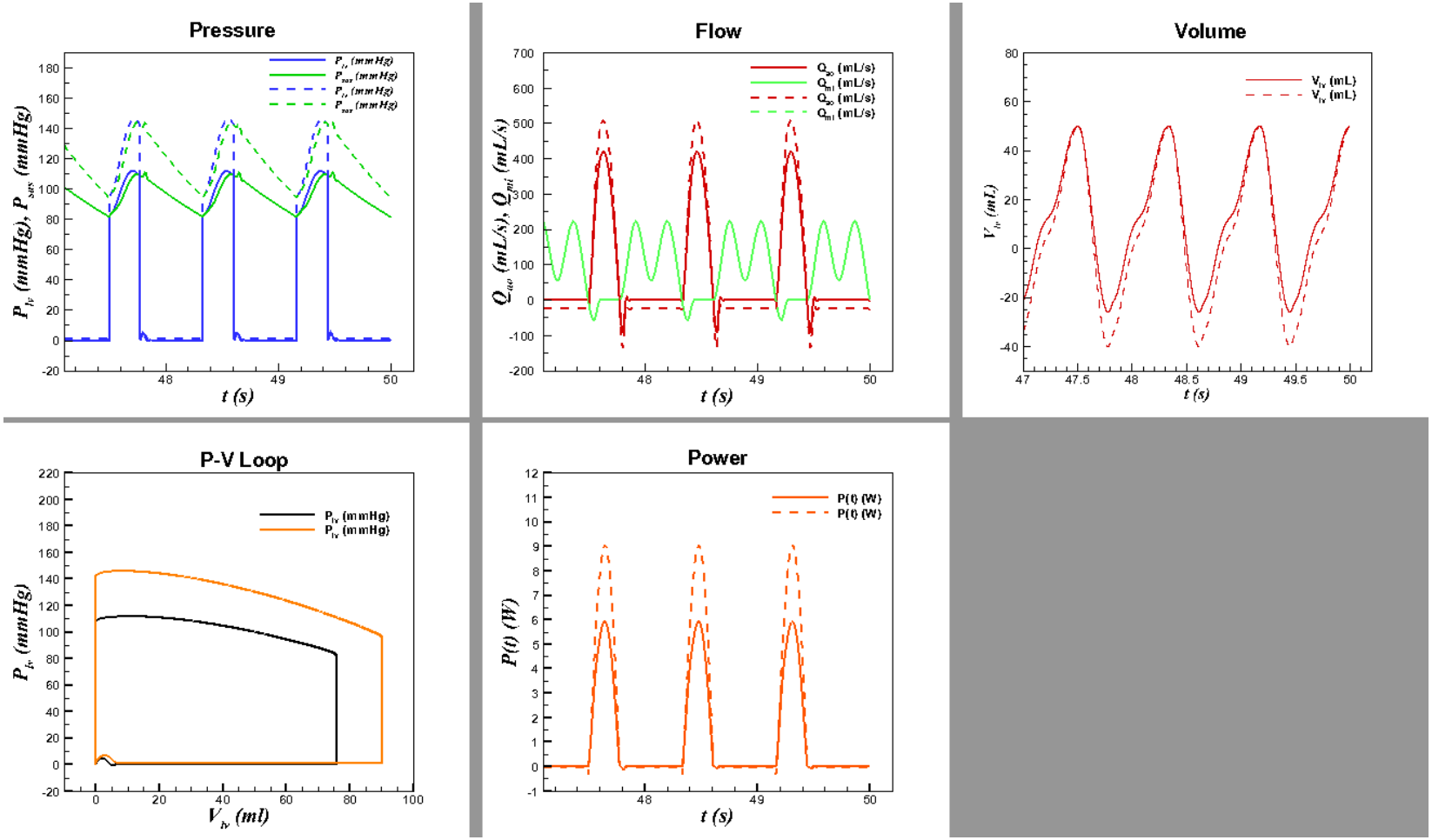

Figure 73 Results for the combined mild hypertension/mild aortic regurgitation model. The pressure (upper-left hand corner), flow (upper-middle), volume (upper-right corner) and power (bottom-middle) graphs show comparisons between the combined disease case with the results using normal case parameters (normal case uses solid lines, diseased case uses dashed lines). The P-V loop (bottom-left hand corner) shows a comparison between normal and diseased case operating pressure and volumes (normal case is in black, diseased case in orange).

The final combined pressure/volume overload disease case is mild hypertension modeled with mild mitral regurgitation. Mild hypertension causes the pressure overload and mitral regurgitation the volume overload. The disease parameters for the cases are shown below:

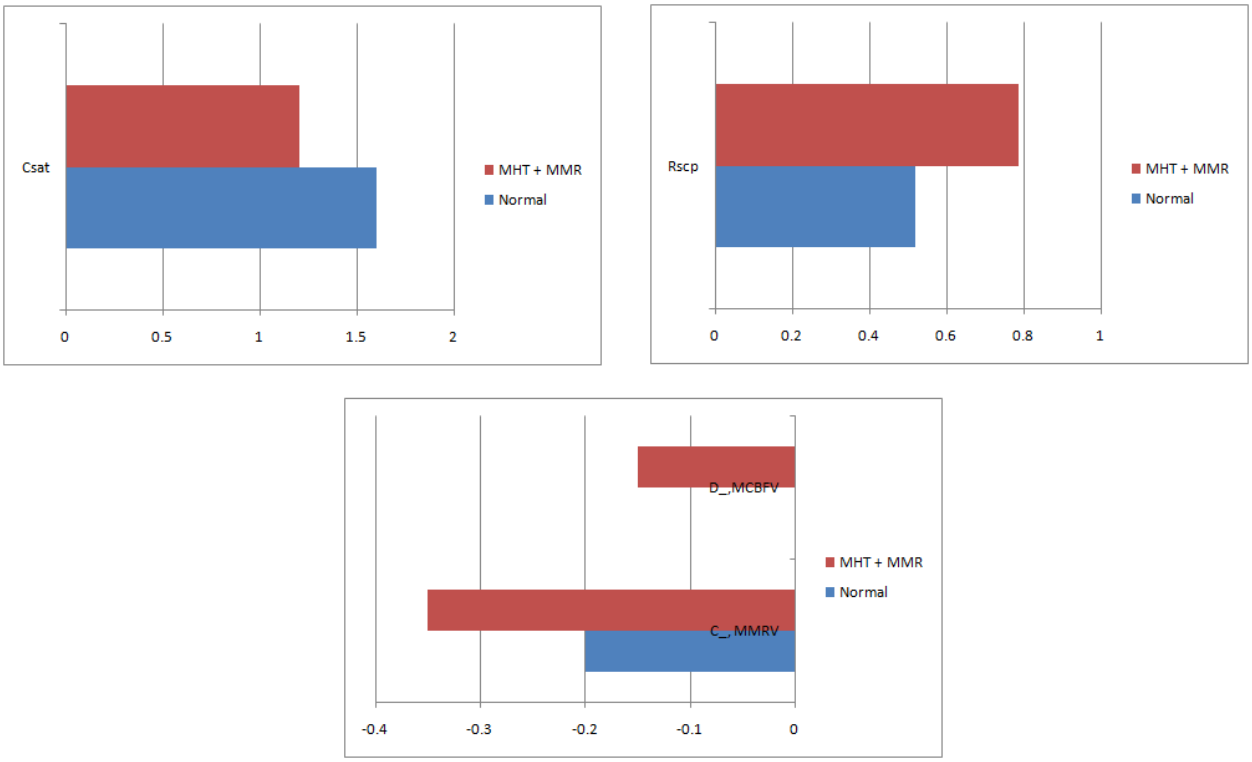

Figure 74 Parameters used to model mild hypertension with mild mitral regurgitation.

Work per beat calculated for the combined mild mitral regurgitation and mild hypertension model saw an increase of 46% over the normal case indicating that the combination is on par with the severe pressure overload diseases delineated earlier. The severe increase in workload created by the combination of mild hypertension and mild mitral regurgitation is an example of how the moderate increase in pressure and mild increase in stroke volume does not rank as a severe disease according to disease guidelines.

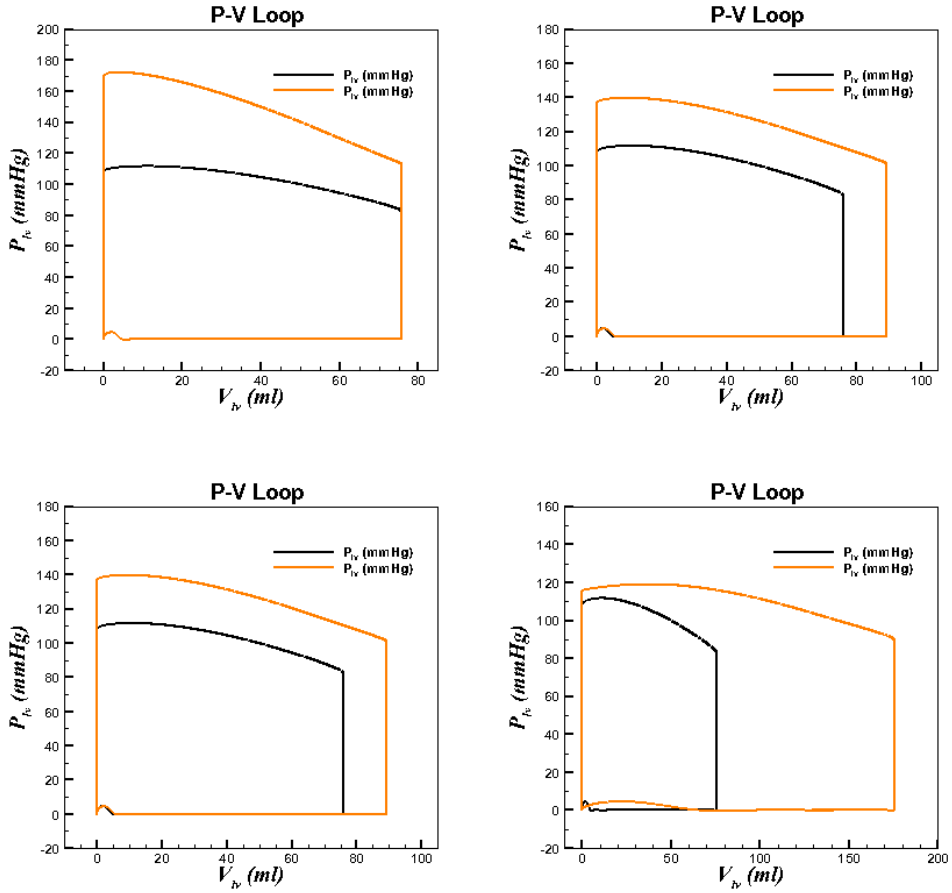

Figure 75 Pressure volume diagrams comparing p-v loops of mild hypertension/mild mitral regurgitation (left column) with severe hypertension (row 1, column 2) and severe mitral regurgitation (row 2, column 2).

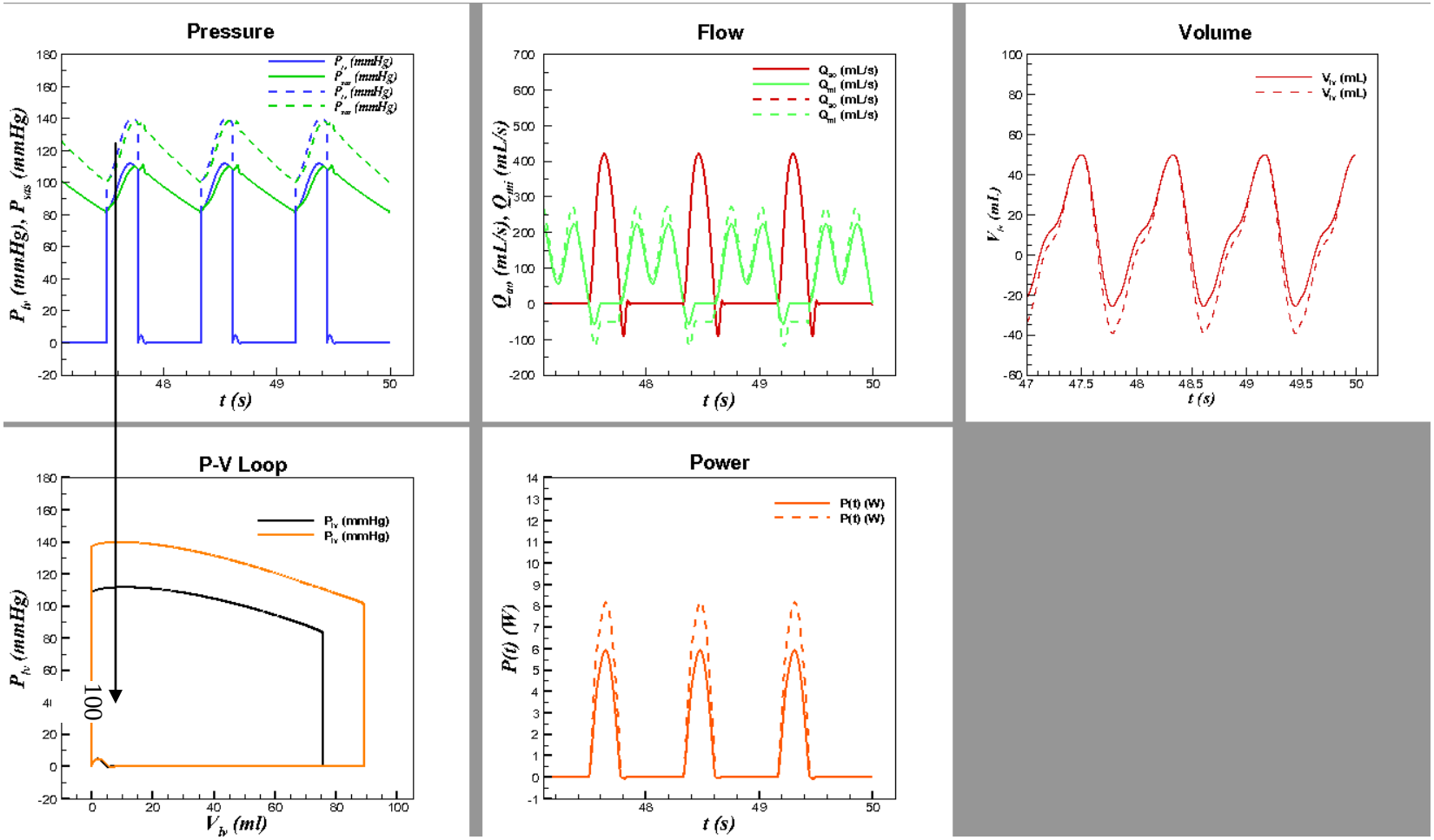

Figure 76 Results for the combined mild hypertension/mild mitral regurgitation model. The pressure (upper-left hand corner), flow (upper-middle), volume (upper-right corner) and power (bottom-middle) graphs show comparisons between the combined disease case with the results using normal case parameters (normal case uses solid lines, diseased case uses dashed lines). The P-V loop (bottom-left hand corner) shows a comparison between normal and diseased case operating pressure and volumes (normal case is in black, diseased case in orange).

The combined case of mild hypertension and mild aortic stenosis forms a model that sees only pressure overload as the cause of work increase for the heart. Parameters for the combined disease model are in the chart below:

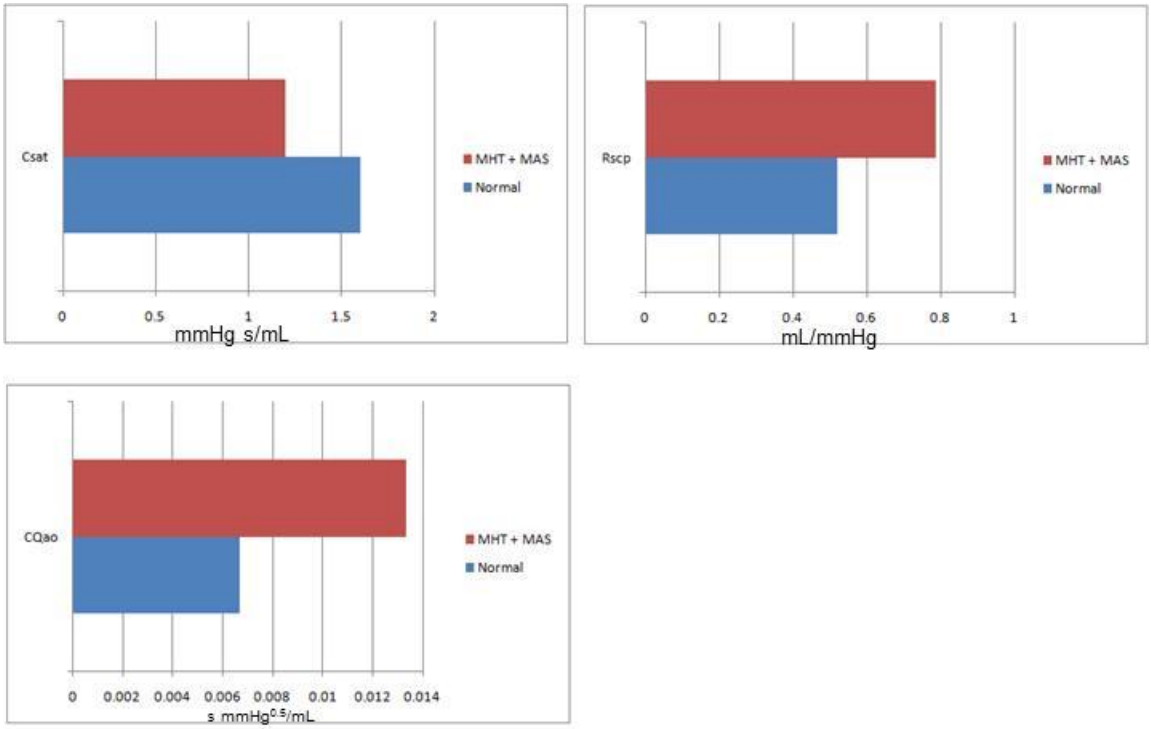

Figure 77 Parameters used to model mild hypertension with mild aortic regurgitation.

Work increases with the two mild case modeled together 39%. The +39% increase is slightly less severe than the 42% increase caused by severe aortic stenosis; showing that the two diseases combined can endanger the heart to succumb to congestive heart failure. The increased operating is in the severe range of the hypertension classification and probably be easily identified as severe using that guideline.

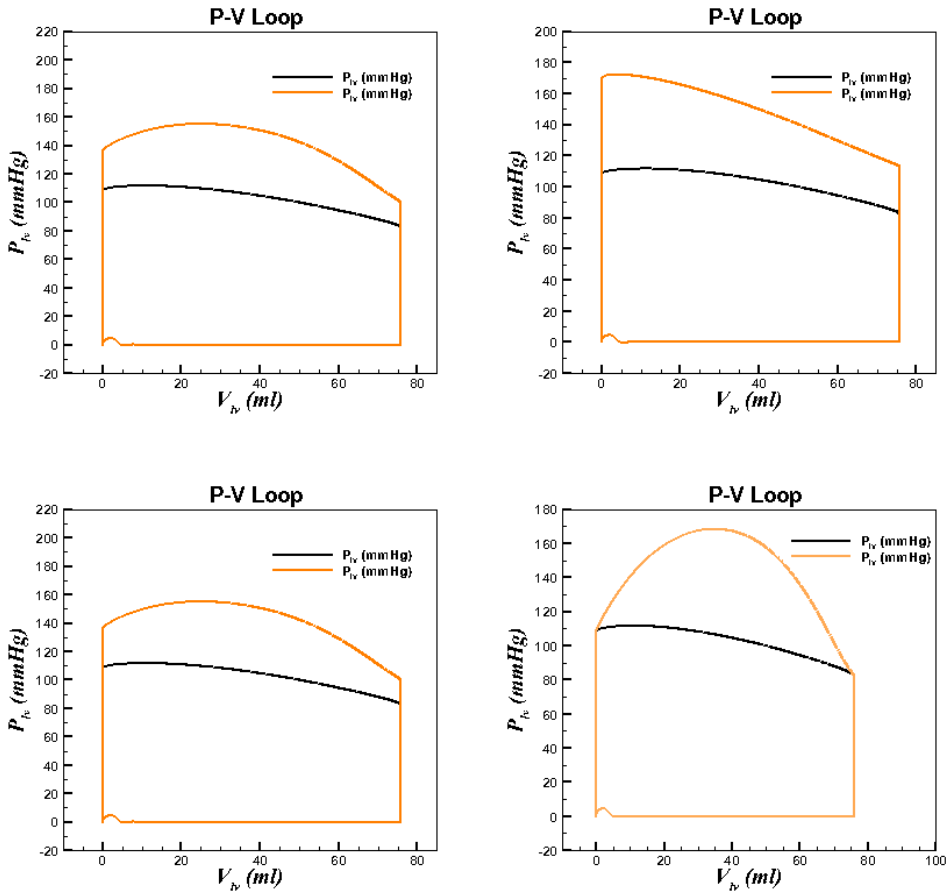

Figure 78 Pressure volume diagrams comparing p-v loops of mild hypertension/mild aortic stenosis (left column) with severe hypertension (row 1, column 2) and severe aortic stenosis (row 2, column 2).

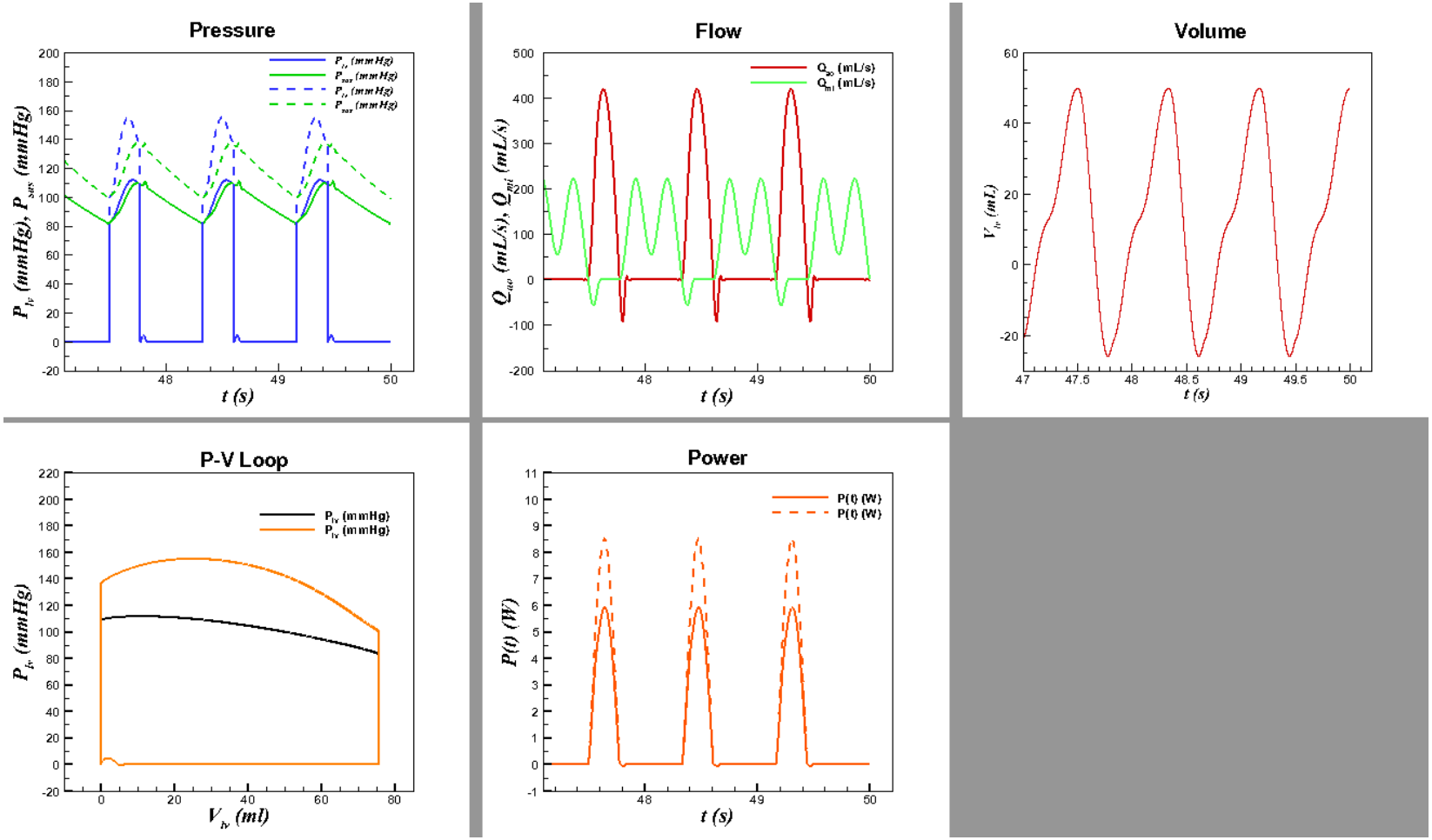

Figure 79 Results for combined mild hypertension/ mild aortic stenosis model. The pressure (upper-left hand corner) and power (bottom-middle) graphs show comparisons between the combined disease case with the results using normal case parameters (normal case uses solid lines, diseased case uses dashed lines). The flow (top-middle) and volume (upper-right corner) graphs do not change since parameters affecting their calculation do not change to model the combined disease case. The P-V loop (bottom-left hand corner) shows a comparison between normal and diseased case operating pressure and volumes (normal case is in black, diseased case in orange).

The final combined disease case modeled was the pure volume overload case of mild mitral regurgitation and mild aortic regurgitation. The figure below lists parameters declared for the model simulation:

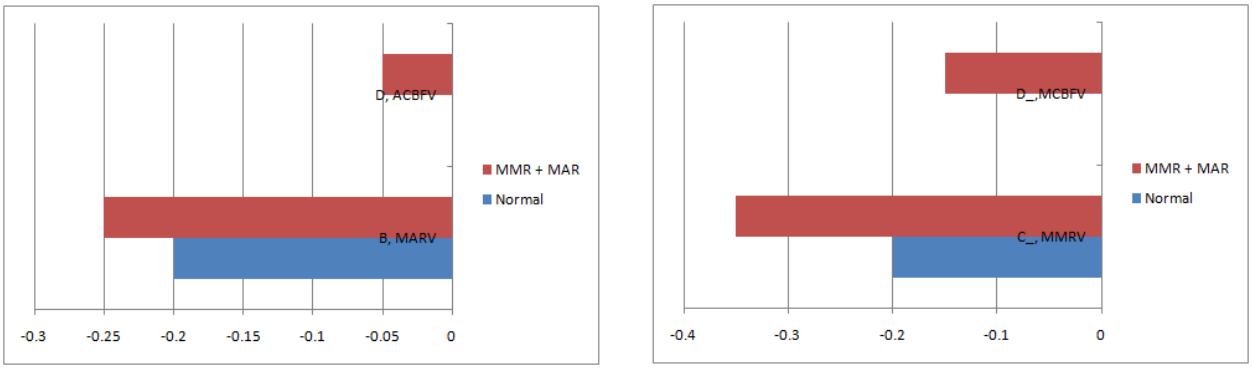

Figure 80 Parameters used to model mild mitral regurgitation with mild aortic regurgitation.

The 44% increase that resulted from the combination of the two mild forms of regurgitation was in the range of severe increase in workload due to severe individual pressure overload diseases. The two cases working together, albeit in a mild form, affect the heart strongly enough to precipitate congestive heart failure from a workload standpoint.

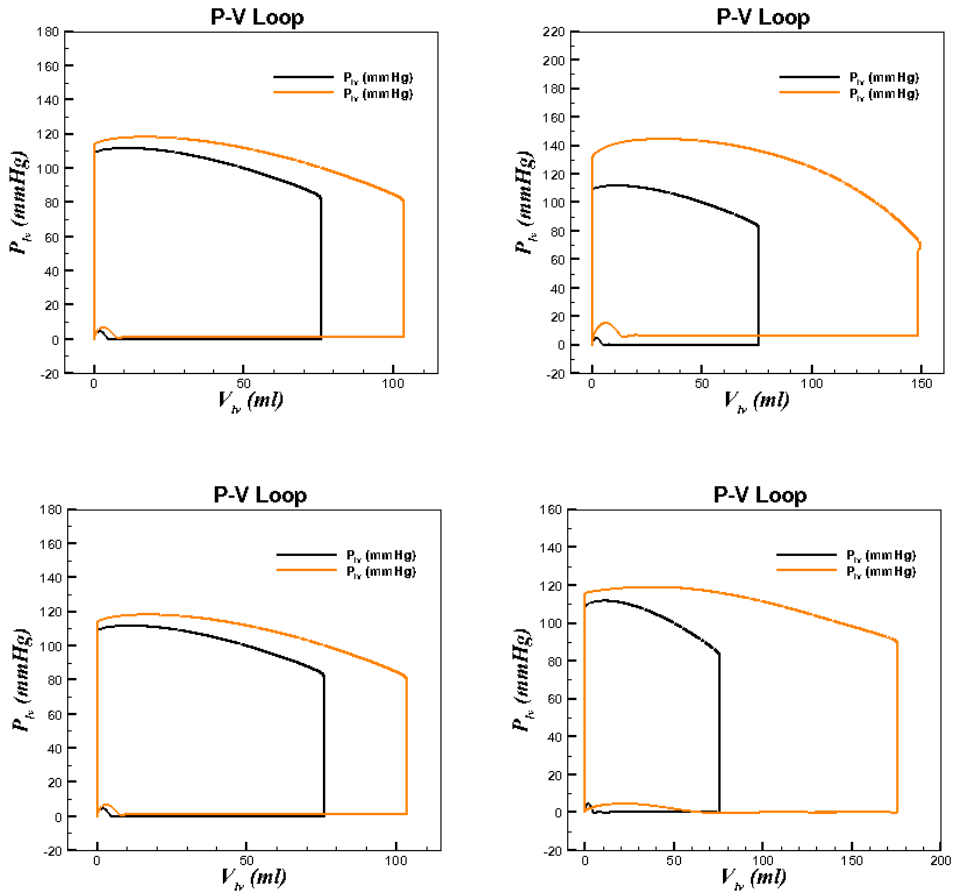

Figure 81 Pressure volume diagrams comparing p-v loops of mild mitral regurgitation/mild aortic regurgitation (left column) with severe aortic regurgitation (row 1, column 2) and severe mitral regurgitation (row 2, column 2).

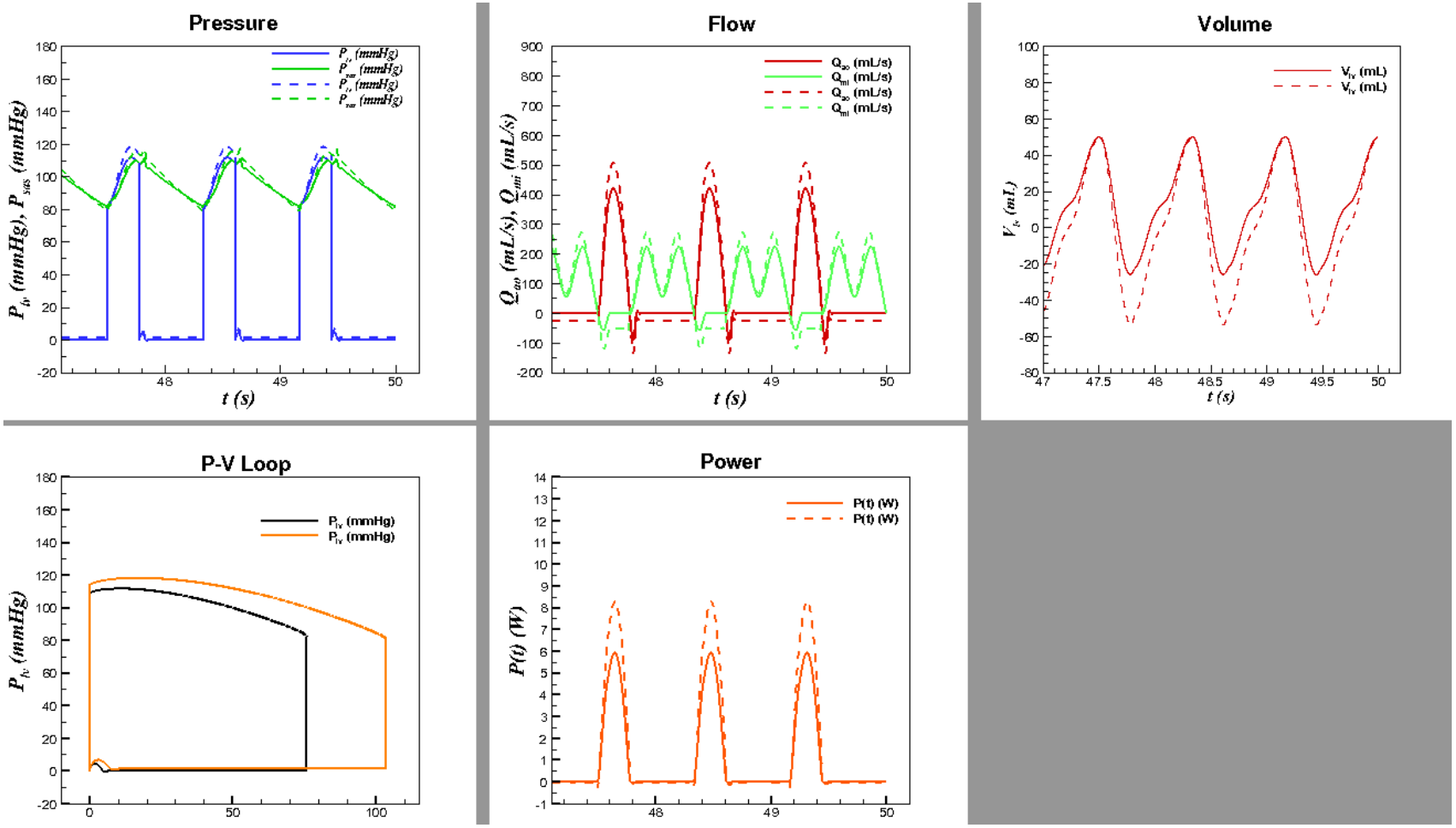

Figure 82 Results for the combined mild aortic regurgitation/mild mitral regurgitation model. The pressure (upper-left hand corner), flow (upper-middle), volume (upper-right corner) and power (bottom-middle) graphs show comparisons between the combined disease case with the results using normal case parameters (normal case uses solid lines, diseased case uses dashed lines). The P-V loop (bottom-left hand corner) shows a comparison between normal and diseased case operating pressure and volumes (normal case is in black, diseased case in orange).

The combined disease models showed that in five of the six cases, combined mild forms of diseases actually created a greater amount of workload on the left ventricle than had the increase in the added workload of the individual diseases considered in the combined models been summed separately.

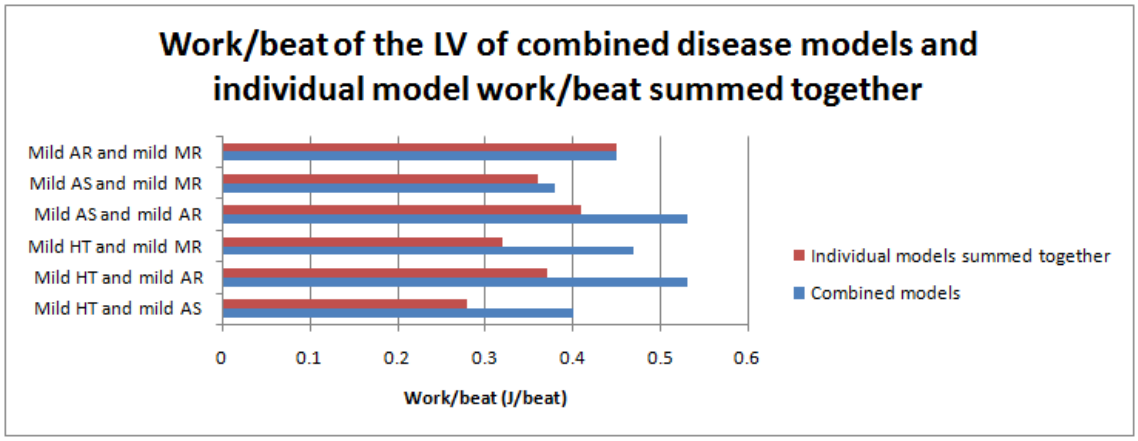

Figure 83 Work per beat analysis of combined diseases compared to work per beat of individual case simulations summed together.

Five of the six disease combinations showed amplification of workload, the only case not showing amplification being the volume overload combination of mitral and aortic regurgitation (see Figure 83 above). It is interesting that mild aortic and mild mitral regurgitation did not increase workload when combined together but at the same time had the highest workload impact on the heart as individual actors on the heart. It can be reasoned that as individual actors aortic and mitral regurgitation are tax the left ventricle quite highly but do not offer mechanisms to one another that additionally burden the left ventricle when working together.

Workload increase caused by the combination of diseases can be looked at in two ways to get some understanding of how diseases work together to increase workload. The first way is to look at gross workload increase as is done in Figure 83. The highest overall increases in workload are seen when aortic regurgitation is combined with a pressure overload case disease. Mild aortic regurgitation combined with mild hypertension or mild aortic stenosis increased workload from the normal case over 0.5 J/beat. The high increase in workload mostly has to do with how

expensive a disease aortic regurgitation is on energy expenditure for the heart. When aortic regurgitation is paired with any disease, workload cost will be high.

The second way to look at the amplification of workload is to look at increase in workload relative of combined cases relative to the individual sums of diseases cases acting by themselves which is what Figure 84 identifies.

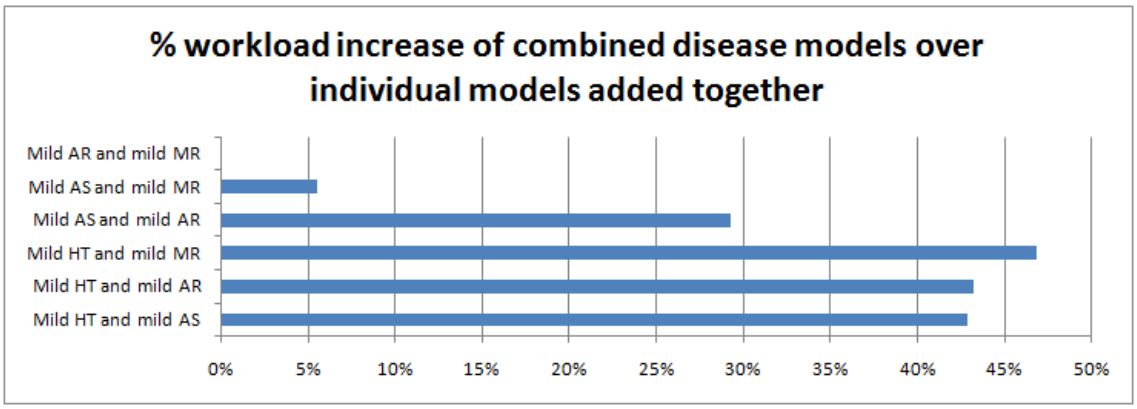

Figure 84 % increase in work of the left ventricle calculated for combined disease model runs and separately summed individual case counterparts.

Workload increases most non-linearly in the cases where hypertension is combined with a different disease. The three highest *relative* increases in workload occur when hypertension is part of the simulation, the greatest relative impact being when mild hypertension was combined with mild mitral regurgitation.

Unlike the pressure overload disease case of aortic stenosis which only raises the operating pressure of the left ventricle and affects no other component of the cardiovascular system, hypertension affects both the left ventricle and the systemic circulation. While aortic stenosis affects the left ventricle directly, hypertension affects left ventricular pressure indirectly by raising the overall systemic circulatory resistance so that the left ventricle must pump harder to move blood at a sufficient rate. Raising both the operating pressures of the left ventricle and the resistance of the system provides a mechanism that amplifies the severity of disease cases that are combined with hypertension otherwise similar workload amplification would be seen with cases combined with aortic stenosis.

4.4 Model Limitations

The current model has been presented as a tool that can be used to directly compute energy cost under physiological and pathophysiological conditions. As workload calculation is the goal of the model, there are some limitations to what the model can do in terms of accurate physiological modeling.

The method used to create flow curves using the splining of several points together to form a continuous function is easily able to spline points together that are not separated by sharp slopes. Certain points of the aortic and mitral flow curves do contain sharp slopes and due to the nature of how the spline code connects points together does not handle the steep slope perfectly accurately, but close enough to look physiologically representative of what a flow curve should look like.

Figure 40 in section 4.3 displays a comparison of the resulting pressure versus time graph from the current model compared to an accepted representation of what pressure versus time should look like for the left ventricle. The current model's representation of left ventricular pressure versus time contains pressure values that rise and fall instantaneously corresponding to when the cardiac cycle enters into systole and ends systole, respectively. Left ventricular operating pressures are physiologically shown to rise and fall gradually, not instantaneously, demonstrating a limitation of the model's ability to represent pressure. Workload calculation is not severely affected by the instantaneous pressure change so the model is still considered valid in the capacity of calculating workload.

The model also does not demonstrate a gradual rise in pressure that is physiologically observed during diastole in the left ventricle. During normal operation, the left ventricle operating pressure will gradually rise about 10 mmHg as the left ventricle distends with blood during diastole. The model makes the assumption that the pressure increase during diastole is not a result of left ventricular contraction and is not used to perform any useful work during systole. The

useful work calculation made by the model is not affected by not including a pressure rise in the left ventricle during diastole.

The current model does not account for ischemic heart failure, a problem that usually results in the death of most patients affected by left ventricular heart diseases before congestive heart failure does. Myocardial ischaemia which causes ischaemic heart failure is caused mainly by the failure of coronary arteries to circulate enough blood to the heart. The coronary arteries, and any diseases associated with their operation, are not included in the current model and represent an area for improvement in future models/

The last limitation that needs to be noted is how the model does not adjust its cardiac output to account for changing conditions as is observed physiologically in cardiac operation. In physiological response to varied conditions, the heart will change in both how hard it works and how much output it is creating. The model chooses to control the variable of cardiac output, maintaining it at a 5 L/min cardiac output, so that only workload is able to change. The maintenance of a cardiac output at only one value creates a model that calculates the energy cost of varying conditions at one cardiac output level, greatly simplifying the complexity of how the heart function so that energy cost can be analyzed without needing to correct for changing output levels.

4.5 Summary and Future Work

A lumped parameter model of the cardiovascular system was developed that produced numerical solutions to blood flow and pressure that were physiologically accurate. The model improves on the model created by Korakianitis and Shi by employing a simple approach to modeling the cardiovascular system while still providing accurate physiological representations of flow and pressure in the cardiovascular system.

The model calculates workload per beat of the left ventricle in physiological and pathophysiological cases, a use for lumped parameter modeling that gives some understanding of how changing conditions on the heart affect the heart in terms of energy cost. Currently, literature

focuses on physiological modeling of the cardiovascular system, irrespective of changing workload on the heart. The current model gives the ability for further research to directly study workload impact created by diseased conditions.

When applied to modeling the disease cases of hypertension, aortic stenosis, aortic regurgitation, and mitral regurgitation, the model provided results showing that diseases that rely on volume overload to overwork the heart are shown to overwork the heart much more severely as disease severity increases compared to pressure overload diseases. Currently, disease guidelines are set up in a manner that does not differentiate disease severity based on workload. The simulation of the four disease cases showed that the current guidelines are allowing for disease cases that are overworking the heart much more severely, specifically volume overload cases, because guidelines do not capture the increased workload impact that diseased cases have on the heart. The results of modeling individual diseased cases show that guidelines need to be improved so that workload severity is better assessed, possibly by a workload index that bases disease severity solely on workload impact on the heart.

Mild forms of disease modeled separately were seen to increase in workload effect when combined together in five of six simulations. The non-linear addition of workload when diseases are combined suggest disease severity guidelines for risk of developing congestive heart failure should account for the effect of combined mild forms of diseases and not just severe cases of individual diseases. Combined disease modeling showed an acute effect on relative workload created when hypertension was combined with another disease case. Hypertension was identified as a disease with unique ability to amplify the severity of other diseases and increase the severity that those diseases impose in terms of increased workload.

Future work to the model include enhancing the models robustness to include parameters that model for coronary artery circulation so that ischaemic diseases can be modeled for alongside diseases that cause congestive heart failure since the disease cases often occur together.

Improvement in how the aortic and mitral valves operate is also a goal for future work. Currently, the model employs a simple method for valve simulation, completely opening the valves instantaneously during the appropriate times within the cardiac cycle. Instantly opening and shutting valves leads to instantaneous pressure changes evident in operating pressure graphs of the left ventricle and are not physiologically representative of what is happening inside the heart. Upgrading the complexity of the aortic and mitral valve models will improve the pressure response of the pumping chambers to create more physiologically representative flow curves.

Incorporating recent research done by Dr L Prasad Dasi into how energy dissipation is affected by diseased conditions within systemic circulation is also part of future work. Research has shown that vascular bifurcations affect energy dissipation response, and changes in the physiology of the bifurcations can signal disease severity of certain types of diseases. Upgrading the model from a zero-dimensional to a one dimensional model that takes into account vascular bifurcations can then be applied to understanding how energy dissipation is affected by vascular bifurcations.

Reincorporating the Korakianitis model's design so that the current model would contain pulmonic and systemic circulation as well as a four chamber heart that uses an elastance model is a goal as well. The re-imagined four chamber model would aim to create physiological representations of flow where the Korakianitis model failed.

REFERENCES

Avolio, A. P. (1980). "MULTI-BRANCHED MODEL OF THE HUMAN ARTERIAL SYSTEM." Medical & Biological Engineering & Computing **18**(6): 709-718.

Berne, R. M. and M. N. Levy (2001). Cardiovascular physiology. St. Louis, MO, Mosby.

Bodley, W. E. (1971). "NON-LINEARITIES OF ARTERIAL BLOOD FLOW." Physics in Medicine and Biology **16**(4): 663-&.

Bonow (2007). "ACC/AHA 2006 guidelines for the management of patients with valvular heart disease - executive summary: A report of the American College of Ccardiology/American Heart Association task force on practice guidelines (writing committee to develop guidelines for the management of patients with valvular heart disease) (vol 114, pg 450, 2006)." Circulation **115**(15): E410-E410.

Bronzino, J. D. (1995). The biomedical engineering handbook. Boca Raton, CRC Press : IEEE Press.

Burkhoff, D., P. P. Detombe, et al. (1993). "IMPACT OF EJECTION ON MAGNITUDE AND TIME-COURSE OF VENTRICULAR PRESSURE-GENERATING CAPACITY." American Journal of Physiology **265**(3): H899-H909.

Burkhoff, D., I. Mirsky, et al. (2005). "Assessment of systolic and diastolic ventricular properties via pressure-volume analysis: a guide for clinical, translational, and basic researchers." American Journal of Physiology-Heart and Circulatory Physiology **289**(2): H501-H512.

Chandran, K. B., S. E. Rittgers, et al. (2007). Biofluid mechanics : the human circulation. Boca Raton, CRC/Taylor & Francis.

Cicala, R. (1997). The heart disease sourcebook. Los Angeles, Chicago, Lowell House; Contemporary Books.

Claessens, T. E., D. Georgakopoulos, et al. (2006). "Nonlinear isochrones in murine left ventricular pressure-volume loops: how well does the time-varying elastance concept hold?" American Journal of Physiology-Heart and Circulatory Physiology **290**(4): H1474-H1483.

Dasi, LP; Pekkan, K; de Zelicourt, D, et al. Hemodynamic Energy Dissipation in the Cardiovascular System: Generalized Theoretical Analysis on Disease States. Annals of Biomedical Engineering **37(**4) 661-673, 2009

Elstad, M., K. Toska, et al. (2002). "Model simulations of cardiovascular changes at the onset of moderate exercise in humans." Journal of Physiology-London **543**(2): 719-728.

Funai, J. T. and M. D. Thames (1988). "ISOCHRONAL BEHAVIOR IN LEFT-VENTRICULAR SYSTOLIC PRESSURE-WALL THICKNESS RELATIONS." American Journal of Physiology **255**(5): H1136-H1143.

Fung, Y. C. (1984). Biodynamics : circulation. New York, Springer-Verlag.

Grodins, F. S. (1959). "INTEGRATIVE CARDIOVASCULAR PHYSIOLOGY - A MATHEMATICAL SYNTHESIS OF CARDIAC AND BLOOD VESSEL HEMODYNAMICS." Quarterly Review of Biology **34**(2): 93-116.

Guyton, A. C., T. G. Coleman, et al. (1984). "SOME PROBLEMS AND SOLUTIONS FOR MODELING OVERALL CARDIOVASCULAR REGULATION." Mathematical Biosciences **72**(2): 141-155.

Henderson, W. R., D. E. G. Griesdale, et al. (2010). "Clinical review: Guyton - the role of mean circulatory filling pressure and right atrial pressure in controlling cardiac output." Critical Care **14**(6).

Klabunde, R. E. (2005). Cardiovascular physiology concepts. Philadelphia, Lippincott Williams & Wilkins.

Korakianitis, T. and Y. B. Shi (2006). "Numerical simulation of cardiovascular dynamics with healthy and diseased heart valves." Journal of Biomechanics **39**(11): 1964-1982.

Kvitting, J.-P. E., T. Ebbers, et al. (2004). "Flow patterns in the aortic root and the aorta studied with time-resolved, 3-dimensional, phase-contrast magnetic resonance imaging: implications for aortic valve-sparing surgery." The Journal of Thoracic and Cardiovascular Surgery **127**(6): 1602-1607.

Langewouters, G. J., K. H. Wesseling, et al. (1984). "THE STATIC ELASTIC PROPERTIES OF 45 HUMAN THORACIC AND 20 ABDOMINAL AORTAS INVITRO AND THE PARAMETERS OF A NEW MODEL." Journal of Biomechanics **17**(6): 425-435.

Lankhaar, J. W., F. A. Rovekamp, et al. (2009). "Modeling the Instantaneous Pressure-Volume Relation of the Left Ventricle: A Comparison of Six Models." Annals of Biomedical Engineering **37**(9): 1710-1726.

Lecarpentier, Y. C., L. H. S. Chuck, et al. (1979). "NATURE OF LOAD DEPENDENCE OF RELAXATION IN CARDIAC-MUSCLE." American Journal of Physiology **237**(4): H455-H460.

Liang, F. Y. and H. Liu (2005). "A closed-loop lumped parameter computational model for human cardiovascular system." Jsme International Journal Series C-Mechanical Systems Machine Elements and Manufacturing **48**(4): 484-493.

Lu, K., J. W. Clark, et al. (2001). "A human cardiopulmonary system model applied to the analysis of the Valsalva maneuver." American Journal of Physiology-Heart and Circulatory Physiology **281**(6): H2661-H2679.

Melchior, F. M., R. S. Srinivasan, et al. (1992). "MATHEMATICAL-MODELING OF HUMAN CARDIOVASCULAR-SYSTEM FOR SIMULATION OF ORTHOSTATIC RESPONSE." American Journal of Physiology **262**(6): H1920-H1933.

Montani, J. P., T. H. Adair, et al. (1986). "PHYSIOLOGICAL MODELING - A SIMULATOR FOR THE IBM PC." Federation Proceedings **45**(4): 1139-1139.

Montani, J. P. and B. N. Van Vliet (2009). "Understanding the contribution of Guyton's large circulatory model to long-term control of arterial pressure." Experimental Physiology **94**(4): 382-388.

National Center for Chronic Disease Prevention and Health Promotion, D. f. H. D. a. S. P. (2010). "Heart disease facts and statistics."

Noordergraaf, A., P. D. Verdouw, et al. (1963). "THE USE OF AN ANALOG COMPUTER IN A CIRCULATION MODEL." Progress in Cardiovascular Diseases **5**(5): 419-439.

Paredes, S., T. Rocha, et al. (2011). "Long term cardiovascular risk models' combination." Computer Methods and Programs in Biomedicine **101**(3): 231-242.

Shi, Y. B., P. Lawford, et al. (2011). "Review of Zero-D and 1-D Models of Blood Flow in the Cardiovascular System." Biomedical Engineering Online **10**.

Shim, E. B., J. Y. Sah, et al. (2004). "Mathematical modeling of cardiovascular system dynamics using a lumped parameter method." Japanese Journal of Physiology **54**(6): 545-553.

Suga, H., K. Sagawa, et al. (1973). "LOAD INDEPENDENCE OF INSTANTANEOUS PRESSURE-VOLUME RATIO OF CANINE LEFT VENTRICLE AND EFFECTS OF EPINEPHRINE AND HEART-RATE ON RATIO." Circulation Research **32**(3): 314-322.

Sunagawa, K. (2010). The pressure-volume relationship of the heart: Past, present and future.

Terkildsen, J., J. P. Montani, et al. (2009). "IMPLEMENTING THE GUYTON LARGE CIRCULATORY MODEL IN CELLML." Journal of Physiological Sciences **59**: 262-262.

Uemura, K., M. Sugimachi, et al. (2004). "A novel framework of circulatory equilibrium." American Journal of Physiology-Heart and Circulatory Physiology **286**(6): H2376-H2385.

Vander, A. J., J. H. Sherman, et al. (2001). Human physiology : the mechanisms of body function. Boston, McGraw-Hill.

Verdonck, P. and K. Perktold (1998). Intra and extracorporeal cardiovascular fluid dynamics. Southampton ; Boston, Computational Mechanics Publications.

Wolf, M. B. and R. P. Garner (2007). "A mathematical model of human respiration at altitude." Annals of Biomedical Engineering **35**(11): 2003-2022.

Womersley, J. R. (1958). "OSCILLATORY FLOW IN ARTERIES .3. FLOW AND PULSE-VELOCITY FORMULAE FOR A LIQUID WHOSE VISCOSITY VARIES WITH FREQUENCY." Physics in Medicine and Biology **2**(4): 374-382.

Yoganathan AP, He ZM, Jones SC. Fluid mechanics of heart valves. ANNUAL REVIEW OF BIOMEDICAL ENGINEERING Vol VI, 331-362, 2004.

APPENDIX A SOURCE CODE

```
#include "stdio.h"
#include <conio.h>
#include <math.h>
#include <string.h>

#include "nrutil.h"
#include "nrutil.cpp"
#define NUMPTS 30

const double pi = 3.1415926535;
double heart_rate = 60.0; // heart rate in bpm
double CO = 5.0*1000.0/60.0; // cardiac output in mL/s
double systolic_fraction = 1.0/3.0; // systolic fraction
double diastolic_fraction = 1.0 - systolic_fraction; // diastolic fraction
double delta_t = 0.000001; // the time step for each iteration of the lumped parameter model
double TOTAL_RUN_TIME = 50.0; // the total amount of time that the model runs
const int SKIP = 200;


// --- systemic constants
// the capitalized first letters of the systemic constants use the following naming system:
// C = capacitance, R = resistance, L = inductance

// aorta
double Csas = 0.08;
double Rsas = 0.003;
double Lsas = 0.000062;

// systemic artery
double Csat = 1.6;
double Rsat = 0.05;
double Lsat = 0.0017;

// systemic aerteriole
double Rsar = 0.5;

// systemic capillary
double Rscp = 0.52;
// systemic vein

double Rsvn = 0.075;
double Csvn = 20.5;
double A, B, C, D, Norm_aortic=1.0; // A, B, C, D are parameters used to model a blood flow curve
coming out of the aortic valve
```

```
                    // norm _aortic is used to calculate an average value for a given flow curve
double A_, A1, A2, A3, B_, C_, D_, Norm_mitral=1.0; // A_, A1, A2, A3, B_, C_, D_ are parameters used to model a blood flow curve
                    // coming out of the mitral valve


double Lao = 0.000, Lmi = 0.000;   //inductance of aortic valve, mitral valve.
double qao_x[NUMPTS*3+2], qao_y[NUMPTS*3+2], qao_y2[NUMPTS*3+2]; // arrays that will be used to spline a blood flow curve
double qmi_x[NUMPTS*3+2], qmi_y[NUMPTS*3+2], qmi_y2[NUMPTS*3+2]; // arrays that will be used to spline a blood flow curve

//SUB FUNCTION DEFINITIONS
void systemic_circuit(); // function that calculates pressure and blood flow through the systemic circuit
void aortic_flow(double t); // function that primes the lumped parameter model by creating a sinusoidal blood flow curve that provides
                                                    // pressure and blood flow input into the systemic circuit
void left_ventricle(double t); // function that models the mechanical function of the left ventricle
void aortic_valve(double t); // function that models the mechanical function of the aortic valve
void left_atrium(double t); // function that models the mechanical function of the left atrium
void mitral_valve(double t); // function that models the mechanical function of the mitral valve
void spline(double x[], double y[], int n, double yp1, double ypn, double y2[]); // a function that creates an array defined by the user that will be splined by another function
void splint(double xa[], double ya[], double y2a[], int n, double x, double *y); // a function that splines an array created by the spline function which becomes the blood flow inputes into the lumped parameter model
void setup_aortic_spline();
double Qao_function(double t); // a function that defines aortic blood flow
void create_aortic_spline_template(double A, double B, double C, double D); // a function that takes parameters for the shape of a blood flow curve and makes an array that will be splined so that a continuosly diffrentiable funtion is made
void setup_mitral_spline();
double Qmi_function(double t); // a function that defines mitral blood flow
void create_mitral_spline_template(double A_, double A1, double A2, double A3, double B, double C, double D); // a function that takes parameters for the shape of a blood flow curve and makes an array that will be splined so that a continuosly diffrentiable funtion is made
void read_patient_file(char *);

//universal variables
        FILE *PT;
        char patient_file_name[200]; // = {"C:\\Users\\Dasi\\Documents\\Visual 6\\02May11\\Patient files\\Patient1.txt"};
        double dPsas=0.0, dQsas=0.0, dPsat=0.0, dQsat=0.0, dPsvn=0.0, Qsas=0.0,Psas=0.0, Psat=0.0, Psvn=0.0, Qsat=0.0, Pra=0.0, Qsvn=0.0;
        double Qmi = 0.0, Qao = 0.0, Vlv = 50.0;
        double CQao = 150.0, CQmi = 400.0,_CQao = 7.0,_CQmi = 10.0;
        double Plv, dVlv=0.0;
        double Vla, dVla = 0.0, Vla0 = 4.0, Pla = 10.0, Pla0 = 1.0;
        double dqao[5];

        double dQao, dQmi;
        double instantaneous_power,avg_power,count=0.0,work_per_beat=0.0;
```

```
int main(int argc, char* argv[])
{
	FILE *fp;
	double time,T,t;
	int skip = 0;
	char outfilename[200];
	int length;

//	printf("argc = %d\n",argc);

//	for(i=0;i<argc;i++) printf("%s\n",argv[i]);

	if(argc != 2) {printf("error\n"); exit(0);}

	sprintf(patient_file_name,"%s",argv[1]);

	printf("reading file %s...",patient_file_name);

	read_patient_file(patient_file_name);


	T = 60.0/heart_rate;
	double   avg_qao=0.0, avg_qmi=0.0,ctr=0.0;

	A = systolic_fraction; //systolic duration fraction
	A_ = diastolic_fraction; //diastolic duration fraction

	A1 = (1.0-A_)+1.0/4.0*A_; // first local Qmi max fraction
	A2 = (1.0-A_)+1.0/2.0*A_; // local Qmi min value fraction
	A3 = (1.0-A_)+3.0/4.0*A_; // second local Qmi max fraction

/*
	B = -0.2; // max backflow
	C = 1.0/12.0; // width of falling fraction
	D = -0.1; // constant backflow value

	B_ = 1.0/8.0; // backflow duration fraction
	C_ = -0.2; // max blackflow value
	D_ = -0.1; // constant backflow value
*/
//	printf("\n%lf \n%lf \n%lf \n%lf \n%lf \n%lf \n%lf \n%lf \n%lf \n%lf
\n",A,B,C,D,A_,A1,A2,A3,B_,C_,D_);
//	exit(0);

	setup_aortic_spline();
	setup_mitral_spline();

	// the for loop below calculates stroke volumes by averaging the amount of blood flow for one
cardiac cycle. The average of the flow coming out of
	// the mitral valve must equal the aortic valve for lumped parameter model to function
correctly, otherwise a volume of blood would accumulate
```

```
	// wither in the atrium or the ventricle depending on which chamer of the heart was holding
more blood.
	for(t=0.0;t<=60.00/heart_rate;t+=delta_t) {
	avg_qao += Qao_function(t);
	avg_qmi += Qmi_function(t);
	ctr++;
	}
	Norm_aortic = avg_qao/ctr;
	Norm_mitral = avg_qmi/ctr;

	length=strlen(patient_file_name);
	sprintf(outfilename,"%s",patient_file_name);
	sprintf(&outfilename[length-3],"dat");

//	printf("%s  %d\n",outfilename,length);
//	exit(0);
	printf("writing...");
	fp = fopen(outfilename,"w"); // the out.dat file contains the blood flow and pressure data
defined below


//	fprintf(fp,"sd\"s");

	fprintf(fp,"TITLE = \"%s\"\nVARIABLES = \"t (s)\"\n\"P<sub>lv</sub>
(mmHg)\"\n\"V<sub>lv</sub> (mL)\"\n\"Q<sub>ao</sub> (mL/s)\"\n\"Q<sub>mi</sub>
(mL/s)\"\n\"P<sub>sas</sub> (mmHg)\"\n\"P<sub>la</sub> (mmHg)\"\n\"Q<sub>svn</sub>
(mL/s)\"\n\"P(t) (W)\"\n\"P<sub>avg</sub>(t) (W)\"\n\"W/beat (J/b)\"\n",outfilename);
//	fclose(fp);
//	exit(0);

	// the for loop below is responsible for the ordering of the sub-functions defined. It is in
essesnce the organization of the cardiac circuit.
		for(time=0.0,t=0.0;time<TOTAL_RUN_TIME;time+=delta_t,t+=delta_t) {
			if(t>T) {
				t = 0.0;
			}

			if(time < 20.0*T) {  // the if statement defines how long the sistem is primed
with a simple blood flow curve.
				// priming of the system allows for a method of providing input
values into the lumped parameter
				// model for aortic blood flow and aortic pressure without having to
randomly guess. It is a more gentle way to
				// start the heart with a volume of blood based off of the heart's own
operation for a given amount of time
			aortic_flow(t);
			}

			if(time >= 20.0*T) { // after the system is primed, the heart starts pumping
blood using parameters that are supposed to
				// closely resemble the parameter values of a healthy heart
			left_atrium(t);
			mitral_valve(t);
```

```
                        left_ventricle(t);
                        aortic_valve(t);
                        }

                        systemic_circuit();

                if(skip == 0)
                {

        fprintf(fp,"%lf\t%lf\t%lf\t%lf\t%lf\t%lf\t%lf\t%lf\t%lf\t%lf\t%lf\n",time,Plv, Vlv, Qao, Qmi,
Psas, Pla, Qsvn,instantaneous_power,avg_power,work_per_beat);
                        skip = SKIP;
                }
                else skip--;
                }

        fclose(fp);

        printf("done\n");
        return 0;
}

////////////////////////////HARD CODED FLOW CURVES//////////////////////////////////
// the hard coded flow curves passively model the mechanical function of the heart's valves in that
// the curve itself is the result of the action of a hypothetical valve at work. The goal of this method
// of valve modeling is to tak a given flow (whether it is healthy or not) and see how the CVS reacts as
a whole
void aortic_valve(double t) {
        Qao = CO * Qao_function(t) ; // instantaneous aortic flow is calculated here

        dQao = CO * (Qao_function(t+delta_t) - Qao_function(t-delta_t)) / (2.0*delta_t); // the
instantaneous change in aortic flow is
                // calculated by using the definition of a derivative from simple calculus
}

void mitral_valve(double t) { // instantaneous mitral flow is modelled here
        Qmi = CO*Qmi_function(t) ;

        dQmi = CO*(Qmi_function(t+delta_t) - Qmi_function(t-delta_t)) / (2.0*delta_t);

}

////////////////////////////HARD CODED FLOW CURVES - END//////////////////////////////////

void aortic_flow(double t) {
        double T;
        T = 60.0/heart_rate; // defines the period of the heart
        if (t >= 0 && t <= systolic_fraction * T) { // this if loop defines the curve that primes the
circulatory system with a simusoidal blood flow
                Qao = 416.6 * sin(t * pi/(systolic_fraction * T));
        }
        else Qao = 0;
}
```

```
void systemic_circuit() { // formulas below provide input and output values for the different vessels of the systemic circuit
   dPsas = ((Qao - Qsas) / Csas);
   dQsas = (Psas - Psat - Rsas*Qsas)/Lsas;

  // systemic artery
   dPsat = ((Qsas - Qsat) / Csat);
   dQsat = ((Psas - Psvn - (Rsat + Rsar + Rscp) * Qsat)/ Lsat);

   //systemic vein
   dPsvn = ((Qsat - Qsvn) / Csvn);

   // now advance in time
   Psas = Psas + delta_t*dPsas;
   Qsas = Qsas + delta_t*dQsas;
   Psat = Psat + delta_t*dPsat;
   Qsat = Qsat + delta_t*dQsat;
   Psvn = Psvn + delta_t*dPsvn;
        Qsvn = (Psvn - Pla)/Rsvn;  //important: I am looping the Qsvn back into the left atrium
}

void left_atrium(double t) {
        double T;
        T = 60.0/heart_rate;
        if(t >= systolic_fraction * T)
                Pla = Plv + Lmi*dQmi + Qmi*Qmi/(CQmi*CQmi); // pressure calcultion in the left atrium is different in systole than in diastole
        else
                Pla = -Qmi/20.0; // the 20.0 value is suposed to represent the resistance to flow created by the closing of the valve during systole
        dVla = Qsvn - Qmi;
        Vla += dVla*delta_t;
}

void left_ventricle(double t) {
        double T,temp;
        T = 60.0/heart_rate;

        dVlv = Qmi - Qao;
        Vlv += dVlv * delta_t;

        if (t <= systolic_fraction * T) {
                Plv = (Psas + Lao * dQao + Qao * Qao/(CQao * CQao));
        }

        if((t >= systolic_fraction * T)) {
                Plv = -Qao/20.0;
        }

        instantaneous_power = Plv*-1.0*dVlv*1E-6*133.32239;

        if (t==0) {
```

```
                work_per_beat = avg_power*T;
                avg_power = 0.0;
                count = 0.0;

        }

        count = count + 1.0;
        temp = avg_power*(count-1.0);

        if(instantaneous_power >= 0.0) avg_power = temp + instantaneous_power; else avg_power =
temp;
        avg_power /=count;

//      avg_power = (avg_power*(ctr-1.0)+instantaneous_power)/ctr;
//      printf("%lf %lf %lf\n",count, instantaneous_power,avg_power);
//      getch();
}

void spline(double x[], double y[], int n, double yp1, double ypn, double y2[])
/*
Given arrays x[1..n] and y[1..n] containing a tabulated function, i.e., yi = f(xi), with
x1 < x2 < .. . < xN, and given values yp1 and ypn for the first derivative of the interpolating
function at points 1 and n, respectively, this routine returns an array y2[1..n] that contains
the second derivatives of the interpolating function at the tabulated points xi. If yp1 and/or
ypn are equal to 1 × 1030 or larger, the routine is signaled to set the corresponding boundary
condition for a natural spline, with zero second derivative on that boundary.
*/
{
int i,k;
double p,qn,sig,un,*u;
u=vector(1,n-1);
if (yp1 > 0.99e30) y2[1]=u[1]=0.0;
else {
        y2[1] = -0.5;
        u[1]=(3.0/(x[2]-x[1]))*((y[2]-y[1])/(x[2]-x[1])-yp1);
}


for (i=2;i<=n-1;i++) {
        sig=(x[i]-x[i-1])/(x[i+1]-x[i-1]);
        p=sig*y2[i-1]+2.0;
        y2[i]=(sig-1.0)/p;
        u[i]=(y[i+1]-y[i])/(x[i+1]-x[i]) - (y[i]-y[i-1])/(x[i]-x[i-1]);
        u[i]=(6.0*u[i]/(x[i+1]-x[i-1])-sig*u[i-1])/p;
}

if (ypn > 0.99e30) qn=un=0.0;
else {
        qn=0.5;
        un=(3.0/(x[n]-x[n-1]))*(ypn-(y[n]-y[n-1])/(x[n]-x[n-1]));
}

y2[n]=(un-qn*u[n-1])/(qn*y2[n-1]+1.0);
```

```
for (k=n-1;k>=1;k--) y2[k]=y2[k]*y2[k+1]+u[k];

free_vector(u,1,n-1);
}


void splint(double xa[], double ya[], double y2a[], int n, double x, double *y)
/*Given the arrays xa[1..n] and ya[1..n], which tabulate a function (with the xai's in order),
and given the array y2a[1..n], which is the output from spline above, and given a value of
x, this routine returns a cubic-spline interpolated value y.
*/
 {
void nrerror(char error_text[]);
int klo,khi,k;
double h,b,a;
klo=1;
khi=n;
while (khi-klo > 1) {
        k=(khi+klo) >> 1;
        if (xa[k] > x) khi=k;
        else klo=k;
}
h=xa[khi]-xa[klo];

if (h == 0.0) nrerror("Bad xa input to routine splint");

a=(xa[khi]-x)/h;
b=(x-xa[klo])/h;
*y=a*ya[klo]+b*ya[khi]+((a*a*a-a)*y2a[klo]+(b*b*b-b)*y2a[khi])*(h*h)/6.0;
}

void setup_aortic_spline()  // this function takes the user defined blood flow parameters and creates an
array that will be splined into
        // a continuous differentiable function
 {

        int i;
   create_aortic_spline_template(A, B, C, D);
///// SPLINE INTERPOLATE
        FILE *in;
        in = fopen("aortic_spline_template_.dat","r");
                for(i=1;i<NUMPTS*3+2;i++) {
                fscanf(in,"%lf%lf",&qao_x[i],&qao_y[i]);
        }

        fclose(in);


        spline(qao_x,qao_y,NUMPTS*3+1,0.0,0.0,qao_y2);
///// END SPLINE INTERPOLATE
}
```

```
void setup_mitral_spline() // this function takes the user defined blood flow parameters and creates an array that will be splined into
	// a continuous differentiable function
 {

	int i;
   create_mitral_spline_template(A_, A1, A2, A3, B_, C_, D_);
///// SPLINE INTERPOLATE
	FILE *in;
	in = fopen("mitral_spline_template_.dat","r");

	for(i=1;i<NUMPTS*3+2;i++) {
		fscanf(in,"%lf%lf",&qmi_x[i],&qmi_y[i]);
	}

	fclose(in);

	spline(qmi_x,qmi_y,NUMPTS*3+1,0.0,0.0,qmi_y2);
///// END SPLINE INTERPOLATE
}

double Qao_function(double t)
{ // Qao_function is the actual splined array that is used as a flow curve
	double f;

	splint(qao_x,qao_y,qao_y2,NUMPTS*3+1,t,&f);
	f = f/Norm_aortic; // f is a normalized value for flow

	return f;
}

double Qmi_function(double t)
{
	double f;

	splint(qmi_x,qmi_y,qmi_y2,NUMPTS*3+1,t,&f);
	f = f/Norm_mitral;

	return f;
}



void create_aortic_spline_template(double A, double B, double C, double D)
{ // a function that takes user parameters for a flow curve and makes a template that can be splined into a blood flow curve
	int i = 0;
	int l = 1;
	double T;
	T = 60.0/heart_rate;

	double x[NUMPTS], y[NUMPTS], e;
	e = (1.0 - A - C)/(NUMPTS - 7);
```

```
	while (i  < NUMPTS)
	{
		if (i == 0) {
			x[i] = 0;
			y[i] = D;
		};
		if (i >= 1 && i <= 4) {
			x[i] = (i)*A/4.0*T;
			y[i] = sin(3.1415927*x[i]/(A*T));
		}
		if (i == 5 ) {
			x[i] = (A + (i-4)*C/2.0)*T;
			y[i] = B;
		}
		if (i >= 6) {
			x[i] = x[i-1]+ e*T;
			y[i] = D;
		}
		i++;
	}


	FILE *in;
	in = fopen("aortic_spline_template_.dat", "w");
	for(l = 0;  l < NUMPTS; l++){
		fprintf(in,"%lf\t%lf\n", x[l]-1.0*T, y[l]);
	}
	for(l = 0;  l < NUMPTS; l++){
		fprintf(in,"%lf\t%lf\n", x[l], y[l]);
	}
	for(l = 0;  l < NUMPTS; l++){
		fprintf(in,"%lf\t%lf\n", x[l]+1.0*T, y[l]);
	}
		fprintf(in,"%lf\t%lf\n", x[0]+2.0*T, y[0]);

	fclose(in);

}

void create_mitral_spline_template(double A_, double A1, double A2, double A3, double B_, double
C_, double D_)
{
	int i = 0;
	int k = 0;
	double T,alpha;
	T = 60.0/heart_rate;

	double x[NUMPTS], y[NUMPTS], e;

	e = (1.0 - A_ - B_)/(NUMPTS - 11.0);
```

```
                for(k=0;k<NUMPTS-12;k++) {
                        x[k+3] = B_*T + e*T*(k+1);
                        y[k+3] = D_;

                }


/*
0st additional point at:   0.5*((1-A_)*T +  0.5*((1-A_)*T + A1*T) )  ,   0.2

1st additional point at:   0.5*((1-A_)*T + A1*T)  ,   0.4
2nd additional point at:   0.5*(A1*T + A2*T ) , 0.5
3rd additional point at:   0.5*(A2*T + A3*T )  , 0.5
4rd additional point at:   0.5*(A3*T + 1.0*T) , 0.4



*/

alpha = 0.9;

        while (i  < NUMPTS)
        {
                if (i == 0) {
                        x[i] = 0.0;
                        y[i] = 0.0;
                };
                if (i == 1) {
                        x[i] = B_/2.0*T;
                        y[i] = C_;
                }
                if (i == 2) {
                        x[i] = B_*T;
                        y[i] = D_;
                }

                if (i == NUMPTS-9) {
                        x[i] = (1-A_)*T;
                        y[i] = 0.0;
                }

                if (i == NUMPTS-8) {
                        x[i] = alpha*((1-A_)*T) + (1.0-alpha)*(0.5*((1-A_)*T + A1*T)) ;
                        y[i] = alpha*0.0+ (1.0-alpha)*0.4;
                }
                if (i == NUMPTS-7) {
                        x[i] = 0.5*((1-A_)*T + A1*T);
                        y[i] = 0.4;
                }

                if (i == NUMPTS-6) {
                        x[i] = A1*T;
                        y[i] = 0.8;
```

```
                }
                if (i == NUMPTS-5) {
                        x[i] = 0.5*(A1*T + A2*T);
                        y[i] = 0.5;
                }
                if (i == NUMPTS-4) {
                        x[i] = A2*T;
                        y[i] = 0.2;
                }
                if (i == NUMPTS-3) {
                        x[i] = 0.5*(A2*T + A3*T );
                        y[i] = 0.5;
                }
                if (i == NUMPTS-2) {
                        x[i] = A3*T;
                        y[i] = 0.8;
                }
                if (i == NUMPTS-1) {
                        x[i] = 0.5*(A3*T + 1.0*T);
                        y[i] = 0.4;
                }

                i++;
        }



        FILE *in;
        in = fopen("mitral_spline_template_.dat", "w");
        for(k = 0;  k < NUMPTS; k++){
                fprintf(in,"%lf\t%lf\n", x[k]-1.0*T, y[k]);
        }
        for(k = 0;  k < NUMPTS; k++){
                fprintf(in,"%lf\t%lf\n", x[k], y[k]);
        }
        for(k = 0;  k < NUMPTS; k++){
                fprintf(in,"%lf\t%lf\n", x[k]+1.0*T, y[k]);
        }
                fprintf(in,"%lf\t%lf\n", x[0]+2.0*T, y[0]);

        fclose(in);

}


void read_patient_file(char *filename) {

        PT = fopen(filename,"r");
//      double temp;
//      fscanf(PT,"%lf",&temp);
//      printf("%lf",temp);
```

```
	fscanf(PT,"%lf%lf%lf%lf%lf%lf%lf%lf%lf%lf%lf%lf%lf%lf%lf%lf%lf%lf%lf%lf%lf%l
f",&heart_rate, &CO, &systolic_fraction, &Csas, &Rsas, &Lsas, &Csat, &Rsat, &Lsat, &Rsar,
&Rscp, &Rsvn, &Csvn, &B, &C, &D, &B_, &C_, &D_, &CQao, &CQmi, &_CQao, &_CQmi);
	if(0==1)printf("%lf\n%lf\n%lf\n%lf\n%lf\n%lf\n%lf\n%lf\n%lf\n%lf\n%lf\n%lf\n%lf\n%lf\n%lf\n
%lf\n%lf\n%lf\n%lf\n%lf\n%lf\n%lf\n%lf\n%lf\n",heart_rate, CO, systolic_fraction, Csas, Rsas, Lsas,
Csat, Rsat, Lsat, Rsar, Rscp, Rsvn, Csvn, B, C, D, B_, C_, D_, CQao, CQmi, _CQao, _CQmi);

	fclose(PT);
//	exit(0);
;
}
```

APPENDIX B NORMAL CASE AND DISEASE CASE PARAMETERS

Table 12 Normal case parameters

Normal Case	
Parameter name	Value
HR (beat/min)	72
CO (mL/s)	83.33
Systolic fraction (s/s)	0.333
Csas (mL/mmHg)	0.0004
Rsas (mmHg s/mL)	0.003
Lsas (mmHg s^2/mL)	0.000744
Csat (mL/mmHg)	1.6
Rsat (mmHg s/mL)	0.05
Lsat (mmHg s^2/mL)	0.0017
Rsar (mmHg s/mL)	0.5
Rscp (mmHg s/mL)	0.52
Rsvn (mmHg s/mL)	0.075
Csvn (mL/mmHg)	20.5
B, MARV	-0.2
C, ARDF	0.08333
D, ACBFV	0
B_, MRDF	0.125
C_, MMRV	-0.2
D_, MCBFV	0
CQao ((s mmHg)$^{0.5}$/mL)	0.006667
CQmi ((s mmHg)$^{0.5}$/mL)	0.0025

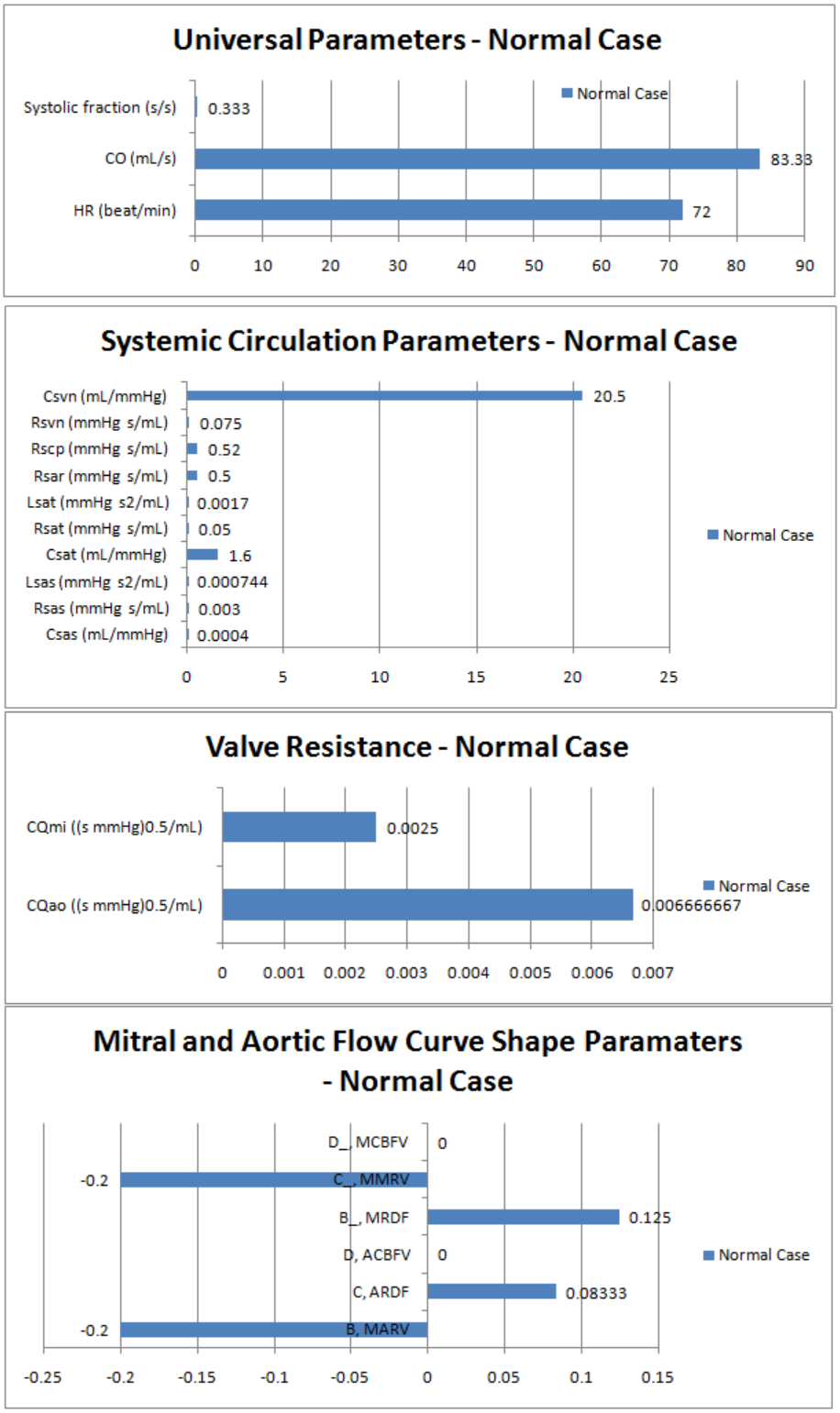

Figure 85 Normal case parameters

Table 13 Mild Hypertension case parameters.

Mild Hypertension Case	
Parameter name	Value
HR (beat/min)	72
CO (mL/s)	83.33
Systolic fraction (s/s)	0.333
Csas (mL/mmHg)	0.0004
Rsas (mmHg s/mL)	0.003
Lsas (mmHg s^2/mL)	0.000744
Csat (mL/mmHg)	1.2
Rsat (mmHg s/mL)	0.05
Lsat (mmHg s^2/mL)	0.0017
Rsar (mmHg s/mL)	0.5
Rscp (mmHg s/mL)	0.7875
Rsvn (mmHg s/mL)	0.075
Csvn (mL/mmHg)	20.5
B, MARV	-0.2
C, ARDF	0.08333
D, ACBFV	0
B_, MRDF	0.125
C_, MMRV	-0.2
D_, MCBFV	0
CQao ((s mmHg)$^{0.5}$/mL)	150
CQmi ((s mmHg)$^{0.5}$/mL)	400

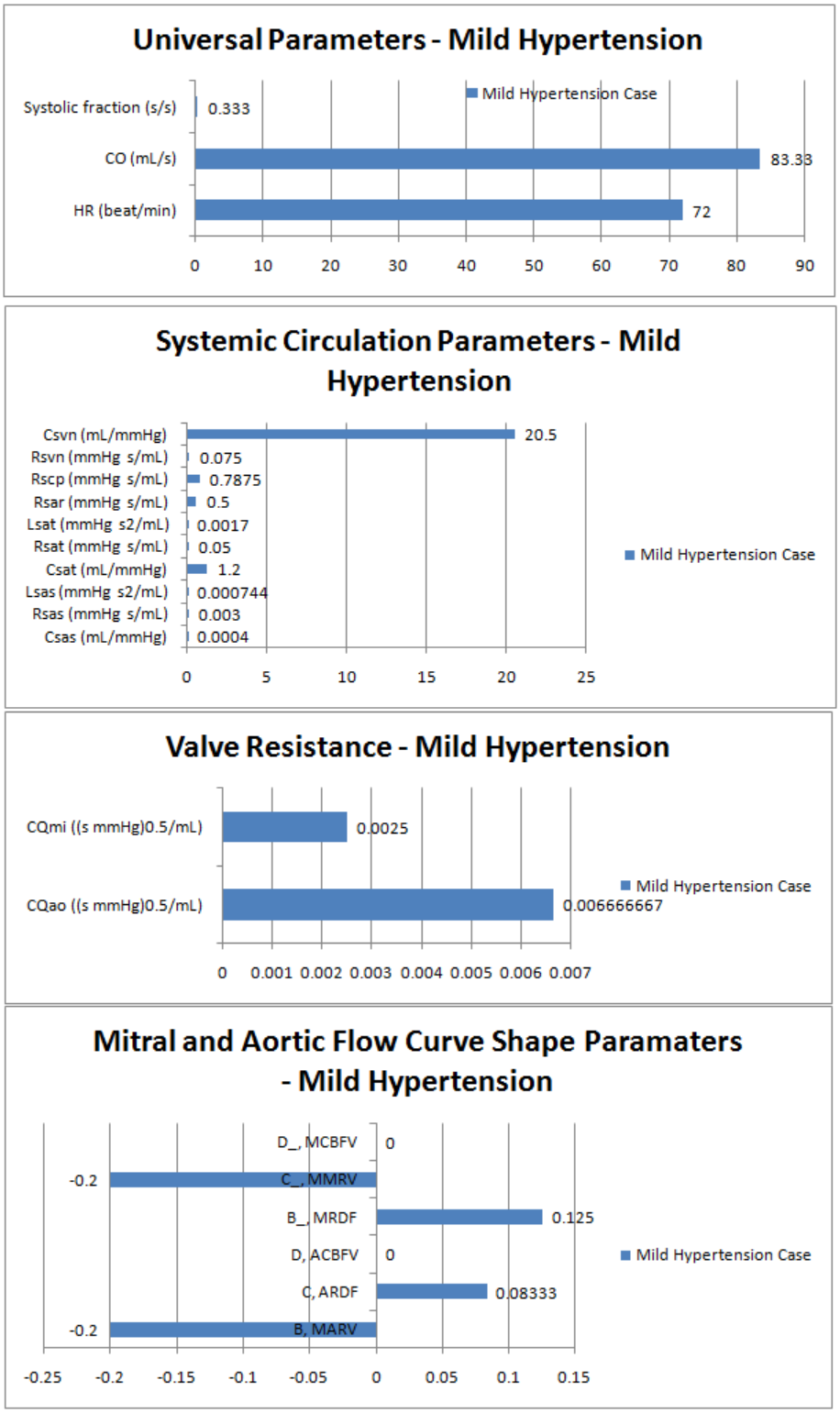

Figure 86 Mild Hypertension case parameter values.

Table 14 Moderate Hypertension case parameters.

Moderate Hypertension Case	
Parameter name	Value
HR (beat/min)	72
CO (mL/s)	83.33
Systolic fraction (s/s)	0.333
Csas (mL/mmHg)	0.0004
Rsas (mmHg s/mL)	0.003
Lsas (mmHg s^2/mL)	0.000744
Csat (mL/mmHg)	1.2
Rsat (mmHg s/mL)	0.05
Lsat (mmHg s^2/mL)	0.0017
Rsar (mmHg s/mL)	0.5
Rscp (mmHg s/mL)	0.8767
Rsvn (mmHg s/mL)	0.075
Csvn (mL/mmHg)	20.5
B, MARV	-0.2
C, ARDF	0.08333
D, ACBFV	0
B_, MRDF	0.125
C_, MMRV	-0.2
D_, MCBFV	0
CQao ((s mmHg)$^{0.5}$/mL)	0.006666667
CQmi ((s mmHg)$^{0.5}$/mL)	0.0025

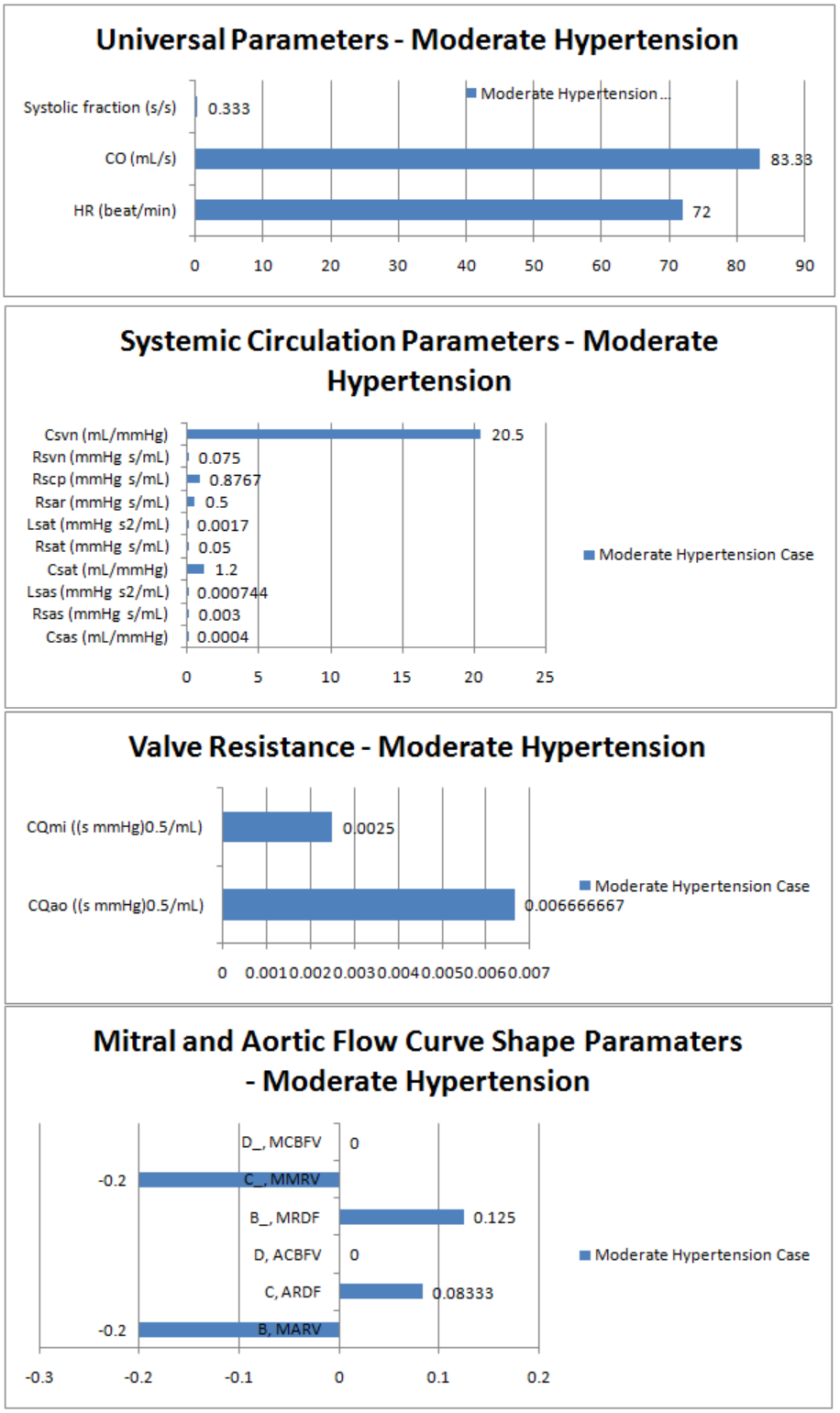

Figure 87 Moderate Hypertension case parameters.

Table 15Severe Hypertension case parameters.

Severe Hypertension Case	
Parameter name	Value
HR (beat/min)	72
CO (mL/s)	83.33
Systolic fraction (s/s)	0.333
Csas (mL/mmHg)	0.0004
Rsas (mmHg s/mL)	0.003
Lsas (mmHg s^2/mL)	0.000744
Csat (mL/mmHg)	0.8
Rsat (mmHg s/mL)	0.05
Lsat (mmHg s^2/mL)	0.0017
Rsar (mmHg s/mL)	0.5
Rscp (mmHg s/mL)	1.055
Rsvn (mmHg s/mL)	0.075
Csvn (mL/mmHg)	20.5
B, MARV	-0.2
C, ARDF	0.08333
D, ACBFV	0
B_, MRDF	0.125
C_, MMRV	-0.2
D_, MCBFV	0
CQao ((s mmHg)$^{0.5}$/mL)	0.006666667
CQmi ((s mmHg)$^{0.5}$/mL)	0.0025

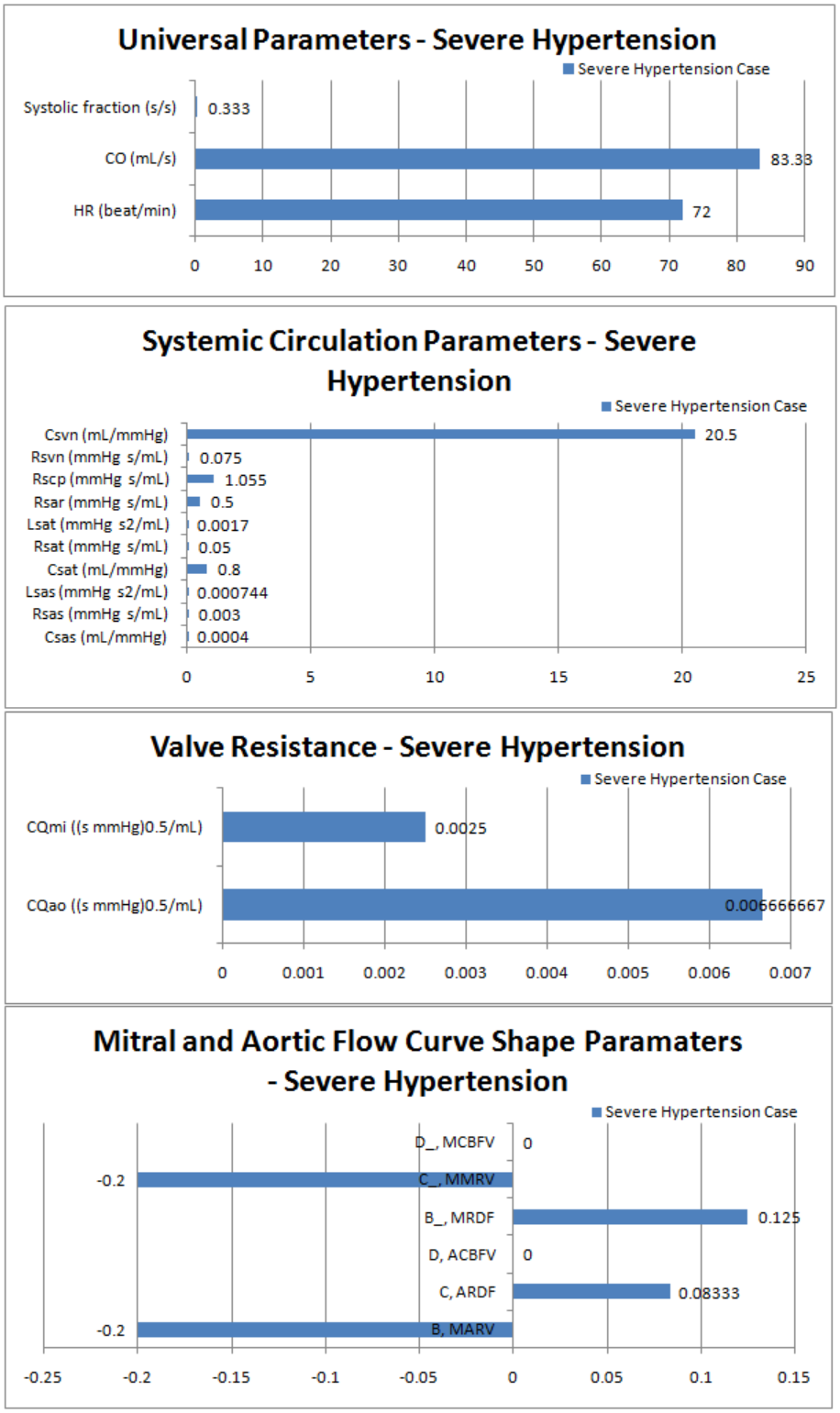

Figure 88 Severe Hypertension case parameters.

Table 16 Mild Aortic Stenosis case parameters.

Mild Aortic Stenosis Case	
Parameter name	Value
HR (beat/min)	72
CO (mL/s)	83.33
Systolic fraction (s/s)	0.333
Csas (mL/mmHg)	0.0004
Rsas (mmHg s/mL)	0.003
Lsas (mmHg s^2/mL)	0.000744
Csat (mL/mmHg)	1.6
Rsat (mmHg s/mL)	0.05
Lsat (mmHg s^2/mL)	0.0017
Rsar (mmHg s/mL)	0.5
Rscp (mmHg s/mL)	0.52
Rsvn (mmHg s/mL)	0.075
Csvn (mL/mmHg)	20.5
B, MARV	-0.2
C, ARDF	0.08333
D, ACBFV	0
B_, MRDF	0.125
C_, MMRV	-0.2
D_, MCBFV	0
CQao ((s mmHg)$^{0.5}$/mL)	0.013333333
CQmi ((s mmHg)$^{0.5}$/mL)	0.0025

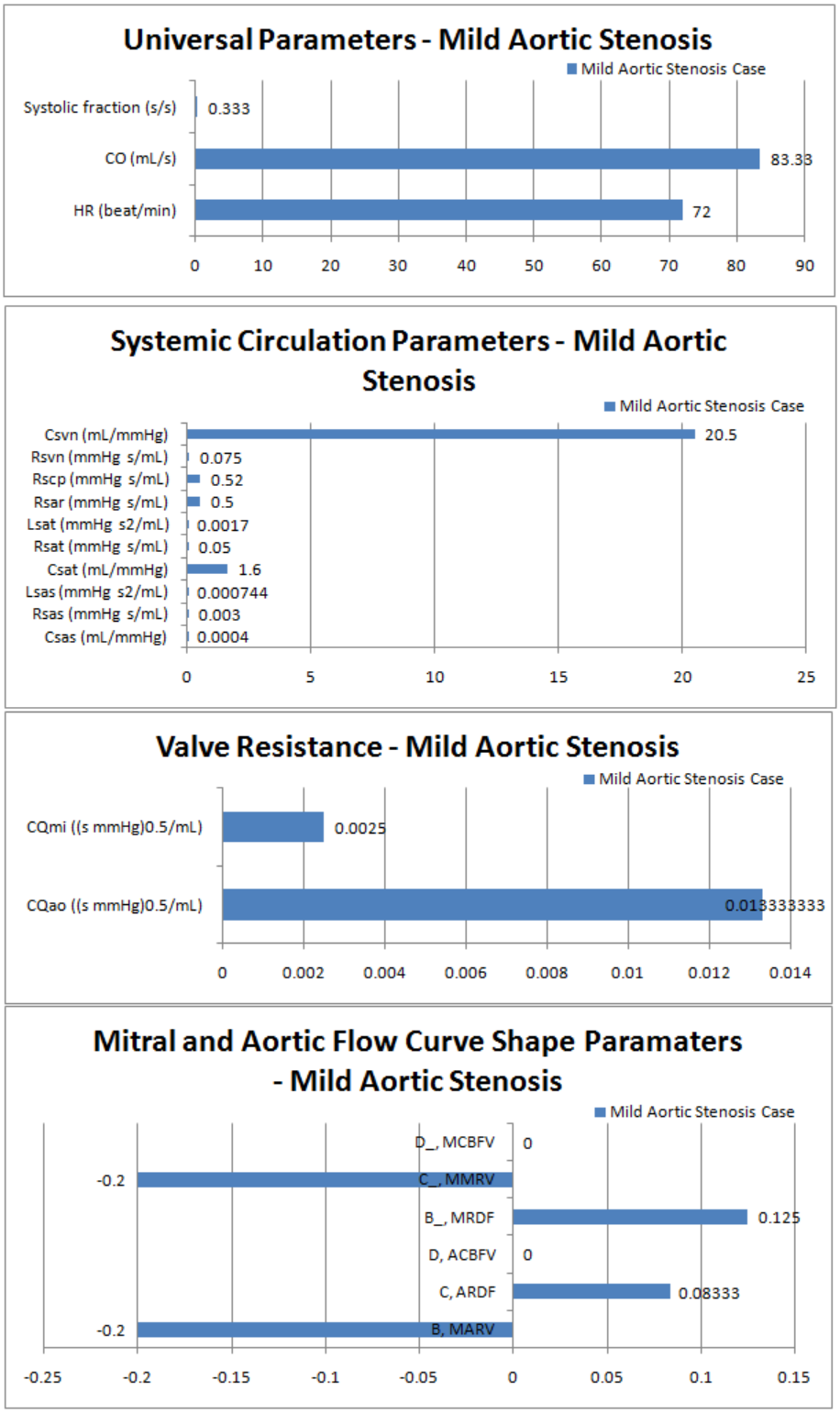

Figure 89 Mild Aortic Stenosis case parameters.

Table 17Moderate aortic stenosis case parameters.

Moderate Aortic Stenosis Case	
Parameter name	Value
HR (beat/min)	72
CO (mL/s)	83.33
Systolic fraction (s/s)	0.333
Csas (mL/mmHg)	0.0004
Rsas (mmHg s/mL)	0.003
Lsas (mmHg s^2/mL)	0.000744
Csat (mL/mmHg)	1.6
Rsat (mmHg s/mL)	0.05
Lsat (mmHg s^2/mL)	0.0017
Rsar (mmHg s/mL)	0.5
Rscp (mmHg s/mL)	0.52
Rsvn (mmHg s/mL)	0.075
Csvn (mL/mmHg)	20.5
B, MARV	-0.2
C, ARDF	0.08333
D, ACBFV	0
B_, MRDF	0.125
C_, MMRV	-0.2
D_, MCBFV	0
CQao ((s mmHg)$^{0.5}$/mL)	0.02
CQmi ((s mmHg)$^{0.5}$/mL)	0.0025

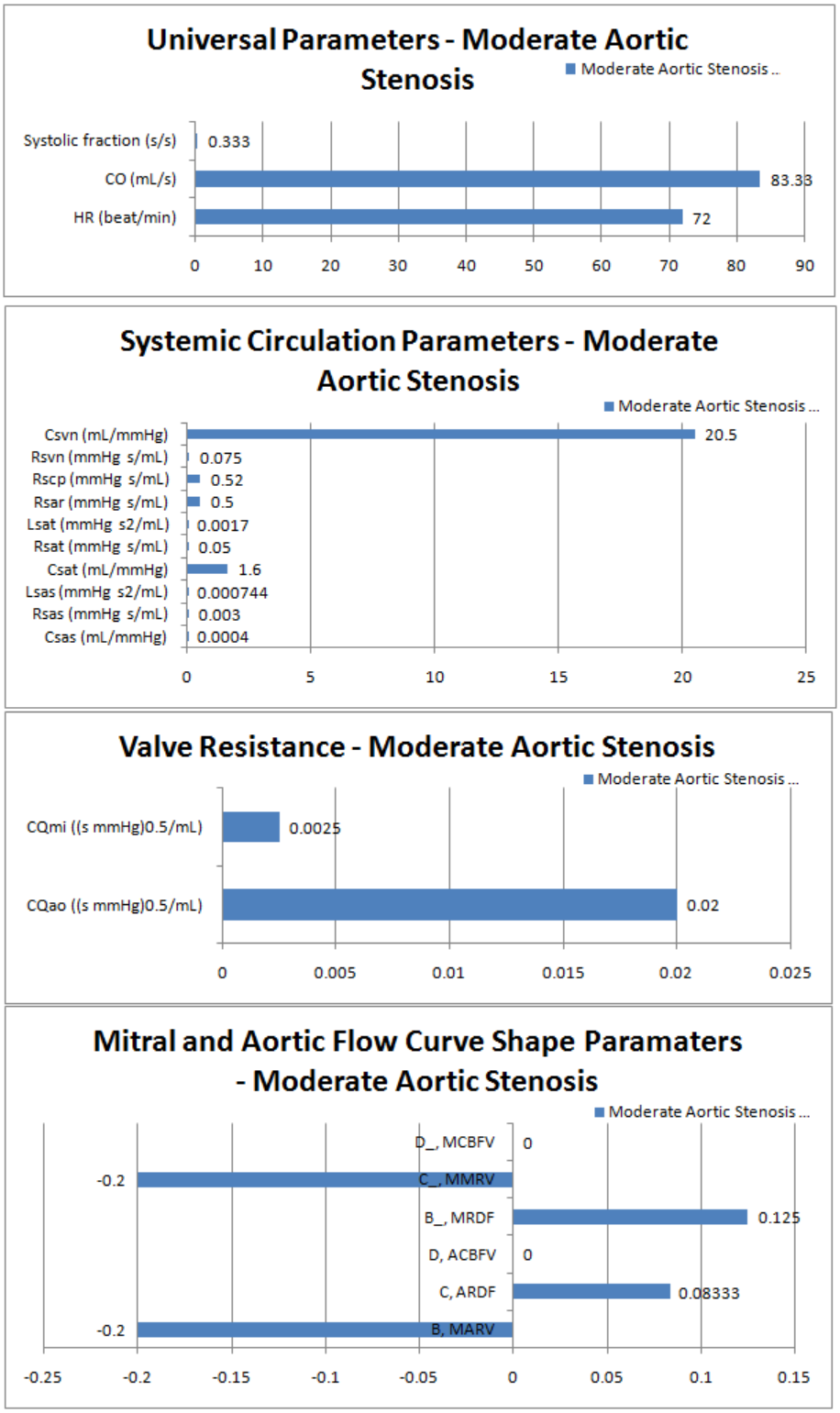

Figure 90 Moderate aortic stenosis cases parameters.

Table 18 Severe Aortic Stenosis case parameters.

Severe Aortic Stenosis Case	
Parameter name	Value
HR (beat/min)	72
CO (mL/s)	83.33
Systolic fraction (s/s)	0.333
Csas (mL/mmHg)	0.0004
Rsas (mmHg s/mL)	0.003
Lsas (mmHg s^2/mL)	0.000744
Csat (mL/mmHg)	1.6
Rsat (mmHg s/mL)	0.05
Lsat (mmHg s^2/mL)	0.0017
Rsar (mmHg s/mL)	0.5
Rscp (mmHg s/mL)	0.52
Rsvn (mmHg s/mL)	0.075
Csvn (mL/mmHg)	20.5
B, MARV	-0.2
C, ARDF	0.08333
D, ACBFV	0
B_, MRDF	0.125
C_, MMRV	-0.2
D_, MCBFV	0
CQao ((s mmHg)$^{0.5}$/mL)	0.015384615
CQmi ((s mmHg)$^{0.5}$/mL)	0.0025

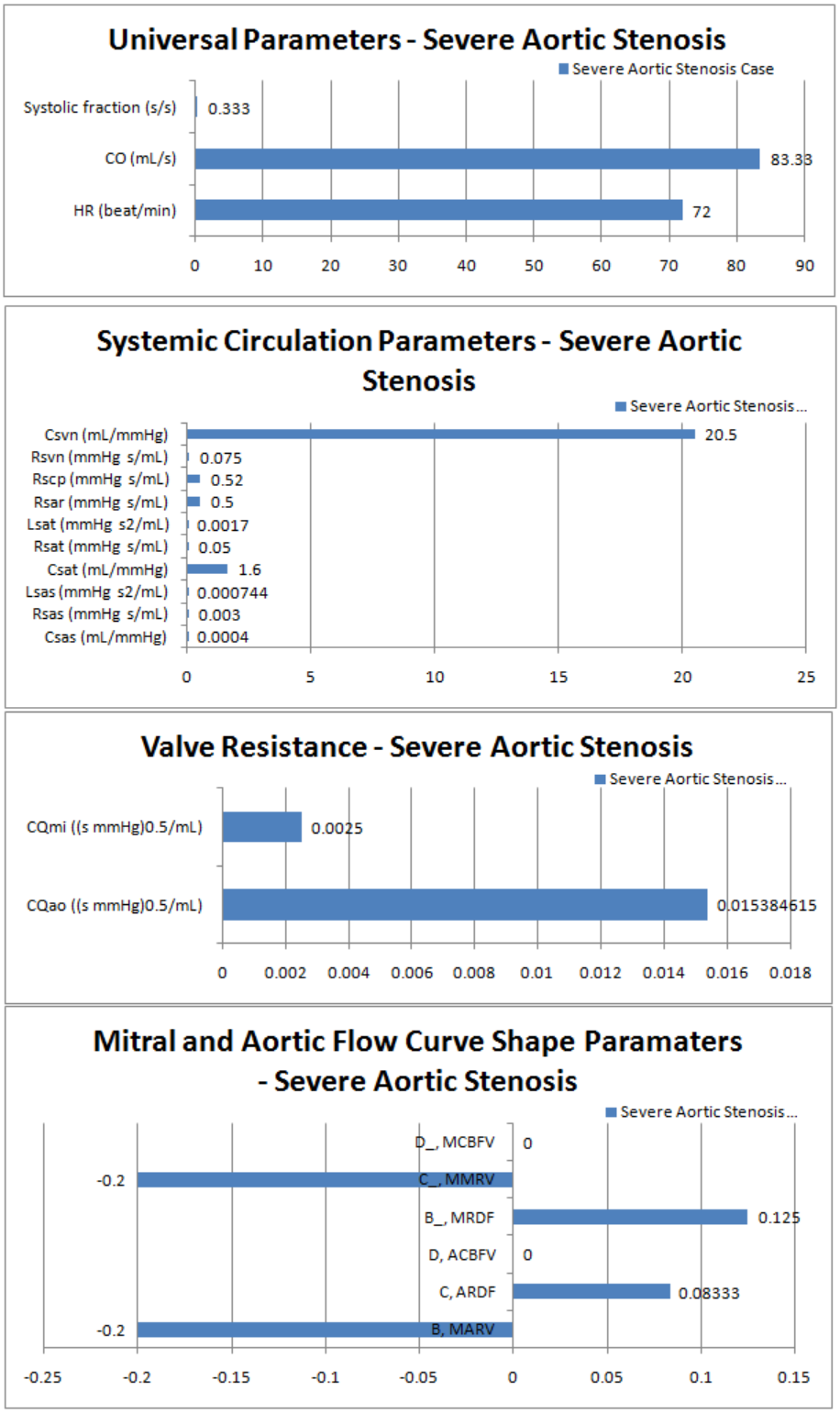

Figure 91 Severe Aortic Stenosis case parameters.

Table 19 Mild Aortic Regurgitation case parameters.

Mild Aortic Regurgitation Case	
Parameter name	Value
HR (beat/min)	72
CO (mL/s)	83.33
Systolic fraction (s/s)	0.333
Csas (mL/mmHg)	0.0004
Rsas (mmHg s/mL)	0.003
Lsas (mmHg s^2/mL)	0.000744
Csat (mL/mmHg)	1.6
Rsat (mmHg s/mL)	0.05
Lsat (mmHg s^2/mL)	0.0017
Rsar (mmHg s/mL)	0.5
Rscp (mmHg s/mL)	0.52
Rsvn (mmHg s/mL)	0.075
Csvn (mL/mmHg)	20.5
B, MARV	-0.25
C, ARDF	0.08333
D, ACBFV	-0.05
B_, MRDF	0.125
C_, MMRV	-0.2
D_, MCBFV	0
CQao ((s mmHg)$^{0.5}$/mL)	0.006666667
CQmi ((s mmHg)$^{0.5}$/mL)	0.0025

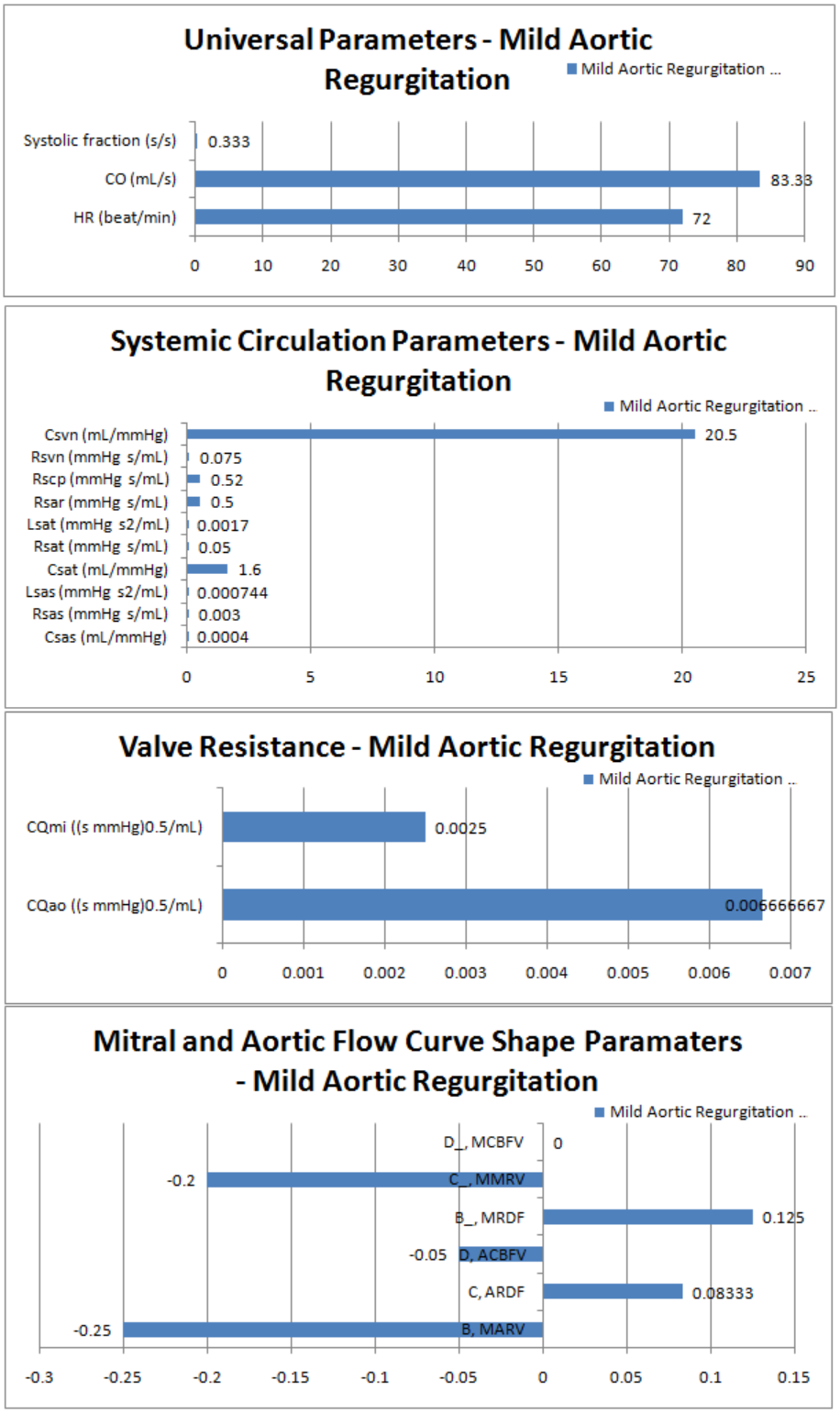

Figure 92 Mild Aortic Regurgitation case parameters.

Table 20 Moderate Aortic regurgitation case parameters.

Moderate Aortic Regurgitation Case	
Parameter name	Value
HR (beat/min)	72
CO (mL/s)	83.33
Systolic fraction (s/s)	0.333
Csas (mL/mmHg)	0.0004
Rsas (mmHg s/mL)	0.003
Lsas (mmHg s^2/mL)	0.000744
Csat (mL/mmHg)	1.6
Rsat (mmHg s/mL)	0.05
Lsat (mmHg s^2/mL)	0.0017
Rsar (mmHg s/mL)	0.5
Rscp (mmHg s/mL)	0.52
Rsvn (mmHg s/mL)	0.075
Csvn (mL/mmHg)	20.5
B, MARV	-0.3
C, ARDF	0.08333
D, ACBFV	-0.1
B_, MRDF	0.125
C_, MMRV	-0.2
D_, MCBFV	0
CQao ((s mmHg)$^{0.5}$/mL)	0.006666667
CQmi ((s mmHg)$^{0.5}$/mL)	0.0025

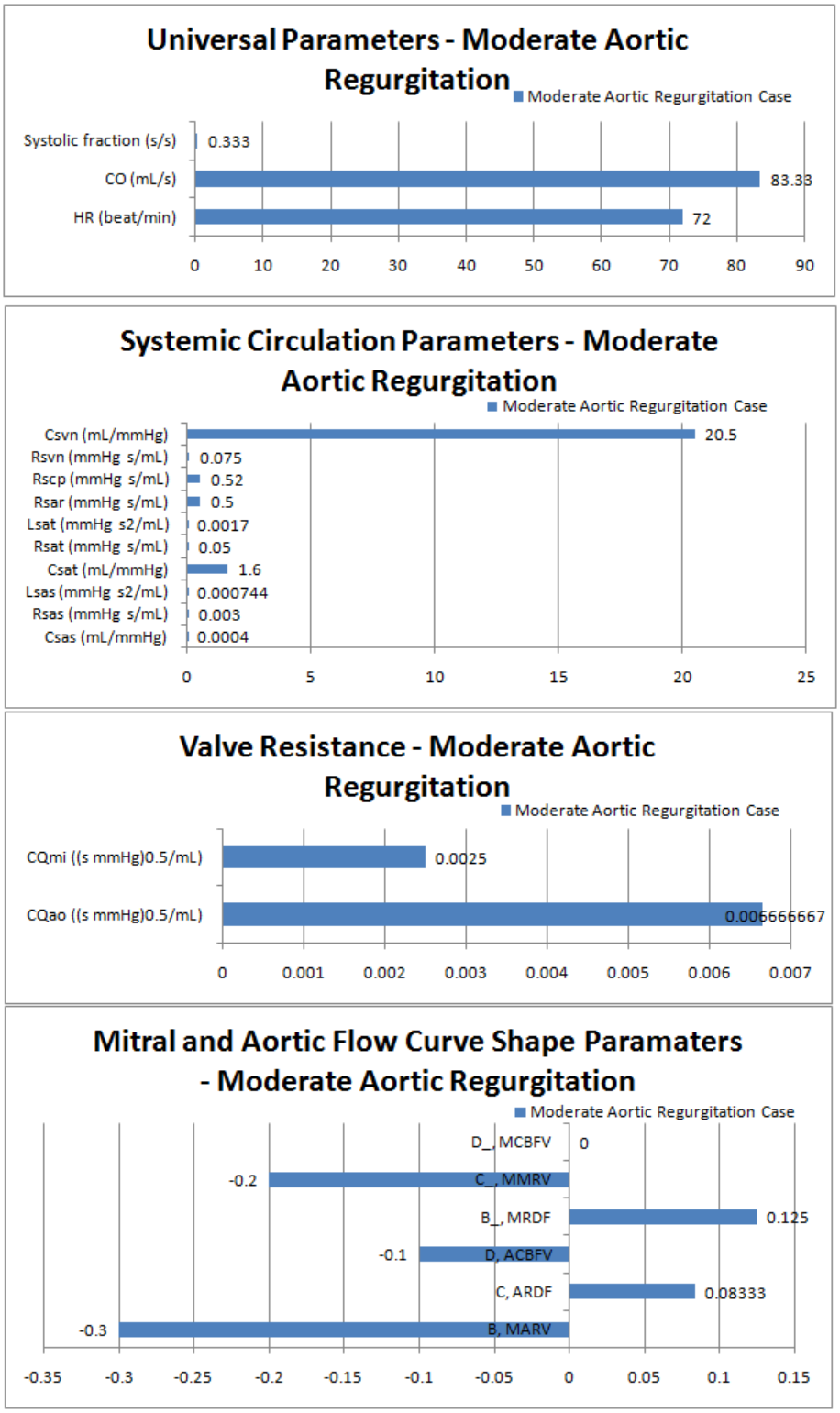

Figure 93 Moderate Aortic Regurgitation case parameters.

Table 21 Severe Aortic Regurgitation Case Parameters.

Severe Aortic Regurgitation Case	
Parameter name	Value
HR (beat/min)	72
CO (mL/s)	83.33
Systolic fraction (s/s)	0.333
Csas (mL/mmHg)	0.0004
Rsas (mmHg s/mL)	0.003
Lsas (mmHg s^2/mL)	0.000744
Csat (mL/mmHg)	1.6
Rsat (mmHg s/mL)	0.05
Lsat (mmHg s^2/mL)	0.0017
Rsar (mmHg s/mL)	0.5
Rscp (mmHg s/mL)	0.52
Rsvn (mmHg s/mL)	0.075
Csvn (mL/mmHg)	20.5
B, MARV	-0.4
C, ARDF	0.08333
D, ACBFV	-0.2
B_, MRDF	0.125
C_, MMRV	-0.2
D_, MCBFV	0
CQao ((s mmHg)$^{0.5}$/mL)	0.006666667
CQmi ((s mmHg)$^{0.5}$/mL)	0.0025

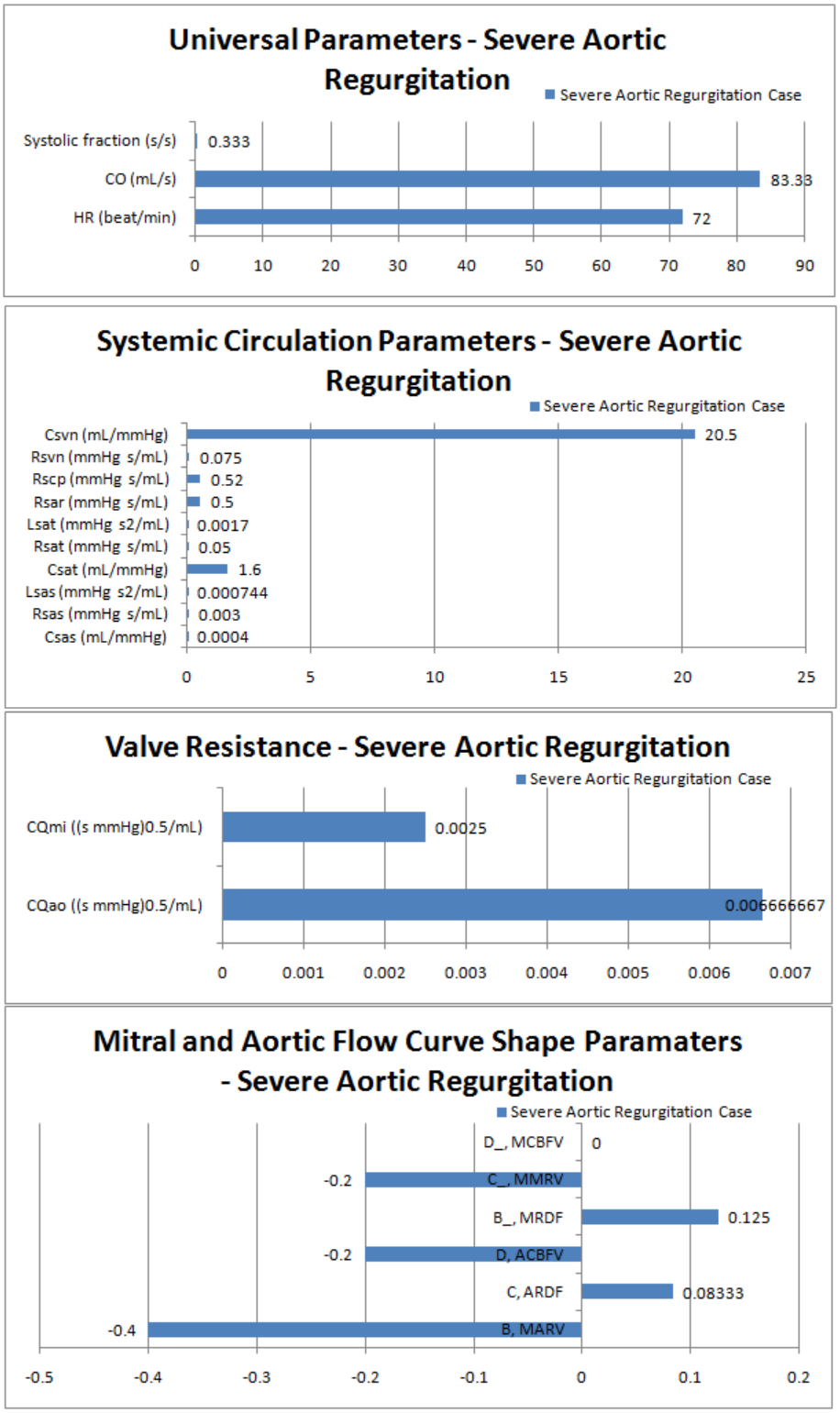

Figure 94 Severe Aortic Regurgitation case parameters.

Table 22 Mild Mitral Regurgitation case parameters.

Mild Mitral Regurgitation Case	
Parameter name	Value
HR (beat/min)	72
CO (mL/s)	83.33
Systolic fraction (s/s)	0.333
Csas (mL/mmHg)	0.0004
Rsas (mmHg s/mL)	0.003
Lsas (mmHg s^2/mL)	0.000744
Csat (mL/mmHg)	1.6
Rsat (mmHg s/mL)	0.05
Lsat (mmHg s^2/mL)	0.0017
Rsar (mmHg s/mL)	0.5
Rscp (mmHg s/mL)	0.52
Rsvn (mmHg s/mL)	0.075
Csvn (mL/mmHg)	20.5
B, MARV	-0.2
C, ARDF	0.08333
D, ACBFV	0
B_, MRDF	0.125
C_, MMRV	-0.35
D_, MCBFV	-0.15
CQao ((s mmHg)$^{0.5}$/mL)	0.006666667
CQmi ((s mmHg)$^{0.5}$/mL)	0.0025

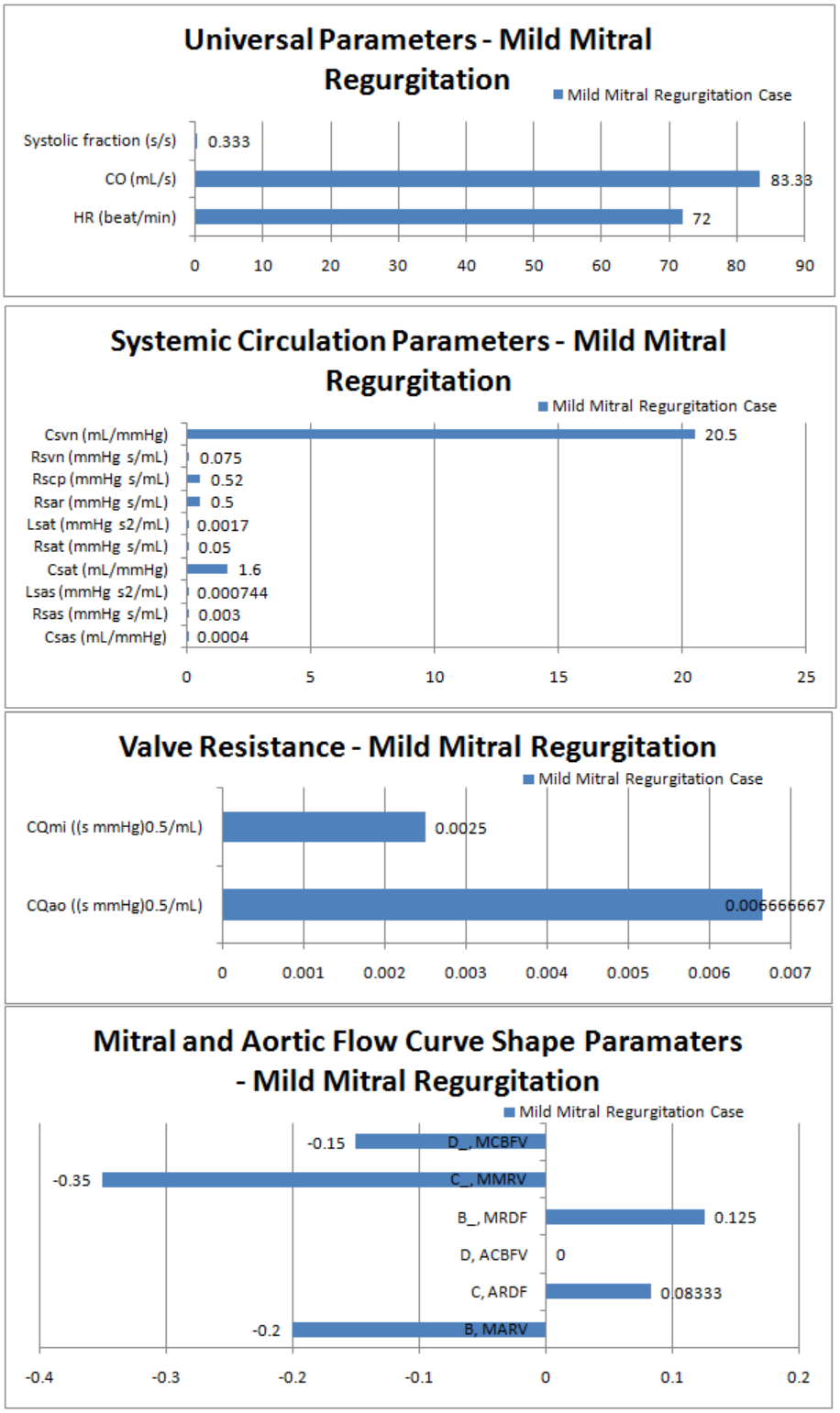

Figure 95 Mild Mitral Regurgitation case parameters.

Table 23 Moderate Mitral Regurgitation case parameters.

Moderate Mitral Regurgitation Case	
Parameter name	Value
HR (beat/min)	72
CO (mL/s)	83.33
Systolic fraction (s/s)	0.333
Csas (mL/mmHg)	0.0004
Rsas (mmHg s/mL)	0.003
Lsas (mmHg s^2/mL)	0.000744
Csat (mL/mmHg)	1.6
Rsat (mmHg s/mL)	0.05
Lsat (mmHg s^2/mL)	0.0017
Rsar (mmHg s/mL)	0.5
Rscp (mmHg s/mL)	0.52
Rsvn (mmHg s/mL)	0.075
Csvn (mL/mmHg)	20.5
B, MARV	-0.2
C, ARDF	0.08333
D, ACBFV	0
B_, MRDF	0.125
C_, MMRV	-0.65
D_, MCBFV	-0.45
CQao ((s mmHg)$^{0.5}$/mL)	0.006666667
CQmi ((s mmHg)$^{0.5}$/mL)	0.0025

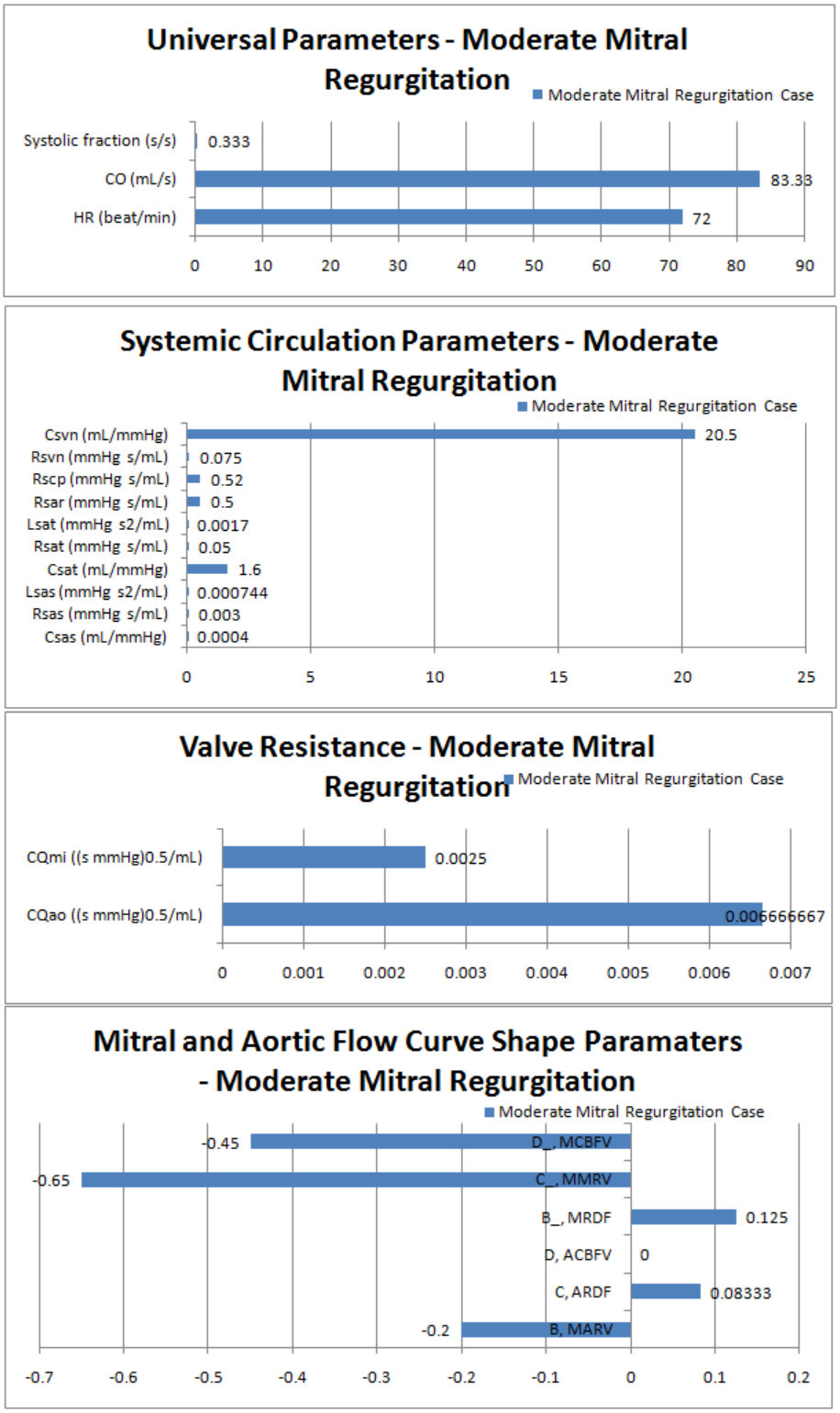

Figure 96 Moderate Mitral Regurgitation case parameters.

Table 24 Severe Mitral Regurgitation case parameters.

Severe Mitral Regurgitation Case	
Parameter name	Value
HR (beat/min)	72
CO (mL/s)	83.33
Systolic fraction (s/s)	0.333
Csas (mL/mmHg)	0.0004
Rsas (mmHg s/mL)	0.003
Lsas (mmHg s^2/mL)	0.000744
Csat (mL/mmHg)	1.6
Rsat (mmHg s/mL)	0.05
Lsat (mmHg s^2/mL)	0.0017
Rsar (mmHg s/mL)	0.5
Rscp (mmHg s/mL)	0.52
Rsvn (mmHg s/mL)	0.075
Csvn (mL/mmHg)	20.5
B, MARV	-0.2
C, ARDF	0.08333
D, ACBFV	0
B_, MRDF	0.125
C_, MMRV	-2.1
D_, MCBFV	-1.9
CQao ((s mmHg)$^{0.5}$/mL)	0.006666667
CQmi ((s mmHg)$^{0.5}$/mL)	0.0025

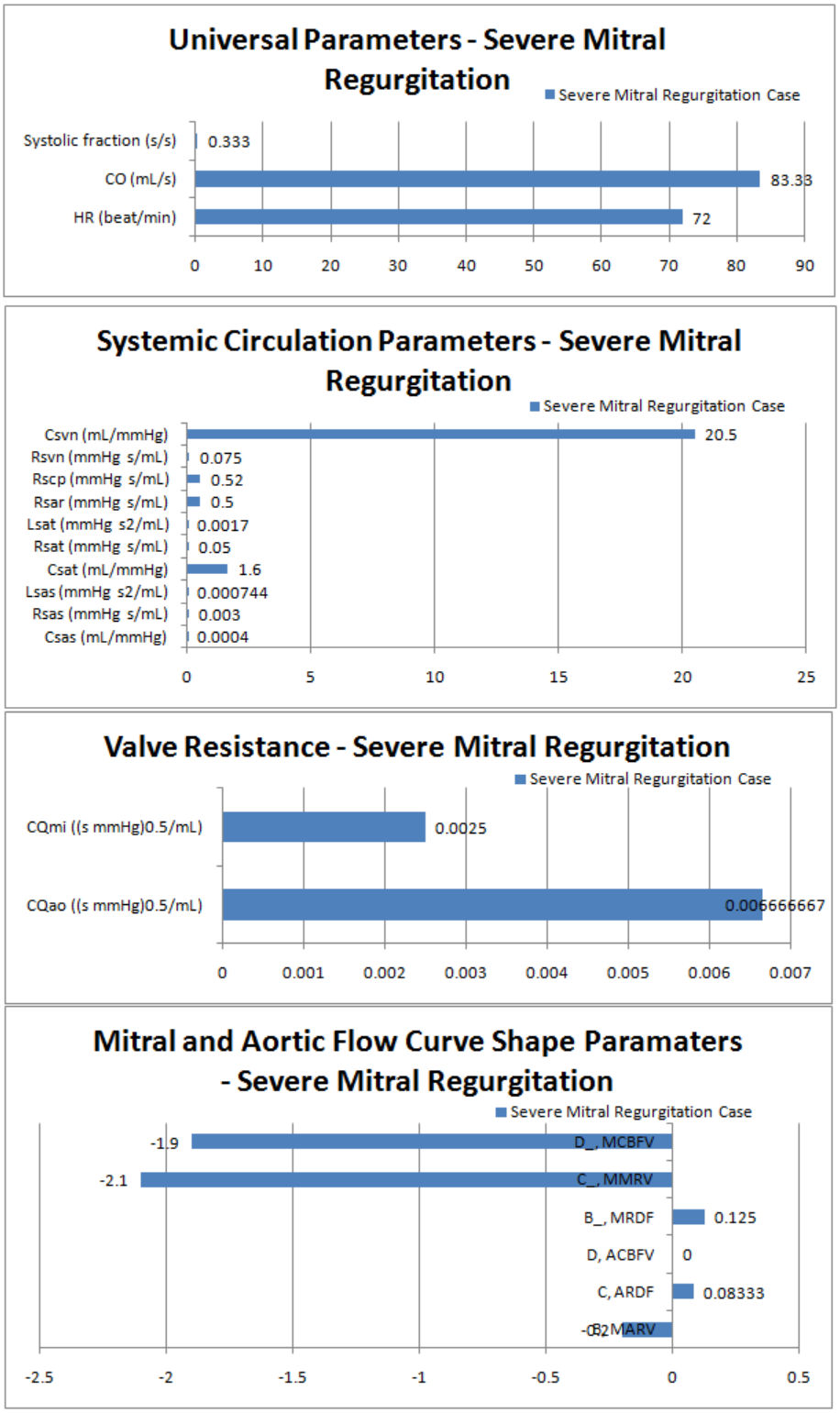

Figure 97 Severe mitral regurgitation case parameters.

Table 25 Mild hypertension and Mild Aortic Stenosis combined case parameters.

Mild Hypertension and Mild Aortic Stenosis Combined Case	
Parameter name	Value
HR (beat/min)	72
CO (mL/s)	83.33
Systolic fraction (s/s)	0.333
Csas (mL/mmHg)	0.0004
Rsas (mmHg s/mL)	0.003
Lsas (mmHg s^2/mL)	0.000744
Csat (mL/mmHg)	1.2
Rsat (mmHg s/mL)	0.05
Lsat (mmHg s^2/mL)	0.0017
Rsar (mmHg s/mL)	0.5
Rscp (mmHg s/mL)	0.7875
Rsvn (mmHg s/mL)	0.075
Csvn (mL/mmHg)	20.5
B, MARV	-0.2
C, ARDF	0.08333
D, ACBFV	0
B_, MRDF	0.125
C_, MMRV	-0.2
D_, MCBFV	0
CQao ((s mmHg)$^{0.5}$/mL)	0.013333333
CQmi ((s mmHg)$^{0.5}$/mL)	0.0025

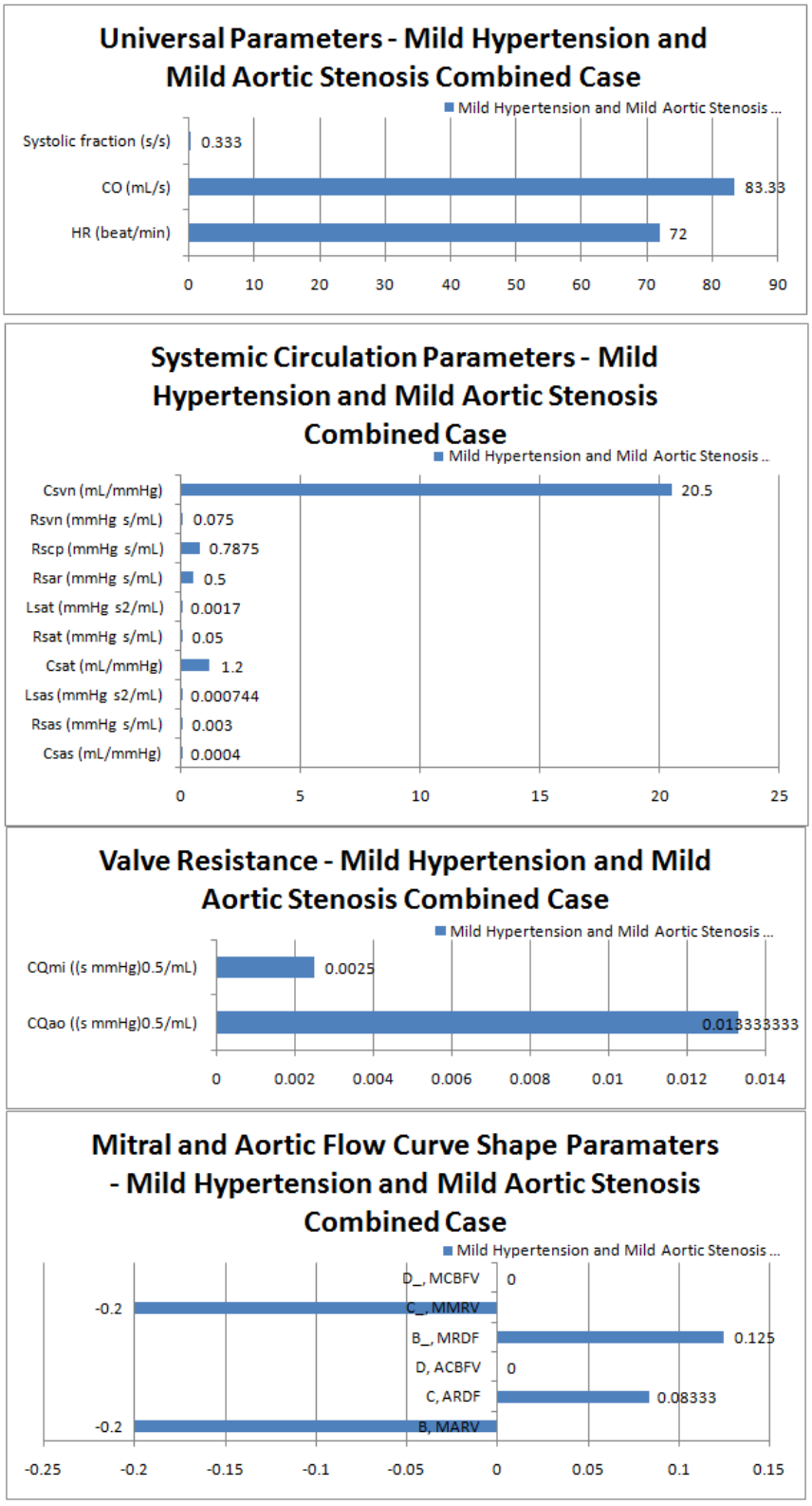

Figure 98 Mild hypertension and Mild Aortic Stenosis combined case parameters.

Table 26 Mild Hypertension and Mild Aortic Regurgitation combined case parameters.

Mild Hypertension and Mild Aortic Regurgitation Combined Case	
Parameter name	Value
HR (beat/min)	72
CO (mL/s)	83.33
Systolic fraction (s/s)	0.333
Csas (mL/mmHg)	0.0004
Rsas (mmHg s/mL)	0.003
Lsas (mmHg s^2/mL)	0.000744
Csat (mL/mmHg)	1.2
Rsat (mmHg s/mL)	0.05
Lsat (mmHg s^2/mL)	0.0017
Rsar (mmHg s/mL)	0.5
Rscp (mmHg s/mL)	0.7875
Rsvn (mmHg s/mL)	0.075
Csvn (mL/mmHg)	20.5
B, MARV	-0.25
C, ARDF	0.08333
D, ACBFV	-0.05
B_, MRDF	0.125
C_, MMRV	-0.2
D_, MCBFV	0
CQao ((s mmHg)$^{0.5}$/mL)	0.006666667
CQmi ((s mmHg)$^{0.5}$/mL)	0.0025

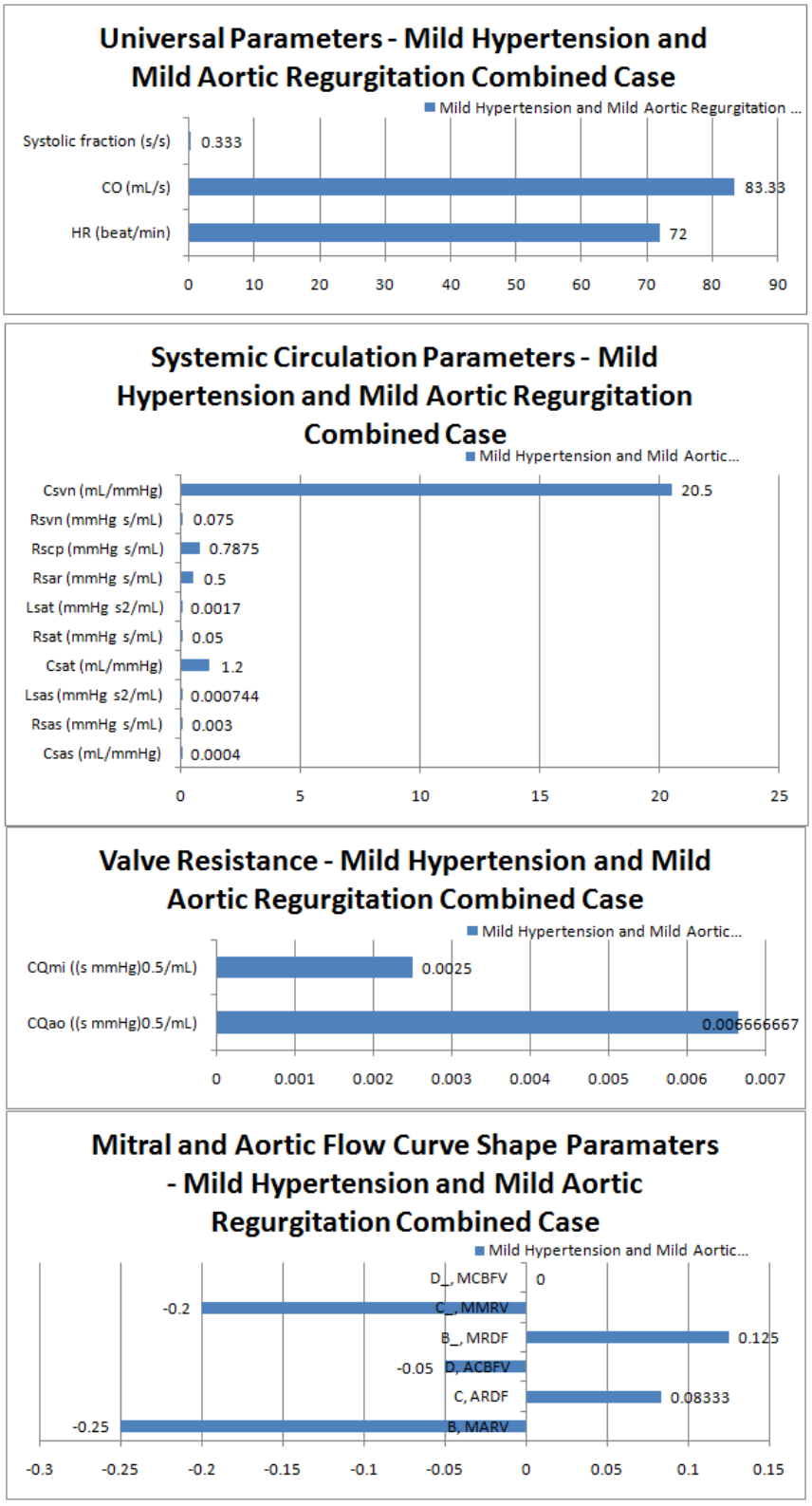

Figure 99 Mild Hypertension and Mild Aortic Regurgitation combined case parameters.

Table 27 Mild Hypertension and Mild Mitral Regurgitation combined case parameters.

Mild Hypertension and Mild Mitral Regurgitation Combined Case	
Parameter name	Value
HR (beat/min)	72
CO (mL/s)	83.33
Systolic fraction (s/s)	0.333
Csas (mL/mmHg)	0.0004
Rsas (mmHg s/mL)	0.003
Lsas (mmHg s^2/mL)	0.000744
Csat (mL/mmHg)	1.2
Rsat (mmHg s/mL)	0.05
Lsat (mmHg s^2/mL)	0.0017
Rsar (mmHg s/mL)	0.5
Rscp (mmHg s/mL)	0.7875
Rsvn (mmHg s/mL)	0.075
Csvn (mL/mmHg)	20.5
B, MARV	-0.2
C, ARDF	0.08333
D, ACBFV	0
B_, MRDF	0.125
C_, MMRV	-0.35
D_, MCBFV	-0.15
CQao ((s mmHg)$^{0.5}$/mL)	0.006666667
CQmi ((s mmHg)$^{0.5}$/mL)	0.0025

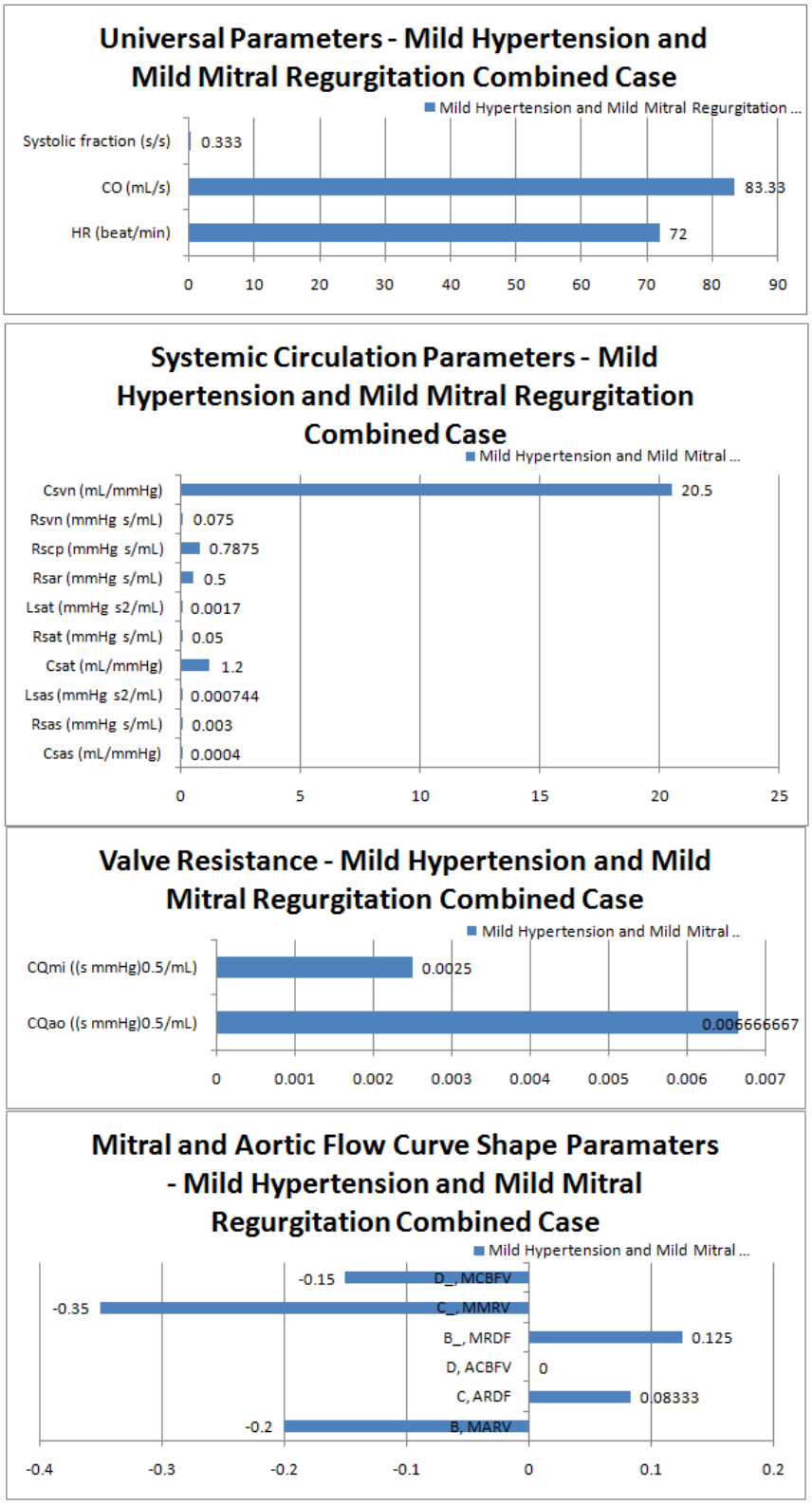

Figure 100 Mild Hypertension and Mild Mitral Regurgitation combined case parameters.

Table 28 Mild Aortic Stenosis and Mild Mitral Regurgitation combined case parameters.

Mild Aortic Stenosis and Mild Mitral Regurgitation Combined Case	
Parameter name	Value
HR (beat/min)	72
CO (mL/s)	83.33
Systolic fraction (s/s)	0.333
Csas (mL/mmHg)	0.0004
Rsas (mmHg s/mL)	0.003
Lsas (mmHg s^2/mL)	0.000744
Csat (mL/mmHg)	1.6
Rsat (mmHg s/mL)	0.05
Lsat (mmHg s^2/mL)	0.0017
Rsar (mmHg s/mL)	0.5
Rscp (mmHg s/mL)	0.52
Rsvn (mmHg s/mL)	0.075
Csvn (mL/mmHg)	20.5
B, MARV	-0.2
C, ARDF	0.08333
D, ACBFV	0
B_, MRDF	0.125
C_, MMRV	-0.35
D_, MCBFV	-0.15
CQao ((s mmHg)$^{0.5}$/mL)	0.013333333
CQmi ((s mmHg)$^{0.5}$/mL)	0.0025

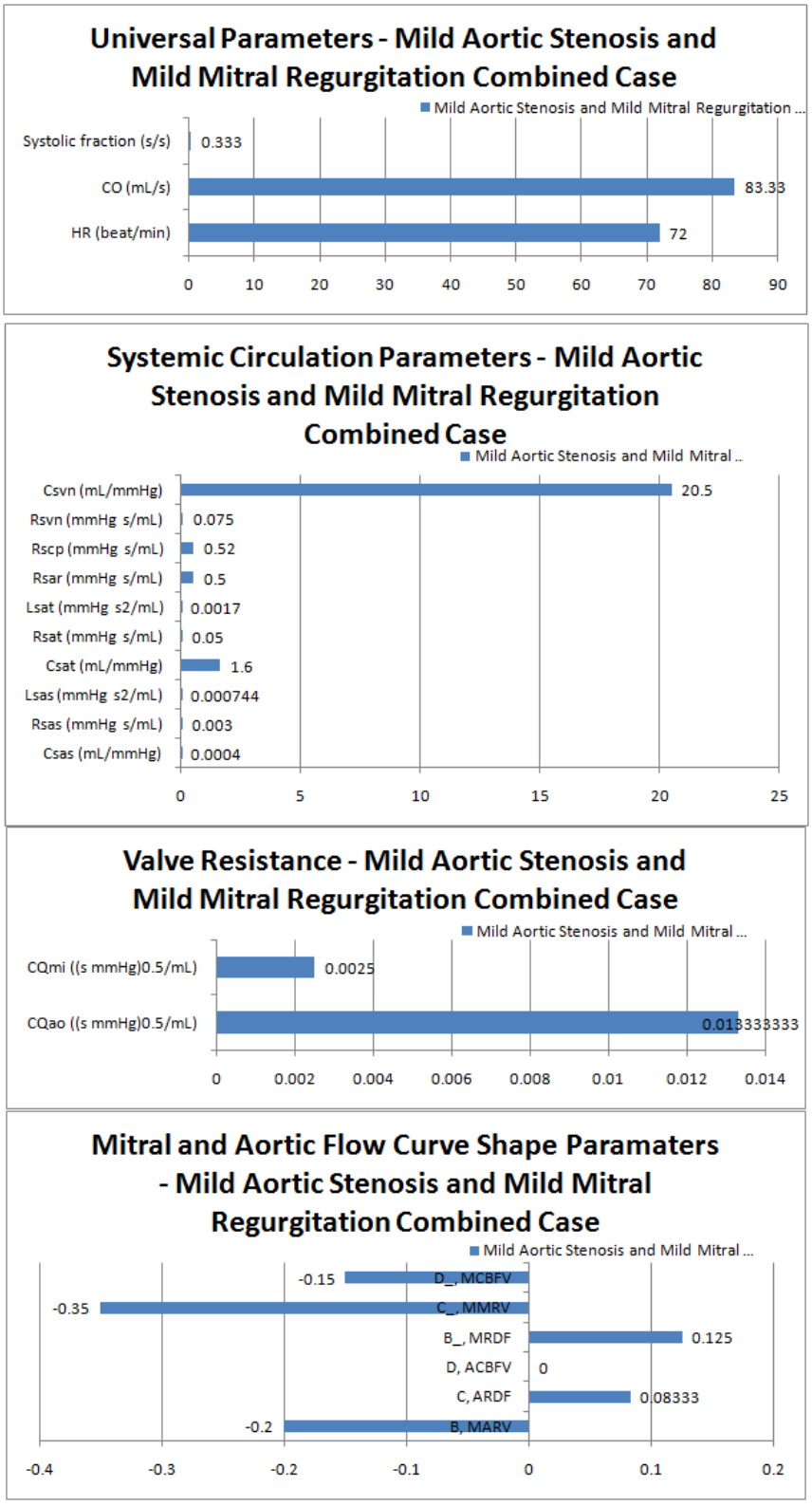

Figure 101 Mild Aortic Stenosis and Mild Mitral Regurgitation combined case parameters.

Table 29 Mild Aortic Stenosis and Mild Aortic Regurgitation combined case parameters.

Mild Aortic Stenosis and Mild Aortic Regurgitation Combined Case	
Parameter name	Value
HR (beat/min)	72
CO (mL/s)	83.33
Systolic fraction (s/s)	0.333
Csas (mL/mmHg)	0.0004
Rsas (mmHg s/mL)	0.003
Lsas (mmHg s^2/mL)	0.000744
Csat (mL/mmHg)	1.6
Rsat (mmHg s/mL)	0.05
Lsat (mmHg s^2/mL)	0.0017
Rsar (mmHg s/mL)	0.5
Rscp (mmHg s/mL)	0.52
Rsvn (mmHg s/mL)	0.075
Csvn (mL/mmHg)	20.5
B, MARV	-0.25
C, ARDF	0.08333
D, ACBFV	-0.05
B_, MRDF	0.125
C_, MMRV	-0.2
D_, MCBFV	0
CQao ((s mmHg)$^{0.5}$/mL)	0.013333333
CQmi ((s mmHg)$^{0.5}$/mL)	0.0025

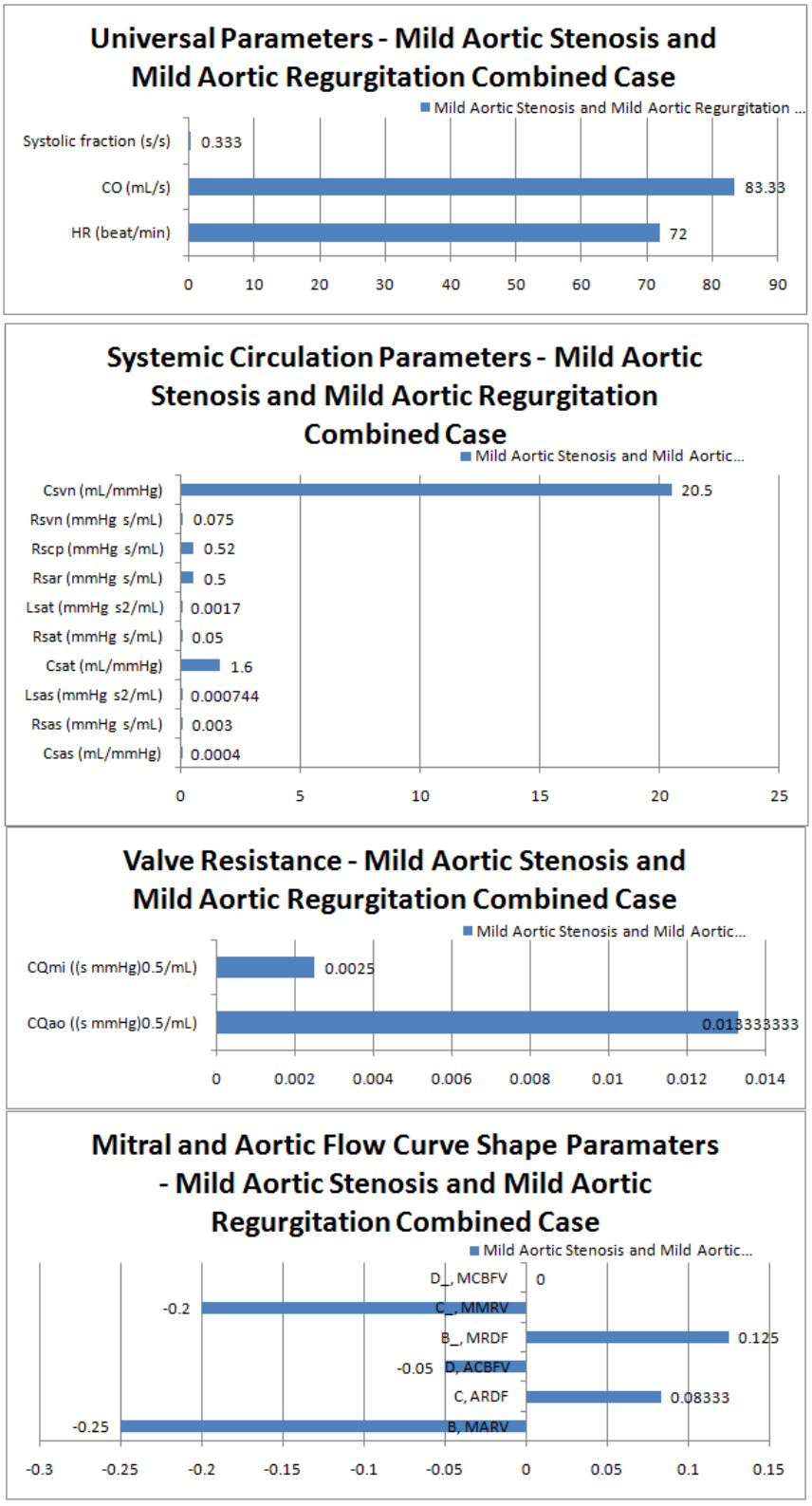

Figure 102 Mild Aortic Stenosis and Mild Aortic Regurgitation combined case parameters.

Table 30 Mild Mitral Regurgitation and Mild Aortic Regurgitation combined case parameters.

Mild Mitral Regurgitation and Mild Aortic Regurgitation Combined Case	
Parameter name	Value
HR (beat/min)	72
CO (mL/s)	83.33
Systolic fraction (s/s)	0.333
Csas (mL/mmHg)	0.0004
Rsas (mmHg s/mL)	0.003
Lsas (mmHg s^2/mL)	0.000744
Csat (mL/mmHg)	1.6
Rsat (mmHg s/mL)	0.05
Lsat (mmHg s^2/mL)	0.0017
Rsar (mmHg s/mL)	0.5
Rscp (mmHg s/mL)	0.52
Rsvn (mmHg s/mL)	0.075
Csvn (mL/mmHg)	20.5
B, MARV	-0.25
C, ARDF	0.08333
D, ACBFV	-0.05
B_, MRDF	0.125
C_, MMRV	-0.35
D_, MCBFV	-0.15
CQao ((s mmHg)$^{0.5}$/mL)	0.006666667
CQmi ((s mmHg)$^{0.5}$/mL)	0.0025

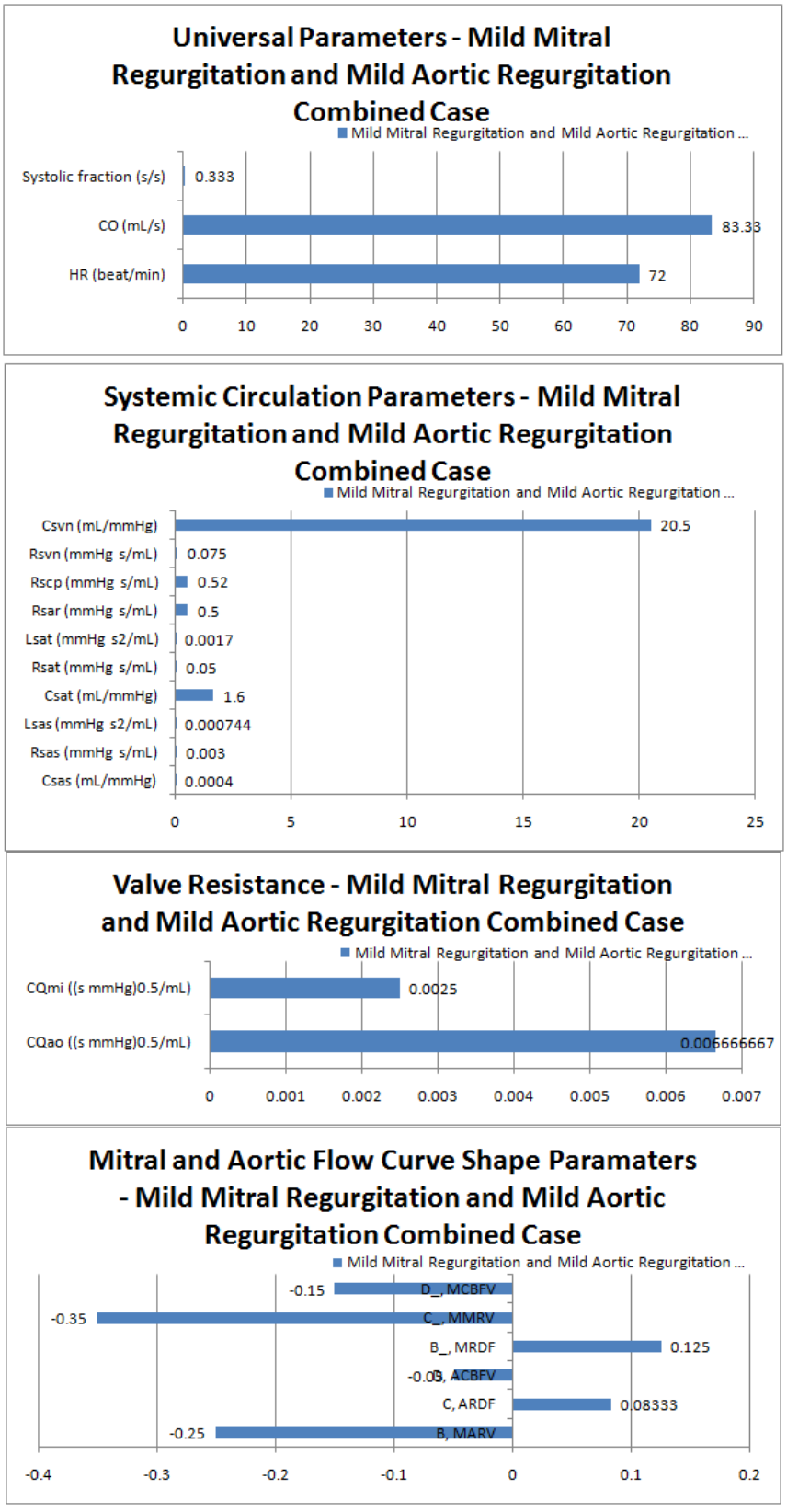

Figure 103 Mild Mitral Regurgitation and Mild Aortic Regurgitation combined case parameters.